“There is nothing like looking, if you want to find something. You certainly usually find something, if you look, but it is not always quite the something you were after.”

J.R.R. Tolkien

Promoters **prof. dr. ir. Luc Tirry**
prof. dr. ir. Thomas Van Leeuwen
dr. ir. Wannes Dermauw

Department of Plants and Crops
Faculty of Bioscience Engineering
Ghent University

Dean **prof. dr. ir. Marc Van Meirvenne**

Rector **prof. dr. ir. Rik Van de Walle**

Genetic and molecular mechanisms of pesticide resistance and host plant acclimation in the generalist herbivore *Tetranychus urticae*

ir. Simon Snoeck

Thesis submitted in fulfillment of the requirements for the degree of Doctor (PhD) in Applied Biological Sciences

Dutch translation of the title of this PhD:

Genetische en moleculaire mechanismen betrokken in pesticiden resistentie en waardplant acclimatisatie in de herbivoor en generalist *Tetranychus urticae.*

To refer to this thesis:

Snoeck S. (2019). Genetic and molecular mechanisms of pesticide resistance and host plant acclimation in the generalist herbivore *Tetranychus urticae*. PhD thesis. Ghent university, Ghent, Belgium.

ISBN-number: 9789463572422

The author and the promoters give the authorization to consult and to copy parts of this work for personal use only. Every other use is subject to copyright laws. Permission to reproduce any material contained in this work should be obtained from the author.

The promoters,

prof. dr. ir. Luc Tirry

The author,

ir. Simon Snoeck

prof. dr. ir. Thomas Van Leeuwen

dr. ir. Wannes Dermauw

Members of the examination committee:

prof. dr. ir. Luc Tirry

Laboratory of agrozoology
Department of plants and crops
Ghent University

prof. dr. ir. Thomas Van Leeuwen

Laboratory of agrozoology
Department of plants and crops
Ghent University

dr. ir. Wannes Dermauw

Laboratory of agrozoology
Department of plants and crops
Ghent University

prof. dr. Rene Feyereisen

Department of plant and environmental sciences
University of Copenhagen

prof. dr. ir. Tim De Meyer

Department of data analysis and mathematical modelling
Ghent University

prof. dr. ir. Patrick De Clercq

Laboratory of agrozoology
Department of plants and crops
Ghent University

prof. dr. ir. Bartel Vanholme

Department of plant biotechnology and bioinformatics
Ghent University

dr. Christoph T. Zimmer

Syngenta crop protection

Acknowledgements/Dankwoord

"There is nothing like looking, if you want to find something..."

Mijn zoektocht begon in het koffiekot, de rode draad doorheen mijn doctoraat. Alsook de locatie voor mijn sollicitatiegesprek (in korte broek, sorry TVL). Dank je wel Luc, Thomas en Wannes, voor het vertrouwen. Thomas, je passie werkte inspirerend, je kritisch oordeel hield me scherp. Bedankt voor de talloze koffies, advies en aangereikte kansen, de opleiding, de collaboraties, de conferenties en de opeengestapelde levenservaringen die hiermee gepaard gingen. Wannes, mijn wetenschappelijke peter, ware het niet dat jouw deur altijd openstond, ik had ze plat gelopen. Bedankt voor je begeleiding de afgelopen vier jaar, van de eerste kennismaking met een terminal tot het "proofreaden" van nonchalant gefabriceerde mendeley referenties. Dit schrift had serieus ingeboet aan kwaliteit zonder jou.

Leen, Rik (15u30 ~ koffie), Bjorn, Stephanie, Agnes en Didier, bedankt voor jullie hulp en advies, zowel op technisch, administratief en mentaal vlak.

Astrid, Wim, Wannes, Arash, Catherine (topmadam/kapster), Wenxin, Ibrahim, Peng, Nicky, Sabina, Berdien, Lore, Marilou, Christine, Xueping and Andre. No day past by without a laugh, it was a pleasure to share the "lab" with you all, talk (no) science, drink a beer, the conferences, … I will definitely miss the atmosphere of our mite group.

Dear office members (Wim, Freya, Maxim, Nicky, Hamshou, Nathaly, Mona and Katterine), thanks for all the talks, laughs, proofreading, figure optimizing… From now on, no smell of French cheeses anymore.

Throughout my PhD, I spent a few months at the University of Utah. Richard, thanks for the guidance, awakening my interests in bioinformatics and the fruitful collaboration. I also had the pleasure to meet, dine and work with Robert, Huyen, Andre and Olivia. Thanks for the memorable nights, thanksgivings and travels. Looking forward to another visit. Special thanks to Andre, my most joyful co-author, staying long in the office was never as pleasant; you playing lovely (loud) nineties music, while smashing your keyboard, and popping out your dvd-drive (again).

At the University of Amsterdam, I had the pleasure to work together with Nena and Ernesto. Nena, thanks for the collaboration, guidance and advice throughout the only three weeks of my PhD that I solely spent in the lab. Ernesto, you primed my interest for evolution. Elahe and Eba, your visits to Ghent University were a delight. I am glad that I had the opportunity to work together with

both of you. Rene, thanks for your contribution to the MR-VP project (which would not have existed without Sabrina), you definitely won the award for “the funniest comment on an article draft”.

Huis-, reis-, lunchgenoten, stammers, Stürm und Drank’ers en fietsvrienden, bedankt voor de momenten van verpozing.

Mijn oudjes (en zus), dank voor jullie steun, opofferingen, de gekregen kansen, zonder jullie had ik hier niet gestaan.

Liv.

“…You certainly usually find something, if you look, but it is not always quite the something you were after.”

Simon, June 2019

Table of Contents

General introduction

High-resolution QTL mapping reveals target-site resistance but also divergent responses to long-term selection by three METI-I acaracides in *Tetranychus urticae*

The effect of insecticide synergist treatment on genome-wide gene expression in a polyphagous pest

Transcriptomic plasticity in the arthropod generalist *Tetranychus urticae* upon long-term acclimation to different host plants

Substrate specificity and promiscuity of horizontally transferred UDP-glycosyltransferases in the generalist herbivore *Tetranychus urticae*

List of abbreviations

AA	amino acid
ABC	ATP-binding cassette
AChE	acetylcholinesterase
AD	allele depth
AF	allele frequency
Albino-JP	albino japan strain
ATP	adenosine triphosphate
AWD	average window distance
BAPC	branched amphiphilic peptide capsules
BSA	bulked segregant analysis
BWA	burrows wheeler aligner
BX	benzoxazinoid
Cas9	CRISPR associated protein 9
CCE	carboxyl/choline esterase
cDNA	complementary DNA
CDR	carbonyl reducing enzyme
CHS1	*T. urticae* chitin synthase
CON	control
CPR	cytochrome P450 reductase
CRISPR	clustered regularly interspaced short palindromic repeats
cRNA	complementary RNA
CsA	cyclosporin A
CYP	cytochroom P450
DBD	DNA-binding domain
DDT	dichloordifenyltrichloorethaan
DE	differential expression
DEF	S,S,S-tributyl phosphorotrithioate
DEG	differentially expressed gene
DEM	diethyl maleate
DIMBOA	2,4-dihydroxy-7-methoxy-1,4-benzoxazin-3-one
DMSO	dimethylsulfoxide
DNA	deoxyribonucleic acid
DOG	dioxygenases
dsRNA	double stranded RNA
E&R	evolve and resequence
EDTA	ethylenediaminetetraacetic acid
ER	endoplasmatisch reticulum
FAD	flavin adenine dinucleotide
FADH2	flavin adenine dinucleotide hydroquinone form
FC	fold change
FDR	false discovery rate
FMN	flavin mononucleotide
FORM	formulation
FWO	research foundation Flanders
GATK	genome analysis toolkit
GC	gas chromatography
GO	gene ontology
GSH	glutathione
GST	glutathione-S-transferase
GWAS	genome wide association studies
HGT	horizontal gene transfer
His tag	polyhistidine tag
HPLC-MS	high performance liquid chromatography mass spectrometry
HTSeq	high-throughput sequencing
IBP	iprobenfos
IGV	integrative genomics viewer
IPR domain	InterPro domain
IPTG	isopropyl ß-D-1-thiogalactopyranoside
IRAC	insecticide resistance action committee
IRM	insecticide resistance management
JP-R	Japan resistant strain
LB	lysogeny broth
LBD	ligand binding domain
LC50	lethal concentration for 50% subjects
L-ME EGE	luciferin-ME EGE
Lon-Inb	London inbred strain
LS-VL	laboratory susceptible strain Van Leeuwen
MAR-AB	marathonas abamectin resistant strain
MBOA	6-methoxy-benzoxazolin-2-one
METI-I	mitochondrial elector transport inhibitors of complex I
MFS	major facilitator superfamily
MQ	mean root square mapping quality
MQRankSum	mapping quality rank sum
mRNA	messenger RNA
MR-VP	METI-resistant strain Van Pottelberghe
NADH	nicotinamide adenine dinucleotide
NADPH	nicotrinamide adenine dinucleotide phosphate
NCBI	national center for biotechnology information
NHR96	nuclear hormone receptor 96
NMR	nuclear magnetic resonance
NR	nuclear receptor
OH group	hydroxyl group
OP	organophosphorus compound
ORCAE	online resource for community annotation of eukaryotes
ORF	open reading frame
P450	cytochrome P450 monooxygenase
PA2	parental strain 2
PBO	piperonyl butoxide
PC	principal component
PCA	principal component analysis
PCR	polymerase chain reaction
PI	proteinase inhibitor
PLAT	polycystin, lipoxygenase, alpha-toxin and triacylglycerol
PPO	polyphenol oxidase
PR	pathogenesis-related
PSST	NADH-ubiquinone oxidoreductase

QD	quality score normalized by allele depth
qPCR	quantitative realtime PCR
QTL	quantitative trait loci
ReMOT	receptor-mediated ovary transduction of cargo
RH	relative humidity
RISC	RNA-induced silencing complex
RLU	relative luminescence unit
RNA	ribonucleic acid
RNAi	RNA interference
RNA-seq	RNA sequencing
RNP	ribonucleoprotein
RP49	ribosomal protein
SC	solid compound
SDR	short chain dehydrogenase
SDS	sodium dodecyl sulfate
SDS-PAGE	SDS-polyacrylamide gel
SE	standard error
siRNA	short interfering RNA
SLC	solute carrier
SNP	single nucleotide polymorphism
SR-TK	spirodiclofen resistant Tina Kramer
SR-VP	spirodiclofen resistant Van Pottelberghe
TBPT	S,S,S-tributyl phosphorotrithioate
TE	transposable element
TLC	tin layer chromatography
TM	transmembrane domain
TPP	triphenyl phosphate
Tris-HCL	tris hydrochloride
Tu008R	cyflumetofen resistant strain
UDP	uridine diphosphate
UDP-galNAc	UDP-N-acetylglycosamine
UDP-GlcNAc	acetylgalactosamine
UGT	UDP-glycosyltransferase
US$	United States dollars
UV	ultraviolet
VCF	variant call format
VGSC	voltage-gated sodium channel

Chapter 1

General introduction

This chapter has been partially redrafted from:

Kurlovs*, A., Snoeck*, S., Kosterlitz, O., Van Leeuwen, T., Clark, R.M. (2019) Trait mapping in diverse arthropods by bulked segregant analysis. Current Opinion in Insect Science, 36.

1. Arthropod herbivory

1.1. The challenges of arthropod herbivory

Arthropods and plants have a distinct nutrient composition; plants are characterized by a relative high carbohydrate content while arthropods have a relatively high protein content (Mattson, 1980; Strong *et al.*, 1984). Consequently, the “protein/carbohydrate” ratio of a plant is a critical characteristic for host plant acceptance by a herbivore (Behmer, 2009). In addition to nutrient composition, plant defenses play a pivotal role in host plant acceptance. These defenses can either be chemical, physical (e.g., thorns and rough leaves) or a combination of the latter two (trichomes containing defensive compounds, reviewed by Huchelmann *et al.*, 2017). Plant defenses can also be subdivided based on how they affect the susceptibility of the plant, directly or indirectly. Examples of indirect defenses are: (1) the attraction of natural enemies (predators and parasitoids) of the herbivore with volatile compounds, the provision of food such as extrafloral nectar (Pemberton and Lee, 1996), or the provision of shelters (domatia) like cavities or tufts of hair (Sabelis and Dicke, 1988; Vinson, 1976; Walter, 1996), and (2) re-allocation of plant resources towards non-attacked tissues, to minimize the negative fitness consequences of tissue loss due to herbivore feeding (Howe and Jander, 2008; Kant *et al.*, 2015). In contrast, antifeedants have a direct negative effect on the herbivore itself by influencing growth and/or survival (e.g. inhibitors of digestion and toxins), and can be categorized as a direct defense (Howe and Jander, 2008).

Plant defenses can also be classified based on their timing of production. Preformed structural and chemical plant defenses are referred to as ‘constitutive defenses’ and offer immediate protection against many herbivores. However, defenses can be costly to produce and maintain, and therefore not all of them are active at all times (Kessler and Baldwin 2002). A second line of defense, the ‘induced defenses’, is only activated in response to herbivore attack via damage recognition and mediated by well characterized plant hormone systems (Dixon, 2001; Kant *et al.*, 2015; Kessler and Baldwin, 2002; Rioja *et al.*, 2017; Stahl *et al.*, 2018). Induced defenses can be composed of defense proteins and/or defense metabolites and repulse, poison or interfere with the assimilation of plant nutrients by the herbivore (Carlini and Grossi-De-Sá, 2002; Whittaker and Feeny, 1971). For example, upon herbivory of the two-spotted spider mite *Tetranychus urticae* on *Arabidopsis*, activation of indole glucosinolate production was observed (Zhurov *et al.*, 2014). Several types of defense proteins exist, including protease inhibitors (PIs), peptidases/proteases, amino acid degrading proteins, oxidases (e.g. polyphenol oxidases (PPOs)), plant defensive lectins, pathogenesis-related (PR) proteins and small cysteine-rich defense proteins. Next to defensive plant proteins, a staggering diversity of plant secondary metabolites evolved across the plant kingdom in the co-evolutionary arms-race between plants and herbivores (Rosenthal and Berenbaum, 1991; Wink, 2010). Despite their rich diversity, they can be classified based on their biosynthetic origin; the phenolics, the isoprenoids and the nitrogen-containing compounds.

1.2. Host plant range

In order to deal with the above-mentioned range of plant defenses, herbivores evolved specific adaptations. This lead to an evolutionary trend of specialization to specific host plants (Ali and Agrawal, 2012; Barrett and Heil, 2012; Kant *et al.*, 2015; Nosil, 2002). Monophagous arthropods solely feed on one or a few related plant species from a single genus, e.g. the spider mite *Tetranychus lintearius* can only feed on gorse species (*Ulex* sp.) (Hill and O'Donnell, 1991). Oligophagous arthropods are able to feed on a group of plants from the same family, such as *Tetranychus evansi*, a spider mite species that is able to infest different plant species of the family of the Solanaceae (de Moraes *et al.*, 1987; Migeon *et al.*, 2010). True polyphagous herbivores are rather scarce (but can be found in diverse arthropod orders, e.g. *Spodoptera exigua* (Lepidoptera), *Schistocerca gregaria* (Orthoptera) and *Bemisia tabaci* (Hemiptera)), and are able to feed on plants of more than one botanical family (Bernays and Graham, 1988; Krantz and Lindquist, 1979; Lindquist, 1998; Schoonhoven *et al.*, 2005; Strong *et al.*, 1984). An extreme example of a polyphagous herbivore is the two-spotted spider mite *T. urticae*, which feeds on over 1100 plants scattered over more than 140 distinct plant families (Jeppson *et al.*, 1975; Migeon *et al.*, 2010). However, this does not necessarily imply that this species consists of generalist individuals (Kant *et al.*, 2008). *T. urticae* has a high intraspecific genetic variability and local populations are known to form host races that do not always perform equally well on different potential host plants (Agrawal *et al.*, 2002; Díaz-Riquelme *et al.*, 2016; Gotoh *et al.*, 1993; Magalhães *et al.*, 2007; Navajas, 1998; Zhurov *et al.*, 2014).

1.3. Chemical control of arthropods and pesticide resistance

Although the first neonicotinoids were discovered in a random screening towards new pesticides, they act on the insect central nervous system as agonists of the post-synaptic nicotinic acetylcholine receptors, just like the chemically related plant defense compound nicotine found in tobacco (Feuer and Lawrence, 1969; Jeschke and Nauen, 2008). Pyrethroid pesticides are based on pyrethrins found in *Chrysanthemum cinerariaefolium* and *C. coccineum* (Elliott *et al.*, 1973). Even more, azadirachtin, a plant secondary metabolite present in the neem tree, is used directly as a botanical pesticide after extraction out of the seeds (Butterworth and Morgan, 1968).

However, whether inspired by nature or derived from chemical synthesis screening programs, arthropods are able to evolve resistance to all of them (Table 1) (Melander, 1914; Mota-Sanchez and Wise, 2019). As defined by Tabashnik *et al.*, 2014, resistance is a genetically based decrease in susceptibility to a pesticide. Field-evolved resistance is defined as a genetically based decrease in susceptibility of a population to a pesticide caused by exposure to the pesticide in the field. In contrast, laboratory-selected resistance results from exposure to a pesticide in the laboratory. Distinction between the latter two selection pressures is of importance because: (1) field-evolved resistance can have practical consequences for pest-control in the field if the efficacy of the pesticide decreases (practical resistance), whereas laboratory-selected resistance is confined to the lab, (2) the genetic basis, mechanism and magnitude of resistance are not necessarily the same in laboratory-selected and field- evolved resistance (Zhang *et al.*, 2012). Cross resistance occurs

when selection for resistance against one pesticide also leads to resistance against another different compound to which the pest population was not earlier exposed (e.g. for *T. urticae*: Khalighi *et al.*, 2014). The term multiple resistance is applied when one population develops distinct resistance mechanisms against pesticides with different mode of actions (MoAs) (e.g. *Myzus persicae* and *T. urticae*, Bass *et al.*, 2014 and Van Leeuwen and Dermauw, 2016, respectively).

Pesticide resistance threatens food supply worldwide (Pimentel and Peshin, 2014), especially since the development of new effective pesticides slowed down due to time consuming, laborious and expensive risk assessments (Sparks, 2013). Hence, it is of utmost importance to preserve the utility and efficacy of the currently available pesticides (Sparks and Nauen, 2015). To do this, the Insecticide Resistance Action Committee (IRAC) is essential (Sparks and Nauen, 2015). The aim of IRAC MoA working group is to describe the different pesticide MoAs and update the MoA classification. The latter information makes it possible to control agricultural pests and disease vectors by applying an optimal insecticide resistance management (IRM) strategy.

The evolutionary origins of pesticide resistance were recently reviewed by Hawkins *et al.*, 2019, and in most cases, insecticide resistance is known to evolve through a combination of standing genetic variation and *de novo* mutations in either target-site genes or genes encoding major metabolic resistance genes. The way resistance spreads through a population depends on multiple factors such as: (1) mode of inheritance, monogenic resistance is thought to be more difficult to control in the field in comparison to polygenic resistance since polygenic traits are easier to lose through mating with susceptible genotypes (Roush and McKenzie, 1987). (2) the degree of dominance, recessive resistance will spread slower than dominant resistance as heterozygote individuals are still killed by pesticide application. (3) mode of reproduction, in haplodiploid species (e.g. thrips, whiteflies and tetranychid mites), resistance might be fixed more rapidly in populations by fast selection on haploid males (Carrière, 2003; Crozier, 1985; Hartl, 1972). However, the strength of this effect depends on multiple factors, such as the potential

Table 1 - Ranking of top 10 pesticide-resistant arthropods (April 2019).

Species	Common name	Taxonomy	Number*
Tetranychus urticae	two-spotted spider mite	Acari	96
Plutella xylostella	diamondback moth	Lepidoptera	95
Myzus persicae	green peach aphid	Hemiptera	80
Musca domestica	house fly	Diptera	64
Bemisia tabaci	sweet potato whitefly	Hemiptera	64
Leptinotarsa decemlineata	colorado potato beetle	Coleoptera	56
Rhipicephalus microplus	southern cattle tick	Ixodida	50
Aphis gossypii	cotton aphid	Hemiptera	50
Panonychus ulmi	european red mite	Acari	48
Helicoverpa armigera	cotton bollworm	Lepidoptera	48

* *number of active ingredients to which the arthropod pest has exhibited documented resistance* (Mota-Sanchez and Wise, 2019)

Figure 1 - the two-spotted spider mite *T. urticae.* © Jan van Arkel

fitness difference between R males and RR females (gene dosage) (Carrière, 2003; Feyereisen *et al.*, 2015). (4) reproductivity, short life cycles and a high fecundity require frequent pesticide applications, which rapidly leads to the development of resistance (Van Leeuwen *et al.*, 2010). (5) origin of resistance alleles, the probability of loss or fixation of a resistance allele depends on the initial frequency and the selection coefficient. Hence, mechanisms conferring only partial resistance, or carrying significant fitness penalties, resulting in a lower selection coefficient, are more likely to emerge from standing variation since higher frequencies of the variant are present in the population (Hawkins *et al.*, 2019).

1.4. Spider mites

The phylum Arthropoda consists of the subphyla Chelicerata (e.g. mites, scorpions and spiders), Myriapoda (e.g. centipedes and millipedes) and Pancrustacea (Crustaceae (e.g. shrimps, crabs and water fleas) and Hexapoda (e.g. insects and springtails)). Mites and ticks belong to the Acari subclass within the chelicerate class of the Arachnida. Compared to other chelicerates, mites are relatively small, have a great diversity in life styles and a unique body plan. Their body consists of one single segment which is artificially divided into the idiosoma and the gnathosoma. The latter contains the mouth parts (e.g. chelicerae and pedipalps) and two pairs of eyes, the idiosoma contains all other body parts. Mites have adapted to various ecological niches and diversified their chelicerae to feed on plants, bacteria, animals and fungi (Walter and Proctor, 2013). Phytophagous mites are mainly found in the order of the Trombidiformes (subclass Acari). More precisely, in the phytophagous clades of the Eriophyoidea, Tetranychoidea and Tarsonemida (Tarsonemoidea) but also in Eupodoidea, Parasitengona, Raphignathoidea and the Tydeoidea (Krantz and Lindquist, 1979; Lindquist, 1998; Wybouw, 2015). All phytophagous mites have chelicerae that form a hollow tube which is commonly called a stylet (Evans, 1992; Jeppson *et al.*, 1975). Within the superfamily of the Tetranychoidea, approximately 1250 species are member of the Tetranychidae family, commonly called spider mites (Migeon *et al.*, 2010). This name refers to their ability to produce silk-like webbing which offers a colonial micro-habitat, protection against biotic and abiotic agents, dispersal, and intraspecific communication (Clotuche *et al.*, 2013, 2012; Helle and Sabelis, 1985). Spider mites feed on spongy plant parenchyma cells and use a lacerate-and-flush mechanism to empty an individual cell (Alba *et al.*, 2015; Jeppson *et al.*, 1975), and avoid penetrating epidermal

cells by inserting their stylet in between epidermal cells or through the stomatal opening (Bensoussan *et al.*, 2016). Spider mite feeding results in foliar chlorotic spots and eventually leads to necrosis and abscission (Helle and Sabelis, 1985; Jeppson *et al.*, 1975; Park and Lee, 2002).

Spider mites are haplodiploid and reproduce through arrhenotokous parthenogenesis. Virgin females only produce haploid males while fertilized females produce both diploid females as well as haploid male offspring (*T. urticae* sex ratio female:male 3:1 (Krainacker and Carey, 1990)). After egg hatching, spider mites develop through four active-feeding stages: six-legged larvae, protonymph, deutonymph and adult. Before each of the last three stages, an immobilized chrysalid phase occurs, called protochrysalis, deutochrysalis and teleochrysalis, respectively (Helle and Sabelis, 1985). Male adult spider mites are easily recognizable since they are typically smaller, leaner, and tapered towards the posterior end. Moreover, they show a so-called guarding behavior, they usually eclose earlier than females and subsequently remain close to teleiochrysalid females. Copulation occurs immediately after female eclosion (Mitchell, 1973; Potter *et al.*, 2015). Spider mite pests of economic importance have typically a high fecundity and a very short life cycle of less than two weeks. For example, fertilized *Tetranychus urticae* females can produce over 50 female offspring and have a life cycle of 8-12d (Jeppson *et al.*, 1975), resulting in an exponential population growth and host plant overexploitation (Alba *et al.*, 2015; Clotuche *et al.*, 2011; Sarmento *et al.*, 2011). Both parameters can vary strongly depending on external (temperature, humidity, light and predation level) and inherent factors like genetic diversity, density of the population and fertilization. Considering oligo- and polyphagous mites, reproductive characteristics are also affected by the host plant species or varieties on which they feed (Gotoh *et al.*, 1993; Jeppson *et al.*, 1975; Taj *et al.*, 2016). To survive unfavorable conditions, spider mites go into diapause in the egg or the adult female stage, depending on the species (Veerman, 1985). In temperate regions for example, adult *T. urticae* females go into a hibernal facultative reproductive diapause (Bryon *et al.*, 2013). The two-spotted spider mite *T. urticae* is the most well-known member of the Tetranychidae. This extremely polyphagous herbivore is an important agricultural pests and causes major agricultural and horticultural losses (Jeppson *et al.*, 1975; Van Leeuwen and Dermauw, 2016). Although biological control with arthropod predators is used to combat phytophagous mite infestations, mites are still primarily controlled by acaricides, with an estimated acaricide treatment cost of 1.1 billion US$ in 2013 (Van Leeuwen and Dermauw, 2016).

2. Xenobiotic metabolism

Arthropod herbivores have developed multiple strategies to deal with pesticides and plant secondary metabolites. These are traditionally classified into (1) toxicodynamic mechanisms that decrease target-site sensitivity and (2) toxicokinetic mechanisms that decrease exposure (Feyereisen *et al.*, 2015; Li *et al.*, 2007; Van Leeuwen and Dermauw, 2016). Both toxicodynamic and toxicokinetic mechanisms are driven by three types of genetic changes (Feyereisen, 2015)

Table 2 - Resistance related target-site mutations in T. urticae

target site	numbering	substitutions	acaricide (+ IRAC mode of action group)	Ref.
PSST homologue of complex I	*Yarrowia lipolytica*	H92R	fenpyroximate (21a), pyridaben (21a), tebufenpyrad (21a)	1
chitin synthase 1 (*CHS1*)	*T. urticae*	I1017F	etoxazole (10b), clofentezine (10a), hexythiazox (10a)	2
glutamate-gated chloride channels subunits	*T. urticae*	G314D (GluCl1), G326E (GluCl3)	abamectin (6)	3
mitochondrial cytochrome b	*T. urticae*	G126S, I136T, S141F, D161G, P262T	bifenazate (20d), acequinocyl (20b)	4
voltage-gated sodium channel (*VGSC*)	*Musca domestica*	L1024V, A1215D, F1538I	fenpropathrin (3a)	5,6
		F1538I, A1215D, F1534S, M918L	bifenthrin (3a)	7,8
acetylcholinesterase (*AChE*)	*Torpedo californica*	G119S, A201S, A208T, T280A/S, G328A	organophosphates (1b), carbamates (1a)	9,10,11
		D128E, F331W/C/Y	organophosphates (1b)	9,10,11

1 (Bajda *et al.*, 2017)
2 (Demaeght *et al.*, 2014; Van Leeuwen *et al.*, 2012)
3 (Dermauw *et al.*, 2012; Kwon *et al.*, 2010e)
4 (Van Leeuwen *et al.*, 2008; Van Nieuwenhuyse *et al.*, 2012)
5 (Kwon *et al.*, 2010a)
6 (Wang *et al.*, 2015)
7 (Tsagkarakou *et al.*, 2009)
8 (Wu *et al.*, 2019)
9 (Anazawa *et al.*, 2003)
10 (Kwon *et al.*, 2010c)
11 (Khajehali *et al.*, 2010)

(1) mutations that affect the coding sequences of the target gene or detoxification genes, (2) mutations that alter expression levels of target/detoxification genes by affecting *cis* or *trans* regulation, or (3) whole target/detoxification gene duplications or deletions. Combinations of these genetic mechanisms are also possible, as shown in organophosphate resistant *T. urticae* populations. Point mutations in acetylcholinesterase (AChE) decreased the enzyme's metabolic efficiency, leading to AChE gene duplication as a compensation mechanism (Kwon *et al.*, 2010b). Of particular note, next to the toxicodynamic and toxicokinetic mechanism, a third category is often added to the traditional classification, behavioral adaptation (Feyereisen *et al.*, 2015; Sparks *et al.*, 1989).

2.1. Toxicodynamic mechanisms

Alterations of the target-site of the toxic compound are a toxicodynamic mechanism and are rarely documented in the context of host plant adaptation (Dobler *et al.*, 2012). This is probably related to the multiple and unspecific mode of actions of plant secondary metabolites (Dermauw *et al.*, 2018; Després *et al.*, 2007). In contrast, target-site mutations underlying pesticide resistance in arthropods have been frequently documented, including spider mites (for a review, see Feyereisen *et al.*, 2015 and Van Leeuwen and Dermauw, 2016). An overview of *T. urticae* target-site resistance mutations can be found in Table 2.

2.2. Toxicokinetic mechanisms

Decreased penetration, sequestration, increased metabolism and excretion are considered as toxicokinetic mechanisms (Feyereisen *et al.*, 2015). Exposure to pesticides can be decreased through modifications in the cuticle that slow down the penetration, as was recently reviewed in Balabanidou *et al.*, 2018. So far, two mechanisms have been described, cuticle thickening and altering of cuticle composition. Likewise, in the context of host plant adaptation, physiological adaptations were described that prevent xenobiotics to reach its target tissue. A key example is the pH adjustment in the digestive tract of *Zygaena filipendulae*, which limits the bioactivation of cyanogenic glucosides by plant β-glucosidases (Pentzold *et al.*, 2014). Some herbivores are even able to use plant secondary (defense) metabolites as oviposition and feeding stimulants. This specialization may further extend to sequestration; the selective uptake, transport, modification, storage and deployment of plant secondary chemicals for the herbivores own defense (reviewed in Heckel, 2014). Sequestration can also contribute to pesticide resistance by sequestering synthetic toxins away from their target-sites and into the fat body or hemolymph (Devonshire and Moores, 1982). In the following paragraphs, metabolic detoxification, i.e. metabolism and excretion of toxins will be further discussed, as well as the major detoxification enzyme families involved in this toxicokinetic mechanism.

2.2.1. Metabolic detoxification

Metabolic detoxification can be categorized into three phases based on the phenotype of underlying genetic changes, and is in the majority of cases mediated by enzymes and transporters belonging to ubiquitous multi-gene families (Després *et al.*, 2007; Erb and Robert, 2016; Feyereisen *et al.*, 2015; Heckel, 2014; Heidel-Fischer and Vogel, 2015). In phase I, the toxic compound is functionalized with nucleophilic groups to make it more reactive and water soluble, typical phase I detoxification enzymes are cytochrome P450 monooxygenases (P450s) and carboxyl/ choline esterases (CCEs). In phase II, the polarity of the metabolite is increased by conjugation of for

Table 3 - Functionally expressed *T. urticae* enzymes that have been linked to pesticide resistance (either inhibition assay with a model substrate or by direct metabolism of the pesticide)

enzyme family	enzyme name	toxin (mode of action classification)	reference
P450	CYP392E10	spirodiclofen (23)	Demaeght *et al.*, 2013
	CYP392A16	abamectin (6)	Riga *et al.*, 2014
	CYP392A11	cyenopyrafen, fenpyroximate (21a)	Riga *et al.*, 2015
CCE	TCE2* (TcCCE14)	fenpropathrin (3a), cyflumetofen (25a)	Shi *et al.*, 2016
	CarE6*	fenpropathrin (3a)	(Wei *et al.*, 2019b)
	TcCCE12*	cyflumetofen (25a)	(Wei *et al.*, 2019a)
GST	TuGSTd14	abamectin (6)	Pavlidi *et al.*, 2015
	TuGSTd05	cyflumetofen (25a)	Pavlidi *et al.*, 2017
	TcGSTm02*	cyflumetofen (25a)	Feng *et al.*, 2019
UGT	UGT201D3*	abamectin (6)	Wang *et al.*, 2018

**Tetranychus cinnabarinus*, considered as a synonymous species of *T. urticae* (Auger *et al.*, 2013)

example glutathione (by glutathione-S-transferases (GSTs)) or a glucose group (by UDP-glycosyltransferases (UGTs)) to increase the water solubility. In phase III, metabolites are excreted out of the cell or into specialized cell compartments by transporters such as ATP-binding cassette (ABC) transporters or solute carrier (SLC) family proteins (Brattsten, 1988; Dermauw and Van Leeuwen, 2014; Després *et al.*, 2007; Heckel, 2014; Kant *et al.*, 2015). Multiple members of the latter enzyme families involved in metabolic detoxification in *T. urticae* were functionally expressed and linked to pesticide resistance (Table 3).

2.2.2. The major detoxification enzyme families

Cytochrome P450 monooxygenases (P450s) or *CYP* genes are one of the largest gene families and have representatives in virtually all living organisms (Feyereisen, 2012). They play an important role in the metabolism of both endogenous compounds (e.g. steroid hormones and lipids) and xenobiotics (e.g. plant secondary metabolites and pesticides) (Feyereisen, 2012). P450s contain a heme cofactor and can act as isomerases, reductases, or oxidases depending on the substrate structure (Ahmad, 1986; Feyereisen, 1999) but are best known for their monooxygenase activity, the catalyzation of the transfer of one oxygen atom of an O_2 molecule to the substrate, while reducing the other oxygen atom to water (Feyereisen, 1999). NADPH cytochrome P450 reductase (CPR) is an obligatory partner of microsomal P450s and serves as an electron donor protein throughout the enzymatic reaction (Murataliev *et al.*, 2004).

Insect P450s are classified into four major clades: CYP2, CYP3, CYP4 and the mitochondrial CYP genes (except for the Palaeoptera, also CYP20 (Ioannidis *et al.*, 2017)). Two mitochondrial groups can be distinguished with different biological roles, involvement in the ecdysteroid metabolism and metabolism of xenobiotic compounds (Feyereisen, 2012). Additionally, insect CYP3 and CYP4 clans, which contain insect-specific families, have been linked to the detoxification of xenobiotics and phytotoxins (Feyereisen, 2012).

Several CYP2 genes are known to be involved in essential physiological functions. The number of CYP2 genes is more diverse in *Daphnia* and Acari than in insects, and a species-specific expansion of intronless CYP2s was found in *T. urticae* (Feyereisen, 2012; Grbić *et al.*, 2011). Several of them were shown to be upregulated after long-term hostplant transfer or in acaricide resistant strains (Demaeght *et al.*, 2013; Dermauw *et al.*, 2013b; Grbić *et al.*, 2011; Khalighi *et al.*, 2015; Wybouw *et al.*, 2015). Furthermore, three of them were functionally expressed; CYP392A11 was able to metabolize both cyenopyrafen (IRAC MoA 25a) and fenpyroximate (IRAC MoA 21a) (Riga *et al.*, 2015), CYP392A16 was shown to metabolize abamectin (IRAC MoA 6) (Riga *et al.*, 2014), while CYP392E10 can metabolize spirodiclofen (IRAC MoA 23) (Demaeght *et al.*, 2013).

The carboxyl/choline esterases (CCEs) are another important phase I detoxification enzyme family, CCEs detoxify xenobiotics by hydrolyzing covalent bonds. Additionally, CCEs can sequester toxins, preventing them to reach their target site (Devonshire and Moores, 1982; Devorshak and Roe, 1998). Just like P450s, CCEs are studied in depth as an important component of insects' xenobiotic defense system. Insect CCEs were grouped into 13 clades based on a phylogenetically-based classification, and the clades were spread over three different biological

function classes: (1) assimilation and detoxification of the diet, (2) generally secreted enzymes, and (3) hormone/semiochemical processing (Claudianos *et al.*, 2006; Oakeshott *et al.*, 2005). The total number of CCEs in *T. urticae* is comparable to other arthropods. However, no homologues were found for the insect dietary CCE class, and the neurodevelopmental class was shown to be expanded with two new clades (Grbić *et al.*, 2011). A neurodevelopmental CCE, AChE, is well-known as the target for organophosphate (OP) and carbamate pesticide compounds (Oakeshott *et al.*, 2005). Multiple target-site mutations as well as a duplication of AChE have been reported in OP resistant *T. urticae* populations (Anazawa *et al.*, 2003; Khajehali *et al.*, 2010; Kwon *et al.*, 2010c, 2010b). Additionally, a role for *Tetranychus* CCE enzymes in metabolic detoxification or sequestration of pesticides was suggested by several studies (Demaeght, 2015; Feng *et al.*, 2011). In *T. cinnabarinus*, a synonymous species of *T. urticae* (Auger *et al.*, 2013), high-performance liquid chromatography (HPLC) and gas chromatography (GC) were used to detect the *in vitro* metabolism of fenpropathrin and/or cyflumetofen by three recombinant CCEs too (Shi *et al.*, 2016a; Wei *et al.*, 2019a, 2019b).

Glutathione-S-transferases (GSTs) are a major phase II detoxification gene family related to pesticide resistance (recently reviewed in Pavlidi *et al.*, 2018). GSTs are best known for the glutathione (GSH) conjugation reaction, where they catalyze conjugation of GSH to a highly reactive nucleophile site of the xenobiotic, resulting in a less toxic and more soluble conjugate (Habig *et al.*, 1974; Mannervik, 1985). Other well-known mechanisms are: (1) the enzymatic catalyzation of the dehydrochlorination reaction (e.g. dichlorodiphenyltrichloroethane (DDT) to non-toxic DDE, using GS^- as a co-factor (Clark and Shamaan, 1984)), (2) GSTs displaying peroxidase activity, reducing the levels of toxic peroxides caused by pesticide related oxidative stress (Mannervik and Danielson, 1988; Vontas *et al.*, 2001), and (3) GSTs passively binding and sequestering the pesticide (Kostaropoulos *et al.*, 2001).

Thirty-one GSTs were identified in the *T. urticae* genome and were classified into the following four GST families: delta, mu, omega, and zeta (Grbić *et al.*, 2011). The delta family was shown to be expanded in *T. urticae*, while the mu-family was previously believed to be vertebrate specific. The GST mu family, however, has been found in many Acari genomes (Bajda *et al.*, 2015; Bartley *et al.*, 2015; Grbić *et al.*, 2011; Niranjan Reddy *et al.*, 2011). Biochemical assays and transcriptomic analysis revealed the putative importance of *T. urticae* GSTs in metabolic detoxification and prioritized candidates for further research (Dermauw *et al.*, 2013b; Ghadamyari and Sendi, 2008; Khalighi *et al.*, 2015; Stumpf and Nauen, 2002; Yang *et al.*, 2009). Subsequently, Pavlidi *et al.*, 2015 functionally expressed two delta- and one mu class GST, of which TuGSTd14 showed high affinity towards abamectin in an indirect competition assay with model substrates. Most recently, TuGSTd05 was functionally expressed and kinetically characterized. Cyflumetofen and its more toxic de-esterified metabolite were identified as potential substrates after transcriptomic analysis, molecular docking and *in vitro* inhibition assays. Subsequently, a very strong affinity was found of TuGSTd05 for the de-esterified metabolite, and the resulting metabolite was identified with HPLC/MS analysis, as well as the possible site of attack (Pavlidi *et al.*, 2017).

Uridine diphosphate (UDP)-glycosyltransferases (UGTs) catalyze the addition of UDP-sugars to small hydrophobic molecules, and are just like GSTs, well-known as phase II detoxification enzymes (Jancova *et al.*, 2010). By catalyzing the conjugation, more hydrophilic compounds are generated, enhancing excretion (Mackenzie *et al.*, 1997). However, in contrast to human UGTs, arthropod UGTs have been marginally studied. Only recently, biochemical and functional studies specifically linked arthropod UGTs to detoxification and sequestration of both plant allelochemicals and insecticides (Highfill *et al.*, 2017; Krempl *et al.*, 2016; Li *et al.*, 2017). UGTs seem to have been lost early in chelicerate evolution history, but Ahn *et al.*, 2014 revealed that spider mites regained UGTs after a horizontal gene transfer from bacteria. Moreover, they are specifically expanded in *T. urticae*, and strong transcriptomic responses were found after host plant switching, host adaptation and acaricide resistance (Ahn *et al.*, 2014; Zhurov *et al.*, 2014). Most recently, it was shown that 1-naphthol (model substrate) glycosylation by UGT201D3 was inhibited by abamectin in *T. cinnabarinus*, but glycosylated abamectin was not detected (M. Y. Wang *et al.*, 2018). Hence, *T. urticae* UGTs await further research to confirm their role in host plant adaptation and/or acaricide resistance.

In addition to the above-mentioned detoxification enzymes, membrane transporters also play a prominent role in xenobiotic detoxification. The genome of *T. urticae* harbors multiple lineage-specific ATP-binding cassette (ABC) transporter expansions and 103 ABC genes in total, the highest number discovered in any metazoan species so far (Dermauw *et al.*, 2013a). ABC transporters have been extensively characterized for their involvement in drug resistance in vertebrates and bacteria, but less is known about their role in arthropod xenobiotic resistance (reviewed in Dermauw and Van Leeuwen, 2014). Some ABC genes were differentially expressed in *T. urticae* after adaptation to a new host plant or in acaricide resistant strains (Dermauw *et al.*, 2013b). However, members of the major facilitator family (MFS), a.k.a. uniporter-symporter-antiporter family (Reddy *et al.*, 2012), have shown rapid and more profound transcriptional changes upon exposure to xenobiotics, suggesting a potential role in the efflux of xenobiotics (Dermauw *et al.*, 2013b; Van Leeuwen and Dermauw, 2016). But the role of MFS transporters in transport of toxic substances is mainly described for bacteria and fungi (Kretschmer *et al.*, 2009; Saidijam *et al.*, 2006). Hence, further research is needed to validate the role of arthropod MFS transporters in metabolic detoxification.

2.3. Behavioral adaptations

Behavioral adaptations that circumvent plant defenses are quite diverse (vein cutting, trenching, girdling, leaf clipping, and application of fluids from exocrine glands) and were reviewed by Dussourd, 2016. Behavior as a mechanism of insecticide resistance was recently reviewed by Zalucki and Furlong, 2017. They state that behavioral resistance should be defined in a manner consistent to toxicodynamic and toxicokinetic mechanisms, and be based on heritable changes. A rare example of this definition was found in resistant populations of the German cockroach, *Blatella germanica*, which were shown to avoid feeding on ‘sugar baits’ laced with a toxicant (Wang *et al.*,

2004). This behavior was later linked to a change in the glucose receptor, which explained the avoidance of glucose (Wada-Katsumata *et al.*, 2013).

3. Acari genomics, transcriptomics and QTL mapping

3.1. *T. urticae* as a model organism

T. urticae was chosen as a chelicerate model organism for multiple reasons (Grbic *et al.*, 2007): (1) its status as a polyphagous, worldwide pest and an acaricide resistance champion, (2) a

Table 4 - Nuclear Acari genomes deposited in the NCBI database (3 May 2019). Third generation long read sequenced genomes are indicated with an asterisk (*). Genomes are sorted based on their time of publication. If multiple genomes were available for a species, only the best assembly was included in this overview.

species	relevance	reference	contig N50 (Kb)	genome size (Mb)
Tetranychus urticae	polyphagous herbivore	Grbić *et al.*, 2011	212.780	90.829
Sarcoptes scabiei	parasite, itch mite (scabies)	Rider *et al.*, 2015	11.197	56.2624
Ixodes ricinus	vector of human and animal pathogens	Cramaro *et al.*, 2015	3.059	514.507
Metaseiulus occidentalis	predatory mite (biological control)	Hoy *et al.*, 2016	200.706	151.724
Achipteria coleoptrata	oribatid mite	Bast *et al.*, 2016	3.360	88.444
Hypochthonius rufulus	oribatid mite	Bast *et al.*, 2016	3.126	172.365
Platynothrus peltifer	oribatid mite	Bast *et al.*, 2016	1.236	100.533
Steganacarus magnus	oribatid mite	Bast *et al.*, 2016	1.617	113.565
Euroglyphus maynei	house dust mite (allergy)	Morgan *et al.*, 2017	786	43.438
Tropilaelaps mercedesae	honey bee parasite	Dong *et al.*, 2017	12.742	352.535
Dermatophagoides pteronyssinus	european house dust mite (allergy)	Waldron *et al.*, 2017	67.954	70.778
*Rhipicephalus microplus**	parasite of livestock	Barrero *et al.*, 2017	15.568	2008.370
*Dermatophagoides farinae**	american house dust mite (allergy)	PRJNA379991 2017	188.869	91.935
*Dermanyssus gallinae**	parasite of poultry, red mite	Burgess *et al.*, 2018	278.630	959.010
Dinothrombium tinctorium	potential biological control agent	Dong *et al.*, 2018	16.055	180.399
Leptotrombidium deliense	parasite of vertebrates, can cause bacterial infection (scrub typhus)	Dong *et al.*, 2018	2.903	117.319
*Ixodes scapularis**	vector of human and animal pathogens	Miller *et al.*, 2018	517.316	3088.620
Brevipalpus yothersi	herbivore and plant virus vector	Navia *et al.*, 2019	56.226	71.163
*Psoroptes ovis**	parasite of sheep (scoroptic mange)	Burgess *et al.*, 2019	2,279.290	63.214
Varroa jacobsoni	honey bee parasite	Techer *et al.*, 2019	96.009	365.586
*Varroa destructor**	honey bee parasite	Techer *et al.*, 2019	201.866	368.942

predicted small genome size on three equally-sized holocentric chromosomes, (3) short generation time, huge progeny and easy maintenance in the lab, (4) haplodiploid sex determination system that has potential for genetic analysis (e.g. mother-son inbreeding), and (5) small transparent eggs which allow observation of embryo development under the microscope. Hence, the *T. urticae* genome (London strain) was sequenced (sanger sequencing) at about 8-fold coverage, assembled into 640 scaffolds covering 89.6 megabases (Mb) and annotated (Grbić *et al.*, 2011). Roughly 95% of the genome is represented by only 44 scaffolds (Grbic 2011), making it a high-quality genome assembly. More recently, the latter 44 scaffolds were assembled into three chromosomes, facilitating genetic studies such as QTL mapping by bulked segregant analysis (BSA) for polygenic traits (Wybouw *et al.*, 2019).

In recent years, next-generation sequencing methods became more affordable, resulting in the release/announcement of additional Acari genomes, mainly with an agricultural, veterinary or medical impact. However, the quality of assemblies built from short reads varied from good to relatively poor quality (high quality gene annotation requires assemblies with an N50 of more than 250-350Kb (Richards and Murali, 2015), see table 4). The advent of third generation long read sequencing methods now provides an opportunity for the generation of high quality genome assemblies (Saha, 2019). This is supported by the genome statistics of the long-read sequenced Acari (Stewart T. G. Burgess *et al.*, 2018; Stewart T.G. Burgess *et al.*, 2018; Miller *et al.*, 2018; Techer *et al.*, 2019), with the exception of the genomes of *Rhipicephalus microplus* due to insufficient genome coverage (7.0x) (Barrero *et al.*, 2017). Next to increasing the N50, long reads can help with assembly problems caused by the prevalence of complex gene families like olfactory receptors and P450s, DNA polymorphisms and transposable elements (Maumus *et al.*, 2015; Richards *et al.*, 2010; Richards and Murali, 2015).

3.2. Annotation of the *T. urticae* genome

The completion of the *T. urticae* genome, the first chelicerate genome, expanded the arthropod genetic toolkit and provided an important out-group for comparative arthropod genomics. Additionally, it facilitates the study of pesticide resistance and host plant interaction among other characteristics. Annotation of the *T. urticae* genome revealed lineage-specific expansions of gene families known to be implicated in digestion, detoxification and transport of xenobiotics: cysteine peptidases, P450s, CCEs, GSTs, ABC transporters and chemosensory receptors (section 2.2.2, (Grbić *et al.*, 2011; Ngoc *et al.*, 2016)). Additionally, numerous clues were discovered for horizontal gene transfers (HGT). HGT is defined as the biological process whereby genetic material is asexually transferred across species boundaries (Li and Graur, 1991). Recently, the *T. urticae* genome was thoroughly mined for HGT genes (for a complete overview, see (Wybouw *et al.*, 2018)). The authors suggested that HGT made a significant and underestimated impact on the metabolic repertoire of herbivorous spider mites. In *T. urticae*, HGT genes were linked to xenobiotic adaptation, pigmentation, diapause, predicted biochemical functions in carbohydrate, lipid and folate metabolism, and vitamin B5 production (Wybouw *et al.*, 2018).

The strongest example for a role of HGT in xenobiotic adaptation was delivered by Wybouw *et al.*, 2014. They identified a horizontally transferred enzyme from bacteria, beta-cyanoalanine synthase, and showed that it was involved in the detoxification of hydrogen cyanide released by cyanogenic plants upon tissue disruption. Additionally, the *T. urticae* genome harbors 80 UGTs and 17 intradiol ring-cleavage dioxygenases (DOGs) that were acquired through HGT (Ahn *et al.*, 2014; Grbić *et al.*, 2011). Although both gene families (UGTs and DOGs) await further functional characterization, current transcriptomic data suggests that they are involved in metabolic detoxification of plant defense compounds and acaricides (Ahn *et al.*, 2014; Dermauw *et al.*, 2013b; Grbić *et al.*, 2011; Zhurov *et al.*, 2014). DOGs might even be able to split aromatic ring structures of xenobiotics (Dermauw *et al.*, 2013b). This hypothesis was strengthened after a recombinant *T. urticae* DOG was shown to cleave the aromatic ring of the model substrate catechol (Schlachter *et al.*, 2019). Additionally, Bryon *et al.*, 2017a found that the acquisition of HGT carotenoid biosynthetic genes from fungi eliminated the spider mites need of dietary carotenoids. Moreover, they showed that a carotenoid biosynthetic gene was essential for normal pigmentation and diapause induction.

3.3. Whole genome expression profiling: microarrays and RNAseq

Whole genome expression profiling can help to identify a set of candidate genes involved in pesticide resistance or host plant adaptation. It's a snapshot of the expressed transcripts in a cell/organism at a given time point. Various technologies have been developed to deduce and quantify messenger RNA (mRNA), and they can be divided in two categories: hybridization- and sequence-based approaches. Both of them were used throughout this PhD thesis.

The hybridization-based approach typically involves the preparation of fluorescent (or biotin) labelled cRNA or directly labelled RNA with fluorescent tags, and incubation with a microarray that contains gene-specific designed probes (short nucleotide oligomers). Hence, hybridization between the probes and the labelled cRNA/RNA occurs (and if biotin-labelled cRNA was used, post staining with fluorescently labeled streptavidin), followed by the measurement of fluorescence intensity, which is then related to the transcript abundance (Bumgarner, 2013). A *T. urticae* microarray platform was designed using the Agilent eArray platform by (Dermauw *et al.*, 2013b)s, and covered 87.7% of the genes with at least 3 probes. The availability of this array facilitated the study of gene expression patterns in *T. urticae* (Demaeght *et al.*, 2013; Dermauw *et al.*, 2013b; Khalighi *et al.*, 2015; Wybouw *et al.*, 2015, 2014).

RNA-seq is a sequence-based approach, and replaced from 2015 onwards microarrays as the dominant transcriptomic approach (Lowe *et al.*, 2017). It uses deep-sequencing technologies and allows the entire transcriptome to be surveyed in a qualitative high-throughput manner. It requires the preparation of a fragmented cDNA library, after which each molecule is sequenced to obtain short sequences from one end (single-end sequencing) or both ends (pair-end sequencing). The resulting sequence reads are aligned with the reference genome or *de novo* transcriptome assembly to eventually generate read counts and create an expression profile for each gene (Lowe *et al.*, 2017; Wang *et al.*, 2009). In the last years, RNA-seq also became the preferred approach for

T. urticae transcriptomic studies (e.g. (Díaz-Riquelme *et al.*, 2016; Grbić *et al.*, 2011; Mo *et al.*, 2017; Zhao *et al.*, 2017; Zhou *et al.*, 2019)).

RNA-seq has several advantages: (1) Unlike hybridization-based approaches, it is not limited to the detection of transcripts corresponding to existing genome sequence/assembly/annotation, and the quality of the latter three. (2) It requires less RNA as input (nanograms instead of micrograms), which allows finer examination of cellular structures and even single-cell level analysis (Hashimshony *et al.*, 2012), (3) RNA-seq does not have an upper limit for quantification resulting in a large dynamic detection range of expression, in contrast to DNA microarrays, which lack sensitivity for low or very high expressed genes (Wang *et al.*, 2009), (4) Microarrays can have high background due to cross-hybridization (Okoniewski and Miller, 2006), and (5) RNA-seq can be used to detect sequence variations and different isoforms.

3.4. Trait mapping in arthropods

Elucidating the genetic architecture of resistance in arthropods, as well as the immense variation in other phenotypes, has been challenging. For instance, it was only in 2002 that a variant at a cytochrome P450 gene was implicated in *Drosophila melanogaster* as conferring resistance to the infamous pesticide DDT (Daborn *et al.*, 2002), which had been in use since the early 1940s. This and more recent accomplishments using advanced genetic designs, including genome-wide association mapping (GWAS), have been made possible in this species by the extensive genetic and genomic resources developed over decades by the Drosophila community (Groen and Whiteman, 2016; Hales *et al.*, 2015). Apart from *D. melanogaster* or its congeners, however, such genetic resources are virtually non-existent in arthropods, and uncovering the molecular-genetic underpinnings of phenotypic variation can be daunting, even for monogenic traits. While traditional linkage mapping studies have identified loci for trait variation in a number of insect species (e.g., (Linnen *et al.*, 2018; Smith *et al.*, 2015; Zhan *et al.*, 2009)), they require intensive genotyping of single individuals in segregating populations. Notwithstanding technical advances, genotyping hundreds of individuals remains time-consuming, tedious, and costly. In practice, this limits sample size, and hence power (the ability to detect a genotype-to-phenotype association) and mapping resolution (the size of a genomic region to which a causal variant is localized). Moreover, phenotyping single individuals can be noisy, or simply not feasible for many traits (Van Leeuwen *et al.*, 2012). For instance, the minute size of many arthropods, including micro-insects or mite herbivores or parasites that can be only a few hundred µm in length (Bailey and Keifer, 1943; Polilov, 2015), can make both phenotyping individuals, as well as genotyping them, challenging or not possible in practice. To circumvent these obstacles, a growing number of studies have employed BSA genetic methods.

3.4.1. Bulked segregant analysis (BSA)

BSA concepts were first elaborated by plant geneticists in 1991 (Giovannoni *et al.*, 1991; Michelmore *et al.*, 1991), with Michelmore *et al.* introducing the term “BSA.” Since then, BSA approaches (Figure 2) have been used in many studies in plants to identify loci underlying both

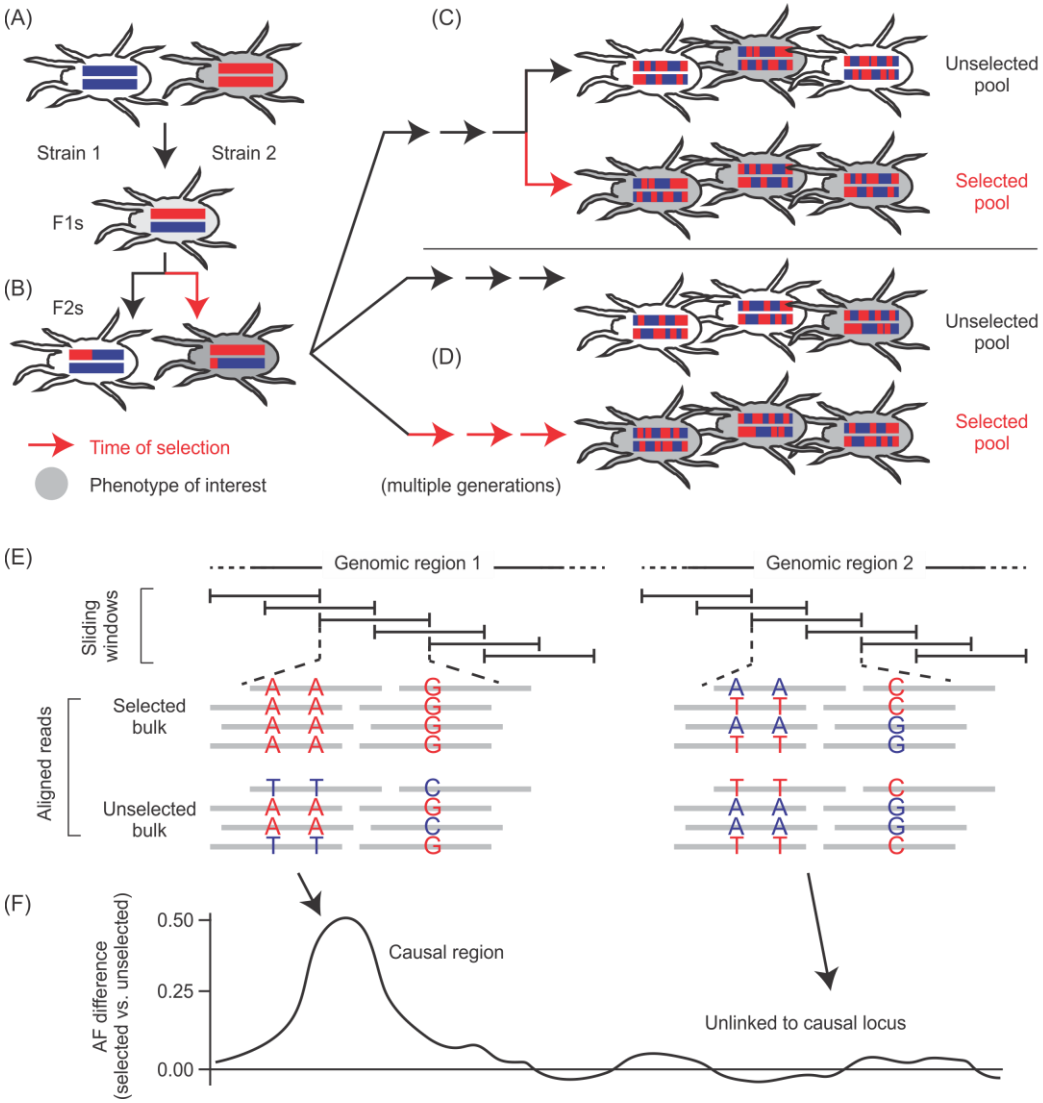

Figure 2 - Experimental designs for BSA genetic mapping. Illustrations depict spider mites, but the methods are generally applicable where crosses can be performed and derived, segregating populations can be expanded in controlled settings in the laboratory, greenhouses, or field settings (e.g., in cage enclosures). (**A**) Parental strains with contrasting genotypes (chromosomes are indicated as blue or red rectangles) and phenotypes (gray shading) are crossed to produce an F2 population (or backcross population, not shown) harboring recombinant chromosomes (**B**). To allow additional recombination events to accrue, populations can also be propagated for additional generations (**C**). In the traditional BSA design, bulks are collected at a defined endpoint (**B** or **C;** red lines with arrows indicate the step at which the phenotype of interest is selected). The bulks consist of individuals with contrasting extremes in the phenotype of interest, e.g., visual differences like pigmentation. Alternatively, fitness differences in response to a selective agent can be assessed, as for a pesticide treatment, in which case "unselected" and resistant "selected" bulks are prepared. The specific scenario illustrated is for a hypothetical case of monogenic, pesticide resistance. A variant of the traditional BSA design involves selection across multiple generations (**D**). Either way, DNA is prepared from bulk samples for genotyping, including by high-throughput, short-read sequencing as indicated (**E**). Read alignments to a reference genome sequence are used for discovery of markers and assessment of allele frequencies in sliding windows. In the case of monogenic recessive inheritance, a single fixation event at and nearby the causal variant in the selected bulk is observed (**F**; AF, allele frequency). To account for systematic deviations in allele frequencies in populations independent of the trait of interest, a comparison of allele frequencies of selected relative to unselected populations is typically performed (see also Figure 3).

monogenic and quantitative traits (Schneeberger *et al.*, 2009; Shen *et al.*, 2003; C. Zou *et al.*, 2016). As the methods are generally applicable to sexually reproducing organisms, they have also been adopted (in various forms) in studies in the yeast *Saccharomyces cerevisiae* (Ehrenreich *et al.*, 2010; Segrè *et al.*, 2006; Swinnen *et al.*, 2012), the roundworm *Caenorhabditis elegans* (Doitsidou *et al.*, 2010), vertebrates (Arnold *et al.*, 2011; Bowen *et al.*, 2012), and major arthropod taxa (Bastide *et al.*, 2016; Jagadeesan *et al.*, 2013; Park *et al.*, 2014; Van Leeuwen *et al.*, 2012). In its simplest iteration, two parental strains with a contrasting phenotype are crossed to generate an F2 population (Figure 2A,B), and separate bulk DNA samples are prepared from pools of individuals that exhibit phenotypic extremes for the trait of interest. In the straightforward case of monogenic inheritance, one pool will be fixed at the causal locus and the region surrounding it (an effect of linkage), while at unlinked genomic locations, alleles from both parents will be represented (Figure 2E,F). For quantitative traits, fixation is not expected, but differences in allele frequencies between offspring pools can be used to locate quantitative trait loci (QTL) (Figure 3) (Bastide *et al.*, 2016; Bryon *et al.*, 2017b; Wybouw *et al.*, 2019). Although crosses with parental strains that are inbred simplifies genotyping and downstream analyses, it is not always a requirement (Bryon *et al.*, 2017a; Demaeght *et al.*, 2014). While pooling of samples eliminates the ability to detect epistatic interactions (Schneeberger, 2014; Sham *et al.*, 2002), single DNA samples are prepared and genotyped from each of the contrasting bulks, and hence the laborious step of individually processing hundreds of samples is eliminated. Importantly, pooling of individuals can allow for relatively large bulk sizes, which can reduce uncertainties in phenotypic ascertainment, and can increase mapping resolution, as more recombination events are captured (Figure 2B). To increase mapping resolution further, segregating populations can also be propagated beyond the F2 generation (Van Leeuwen *et al.*, 2012), allowing additional recombination events to accumulate (Figure 2C). The classic BSA design can also be modified in other ways. For instance, selection can be applied over multiple generations (instead of focusing on a single time point; Figure 2D) (Wybouw *et al.*, 2019); this design is attractive for instances where the genetic architecture is polygenic, and for which multiple rounds of selection may be required to reveal detectable changes in allele frequencies at loci of minor effect size. The multigenerational selection component of this approach bears some similarity to evolve and resequence (E&R) experimental designs that have also attracted attention, especially from Drosophila geneticists (Burke *et al.*, 2010; Kang *et al.*, 2016; Turner *et al.*, 2011; Turner and Miller, 2012). However, E&R studies typically use large, genetically diverse founding populations, as does the related pool-GWAS method (Groen and Whiteman, 2016), and not crosses starting with defined strains selected to vary markedly in phenotypes of interest, as typify BSA study designs. Nevertheless, E&R and related approaches hold promise in cases where the requisite genetic resources exist, and have been covered in several recent reviews (Kofler and Schlötterer, 2014; Schlötterer *et al.*, 2015, 2014).

Considering *T. urticae,* BSAs helped elucidating both monogenic and polygenic traits: (1) a target site mutation (*chitin synthase 1*) was found for the growth inhibitors clofentezine, etoxazole and hexythiazox by looking for a locus with haplotype fixation (Figure 2A,B,C) (Demaeght *et al.*, 2014; Van Leeuwen *et al.*, 2012), (2) a mutation in *phytoene desaturase* causal for the absence of

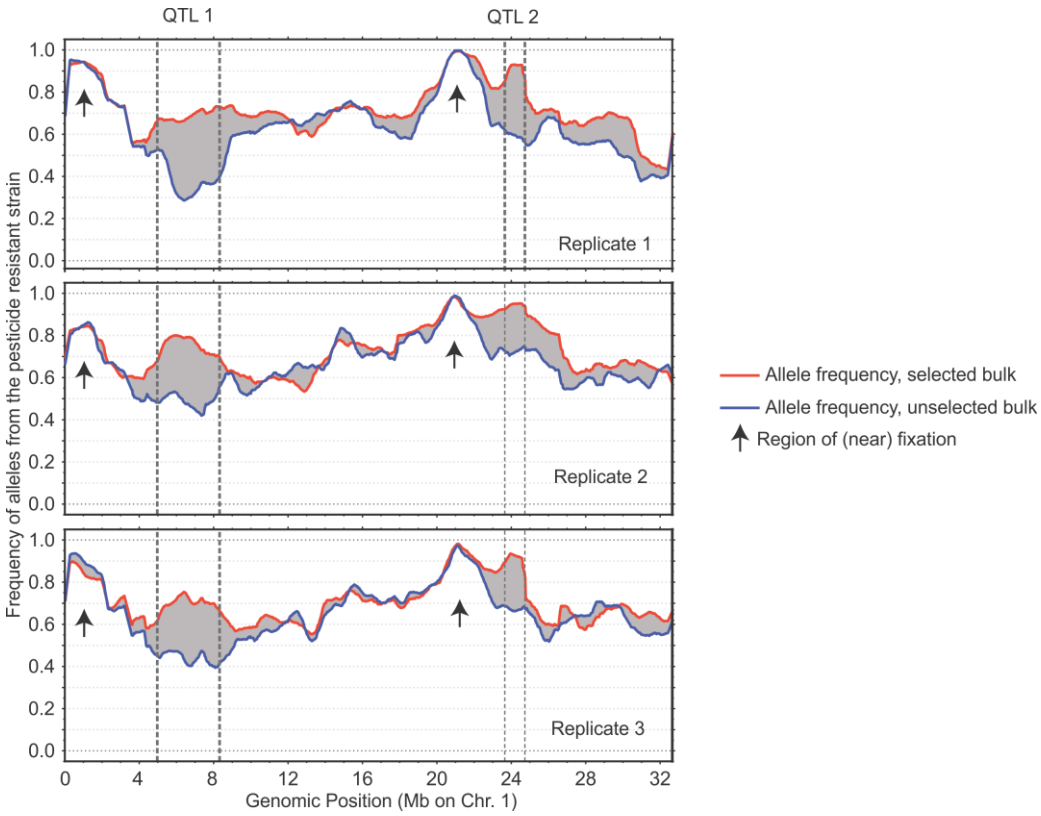

Figure 3 - Example allele frequencies of replicate *T. urticae* populations under selection by the pesticide spirodiclofen in a study that applied selection over many generations. Shown are the raw allele frequencies of three representative replicates of unselected populations (blue lines) and spirodiclofen-selected populations (red lines) as assessed in sliding windows (500 kb with a 25 kb offset). The data used to construct the plots are from Wybouw *et al.* 2019 (the experimental design was after Figure 2A,B,D). As plotted, vertical deflections indicate increases in the frequency of alleles coming from the spirodiclofen-resistant parental strain. Systematic differences in allele frequencies between the paired unselected and selected populations (gray shading) indicate two QTL (Wybouw *et al.*, 2019), and are indicated by vertical dashed lines. Note that several regions of fixation (or near fixation) are observed even in unselected populations (black arrows), potentially reflecting the purging of deleterious alleles or segregation distortion. The code used to plot this figure was adapted from Wybouw *et al.*, 2019 and Chapter 2, and has been made available on Github (https://github.com/rmclarklab/BSA).

carotenoid-based pigmentation in an albino strain was discovered after analyzing allele frequency differences between selected and unselected populations (Figure 2A,B,C) (Bryon *et al.*, 2017a), (3) the latter approach was also used to reveal three QTLs related to resistance against the acetyl-CoA carboxylase inhibitor spirodiclofen after selection over multiple generations (Figure 2A,B,D) (Wybouw *et al.*, 2019).

4. General outline of this thesis

During my PhD work, a variety of approaches were used to study *T. urticae* genetic and molecular mechanisms involved in the detoxification of man-made and plant-derived toxins. These approaches included QTL mapping, transcriptomics and enzyme characterization.

In **Chapter 2**, we used QTL mapping to determine whether similar or different genetic responses underlie resistance to three different acaricides from the METI-I class. The role of a previously documented target-site mutation, and new candidate genes were identified that potentially underlie METI-I resistance.

In **Chapter 3 and 4**, an RNA-seq and microarray approach were used to examine the transcriptomic profile of *T. urticae* females upon application of four synergists, and upon long-term transfer from common bean to five host plant species, respectively. In the former study, we were interested in the transcriptomic response of well-known detoxification genes (specificity, magnitude…) upon synergist exposure. In the latter study, we wanted to extend the knowledge of transcriptomic changes upon acclimation of generalist arthropod herbivores to new host plants (≥ 5 generations, 5 hosts), since most existing studies focus on short term response or within-generation transfer to a single or very few hosts. Additionally, candidate genes potentially linked to host plant acclimation were identified, including members of enzyme families which had never been related to host plant adaptation before.

In **Chapter 5**, we surveyed the potential role of *T. urticae* UGTs in detoxification of pesticides or plant secondary metabolites by screening seven functionally expressed UGTs against 44 substrates. Based on the screening results, nine enzyme-substrate combinations were selected for more comprehensive analysis and steady-state kinetic parameters were determined. Additionally, the preferred activated donor of *T. urticae* for glycosylation was determined.

Finally, in **Chapter 6**, the potential of trait mapping by using bulked segregant analysis in *T. urticae* and other arthropods is discussed. Additionally, an overview of the commonly used validation approaches and recent breakthroughs is provided, while highlighting potential strategies for the validation of hypotheses brought forward in the previous chapters.

Chapter 2

High-resolution QTL mapping reveals target-site resistance but also divergent responses to long-term selection by three METI-I acaricides in *Tetranychus urticae*

This chapter has been partially redrafted from:

Snoeck*, S., Kurlovs*, A., Bajda, S., Feyereisen, R., Greenhalgh, R., Villacis-Perez, E., Kosterlitz, O., Dermauw, W., Clark, R.M., Van Leeuwen, T. (2019) High-resolution QTL mapping reveals target-site resistance but also divergent responses to long-term selection by three METI-I acaricides in *Tetranychus urticae*. Insect Biochemistry and Molecular Biology, 110, 19-33.

1. Abstract

Arthropod herbivores cause dramatic crop losses, and frequent pesticide use has led to widespread resistance in numerous species. One such species, the two-spotted spider mite, *Tetranychus urticae*, is an extreme generalist herbivore and a major worldwide crop pest with a history of rapidly developing resistance to acaricides. Mitochondrial Electron Transport Inhibitors of complex I (METI-Is) have been used extensively in the last 25 years to control *T. urticae* around the globe, and widespread resistance to each has been documented. METI-I resistance mechanisms in *T. urticae* are likely complex, as increased metabolism by cytochrome P450 monooxygenases as well as a target-site mutation have been linked with resistance.

To identify loci underlying resistance to the METI-I acaricides fenpyroximate, pyridaben and tebufenpyrad without prior hypotheses, we crossed a highly METI-I-resistant strain of *T. urticae* to a susceptible one, propagated many replicated populations over multiple generations with and without selection by each compound, and performed bulked segregant analysis genetic mapping. Our results showed that while the known H92R target-site mutation was associated with resistance to each compound, a genomic region that included cytochrome P450-reductase (CPR) was associated with resistance to pyridaben and tebufenpyrad. Within CPR, a single nonsynonymous variant distinguished the resistant strain from the sensitive one. Furthermore, a genomic region linked with tebufenpyrad resistance harbored a non-canonical member of the nuclear hormone receptor 96 (NHR96) gene family. This NHR96 gene does not encode a DNA-binding domain (DBD), an uncommon feature in arthropods, and belongs to an expanded family of 47 NHR96 proteins lacking DBDs in *T. urticae*. Our findings suggest that although cross-resistance to METI-Is involves known detoxification pathways, structural differences in METI-I acaricides have also resulted in resistance mechanisms that are compound-specific.

2. Introduction

Agrochemicals that inhibit electron transport in the mitochondrial respiratory chain have been commonly and successfully used against phytophagous mites (Lümmen, 2007; Van Leeuwen *et al.*, 2014). These compounds are referred to as Mitochondrial Electron Transport Inhibitors (METIs) and have been classified into groups depending on the site or complex they block. Four large transmembrane complexes (I-IV) mediate electron transport in the mitochondrial inner membrane via several redox reactions from NADPH and FADH2 to oxygen, which serves as the final electron acceptor. An outcome of these sequential redox reactions is the proton gradient that drives ATP synthesis by the F_0F_1 ATPase (complex V) (Karp, 2008). Classic METIs like quinolines, pyridinamines, pyrazoles and pyridazinones act on complex I, the proton translocating NADH: ubiquinone oxidoreductase. This is the largest and most complex multi-subunit structure of the respiratory chain, and it is responsible for catalyzing the electron transfer from NADH to coenzyme Q10 (ubiquinone). These acaricides are referred to as METI site I or METI-Is, and belong to Insecticide Resistance Action Committee (IRAC) group 21 (Hollingworth *et al.*, 1994; Hollingworth and Ahammadsahib, 1995; Wirth *et al.*, 2016). Although the specific binding sites for ubiquinone and inhibitors may not be identical (Fendel *et al.*, 2008; Tocilescu *et al.*, 2010), inhibition of complex

I has been described for many structurally diverse compounds that are thought to interfere with ubiquinone reduction (Degli Esposti, 1998; Lümmen, 1998). Competition experiments have shown that hydrophobic inhibitors of complex I share a common binding domain with at least partially overlapping sites (Okun *et al.*, 1999). Structural data on complex I, as well as biochemical studies (Schuler and Casida, 2001; Shiraishi *et al.*, 2012), support the hypothesis that binding sites for both ubiquinone and inhibitors are comprised of the nuclear-encoded PSST and the 49 kDa subunits of complex I (Fiedorczuk *et al.*, 2016; Vinothkumar *et al.*, 2014; Zickermann *et al.*, 2015). The PSST subunit is the most likely carrier of iron-sulfur cluster N2, a proposed direct electron donor for the ubiquinone reduction (Duarte *et al.*, 2002; Friedrich, 1998; Magnitsky *et al.*, 2002).

Acaricide resistance develops via two main mechanisms: the pharmacokinetic mechanism, which is primarily caused by a decreased exposure due to quantitative or qualitative changes in major detoxification enzymes and transporters, and the pharmacodynamic mechanism, which involves a decrease in sensitivity due to changes in the acaricide's target site (Feyereisen *et al.*, 2015; Li *et al.*, 2007; Van Leeuwen and Dermauw, 2016). These mechanisms are driven by three types of genetic changes (Feyereisen, 2015): (1) mutations that affect the coding sequences of the target gene or detoxification genes, (2) mutations that alter expression levels of target/detoxification genes by affecting *cis* or *trans* regulation, or (3) whole target/detoxification gene duplications or deletions. Combinations of these genetic mechanisms are also possible. For instance, point mutations in acetylcholinesterase that make an organism resistant to organophosphates also decrease the enzyme's effectiveness, leading to gene duplications as a compensation mechanism (Kwon *et al.*, 2010b).

Tetranychus urticae (Acari; Tetranychidae), the two-spotted spider mite, is a major crop pest that feeds on over 1000 plant species and has been found on every continent except Antarctica (Migeon *et al.*, 2006-2018). *T. urticae* is notoriously resistant to acaricides and insecticides, with resistance to over 96 active compounds reported to date (Mota-Sanchez and Wise, 2019; Van Leeuwen and Dermauw, 2016). Resistance to METI-Is in *T. urticae* was initially documented in the 1990s and has since become widespread (Cho *et al.*, 1995; Devine *et al.*, 2001; Herron and Rophail, 1998; Ozawa, 1994). METI-I resistance in the spider mite was first associated with increased cytochrome P450 (P450) activity by synergism and enzyme activity tests (Cho *et al.*, 1995; Devine *et al.*, 2001; Herron and Rophail, 1998; Ozawa, 1994; Van Pottelberge *et al.*, 2009c), and based on genome-wide microarray gene expression data, a number of constitutively upregulated P450s were identified in METI-I resistant strains. Subsequent studies revealed that one of those upregulated P450s (CYP392A11) metabolized fenpyroximate – but not pyridaben or tebufenpyrad – to a non-toxic metabolite when expressed in *E. coli* (Riga *et al.*, 2015), suggesting that the enzymes involved in METI-I metabolism may vary depending on the acaricide involved. More recently, targeted sequencing and genetic analysis identified a variant in the *T. urticae* PSST homologue of complex I, H92R (*Yarrowia lipolytica* numbering; H110R in *T. urticae*), that appeared to significantly reduce sensitivity to fenpyroximate, pyridaben, and tebufenpyrad (Bajda *et al.*, 2017). This mutation is currently the only known genetic change associated with resistance to METI-I compounds in *T. urticae*. Introgression into a sensitive strain, however, suggested that the mutation explained only a

fraction of the total resistance phenotype (Bajda *et al.*, 2017). Additional genetic changes underlying other METI-I resistance mechanisms have so far remained elusive.

The two-spotted spider mite is a tractable organism for characterizing resistance mechanisms, as its haplodiploid breeding system (males are haploid while females are diploid) facilitates inbred line construction, its genome size is small (~90Mb), the generation time is as little as a week at optimal temperatures, and very large populations can be propagated (Van Leeuwen and Dermauw, 2016). Bulked segregant analysis (BSA) approaches have been used with *T. urticae* to identify monogenic loci (Bryon *et al.*, 2017a; Demaeght *et al.*, 2014; Van Leeuwen *et al.*, 2012), and these methods were recently extended to successfully describe polygenic resistance to a lipid synthesis inhibiting acaricide, spirodiclofen (Wybouw *et al.*, 2019). For genetic mapping of resistance with BSA methods, a resistant parent is crossed with a sensitive one, and resultant populations are expanded and selected with the pesticide. In *T. urticae*, BSA studies have used multigenerational populations (which allow dense recombination to break apart haplotypes – a prerequisite for high-resolution mapping), with whole-genome sequencing of parents and derived populations to simultaneously genotype and detect allele frequency changes that identify causal loci (i.e., fixation or increases in the frequency of alleles contributed by the resistant parent).

In this study, we adapted recent advances in BSA methods, and a chromosome-level assembly of the *T. urticae* genome (Wybouw *et al.*, 2019), to comprehensively investigate the quantitative (polygenic) genetic architecture of resistance to the METI-I acaricides fenpyroximate, pyridaben and tebufenpyrad. To do so, we performed multiple rounds of acaricide selection on the offspring of a cross between a Belgian greenhouse strain of *T. urticae* (MR-VP) that exhibited high levels of resistance to these commonly used METI-Is (Van Pottelberge *et al.*, 2009c), and the METI-I-sensitive strain Wasatch (Bryon *et al.*, 2017a). As assessed by whole-genome sequencing, multiple quantitative trait loci (QTL) for the three METI-I acaricides were identified, revealing a common target-site mutation and suggesting novel acaricide-specific resistance mechanisms.

3. Materials and methods

3.1. Acaricides

The acaricides used in this study were commercial formulations (Fyto Vanhulle, Belgium) of fenpyroximate (Naja; 50 g a.i. L^{-1} SC), pyridaben (Sanmite; 150 g a.i. L^{-1} SC) and tebufenpyrad (Pyranica; 200 g a.i. L^{-1} SC).

3.2. *T. urticae* strains

The METI-I resistant strain MR-VP was originally collected in September 2005 from bean plants in a greenhouse at the National Botanical Garden (Brussels, Belgium) (Van Pottelberge *et al.*, 2009c), which had a spray history of tebufenpyrad (Pyranica; 200 g a.i. L^{-1} SC) and pyridaben (Sanmite; 150 g a.i. L^{-1} SC); the strain has since been kept in the laboratory at a constant selection pressure of 1000 mg L^{-1} tebufenpyrad. The susceptible Wasatch strain was originally collected from tomato (*Solanum lycopersicum*) in Salt Lake City, Utah, USA (Bryon *et al.*, 2017a), from a public

garden where spraying with synthetic pesticides was prohibited. Both strains were mother-son inbred for six generations as previously described (Bryon *et al.*, 2017a; Van Petegem *et al.*, 2018). Prior to the experiment, both *T. urticae* strains were maintained under laboratory conditions (25° C, 60% RH and 16:8 L:D photoperiod) on detached bean leaves (*Phaseolus vulgaris*) resting on cotton pads in plastic boxes to prevent contamination. LC_{50} assays for strains MR-VP and Wasatch were performed as previously described (Van Leeuwen *et al.*, 2004). For each acaricide, LC_{50} values, slopes and 95% confidence limits of the parental strains were estimated using Probit Analysis (PoloPlus version 2.0; LeOra Software, Berkeley, CA, USA). If 5000 mg L^{-1} did not cause 50% mortality, no further attempts were made to determine LC_{50}.

3.3. Experimental evolution set-up of METI-I resistance

An F_1 hybrid population was generated by crossing 22 one-day-old virgin adult females of the inbred Wasatch strain with a single young male of the inbred MR-VP strain. 332 virgin F_1 teliochrysalis females were collected in total and were backcrossed to 70 males of the Wasatch strain. Subsequently, approximately 500 F_2 females were used for the inoculation of potted bean plants, and the resulting segregating bulk populations were kept in a climatic chamber (Panasonic MLR-352H-PE, Kadoma, Japan) at 28° C with a photoperiod of 16:8 h light:dark for 4-5 generations to expand the population. To set up acaricide selection, 500 individuals from the bulk population were transferred to control plants or those sprayed with 50 mg L^{-1} of either fenpyroximate, pyridaben, or tebufenpyrad; ten replicates were set up for each of the four groups. Experimental evolution on whole bean plants took place in the greenhouse at 21° C over a period of nine months (~25 generations). When the population size was large enough, mites from each treatment group were transferred to new plants with an increasing concentration of the respective acaricide over time. The concentrations varied depending on the acaricide and were empirically determined based on the efficacy of the previous round of selection. Selection was considered complete when no acaricide-related mortality was observed on beans sprayed until run-off with the final concentrations of 3500, 1250, and 750 mg L^{-1}, for fenpyroximate, pyridaben, and tebufenpyrad, respectively.

3.4. METI-I resistance and adaptation assay

Effectiveness of selection to the three acaricides was evaluated by performing toxicity bioassays as previously described (Van Leeuwen *et al.*, 2004). Mites were grown on unsprayed bean plants for two to four generations, depending on the population size, before conducting toxicity tests. To determine toxicity, approximately 30 gravid adult females were transferred to 9 cm^2 square-cut leaf discs on wet cotton wool and then sprayed with 1 ml of fluid at 1 bar pressure with a Potter Spray Tower (Burkard Scientific, Uxbridge, UK) to obtain a homogenous spray film (deposit of 2 mg cm^{-2}). Each of the ten selection replicates of the three acaricide-selected populations and the control populations were tested in four technical replicates at a discriminating concentration of 2500 mg L^{-1} of the relevant acaricide. The leaf discs were kept in a climatically controlled room at 25° C, 60% RH with a 16:8 h light:dark photoperiod for 24 hours. Mites were scored as being alive if they could

walk normally after being prodded with a camel's hair brush. Survival percentages of the three acaricide-selected and control populations were analyzed separately using a generalized linear mixed model with a binomial distribution using the lme4 R package version 1.1 (Bates *et al.*, 2015). Here, selection regime was incorporated as a fixed effect in the linear model, while replicate was regarded as a random effect.

3.5. RNA extraction and sequencing

Total RNA was extracted from about 100 adult female mites from the inbred MR-VP strain using the RNeasy Mini Kit (Qiagen, Belgium) with five-fold biological replication. The quality and quantity of the total RNA was analyzed by a DeNovix DS-11 spectrophotometer (DeNovix, Wilmington, DE, USA) and by running an aliquot on a 1% agarose gel. Illumina libraries were constructed from the RNA samples with the TruSeq Stranded mRNA Library Preparation Kit with polyA selection (Illumina, San Diego, CA, USA), and the resulting libraries were sequenced on an Illumina HiSeq 2000 to generate strand-specific paired reads of 2 × 100 bp (library construction and sequencing was performed at Centro Nacional de Análisis Genómico [CNAG], Barcelona, Spain). The RNA reads have been placed in the Sequence Read Archive under accession numbers SAMN11334652 through SAMN11334656.

3.6. DNA preparation, genome sequencing and variant detection

Genomic DNA of inbred MR-VP and each selection and control population was extracted from female mites according to Van Leeuwen *et al.* (Van Leeuwen *et al.*, 2008). Briefly, 4 × 200 adult mites/population were homogenized in a 2 ml Eppendorf tube containing 800 µl of SDS buffer (2% SDS, 200 mM Tris-HCl, 400 mM NaCl, 10 mM EDTA, pH = 8.33), followed by DNA extraction using a previously described phenol-chloroform-based protocol (Van Pottelberge *et al.*, 2009b). Prior to adding isopropanol, the four extracts were pooled and precipitated together to obtain sufficient DNA per population. Subsequently, samples were further column-purified using an EZNA Cycle Pure Kit (Omega Bio-tek, Norcross, GA, USA) according to the manufacturer's protocol and quantified using an ND-1000 NanoDrop spectrophotometer (Thermo Fisher Scientific, Waltham, MA, USA).

Illumina genomic DNA libraries were constructed, and sequencing was performed to generate paired-end reads of 101 bp (inbred MR-VP strain) or 125 bp (all other samples). Library construction and sequencing was performed at either the Centro Nacional de Análisis Genómico (CNAG, Barcelona, Spain) for inbred MR-VP strain or the Huntsman Cancer Institute of the University of Utah (Salt Lake City, UT, USA) (all segregating populations). Genomic sequence reads for strain MR-VP and the segregating populations have been deposited in the Sequence Read Archive under accession numbers SAMN11350708-SAMN11350748. Illumina reads were aligned to the reference Sanger draft *T. urticae* genome from the London strain (Grbić *et al.*, 2011) using the default settings of the Burrows-Wheeler Aligner (BWA) version 0.7.15-r1140 (Li and Durbin, 2009) and processed into position-sorted BAM files using SAMtools 1.3.1 (Li *et al.*, 2009). Following

recommendations described in the Genome Analysis Toolkit (GATK) best practices pipeline (Van der Auwera *et al.*, 2013), duplicates were marked using Picard tools 2.6.0 (https://broadinstitute.github.io/picard), followed by indel realignment with GATK version 3.6.0-g89b7209 (McKenna *et al.*, 2010). Joint variant calling across all 40 populations and the parental strains was carried out with GATK's UnifiedGenotyper tool to produce a variant call format (VCF) file containing single nucleotide polymorphisms (SNPs) and indels.

3.7. Quality control on predicted variants

To be informative for downstream genetic analyses, variants needed to segregate (i.e., be fixed for contrasting alleles in the MR-VP and Wasatch inbred parental strains) and be of high quality. SNPs were therefore selected according to the following criteria, which were adapted from the hard-filtering recommendations in GATK post #2806 (https://gatkforums.broadinstitute.org/gatk/discussion/2806/howto-apply-hard-filters-to-a-call-set, accessed 9 July 2018): (1) have a minimum quality score normalized by allele depth (QD; this and subsequent acronyms and abbreviations refer to how the metrics appear in the VCF 4.2 standard) of 2, (2) mean root square mapping quality (MQ) of at least 50, (3) strand odds ratio (SOR) below 3, (4) mapping quality rank sum (MQRankSum) higher than or equal to -8, (5) rank sum for relative positioning of alleles in reads (ReadPosRankSumTest) of at least -8, and (6) be within 25% and 150% of the sample's genome-wide mean SNP read coverage to minimize false heterozygous variant calls caused by copy number variable regions (see also Wybouw *et al.*, 2019); this was calculated using total depth per allele per sample (AD).

3.8. Responses to selection and validation of the *T. urticae* three-chromosome assembly

For most downstream analyses, we transformed variant positions as assessed on the *T. urticae* draft Sanger genome assembly onto the recently reported *T. urticae* three-chromosome assembly (Wybouw *et al.*, 2019). For simplicity, we refer to pseudochromosomes 1-3 in this assembly as chromosomes 1-3 (Chr1-3). This assembly was constructed with replicated population allele frequency data from 22 populations in an earlier study, and was partially validated with short-read *de novo* assemblies from multiple *T. urticae* strains (Wybouw *et al.*, 2019). The authors of this study noted that additional, dense population allele frequency would be important to validate the assembly. To do this, and to assess the appropriateness of the assembly for use in our study, we calculated the average window distance (AWD) metric across Chr1-3 using the allele frequency data of all of our 39 individual population samples (one of the 40 segregating populations was excluded from the analysis, see Section 2.10). Briefly, as assessed from highly replicated population allele frequency data, positive deflections of the AWD metric by position in genome-wide scans detect assembly errors; our implementation of AWD calculations followed that of Wybouw *et al.* (2019).

3.9. Heterozygosity estimates

To verify that strains MR-VP and Wasatch were inbred to fixation, we used a separate joint variant call analysis to estimate genome-wide levels of heterozygosity. Briefly, to improve variant call accuracy, and to provide an expectation for inbreeding to homozygosity, we included, in addition to MR-VP and Wasatch, previously published inbred and non-inbred sequenced strains of *T. urticae* (Albino-JP, Foothills, Lon-Inb, MAR-AB, PA2, SR-VP; (Bryon *et al.*, 2017a; Wybouw *et al.*, 2019)). The predicted variants were filtered as described above, with modifications and additional filtering steps to reduce the number of false positives. Specifically, MQRankSum and ReadPosRankSumTest filters were bidirectional, meaning we kept alleles that fell between -8 and 8 for both. In addition, to prevent copy number variable regions from falsely elevating the heterozygosity estimates, only alleles falling within 25% of the mean genome-wide SNP coverage depth for each strain were considered. The extent of heterozygosity, as assessed from counts for alleles at high-quality SNP positions in sliding windows, was visualized genome-wide.

3.10. Principle component analysis

A principal component analysis (PCA) was performed in R version 3.4.3 (R Developement Core Team, 2015). A correlation matrix containing the individual SNP frequencies for specific alleles was used as input for the R function prcomp, which is part of the R package 'stats' (version 3.3.0). We selected only those SNP alleles that were present in all treatments (fenpyroximate-selected, pyridaben-selected, tebufenpyrad-selected and control). The PCA plots were created with autoplot, a function of the R package 'ggplot2' (version 2.1.0) (Wickham, 2009). An examination of the resulting PCA analysis identified an extreme outlier in the pyridaben-selected group (Figure S1), presumably reflecting contamination by an unrelated strain; this sample, P9, was therefore excluded from all subsequent analyses, and a PCA with all samples except P9 was then generated.

3.11. Bulked segregant analysis genetic mapping

The ~590,400 loci from strains MR-VP and Wasatch were analyzed using BSA methods adapted from earlier studies (Bryon *et al.*, 2017a; Demaeght *et al.*, 2014; Van Leeuwen *et al.*, 2012; Wybouw *et al.*, 2019). The difference in MR-VP allele frequency between the acaricide-selected and the control samples was averaged for each pesticide treatment in overlapping 75kb genomic windows with 5kb offsets. Statistical significance of BSA peaks, as assessed across all replicates, was determined with the permutation approach of Wybouw *et al.* (2019). Briefly, in replicated BSA data, responses to selection among independent replicates are expected to co-occur at the same genomic locations. Alternatively, where minor peaks are solely due to drift, no systematic co-occurrence between replicates is expected. The permutation method implemented by Wybouw *et al.* (2019) assigns genomic regions responding to selection across samples (concerted responses at specific genomic locations) from multigenerational, replicated unselected and selected populations by establishing a significance threshold for QTL detection at a specified genome-wide false discovery rate (FDR). The permutation method requires pairing of selected and unselected

samples. In this study, we adapted the sample matching approach that Wybouw *et al.* (2019) applied to the same experimental design to detect a QTL for host plant adaptation using five selected and unselected populations. An exception was that, as the current study used many more replicates – 9 for pyridaben and 10 for fenpyroximate and tebufenpyrad (hence 9! and 10! potential pairings) – subsets of 120 potential pairings were chosen to make it computationally feasible. For each of the 120 sets, 5% FDR thresholds for QTL detection were calculated from the distribution of maximal allele frequency values for 10^4 permutations as described by Wybouw *et al.* (2019). Across the entire set of 120 permutations, the most conservative 5% FDR cutoff was used for QTL assignment.

3.12. Predicted effects of genetic variants in coding sequences

To assess coding sequence changes in genomic (QTL) regions for response to pesticide selection, coding effects of SNPs and small indels identified by the GATK analysis were predicted using SnpEff 4.2 (Cingolani *et al.*, 2012) with a *T. urticae* coding sequence database derived from the June 23, 2016 annotation available from the Online Resource for Community Annotation of Eukaryotes (ORCAE) (Sterck *et al.*, 2012). The QTL were also visually inspected in Integrative Genomics Viewer (IGV) version 2.3.90 (Robinson *et al.*, 2011).

3.13. Alignment of CPR proteins

All protein sequences used in the alignment were accessed either using the UniProt database (Bateman *et al.*, 2015): (*T. urticae* (tetur18g03390), *H. sapiens* (NP_000932.3), *R. norvegicus* (NP_113764.1), *M. domestica* (NP_001273818.1) and *D. melanogaster* (NP_477158.1) or NCBI: *C. sculpturatus* (XP_023225549.1). The sequences were aligned using Clustal W version 2.1 (Larkin *et al.*, 2007).

3.14. Gene duplication of the DNA-binding domain (DBD)-lacking nuclear hormone receptor (NHR-96)-like gene within a QTL connected with tebufenpyrad selection

De novo assemblies of inbred strains MR-VP and Wasatch were constructed from paired-end Illumina data using CLC Genomics Workbench 9.0.1 (https://www.qiagenbioinformatics.com). Reads were imported and trimmed using the “Trim Sequences” tool prior to assembly with the “De Novo Assembly” tool; default settings were used for both. Contigs from the *de novo* assemblies were aligned to the London reference genome using the default settings of BLASR 1.3.1 (Chaisson and Tesler, 2012) with soft-clipping enabled. Contig sequences aligning to the DBD-lacking NHR 96-like gene in the QTL region for response to tebufenpyrad (*tetur06g04270*) were extracted (File S1) and their open reading frames (ORFs) determined using ExPASy (Gasteiger *et al.*, 2003). RNA-seq alignments were performed using Spliced Transcripts Alignment to a Reference (STAR) version 2.5.3a (Dobin *et al.*, 2013), with the two-pass mode and a maximum intron size of 20 kb; the RNA-seq reads were aligned to a modified version of the London reference sequence that was adjusted to include an MR-VP *de novo* assembled contig in the genomic region spanning *tetur06g04270*. Gene duplications in both Wasatch and MR-VP *de novo* contigs were annotated (File S2) based on

the ORF information and the MR-VP RNA-seq alignment visualization in IGV version 2.3.90 (Robinson *et al.*, 2011).

3.15. Analysis of DBD-lacking NHR96-like genes in *T. urticae*: manual reannotation, phylogeny, and genomic distribution

The *T. urticae* genome was mined for other DBD-lacking NHR96-like genes by using the eight conserved NHR96-like ligand binding domains (LBDs) as queries in tBLASTn and BLASTp searches (e-value threshold of e^{-3}, BLAST+ version 2.2.31) against the *T. urticae* genome (Grbić *et al.*, 2011) and proteome (version of 11 August, 2016), respectively. *T. urticae* gene models were modified when necessary or new gene models were created using GenomeView version N39 (Abeel *et al.*, 2012). The DBD-lacking NHR96-like sequences can be found in File S3. To test for evidence of other tandem duplications of DBD-lacking *T. urticae* NHR-like genes, Chr1-3 and the smaller unplaced scaffolds were scanned for regions where at least two DBD-lacking NHR genes occurred in the same orientation with 50kb or less between each pair of genes within the cluster.

Subsequently, nuclear receptor sequences were obtained for *Drosophila melanogaster*, *Daphnia pulex* and *T. urticae* (Grbić *et al.*, 2011; King-Jones and Thummel, 2005; Thomson *et al.*, 2009) [accession numbers can be found in Table S1]. Using Pfam 31.0 (Finn *et al.*, 2016), each receptor sequence was analyzed for the presence of a conserved LBD (PF00104). Detected LBDs were aligned to those of the mined candidate *T. urticae* DBD-lacking NHR96-like peptides using MAFFT version 7 with the E-INS-i iterative refinement method strategy (Katoh *et al.*, 2002). A phylogenetic analysis was performed on the CIPRES web portal (Miller *et al.*, 2010) using RAxML version 8 HPC2-XSEDE (Stamatakis, 2014) with the automatic protein model assignment algorithm using the maximum likelihood criterion and 1000 bootstrap replicates; the LG + G protein model was selected as the optimal model for analysis. The resulting tree was midpoint rooted, visualized using MEGA6 (Tamura *et al.*, 2013) and edited in CorelDRAW Home & Student X7 (Corel, Austin, TX, USA).

3.16. NHR-like genes lacking DBD in other arthropods

To determine if DBD-lacking NHR genes (including DBD-lacking NHR96-like genes) were common in other arthropods, we used two approaches: one relying on comprehensive searches of the NCBI nr database (downloaded 13 June, 2018) for DBD-lacking NHR-like genes using keywords, and the other based on BLASTp (version 2.7.1) searches with DBD-lacking NHR96-like *T. urticae* gene queries against the same database; the latter approach was undertaken to find NHR-like genes that had not been annotated. Using the first approach, we extracted all protein sequences that had “nuclear receptor”, “hormone receptor”, or “ecdysone” in their description; the last keyword was used as many insect NHRs are involved in molting and metamorphosis (Fahrbach *et al.*, 2012). For the second approach, we used as queries each of the 47 DBD-lacking NHR96-like genes present in the London genome sequence of *T. urticae*, as well as the two copies of the

tetur06g04270 gene from strain Wasatch. We allowed 1000 results for each search and then extracted all the resulting proteins that aligned with an e-value of 1 or below.

From the protein sequences obtained using both approaches, we only kept those belonging to Arthropoda as assessed with the Python package ete3 (version 3.1.1) (Huerta-Cepas *et al.*, 2016). InterProScan version 5.29-68.0 was then used to predict domains and conserved regions. From the resulting sequences, we extracted those that were classified by InterProScan as "nuclear hormone receptor-like domain superfamily" (IPR035500), and that lacked the "Zinc-finger, nuclear hormone receptor type" motif (IPR001628) (Zdobnov and Apweiler, 2001). In the event that several proteins had the same amino acid sequence, only one was retained for analysis.

4. Results

4.1. Characterization of METI-I resistant inbred strains

To facilitate genetic and genomic analyses, strain MR-VP was mother-son inbred for six generations, a level of inbreeding similar to that of strain Wasatch, which was performed in an earlier study (Bryon *et al.*, 2017a). To confirm that the strains were isogenic, we sequenced the MR-VP strain using the Illumina method, and aligned the resulting reads, as well as those from Wasatch and several other strains sequenced previously (Bryon *et al.*, 2017a), to the London reference genome. For strains like MAR-AB and Albino-JP, which were either not inbred, or only inbred for one generation (Bryon *et al.*, 2017a), heterozygosity was observed at 82.14% and 10.29% of SNP sites, respectively. In contrast, for MR-VP and Wasatch, only 1.77% and 1.14% of variable positions were not fixed (Figure S2), respectively, perhaps reflecting sequencing errors or errant predictions in copy number variable regions. Toxicity bioassays revealed that the inbred MR-VP and Wasatch strains varied greatly in their susceptibility to METI-Is, with MR-VP withstanding 190-, 532- and 73-fold higher concentrations of fenpyroximate, pyridaben and tebufenpyrad, respectively (Table 1). In fact, MR-VP's LC_{50} for fenpyroximate could not be calculated as it exceeded 5000 mg a.i. L^{-1}.

Table 1 - Results of toxicity bioassays for the inbred parental strains MR-VP and Wasatch. Strain MR-VP showed significantly higher levels of resistance compared to strain Wasatch for every acaricide tested. METI-I resistance of MR-VP had also been determined prior to the strain's inbreeding by Van Pottelberge *et al.* (2009b).

	Inbred Wasatch LC50 (mg a.i. L^{-1}, 95% CI)	Inbred MR-VP LC50 (mg a.i. L^{-1}, 95% CI)	Resistance factor	MR-VP before inbreeding LC50 (mg a.i. L^{-1}, 95% CI)
Fenpyroximate	26.4 (18.2 - 32.1)	> 5000	> 190	10581 (8441-13036)
Pyridaben	4.3 (3.8 – 4.8)	2275 (1945 – 2663)	532	36959 (26450-59590)
Tebufenpyrad	5.7 (4.8 – 6.8)	417 (357 – 476)	73	1197 (1080-1309)

4.2. Evolution of METI-I acaricide resistance in experimental mite populations

To establish a segregating population for genetic mapping of resistance, we crossed MR-VP to Wasatch, and then crossed the F_1 hybrid population back to Wasatch. This backcross was performed to maximize the recombination of haplotypes contributed by the resistant MR-VP strain.

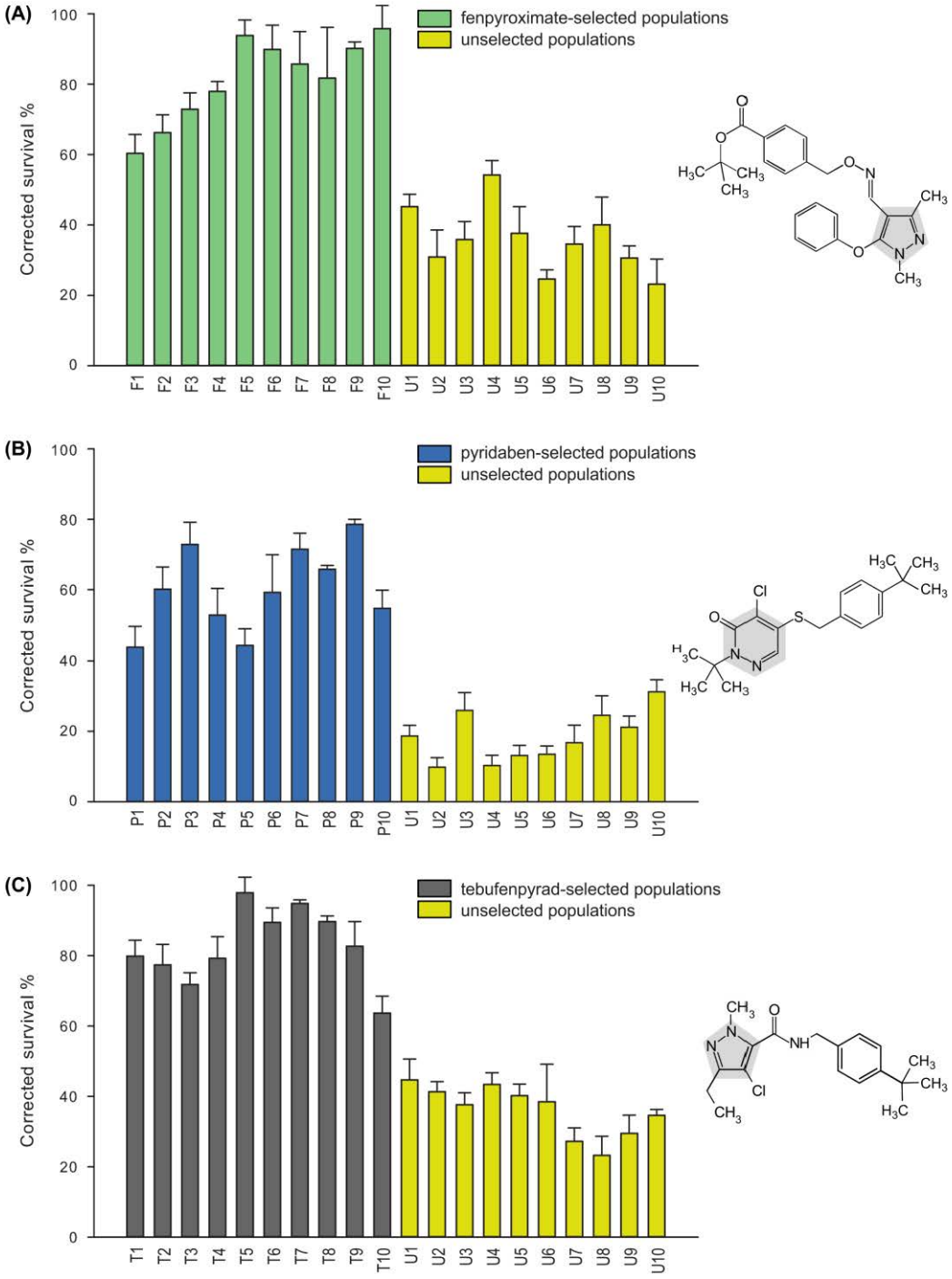

Figure 1 - Response to acaricide treatment for MR-VP × Wasatch recombinant long-term acaricide-selected and control populations. Survival was scored in the adult stage after spraying with 2500 mg a.i. L^{-1} of (A) fenpyroximate, (B) pyridaben and (C) tebufenpyrad. All three sets of acaricide-selected populations showed significantly higher survival rates compared to the control populations ($p < 0.0001$, generalized mixed model). Error bars represent 2 × SE. The molecular structures of the three acaricides are displayed to the right of the bar plots, with nitrogen heterocycles shaded in gray.

After the resulting population was allowed to expand in bulk for several generations, ten subpopulations were established for each of the three acaricide treatments, in addition to ten control subpopulations (see Materials and Methods). The 40 resulting populations were reared in separation in a greenhouse on whole bean plants for over nine months (~25 generations). During that time, each population in the three treatment groups was adapted to gradually increasing concentrations of acaricide, ending with the final concentrations of 3500 mg a.i. L^{-1} fenpyroximate, 1250 mg a.i. L^{-1} pyridaben, and 750 mg a.i. L^{-1} tebufenpyrad. Afterwards, the selected and the control populations were tested at 2500 mg a.i. L^{-1} of each acaricide, which proved to be a discriminating concentration that showed a clear distinction between resistant and sensitive populations (Figure 1). All three acaricide-selected population groups showed significantly higher survival rates compared to the control populations ($p < 0.0001$, generalized mixed model).

4.3. Genomic responses to selection

Following the experimental selections, we extracted DNA from each of the 40 populations and performed genome sequencing to produce a per-sample Illumina read coverage ranging from 58 to 78 (based on the Variant Call Format [VCF] file; see Materials and Methods). As revealed from alignments of the resulting reads, and those of the MR-VP and Wasatch parents, to the *T. urticae* reference genome (London strain, Grbić *et al.*, 2011), ~590,400 high-quality SNP variants were identified as segregating in the experimental populations. To test for responses to selection, we

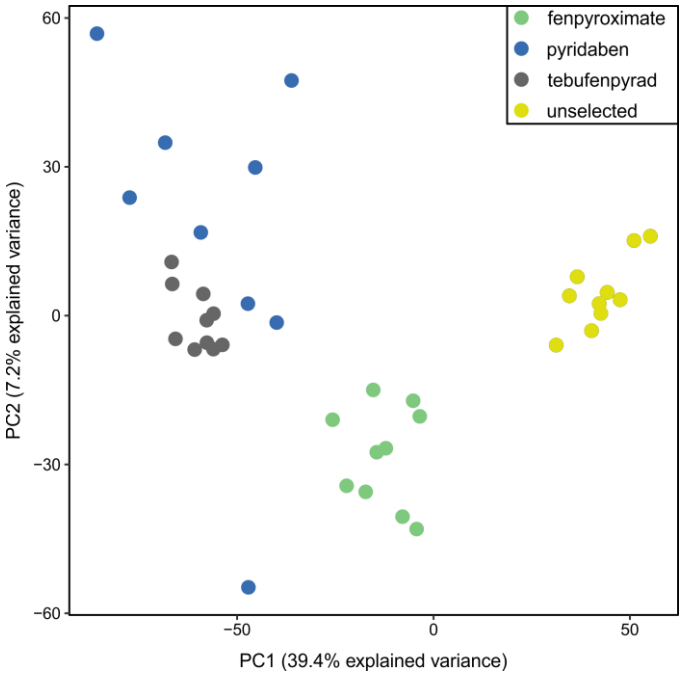

Figure 2 - Principal component analysis (PCA) with control and selected populations based on genome-wide allele frequencies at polymorphic sites. Individual populations are colored according to the treatment group (legend, upper right). The control, fenpyroximate-selected and tebufenpyrad-selected populations clustered tightly by treatment group, and separately from each other. The pyridaben-selected populations clustered less tightly, but nevertheless remained separate from control populations along PC1.

performed PCAs using the genome-wide variant predictions (Figure 2). As a preliminary PCA revealed that one pyridaben population was contaminated by an unknown strain (Figure S1), the analysis was repeated excluding that sample. For the control, fenpyroximate-selected and tebufenpyrad-selected populations, tight clustering was apparent, with no overlap among populations by treatment. Along PC1, which explained 39.4% of the variation, pyridaben- and tebufenpyrad-selected populations clustered separately from control and fenpyroximate-selected populations. However, along PC2 (7.2% of the variation), pyridaben-selected populations were markedly more dispersed as compared to the other treatment groups, consistent with a more heterogeneous response to selection by pyridaben as opposed to the other two acaricides.

4.4. Regional genomic responses to selection and validation of the three-chromosome assembly

As the principle component analysis (PCA) was consistent with genome-wide responses to selection by each acaricide, we assessed the frequency of the MR-VP alleles in sliding windows along Chr1-3 in the consolidated genome assembly recently reported by Wybouw *et al.* (2019). For the control, fenpyroximate and tebufenpyrad treatments, allele frequencies for populations within treatment groups were highly correlated, as they were between treatment groups over much of the genome length. For the pyridaben populations, greater variation was observed, consistent with the findings of the PCA. A potential explanation for this result is that the pyridaben populations went through a more severe bottleneck during acaricide selection as compared to the selections with the other two compounds (during a bottleneck event, the effect of genetic drift is elevated). Nevertheless, systematic differences were observed in allele frequencies between the control populations and those in each acaricide treatment group (e.g., at ~30Mb on Chr1), identifying putative regions for adaptation. Using the population allele frequency data from the control and the fenpyroximate-selected, pyridaben-selected and tebufenpyrad-selected populations, we also calculated the average window distance (AWD) metric along the lengths of Chr1-3 (Figure S3); positive deflections in this metric are indicative of assembly errors, see Wybouw *et al.* (2019) and Materials and Methods. As no such errors were apparent (confirming the integrity of the three-chromosome assembly), we used this chromosome-level assembly for all further analyses.

4.5. Population bulked segregant analysis mapping of QTL

To detect genomic intervals that responded to acaricide selections, we tested for significant deviations in allele frequencies between fenpyroximate, pyridaben and tebufenpyrad treated populations as compared to the control populations. Using a permutation-based framework for establishing QTL significance that takes into account all replicate data (see Materials and Methods) adapted from Wybouw *et al.* (2019), we identified one or more QTL for resistance for each of the three acaricides at a FDR of 5% (Figure 3). Within an acaricide-control comparison, QTL were prefixed with the acaricide, and numbered in order from strongest to weakest as assessed by the magnitude of the allele frequency deviations. In all cases, significant QTL reflected selection for

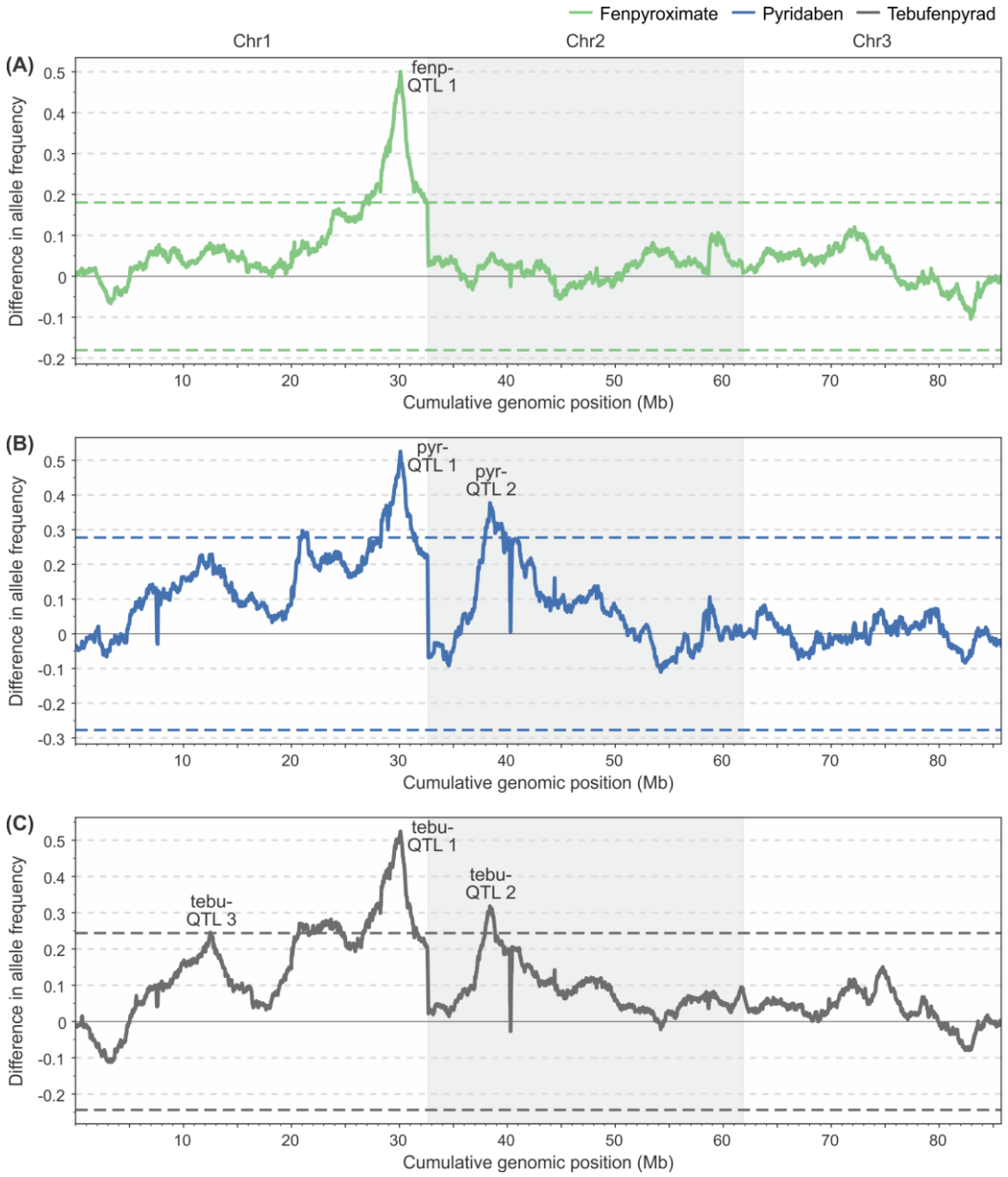

Figure 3 - Genomic responses to acaricide selections. Bulked segregant analysis (BSA) genetic mapping of QTL for resistance to (A) fenpyroximate (green), (B) pyridaben (blue), and (C) tebufenpyrad (gray). Dashed lines delineate statistical significance for QTL detection (FDR of 5%). A QTL at a coincident location at ~30Mb on Chr1 (QTL 1) was observed for selection by each acaricide, and corresponds to the target-site H92R mutation in NADH: ubiquinone oxidoreductase (PSST). Coincident BSA peaks centered on cytochrome P450-reductase (CPR) on Chr2 (QTL 2) and were observed in response to selection by both pyridaben and tebufenpyrad. A less dramatic but nonetheless significant BSA peak at ~12.5Mb on Chr1 (QTL 3) was only observed in response to selection by tebufenpyrad, and is located nearby two tandemly duplicated nuclear hormone receptor 96 (NHR96)-like genes that lack the DNA-binding domains (DBDs).

alleles contributed by the resistant MR-VP parent. For each QTL region, we analyzed genes and genetic variants in the top 75kb window as assessed from the BSA genomic scans.

All three acaricide-selected groups shared a QTL at a coincident location at ~30Mb on Chr1 (fenpyroximate-, pyridaben- and tebufenpyrad-QTL 1; Figure 3A-C, respectively). Strikingly, in all the METI-I-selected populations, the haplotype contributed by the resistant MR-VP strain went to complete (or nearly complete) fixation (Figure S3A-C). The top windows for each of these three QTL all harbored NADH: ubiquinone oxidoreductase (also known as PSST, *tetur07g05240*), and the putative H92R target-site resistance allele for fenpyroximate, pyridaben, and tebufenpyrad (Bajda *et al.*, 2017), among a total of 21 genes in the collective region of 80kb spanning the three peak windows of response (Figure 4; Table S2).

In addition, for the pyridaben and tebufenpyrad selections, a QTL for resistance was also observed at a coincident location on Chr2 (at ~5.7Mb, pyridaben- and tebufenpyrad-QTL 2; Figure. 3B,C, respectively). The top 75kb peak genomic windows overlapped exactly for these two QTL, and the region harbored 27 annotated genes (Table S3). Within this region, cytochrome P450 reductase (CPR, *tetur18g03390*), which encodes an enzyme required for P450 function (Phillips and Langdon, 1962; Wang and Roberts, 1997), was located within 20kb of the maximal allele frequency deviations (Figure 4B). An analysis of the MR-VP haplotype revealed that it was identical to that of the spirodiclofen-resistant strain SR-VP studied by Wybouw *et al.* (2019); in this study, the authors identified a nonsynonymous variant, D384Y, as unique to SR-VP and only one other strain published to date. While this variant was also present in MR-VP, it was absent in the METI-I sensitive parent, Wasatch.

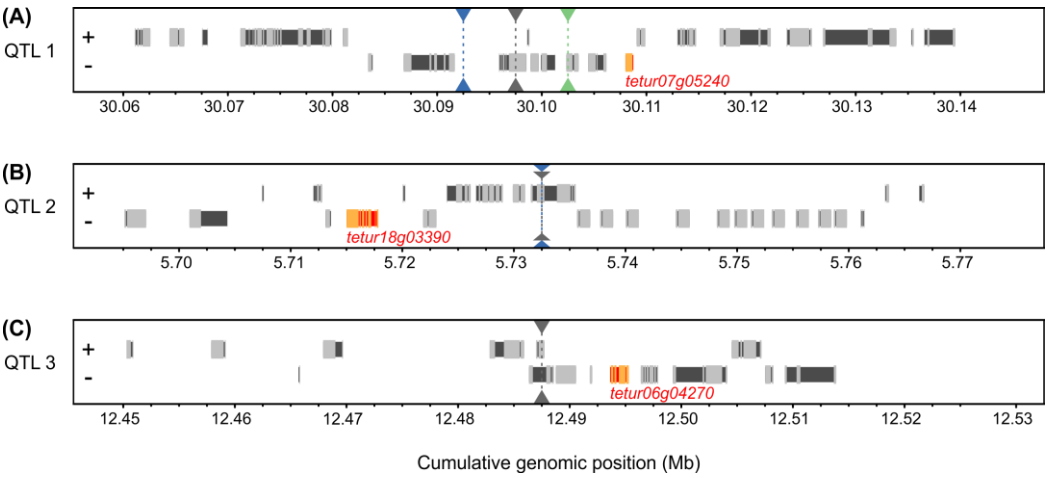

Figure 4 - Genes in 75kb genomic windows of peak response at QTLs 1-3. Triangles positioned along the top and bottom boundaries of each plot represent genomic window midpoints of each acaricide treatment group: fenpyroximate-selected (green), pyridaben-selected (blue), and tebufenpyrad-selected (gray). The orientation of gene models is as indicated ("+" or "-" for forward and reverse strands, respectively). Coding exons are denoted by rectangles shaded in light gray, and introns are shaded in darker gray. Putative candidate genes at the BSA peaks are highlighted in orange (the June 2016 *T. urticae* annotation, Online Resource for Community Annotation of Eukaryotes, or ORCAE, was used). The candidate genes are: (A) QTL 1 (all selections); target enzyme NADH: ubiquinone oxidoreductase (PSST; *tetur07g05240*), (B) QTL 2 (pyridaben and tebufenpyrad selections); cytochrome P450-reductase (CPR) (*tetur18g03390*), and (C) QTL 3 (tebufenpyrad selections only); nuclear hormone receptor 96 (NHR96)-like DNA-binding domain (DBD)-lacking (*tetu06g04270*).

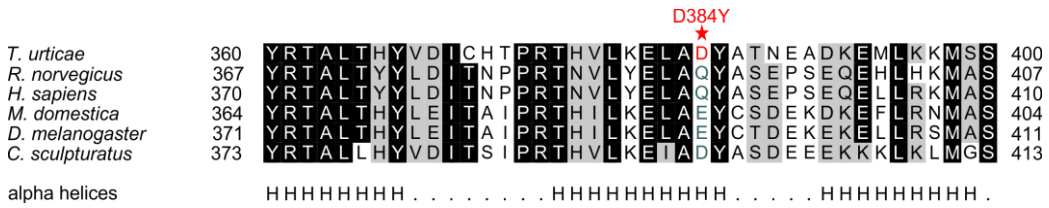

Figure 5 - Alignment of cytochrome P450 reductase (CPR) sequences around the D384Y variant. The conservation of alpha helices H (left), I (middle) and J (right) is shown. An 80% threshold was used for identity (black background) and similarity shading (gray background). The D384Y variant is located at the end of helix I (red star). The residue is charged in arthropods (D in the scorpion *C. sculpturatus* and the spider mite and E in the insects *M. domestica* and *D. melanogaster*), while most vertebrates have a polar Q at that position. The homologous Q391 in the human CPR is predicted to interact with the FMN domain in the open conformation in which electron transfer to P450s occurs.

A QTL at ~12.5Mb on Chr1 was specific for the tebufenpyrad group (tebufenpyrad-QTL 3, Figure 3C; while pyridaben-selected populations also showed elevated MR-VP allele frequencies in this region, they did not pass the significance threshold). The top window for response to tebufenpyrad selection was located near a DNA-binding domain (DBD)-lacking nuclear hormone receptor 96 (NHR96)-like gene (*tetur06g04270*), among a total of 15 genes (Table S4).

In addition, we noted that the pyridaben- and tebufenpyrad-selected populations had elevated frequencies of MR-VP alleles, relative to the control populations, over a broad region from about 20-25Mb on Chr1. Although portions of this large interval passed the threshold for QTL detection, the region is located along the proximal slope of the large response region for pyridaben- and tebufenpyrad-QTL 1. Whether this region reflects one or more independent QTL, or rather the physical proximity to QTL 1 (hitchhiking due to linkage), will require additional investigation.

4.6. Analysis of D384Y mutation in CPR

The D384Y change in the CPR gene of MR-VP was first reported in a genomic region that showed significant response to spirodiclofen selection in *T. urticae* strain SR-VP (Wybouw *et al.*, 2019). The CPR gene is highly conserved in all organisms and therefore alignments and modeling on known CPR structures are straightforward. Figure 5 shows an alignment of the *T. urticae* CPR sequence with other animal CPRs in the region surrounding D384. When modeling CPR with Phyre2 (Kelley *et al.*, 2015), an excellent match with rat CPR (pdb: c1j9zB) was obtained (score of 1184.13, e-value = 0, probability 100% with 58% identities). Spider mite D384, which corresponds to rat or human Q391, was located on the surface of the protein, specifically at the end of alpha helix I (nomenclature of Wang and Roberts, 1997) in the connecting domain between the conserved FAD/NADPH and FMN domains. This region is not implicated in flavin cofactor or NADP(H) binding, and is distant from the short “hinge” connecting the two flavin domains of CPR. Hence, the mutation was not predicted to interfere in any major and obvious way with electron transfer from NADPH to FAD and FMN, or electron transfer between the reductase and P450, but it may have more subtle effects (see Discussion section 5).

4.7. Nuclear hormone receptor analysis

We identified a DBD-lacking NHR96-like gene (*tetur06g04270*) as one of the candidate genes potentially linked with tebufenpyrad resistance. Aligning *de novo* assembled contigs to the three-chromosome assembly suggested that *T. urticae* strains MR-VP and Wasatch both harbored two copies of the DBD-lacking NHR96-like gene in tandem in a head-to-tail orientation. Next, to verify gene models and to determine if the genes were expressed, we aligned MR-VP RNA-seq reads to a copy of the three-chromosome assembly in which a *de novo* assembled MR-VP contig spanned the *tetur06g04270* region in place of the original sequence. As the RNA reads uniquely mapped to each gene, the alignments confirmed the presence of the duplication and showed that both genes were expressed in MR-VP (Figure S4).

The NR1J group represented in insects by the single NHR96 receptor was shown to be expanded in *T. urticae*, where eight NHR96-like genes were found (Grbić *et al.*, 2011). However, all of them contained the DBD. In this study, we annotated DBD-lacking NHR96-like genes in the *T. urticae* genome and identified 47 genes that had a ligand-binding domain (LBD) most similar to the eight canonical NHR96-like genes previously reported (Cheng *et al.*, 2008; Grbić *et al.*, 2011; Robinson-Rechavi *et al.*, 2003; Thomson *et al.*, 2009), but that lacked the DBD (Figure 6, panel A). Most DBD-lacking NHR96-like genes in *T. urticae* (37/47) occurred in clusters (i.e., within 50kb of another DBD-lacking NHR-gene in a head-to-tail orientation) of up to seven genes, suggesting sequential duplication events (Figure 6B).

To determine if DBD-lacking NHR-like (and specifically, NHR96-like) peptides were common in other arthropods, we comprehensively searched the NCBI database for NHR-like DBD-lacking proteins. By far the most common types of previously annotated DBD-lacking NHR-like receptors were E75s (88 in total), followed by FTZ-F1s (44), E78s (41), and photoreceptors (20). DBD-lacking NHR96-like genes, on other hand, appeared to be relatively rare. Our nr database search only identified a single annotated DBD-lacking NHR96 peptide in each of the following species: *Agrilus planipennis*, *Centruroides sculpturatus*, *Drosophila miranda*, *Plutella xylostella*, and *Rhagoletis zephyria*.

5. Discussion

Previous investigations into METI-I resistance in MR-VP revealed that fenpyroximate and pyridaben resistance were inherited as a monogenic and dominant trait, whereas resistance to tebufenpyrad was polygenic and incompletely dominant (Van Pottelberge *et al.*, 2009c). Subsequently, sequencing of several subunits presumably making up the target/binding-site identified a nonsynonymous H92R change in the PSST subunit of NADH:ubiquinone oxidoreductase, which was significantly associated with resistance (Bajda *et al.*, 2017). Nevertheless, the introgression of this mutation into a susceptible genetic background revealed that the H92R variant alone failed to explain the strength of the resistance phenotype to any of the three acaricides. This suggested roles for other loci and alleles in resistance.

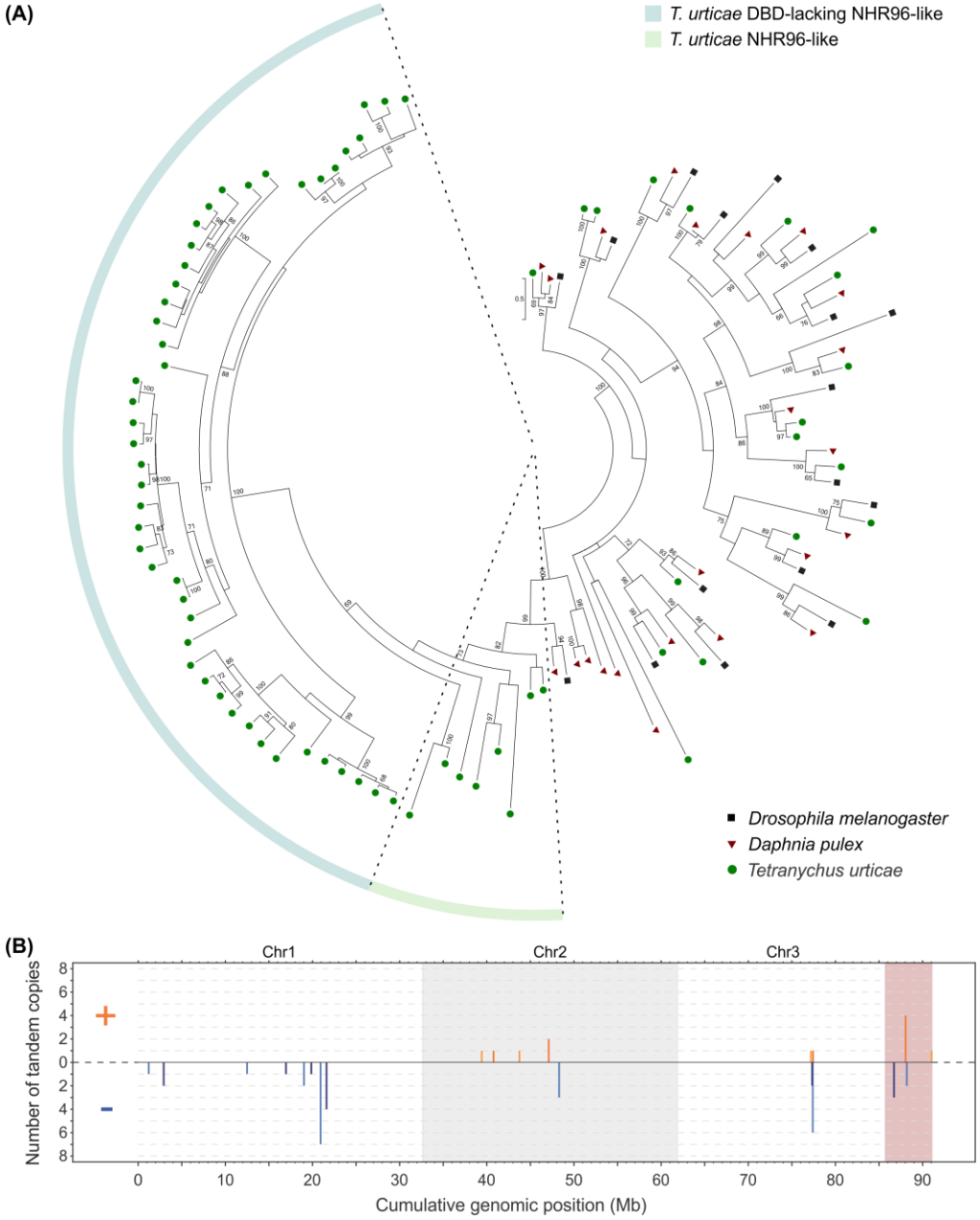

Figure 6 - Phylogenetic analysis of *T. urticae* nuclear hormone receptor (NHR) genes, and genomic distribution of *T. urticae* DNA-binding domain (DBD)-lacking NHR96-like genes. (A) Maximum likelihood LG + G phylogenetic tree of NHRs in *D. melanogaster*, *D. pulex* and *T. urticae*. Only bootstrapping values higher than 65 are shown. The scale bar represents 0.5 amino acid substitutions per site. Both *T. urticae*-specific DBD-lacking NHR96-like and canonical NHR96-like gene expansions are shaded. (B) Genomic distribution of *T. urticae*'s DBD-lacking NHR96-like genes is shown with lengths of vertical line segments corresponding to the number of genes clustered (i.e., within 50kb of another such gene) in a head-to-tail orientation. The orientation was delineated by "+" and "-" along the y-axis and by plotting the bars in shades of orange and blue, respectively. Only intact DBD-lacking NHR96-like genes were included in the analysis. The chromosomes are indicated by alternating white and gray shading, while small scaffolds were concatenated and shaded in red to the right of the chromosomes. The original figure, including all gene names, can be found in Snoeck *et al.*, 2019.

In this study, we subjected a segregating population (parental strains MR-VP and Wasatch, which are resistant and sensitive, respectively) to multiple rounds of selection by three METI-Is, and used BSA genetic mapping to identify loci responding to selection for each acaricide. While the H92R change played a significant role in resistance to each acaricide, one additional genomic region was significantly associated with resistance to both pyridaben and tebufenpyrad, and a further QTL was identified for tebufenpyrad resistance alone. The peak regions of response for both additional QTL harbored candidate genes encoding an enzyme or putative receptors associated directly or indirectly with xenobiotic detoxification (CPR, and two tandem NHR96-like genes lacking DBDs). The candidate genes, and in some cases putative variants for QTL, are discussed below, although for CPR and the NHR96-like genes our conclusions are speculative.

The target-site H92R variant in the PSST subunit was coincident with the most prominent peak in all three BSA scans (QTL 1). The unselected populations were relatively resistant compared to the susceptible parent (Figure 2), presumably reflecting the high frequency of the H92R variant in the unselected populations – about 0.5 after ~25 generations in the experimental evolution experiment (Figure S3) – likely reflecting the partially dominant nature of the change (Van Pottelberge *et al.*, 2009c). This pattern reveals that contrary to the fitness cost associated with some resistance mutations in *T. urticae* (Riga *et al.*, 2017) and the lethality of the corresponding substitution in *Drosophila melanogaster* (Bajda *et al.*, 2017), there is no major fitness cost associated with the *T. urticae* H92R substitution. The earlier work, as well as our current study, suggest that mutations occurring in this conserved part of the PSST subunit can have species-specific effects on fitness. Further, mutations in the adjacent PSST subunit residue M91 in the aerobic yeast *Yarrowia lipolytica* decreased enzymatic activity of complex I (Fendel, 2008), but had no effect on V_{max} when binding ubiquinone-1 and even increased V_{max} involving ubiquinone-2, which has a longer isoprenoid side chain (Angerer *et al.*, 2012; Fendel *et al.*, 2008).

In addition to the target-site change, mites selected to pyridaben and tebufenpyrad showed significant responses in other genomic regions. This was consistent with the previously reported incompletely dominant inheritance of tebufenpyrad resistance, but contradicted an earlier result, which classified resistance to pyridaben as monogenic (Van Pottelberge *et al.*, 2009c). The likely explanation is that Van Pottelberge and colleagues used a fairly recently collected outbred MR-VP strain, while we used an inbred derivative of the same strain after it had been maintained in the lab for ~11 years under constant selection (minor effect alleles may have been selected in the laboratory as acaricide concentrations become high enough to overcome target-site resistance).

Introgression of the H92R resistant allele into a sensitive background only resulted in a fraction (average of 578 mg L^{-1} (Bajda *et al.*, 2017)) of the MR-VP fenpyroximate resistance phenotype observed in both this study (>5000 mg L^{-1}) and in Van Pottelberge *et al.* (10,581 mg L^{-1}). Nevertheless, fenpyroximate resistance appeared to be monogenic in both Van Pottelberge *et al.* as well as in our study. While most of the resistance phenotype was likely due to multiple alleles of minor effect that could not be detected by our methods, it remains unknown why neither of the two genomic regions associated with selection to the other acaricides showed a significant association with fenpyroximate resistance. Evidence from functional cytochrome P450 expression

in *E. coli* as well as from the application of a selective P450-inhibiting synergist piperonyl butoxide (PBO) suggests that fenpyroximate's metabolism is different from that of pyridaben and tebufenpyrad (see below). The divergent genomic response to selection could thus be related to metabolic resistance, and specifically, to differences in P450-mediated detoxification.

The second most prominent BSA peak (QTL 2) in the tebufenpyrad- and pyridaben-selected *T. urticae* centered on a D384Y mutation in the electron transfer flavoprotein CPR (Wybouw *et al.*, 2019). CPR is an essential enzyme in all eukaryotes that serves as an electron donor protein for all microsomal P450s and several other enzymes found in the endoplasmic reticulum of most cells (Murataliev *et al.*, 2004). CPR was not differentially expressed in MR-VP compared to the METI-I susceptible strain London (Dermauw *et al.*, 2013b). Therefore, the D384Y mutation likely does not affect the expression of CPR. Instead, it is possible that the mutation is advantageous by improving P450 detoxification pathways.

The idea that a mutation in CPR can be implicated in resistance development by interacting with relevant P450s in *trans* is attractive, because detoxification of METI-Is is thought to be mostly P450-based (Cho *et al.*, 1995; Devine *et al.*, 2001; Herron and Rophail, 1998; Ozawa, 1994; Van Pottelberge *et al.*, 2009c). This, however, raises the question of why selection to fenpyroximate did not favor the mutation. Possible explanations include the relative specificity of P450s that metabolize acaricides as well as the relative specificity in the interactions of CPR with P450s. P450 specificity towards acaricides is supported by evidence that certain P450s target fenpyroximate, but do not act on the other two acaricides; CYP392A11, a P450 that is overexpressed in MR-VP compared to the METI-I sensitive strain London (Dermauw *et al.*, 2013b), hydrolyzes fenpyroximate but not pyridaben or tebufenpyrad when expressed in *E. coli* (Riga *et al.*, 2015). Evidence that other P450s may also fall into this pattern comes from treatment with the synergist PBO, which does not suppress every P450 equally (Feyereisen, 2015). Work on strain MR-VP prior to inbreeding showed that PBO significantly decreased resistance to pyridaben and tebufenpyrad, but had little effect on fenpyroximate resistance (Van Pottelberge *et al.*, 2009c), likely because PBO did not sufficiently target P450s that metabolize fenpyroximate. Specificity in the interactions of CPR with P450s is supported by evidence that human variants in CPR differentially affect various P450 activities (Burkhard *et al.*, 2017). The only known human CPR variant with increased activity is Q153R, and the effect of this mutation is positive on CYP19A1 and CYP3A4 activities but negative on CYP17A1 and CYP51A1 (Udhane *et al.*, 2017). Furthermore, P450 activity is directly related to the concentration of the CPR-P450 complex (Murataliev *et al.*, 2008), whose dissociation constant depends on the structure of each P450. Consequently, the D384Y mutation may have a greater effect on P450s that specifically metabolize pyridaben and tebufenpyrad.

It remains unclear from X-ray crystallography alone how the D384Y mutation can affect P450 activity. The position of D384 on the surface of the protein in the connecting domain of CPR would rule out an effect on FAD, FMN or NADP(H) binding. D384 is also located far from the short hinge region that allows the approximately 90-degree rotation of the FMN domain away from the FAD-linker domain seen between the open and closed conformations of CPR (Aigrain *et al.*, 2009; Hamdane *et al.*, 2009). It does not point towards the space expected to be occupied by P450s in

the open conformation of CPR, and superimposition of the open and closed structures indicates little if any movement of the residue at position D384. These considerations rule out a major effect on FAD to FMN to P450 electron transfer. The connecting domain and helix I of CPR are also predicted to remain distant from the ER membrane surface in either open or closed conformations (Laursen *et al.*, 2011). The D384Y mutation has not been documented in human variants of CPR (where the homologous mutation would be E394Y), and the closest human variants S397L or E398A are not associated with any known pathology (Burkhard *et al.*, 2017).

The D384Y mutation additionally introduces a YY dipeptide in the structure. The possible pi-stacking (McGaughey *et al.*, 1998) of the two adjacent aromatic rings might affect protein stability, or cause subtle long-range changes in conformational dynamics which are known to take place during catalysis (Murataliev and Feyereisen, 2000). Moreover, the solution structure of the CPR may differ from the crystal structure in subtle ways (Huang *et al.*, 2013). A model of the extended (open) conformation of human CPR based on solution NMR and small angle X-ray scattering experiments indicates that four residues of helix I of the connecting domain, including the homologous Q391, make polar interactions with the FMN domain (Huang *et al.*, 2013). If this model faithfully represents the changes in the structure of CPR during catalysis, then the most likely explanation for an effect of the D384Y mutation would be a subtle change in the stability of the interaction between the connecting domain and the FMN domain in the open conformation, which is the conformation in which electrons are transferred from FMN to P450s.

Given the conservation of sequence, the homologous mutation to D384Y would be E395Y in *D. melanogaster*. Therefore, the fly may be suitable for studying the effect of the mutation *in vivo* by a reverse genetic approach using CRISPR-Cas9 technology combined with homologous recombination-directed gene modification. An intriguing possibility to explore is that the D384Y mutation has a fitness cost to mites that are not exposed to pesticides. The BSA peak centering on the mutation results not from elevated MR-VP frequency in the acaricide-treated groups, but rather in relatively low MR-VP allele frequencies in mites from control populations (i.e., in the absence of selection, the variant rapidly decreased in allele frequency, Figure S3B-C); the same pattern was also observed when the genomic region surrounding the allele was associated with spirodiclofen resistance in SR-VP, a different strain of *T. urticae* (Wybouw *et al.*, 2019), in which it was also shown that P450s are involved in spirodiclofen resistance (Demaeght *et al.*, 2013; Van Pottelberge *et al.*, 2009b).

Another protein that may be involved in detoxification by way of P450 regulation is a DBD-lacking NHR96-like gene, *tetur06g04270*, which appears in two tandem copies in both sensitive and resistant parental strains; the genes fall roughly at the center of a minor BSA peak (QTL 3) in the tebufenpyrad-selected group (mites in the pyridaben-selected group also showed increased MR-VP allele frequency in that region, albeit not significantly). Most NHRs are transcription factors; a ligand-binding domain (LBD) interacts with hydrophobic signaling molecules, which then cause the NHR to affect transcription of select genes via its DNA-binding domain (DBD). The two NHR96-like genes are not canonical NHRs as they completely lack the DBD. Further genomic analyses revealed that in addition to the *tetur06g04270* genes, the *T. urtica*e genome contains 45 other NHR96-like genes

that contained the LBD but were missing the DBD, and that this gene expansion appears to be unique to *T. urticae* (although genome information is not yet available for other spider mite species).

NHRs are diverse and have many functions; they are classified into groups NR0 through NR6, and into subgroups according to their highly conserved domain structure, with non-canonical NHRs that lack either the LBD or the DBD classified as NR0 regardless of origin (Nuclear Receptors Nomenclature Committee, 1999). Our comprehensive search of the NCBI database showed that E75, E78, and FTZ-F1 DBD-lacking NHR-like genes appear to be common in arthropods, but while canonical E75s, E78s and FTZ-F1s are known for their role in metamorphosis, vitellogenesis and embryogenesis (Fahrbach *et al.*, 2012), little is known about the function of DBD-lacking NHR-like genes or how they interact with their targets. In *D. melanogaster*, DBD-lacking E75B acts by heterodimerizing with DHR3 (Reinking *et al.*, 2005), while a DBD-lacking DHR3 plays a role in regulating cell growth by interacting with *Drosophila* ribosomal protein S6 kinase in a yet unknown fashion (Montagne *et al.*, 2010). Since most of the work on arthropod NHRs has been done on *D. melanogaster*, and NHR96-like DBD-lacking genes are only known to be expanded in *T. urticae*, no information is currently available about their potential mode of action. Given *T. urticae*'s polyphagous lifestyle and pest status, a connection between NHR96-like DBD-lacking genes and xenobiotic metabolism is a possibility warranting further exploration, especially considering that *D. melanogaster*'s canonical NHR96 – which has the highest BLASTp match for either copy of *tetur06g04270* – has been implicated in detoxification. Xenobiotic-independent overexpression of NHR96 in *D. melanogaster* L3 larvae induced expression of detoxification genes (King-Jones *et al.*, 2006), and NHR96 overexpression in the Malpighian tubules increased DDT resistance (Afschar *et al.*, 2016). Additionally, adult NHR96 null mutants of *D. melanogaster* were more sensitive to chronic DDT exposure (King-Jones *et al.*, 2006), the sedative effects of phenobarbital (PB) (King-Jones *et al.*, 2006), permethrin (a pyrethroid) (Beaver *et al.*, 2010) and malathion (Afschar *et al.*, 2016). Many of the genes affected by either the NHR96 loss- or gain-of-function mutations encode members of the classic detoxification enzyme families: P450s, glutathione S-transferases (GSTs), carboxylesterases, and UDP-glucuronosyl transferases (UGTs) (King-Jones *et al.*, 2006). These gene families play key roles in detoxification across the animal kingdom, and some – like the P450s – have been expanded in *T. urticae* (Grbić *et al.*, 2011).

6. Conclusion

In this study, we compared and contrasted selection responses to three METI-I acaricides: fenpyroximate, pyridaben, and tebufenpyrad. We found that crossing a resistant strain of *T. urticae* to a susceptible one and separately selecting the offspring with the three acaricides did not yield the same genetic response. While a previously identified H92R target-site mutation was significantly associated with resistance to all three METI-I acaricides, we found that additional loci were associated with resistance to pyridaben and tebufenpyrad, including a genomic region previously associated with spirodiclofen resistance. This region included a variant in CPR, which may be responsible for improving the efficiency of relevant P450s, but at a likely fitness cost in the absence of acaricide treatment. A region connected with resistance to tebufenpyrad included two tandem

copies of NHR96-like genes that lacked a DNA-binding domain, and further manual annotation revealed a total of 47 such genes in *T. urticae*. An NCBI database search suggested that an expansion of these genes appears to be unique to *T. urticae*, and their function is currently unknown. Although the role of the CPR mutation and the DBD-lacking NHR96-like genes in xenobiotic resistance in *T. urticae* remain speculative, the link between the associated genetic regions and resistance to some, but not all, METI-Is, suggests that adaptation to treatment with those acaricides involves different pathways in the spider mite.

Funding information

This work was supported by the Research Foundation Flanders [grant numbers G009312N, G053815N], the European Research Council under the European Union's Horizon 2020 research and innovation programme [grant numbers 772026-POLYADAPT, 773902-SuperPest], the USA National Science Foundation [grant number 1457346], and the National Institutes of Health Genetics Training [grant number T32GM007464]. WD is a postdoctoral fellow of the Research Foundation Flanders (FWO). Research reported in this publication utilized the High-Throughput Genomics and Bioinformatic Analysis Shared Resource at the Huntsman Cancer Institute at the University of Utah and was supported by the National Cancer Institute of the National Institutes of Health [grant number P30CA042014]. The content is solely the responsibility of the authors and does not necessarily represent the official views of the funding agencies.

Supplementary information

All supplementary data can be found at https://doi.org/10.1016/j.ibmb.2019.04.011

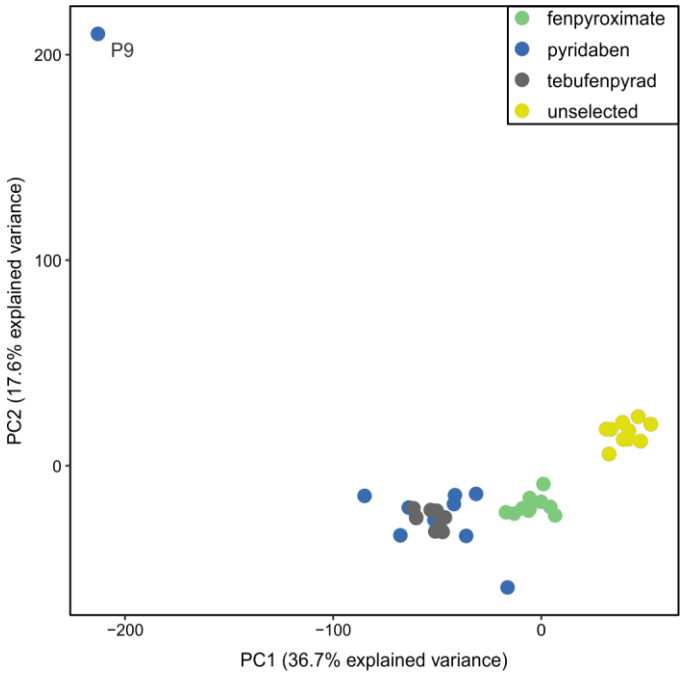

Figure S1. Principal component analysis (PCA) with control and selected populations based on genome-wide allele frequencies at polymorphic sites. Individual populations are colored according to the treatment group (legend, upper right). The extreme outlier in the pyridaben-selected group (population P9) had the genomic profile of an unknown strain not used in this study and was presumed to be contaminated. Hence, P9 was excluded from subsequent analyses.

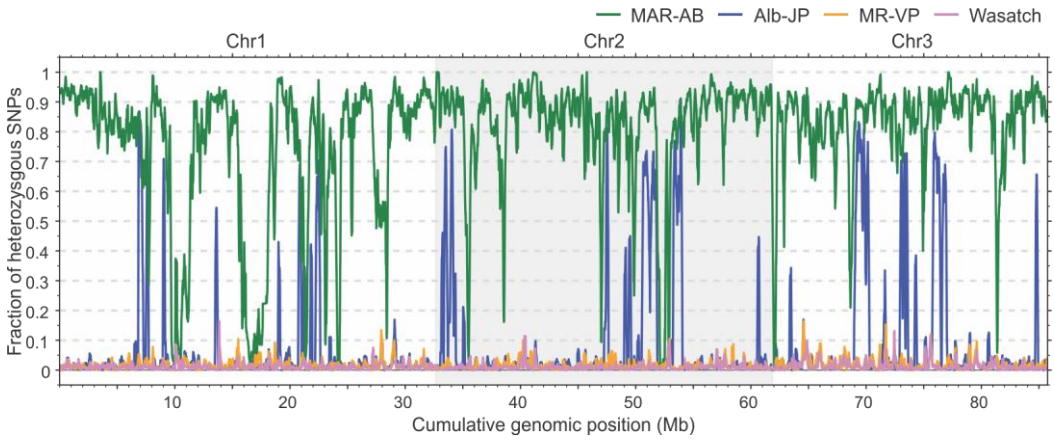

Figure S2. Fraction of heterozygous SNPs plotted across the genome in sliding windows of 150kb with a 10kb offset. Shown is apparent heterozygosity for the outbred strain MAR-AB, a strain that was mother-son (MS) inbred for one generation (Albino-JP) and two strains that were inbred for 6 or more generations (MR-VP and Wasatch).

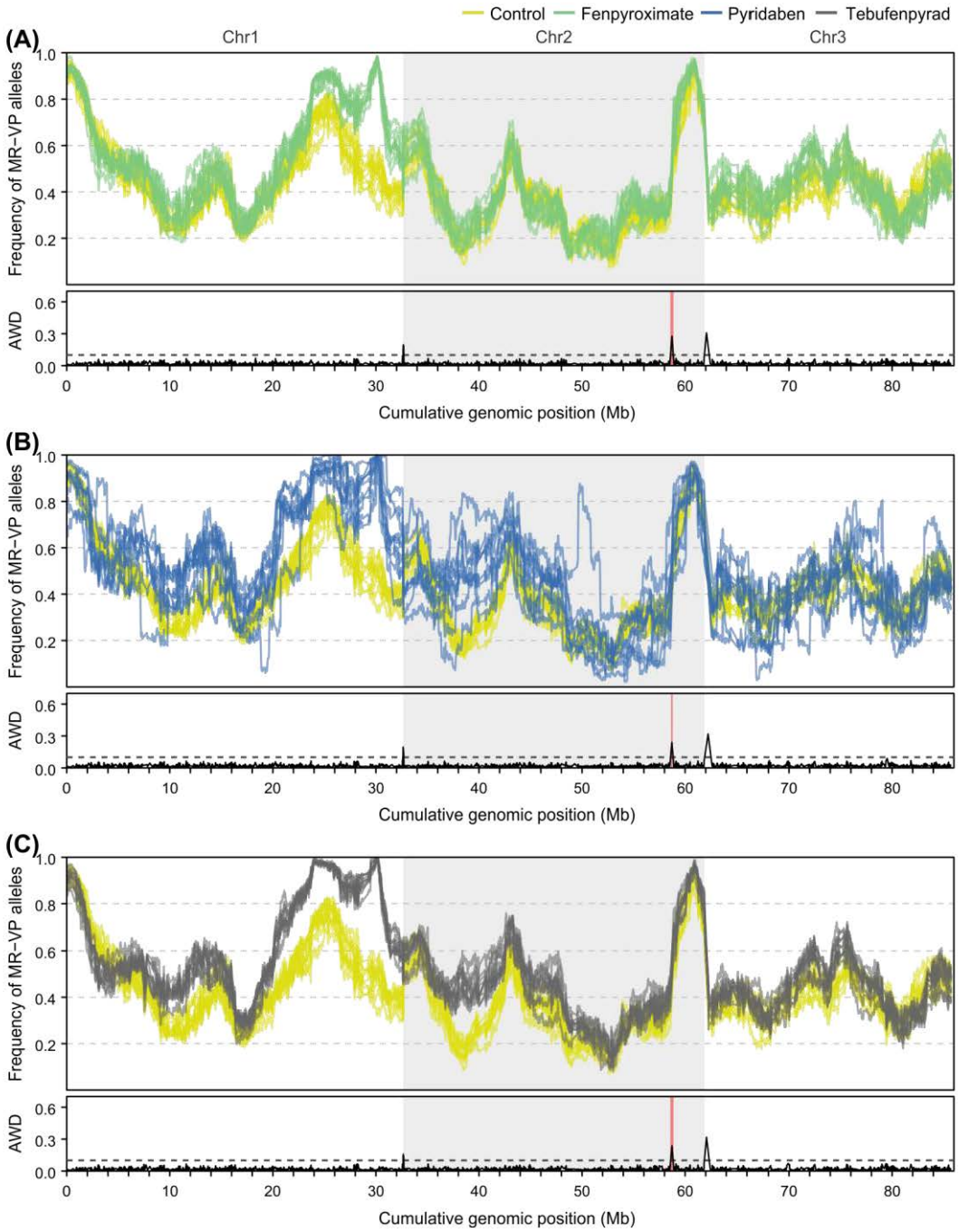

Figure S3. MR-VP allele frequency and average window distance (AWD) values calculated as per Wybouw *et al.* (2019). Each panel (A-C) corresponds to an individual acaricide selection experiment and consists of MR-VP allele frequency information for each relevant sample (top) and the AWD values (bottom) calculated based on the allele frequency information. The samples were colored according to the experimental treatment (legend in the top right corner). The AWD values were used to verify the three-chromosome assembly of Wybouw *et al.*

(2019), with the dashed line representing an AWD value of 0.1 – a threshold indicative of potential misassemblies. One common AWD peak in the fenpyroximate, pyridaben and tebufenpyrad data rises above the threshold (highlighted in red in the bottom panels). The AWD peak, however, was not supported as a misassembly in previous work. Overall, the AWD scan provides strong support for the three-chromosome assembly. The peaks in AWD values between the three chromosomes in the concatenated sequence are expected as they are not adjacent in the genome.

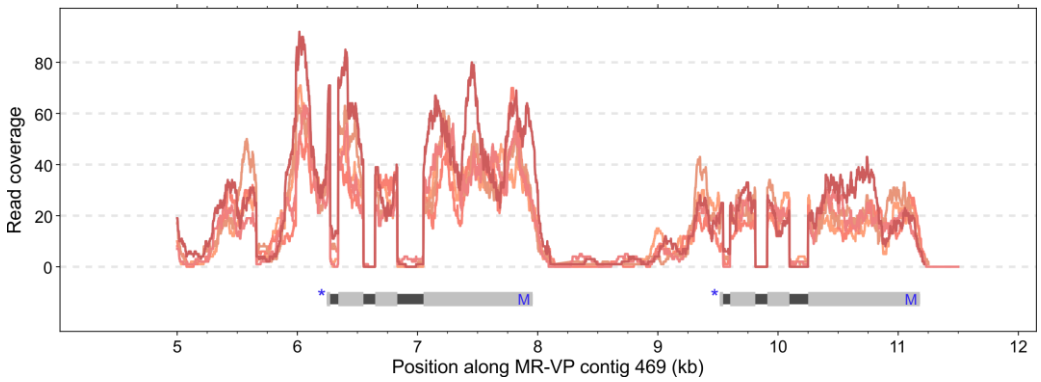

Figure S4 Read coverage of five MR-VP RNA-seq replicates that were aligned to a modified version of the three-chromosome assembly. The modified sequence contained an MR-VP *de novo* assembled contig in the region where *tetur06g04270* duplication was present in both strains MR-VP and Wasatch. The plot zooms in on the part of the contig where the two NHR-like genes are located in tandem. Genetic architecture is shown in the bottom panel with taller rectangles as coding exons, smaller rectangles as introns, "M"s as start codons, and stop codons as asterisks.

Table S1. Accession numbers used for maximum likelihood phylogenetic analysis of nuclear receptors.

Table S2. List of all genes in the 80kb top BSA peak 1 region at ~30Mb on Chr1.

locus_id	strand	start	stop	definition
tetur07g05380	+	3006092	30062624	DnaJ homolog subfamily B member 11 precursor
tetur07g05370	+	3006441	30065831	Myc-type, basic helix-loop-helix (bHLH) domain
tetur07g05360	+	3006754	30068102	Hypothetical protein
tetur07g05350	+	3006988	30080425	Bromodomain protein 4, C-terminal
tetur07g05330	+	3008079	30081662	Hypothetical protein
tetur07g05320	-	3008309	30084201	cytochrome b-c1 complex subunit 7
tetur07g05310	-	3008679	30091676	long-chain fatty acid transport protein 1
tetur07g05300	-	3009545	30098525	Growth factor; receptor
tetur07g05290	+	3009857	30098806	Hypothetical protein
tetur07g05280	-	3009891	30099707	Hypothetical protein
tetur07g05270	-	3009991	30101331	Hypothetical protein
tetur07g05260	-	3010223	30103663	trans-2-enoyl-CoA reductase; mitochondrial precursor
tetur07g05250	-	3010442	30106177	lecithin-cholesterol acyltransferase
tetur07g05240	-	3010790	30108889	NADH dehydrogenase; PSST subunit
tetur07g05220	+	3010896	30109990	serine/threonine-protein kinase 3
tetur07g05210	+	3011253	30115075	Pheromone shutdown, TraB
tetur07g05200	+	3011700	30121882	P-loop containing nucleoside triphosphate hydrolase
tetur07g05190	+	3012239	30125909	translocation protein SEC63 homolog
tetur07g05180	+	3012653	30133880	Tubulin/FtsZ; C-terminal

tetur07g05170	+	3013530	30135533	Hypothetical protein
tetur07g05160	+	3013584	30139508	LY6_UPAR protein

Table S3. List of all genes in the 75kb top BSA peak 2 region at ~5.7Mb on Chr2.

locus_id	strand	start	stop	definition
tetur18g03340	-	5695109	5697050	vesicular acetylcholine transporter
tetur18g03350	-	5700933	5705078	Hypothetical protein
tetur18g03360	+	5706103	5708320	hypothetical protein
tetur18g03370	+	5711979	5712814	archease
tetur18g03380	-	5713069	5713698	large subunit ribosomal protein 23
tetur18g03390	-	5714612	5718880	NADPH cytochome P450 reductase
tetur18g03400	+	5720043	5720491	Hypothetical protein
tetur18g03410	-	5721867	5723368	Folate-binding; YgfZ
tetur18g03420	+	5723969	5726121	Hypothetical protein
tetur18g03430	+	5726607	5728998	DDB1- and CUL4-associated factor 12
tetur18g03440	+	5729912	5730999	Hypothetical protein
tetur18g03450	+	5731332	5735868	PREDICTED: similar to NP95
tetur18g03721	-	5735665	5736837	Chemosensory Receptor; Gustatory receptor family
tetur18g03791	-	5737734	5738891	Chemosensory Receptor; Gustatory receptor family
tetur18g03801	-	5740027	5741194	Chemosensory Receptor; Gustatory receptor family
tetur18g03811	-	5744514	5745752	Chemosensory Receptor; Gustatory receptor family
tetur18g03852	-	5746933	5747712	Chemosensory Receptor; Gustatory receptor family
tetur18g03821	-	5748183	5749331	Chemosensory Receptor; Gustatory receptor family
tetur18g03831	-	5749737	5750908	Chemosensory Receptor; Gustatory receptor family
tetur18g03841	-	5751223	5752427	Chemosensory Receptor; Gustatory receptor family
tetur18g03470	-	5753113	5754272	Chemosensory Receptor; Gustatory receptor family
tetur18g03480	-	5755262	5756427	Chemosensory Receptor; Gustatory receptor family
tetur18g03741	-	5757260	5758432	Chemosensory Receptor; Gustatory receptor family
tetur18g03731	-	5758670	5759841	Chemosensory Receptor; Gustatory receptor family
tetur18g03490	-	5761067	5761411	Hypothetical protein
tetur18g03500	+	5763261	5763606	Hypothetical protein
tetur18g92107	+	5766318	5766774	hypothetical protein

Table S4. List of all genes in the 75kb top BSA peak 3 region at ~12.5Mb on Chr1.

locus_id	strand	start	stop	definition
tetur06g04180	+	1244684	1245751	vacuolar protein sorting 39
tetur06g04190	+	1245751	1245917	galactosyltransferase; putative
tetur06g04200	-	1246563	1246583	Hypothetical protein
tetur06g04210	+	1246613	1247115	CCAAT/enhancer binding protein alpha
tetur06g04220	+	1248282	1248615	SRY sex determining region Y-box 9
tetur06g06761	-	1248635	1248856	Serine proteases, trypsin family, histidine active site
tetur06g04240	+	1248688	1248790	mitochondrial import inner membrane translocase subunit Tim23
tetur06g04250	-	1248863	1249056	Sec1-like protein
tetur06g04260	-	1249180	1249200	Hypothetical protein
tetur06g04270	-	1249357	1249529	Nuclear hormone receptor, ligand-binding domain
tetur06g04280	-	1249637	1249791	PREDICTED: similar to lactation elevated 1
tetur06g04290	-	1249923	1250410	fermitin family homolog 2
tetur06g04300	+	1250446	1250740	Letm1 ribosome-binding domain
tetur06g04310	-	1250740	1250830	mitochondrial import inner membrane translocase subunit Tim23
tetur06g04340	-	1250927	1252711	G-protein coupled receptor for tachykinin

File S1. *De novo* assembled contigs of strains MR-VP and Wasatch that span the DNA-binding domain (DBD)-lacking nuclear hormone receptor 96 (NHR96) like gene (*tetur06g04270*) in the QTL underlying resistance to tebufenpyrad.

File S2. Peptide sequences of tandemly duplicated DBD-lacking NHR96-like genes (annotated as a single gene, *tetur06g04270,* in the London reference genome) in strains MR-VP and Wasatch, as verified by open reading frame (ORF) predictions as well as RNA-seq alignments.

File S3. Genes newly annotated as DBD-lacking NHR96-like in the London assembly of *T. urticae.*

Author contributions

TVL and RMC designed the experiment. SB, EVP and WD conducted the experiments. Analysis and interpretation of the results was done by SS, AK, SB, RF, OK, RG and WD. The manuscript was written by SS, AK and RF, all figures were prepared by SS and AK. All authors reviewed the manuscript.

Chapter 3

The effect of insecticide synergist treatment on genome-wide gene expression in a polyphagous pest

This chapter has been partially redrafted from:

Snoeck, S., Greenhalg, R., Tirry, L., Clark, R.M., Van Leeuwen, T., Dermauw, W. (2017) The effect of insecticide synergist treatment on genome-wide gene expression in a polyphagous pest. Scientific reports, 7(1), 13440.

1. Abstract

Synergists can counteract metabolic insecticide resistance by inhibiting detoxification enzymes or transporters. They are used in commercial formulations of insecticides, but are also frequently used in the elucidation of resistance mechanisms. However, the effect of synergists on genome-wide transcription in arthropods is poorly understood. In this study we used Illumina RNA-sequencing to investigate genome-wide transcriptional responses in an acaricide resistant strain of the spider mite *Tetranychus urticae* upon exposure to synergists such as S,S,S-tributyl phosphorotrithioate (DEF), diethyl maleate (DEM), piperonyl butoxide (PBO) and cyclosporin A (CsA). Exposure to PBO and DEF resulted in a broad transcriptional response and about one third of the differentially expressed genes (DEGs), including cytochrome P450 monooxygenases and UDP-glycosyltransferases, was shared between both treatments, suggesting common transcriptional regulation. Moreover, both DEF and PBO induced genes that are strongly implicated in acaricide resistance in the respective strain. In contrast, CsA treatment mainly resulted in downregulation of Major Facilitator Superfamily (MFS) genes, while DEGs of the DEM treatment were not significantly enriched for any GO-terms.

2. Introduction

Insecticide resistance is a major threat for the agricultural productivity of commercial crops (Pimentel, 2005), and understanding the mechanisms underlying insecticide resistance is a high priority for the design and implementation of effective resistance management programs (Sparks and Nauen, 2015). Resistance mechanisms can generally be classified into either (1) changes in sensitivity of the target-site due to point mutations, or to (2) increased metabolic detoxification through qualitative or quantitative changes in enzymes involved in the detoxification process. The latter process typically occurs in 3 phases. In phase I, the insecticide is functionalized with nucleophilic groups (a hydroxyl, carboxyl or amine group) to make it more reactive and water soluble. In phase II, conjugation occurs with endogenous molecules (such as glutathione (GSH) or sugars), further increasing the compound's polarity. Ultimately, in phase III, the phase II conjugated product is excreted by cellular transporters. Cytochrome P450 monooxygenases (P450s) and carboxyl/choline esterases (CCEs) are well-known examples of enzymes that are responsible for phase I reactions while glutathione-S-transferases (GSTs) and UDP-glycosyltransferases (UGTs) are enzymes that typically operate during phase II. Finally, in phase III, metabolites are often transported out of the cell by ATP-binding cassette (ABC) transporters and solute carrier proteins, of which a major class are proteins of the Major Facilitator Superfamily (MFS) (Feyereisen *et al.*, 2015; Van Leeuwen and Dermauw, 2016).

Insecticide synergists are defined as "compounds that greatly enhance the toxicity of an insecticide, although they are usually practically nontoxic on their own" (Matsumura, 1985). They can either act as a surrogate substrate or an inhibitor of detoxification enzymes and transporters and, as such, are a powerful tool to investigate insecticide resistance mechanisms. Synergists are also of commercial interest as combining them with insecticides increases efficacy and aids in keeping pesticide use to a minimum (Bernard and Philogène, 1993; Casida, 1970; Raffa and

Priester, 1985). As a result of the fast and widespread development of resistance, coupled with the slowdown in the number of registrations of new *pesticides* and a new trend towards “greener” and more “sustainable” pest management (Beck *et al.*, 2012), a renewed interest has arisen in the identification and development of plant-based synergists (Hill, 2008; Joffe *et al.*, 2012; S. Liu *et al.*, 2014). However, as of yet relatively few of these new synergists have made the transition from the laboratory to the field or greenhouse.

The most well-known and commonly used commercial insecticide synergist is the methylene dioxyphenyl compound piperonyl butoxide (PBO), an inhibitor of P450s. PBO has been commercially used since 1940, and since the seventies mainly in combination with pyrethroid insecticides. Its lack of specificity in P450 inhibition has contributed to its success as a synergist (Feyereisen, 2015). The inhibition mechanism of PBO consists of two phases, starting with the binding of PBO to the active site of the P450, followed by the formation of a quasi-irreversible inhibitor complex between the electrophilic carbene moiety of PBO and the ferrous iron of the P450 (Casida, 1970; Correia and Ortiz de Montellano, 2005; Feyereisen *et al.*, 1984). Synergists such as the defoliant S,S,S-tributyl phosphorotrithioate (also known as tribufos, DEF or TBPT), the fungicide iprobenfos (IBP) and triphenyl phosphate (TPP) are well-known carboxyl esterase inhibitors (Plapp *et al.*, 1963; Yeoh *et al.*, 1982). These organophosphorus compounds (OPs) behave like the natural substrate of esterases and enter the active site where they covalently bind to the serine –OH group. Subsequently, the OP is split, with the enzyme being irreversibly phosphorylated, and regeneration of the free enzyme by hydrolyzation not possible (Sogorb and Vilanova, 2002; World Health Organization, 1986). An additional major synergist is the carbonyl compound diethyl maleate (DEM) that is known to conjugate reduced glutathione (GSH), thereby depleting cells of this tripeptide. As a consequence, it reduces the ability of GSTs to utilize GSH for conjugation with insecticides or with the oxidative stress products they induce (Boyland and Chasseaud, 1970; Che-Mendoza *et al.*, 2009; Fujioka and Casida, 2007). Finally, verapamil and cyclosporin A are well-known first generation modulators (competitive inhibitors) of vertebrate P-glycoproteins (ABC transporters of the B subfamily) (Foxwell *et al.*, 1989; Litman *et al.*, 1997; Yusa and Tsuruo, 1989). Human P-glycoproteins are well-known for their role in protecting tissues from toxic xenobiotics and endogenous metabolites (Sharom, 2011) and in the last decade their counterparts in arthropods have also been linked to insecticide transport and/or resistance (Dermauw and Van Leeuwen, 2014; Merzendorfer, 2014). For example, pretreatment with verapamil has been shown to markedly enhance the toxicity of DDT or abamectin in *Drosophila* (Luo *et al.*, 2013; Strycharz *et al.*, 2013)

Synergists, however, do not always act as intended or expected. A frequently reported unanticipated effect is an altered cuticular penetration of the insecticide after pretreatment with a synergist (Gunning *et al.*, 1995; Kennaugh *et al.*, 1993; Sanchez-Arroyo *et al.*, 2001; Sun and Johnson, 1972). In some cases, synergists might also inhibit non-target enzyme systems. PBO has been reported to act as an inhibitor of esterases in *Helicoverpa armigera*, *Frankliniella occidentalis* and *Bemisia tabaci* (López-Soler *et al.*, 2011; Young *et al.*, 2006, 2005) and as an inhibitor of mammalian UGTs (Lucier *et al.*, 1971), while DEF was shown to act, albeit to a much lower extent compared to PBO, as an inhibitor of P450s in *Blatella germanica* (Sanchez-Arroyo *et al.*, 2001).

These studies suggest that in some cases caution should be applied in interpreting results of synergist application as they are not entirely specific to a single detoxification enzyme class (Espinosa *et al.*, 2005; Gunning *et al.*, 1998; López-Soler *et al.*, 2011). However, inhibition of these non-target enzyme systems typically occur in a non-specific way at high synergist concentrations (Philippou *et al.*, 2013; Valles *et al.*, 1997), and results can be cross-checked. For example, confirmation of P450 rather than esterase inhibition by PBO is straightforward and can be done with another class of P450 inhibitors (Feyereisen, 2015).

Insects and mites are known to display a massive and rapid reprogramming of gene expression in response to xenobiotic exposure (Dermauw *et al.*, 2013b; Perry *et al.*, 2011; Wybouw *et al.*, 2015). While synergist compounds are mostly used at concentrations that cause no or very low mortality, they are nonetheless used at high enough concentrations to cause maximal inhibition of the targeted detoxification enzymes (Scott, 1990). Hence, one might expect that synergists also induce gene expression changes on their own (Bernard and Philogène, 1993). Little is known, however, regarding the genome-wide transcriptional changes in arthropods exposed to synergists. Using a full genome and custom ”detox” microarray it was found that a subset of P450s and GSTs, and to a lesser extent UGTs, were induced in *Drosophila melanogaster* upon exposure to PBO (Willoughby *et al.*, 2007), while, using Illumina RNA sequencing, a P450 was shown to be upregulated in the whitefly *B. tabaci* upon exposure to PBO + cypermethrin as compared to cypermethrin alone (Zimmer *et al.*, 2017). However, genome-wide transcriptional changes upon exposure to synergist compounds other than PBO have not been investigated in any herbivorous arthropod pest.

The two-spotted spider mite, *Tetranychus urticae* (Arthropoda: Chelicerata: Acari: Tetranychidae), is a highly polyphagous agricultural pest that is able to colonize more than 1100 plant species (Migeon *et al.*, 2010). Further, among arthropods *T. urticae* is also considered to be the ”pesticide resistance champion” based on the total number of different pesticides to which populations have become resistant (Van Leeuwen *et al.*, 2014, 2010). Synergists such as PBO, DEF and DEM have been frequently used for the identification of metabolic resistance pathways in *T. urticae* (Khalighi *et al.*, 2014; Kim *et al.*, 2006, 2004; Rauch and Nauen, 2002; Stumpf and Nauen, 2002; Tsagkarakou *et al.*, 2002; Van Leeuwen *et al.*, 2004; Van Leeuwen and Tirry, 2007; Van Pottelberge *et al.*, 2009c; Yang *et al.*, 2001), and a high quality Sanger genome assembly is available for this mite species (Grbić *et al.*, 2011). *T. urticae* is therefore an ideal arthropod herbivore to study the impact of synergists at the transcriptional level. In this study, we used Illumina HiSeq 250 technology to generate deep paired-end, strand-specific RNA-seq reads from adult *T. urticae* females that were exposed for 24 hours to either DEF, DEM, PBO, CsA or formulation only. Subsequent differential expression (DE) analyses allowed us to identify genes for which expression was significantly altered upon exposure to synergists. A selection of differentially expressed genes (DEGs) was validated by qPCR and for each comparison (synergist compared to formulation) a Gene Ontology (GO) analysis was performed to shed light on the types of genes and pathways that respond to synergist exposure.

3. Materials and methods

3.1. Mite strains and chemicals

The JP-R strain has previously been described by Khalighi *et al.* (Khalighi *et al.*, 2015). Briefly, this strain is resistant to both cyenopyrafen (LC_{50} of 291 mg L^{-1}) and cyflumetofen (LC_{50} of 146 mg L^{-1}). In addition, cyenopyrafen toxicity in the JP-R strain is synergized by PBO and DEF, while DEM synergizes cyflumetofen toxicity (Khalighi *et al.*, 2015). The JP-R strain was maintained on potted bean plants, *Phaseolus vulgaris* L. var. Prelude, sprayed with 200 mg a.i. cyenopyrafen L^{-1} (STARMITE, 30% SC) until run-off. For the week prior to collection of RNA, the strain was maintained on bean plants without cyenopyrafen selection pressure. The synergists DEF (97% purity), DEM (97% purity) and PBO (90% purity) were of analytical grade and purchased from Sigma-Aldrich (Belgium). CsA had a purity of more than 98% and was purchased from Enzo Life Sciences (Belgium).

3.2. Synergist bioassays

The synergist bioassays were performed as described earlier by Van Pottelberge *et al.* 2009. Briefly, synergists were dissolved in a mixture of N,N-dimethylformamide and emulsifier W (alkylarylpolyglycolether, 3:1 w/w, respectively) and subsequently diluted with deionized water 100-fold. The concentrations used for PBO (1000 ppm), DEF (500 ppm) and DEM (2000 ppm) were identical to those in Khalighi *et al.* and Van Pottelberge *et al.* (Khalighi *et al.*, 2014; Van Pottelberge *et al.*, 2009c) and are known to cause between 5 and 10% mortality. Based on preliminary experiments a concentration of 50 ppm CsA was used, resulting in maximum 5 to 10% mortality. About 30 3-5 day old adult females were transferred to the upper (adaxial) side of a 9 cm^2 square-cut kidney bean leaf discs placed on wet cotton wool. Leaf discs were sprayed at 1 bar pressure in a Cornelis spray tower with 650µl spray fluid (1.56 ± 0.04mg fluid deposit cm^{-2}) containing one of the synergists (DEF, DEM, PBO, CsA) or formulation (FORM; N,N-dimethylformamide and emulsifier W (3:1 w/w) diluted in deionized water 100-fold) only. Unsprayed mites (CON) served as an additional control. About 600 mites (20 leaf discs with mites) were used for each treatment (DEF, DEM, PBO or CsA) and for the controls (FORM, CON). Next, leaf discs were placed in a climatically controlled room at 26°C, 60% RH with a 16:8h light:dark photoperiod. After 24 hours, living mites were scored and collected for RNA extraction. Mites were scored as being alive if they could walk normally after being prodded with a camel's hair brush.

3.3. RNA-seq

Total RNA was extracted from about 100 adult female mites (collected from at least four different leaf discs) using the RNeasy mini kit (Qiagen, Belgium) with four-fold biological replication for each treatment (PBO, DEF, DEM, CsA) and the controls (FORM, CON). The quality and quantity of the total RNA was analyzed by a DeNovix DS-11 spectrophotometer (DeNovix, USA) and by running an aliquot on a 1% agarose gel. From the RNA samples, Illumina libraries were constructed with the TruSeq Stranded mRNA Library Preparation Kit with polyA selection (Illumina, USA), and

the resulting libraries were sequenced on an Illumina HiSeq 2500 to generate strand-specific paired reads of 2 x 125 bp (library construction and sequencing was performed at the High-Throughput Genomics Core of the Huntsman Cancer Institute, University of Utah, Utah, USA). Prior to read-mapping, the quality of the reads was verified using FASTQC version 0.11.4 (Andrews, 2010) (no reads flagged as poor quality or as containing adapter sequences were used in downstream analyses).

3.4. Expression quantification and principal component analysis (PCA)

All reads were aligned to the *T. urticae* genome (Grbić *et al.*, 2011) using the two-pass alignment mode of STAR 2.5.0a (Dobin *et al.*, 2013) with a maximum intron size set to 20 kb. Resulting BAM files were subsequently sorted on read name by using SAMtools 0.1.19 (Li *et al.*, 2009). Read counts per gene using the most recent *T. urticae* annotation (version of June 23, 2016) were then obtained using the default settings of HTSeq 0.6.0 (Anders *et al.*, 2015) with the "STRANDED" flag set to "yes" and the "feature" flag set to "exon". A PCA was created as described by Love *et al.* (Love *et al.*, 2015). Briefly, read counts were first normalized using the regularized-logarithm (rlog) transformation implemented in the DESeq2 (version 1.12.2) R-package (Anders *et al.*, 2013). A PCA was then performed using the stats (version 3.3.0) and ggplot2 (version 2.2.0) R-packages with the 5000 most variable genes across all RNA-seq samples.

3.5. Differential expression (DE) analysis and gene ontology (GO) enrichment analysis

A differential expression (DE) analysis was performed using DESeq2 (version 1.12.2) (Anders *et al.*, 2013) and the read count data obtained by HTSeq (see above). Differentially expressed genes (DEGs, fold change (FC) ≥ 1.5 and Benjamini-Hochberg (Benjamini and Hochberg, 1995) adjusted p-value < 0.05) were determined between unsprayed mites (CON), mites treated with DEF, DEM, PBO or CsA and mites treated with formulation (FORM) (five DE comparisons in total: FORM vs. CON, DEF vs. FORM, DEM vs. FORM, PBO vs. FORM and CsA vs. FORM). For the GO enrichment analysis, the complete *T. urticae* proteome (19087 sequences, version of June 23, 2016) was first used as query in a blastp search against the non-redundant protein database in NCBI (version of October 31, 2016) using the following settings " -outfmt 5 -evalue 1e-5 -word_size 3 -show_gis -num_alignments 20 -max_hsps_per_subject 20". The resulting blastp output was then loaded into the Blast2GO (version 4.0.7) program and *T. urticae* proteins were annotated using the default parameters (Conesa *et al.*, 2005). InterProScan 5 and ANNEX were used to augment the annotation of GO terms. GO terms were condensed using the generic GO Slim subset. For the DESeq2 output of four DE comparisons (DEF vs. FORM, DEM vs. FORM, PBO vs. FORM and CsA vs. FORM), a GO enrichment analysis was performed using the Bioconductor package GOSeq (version 1.24.0) (Young *et al.*, 2010a), which explicitly takes into account gene selection bias due to differences in transcript length (Young *et al.*, 2010b). The resulting p-values from GOSeq were corrected using the Benjamini-Hochberg method (Benjamini and Hochberg, 1995) and only those GO categories with an adjusted p-value of less than 0.05 were

considered significantly enriched. Gene expression heatmaps were generated using the relative transcript levels (fold changes) of four DE comparisons (DEF vs. FORM, DEM vs. FORM, PBO vs. FORM and CsA vs. FORM) and the limma (version 3.28.21) and gplots (version 3.0.1) packages in the R environment. Transcription factor, P450 and UGT gene lists were obtained from previous studies (Ahn *et al.*, 2014; Grbić *et al.*, 2011; Phuong, 2014) while the MFS gene list consisted of those from Dermauw *et al.*, 2013b and those that were differentially expressed in the CsA treatment (Supplementary Table S6). Genes with no read counts in all four DE comparison were not included in the heatplot. Finally, genes were clustered using a Euclidean distance metric and Ward's method.

3.6. qPCR

To validate the RNA-seq results, gene specific primers were designed for differentially expressed *T. urticae* genes (8 up- and 5 downregulated genes) using Primer 3 v.4.0.0 (Rozen and Skaletsky, 2000). The qPCR primers used, including the primers for the genes of interest, as well as those for the two reference genes, ribosomal protein gene RP49 and ubiquitin, can be found in Supplementary Table S8. Total RNA was extracted as described above and cDNA was synthesized with the Maxima First Strand cDNA kit (Fermentas Life Sciences, Aalst, Belgium) and 1.5 µg of total RNA. Three biological and two technical replicates were used and non-template controls were added to exclude sample contamination. The qPCR analysis was performed on a Mx3005P qPCR thermal cycler (Stratagene, Agilent Technologies, Diegem, Belgium) with Maxima SYBR Green qPCR Master Mix and ROX solution (Fermentas Life Sciences, Aalst, Belgium) according to the manufacturer's instructions. The run conditions were as follows: 95°C for 10m followed by 35 cycles of 95°C for 15s, 55°C for 30s, 72°C for 30s. At the end of these cycles, a melting curve was generated (from 65°C to 95°C, 1°C per 2s) to check the presence of a single amplicon. Fourfold dilution series of pooled cDNA were used to determine the standard curves and amplification efficiencies for every gene-specific primer pair. The efficiencies were incorporated in the calculations of the expression values. Relative expression levels and significant gene expression differences (one-sided unpaired t-test) were calculated with qbase+ version 3.0 (Hellemans *et al.*, 2007).

3.7. Data availability and image processing

The RNA-seq expression data generated during the current study are available in the Gene-Expression Omnibus (GEO) repository with accession number GSE98293. CorelDRAW Home & Student X7 and SigmaPlot 12.0 software was used for processing of images.

4. Results

4.1. Synergist bioassays and RNA-seq

Adult female mites of the JP-R strain were either not sprayed (CON) or sprayed with PBO (1000 ppm), DEF (500 ppm), DEM (2000 ppm), CsA (50ppm) or formulation (FORM; N,N-dimethylformamide and emulsifier W (3:1 w/w) diluted in deionized water 100-fold) and collected after 24 hours, a commonly used time point in synergist studies (Khalighi *et al.*, 2015, 2014; Van

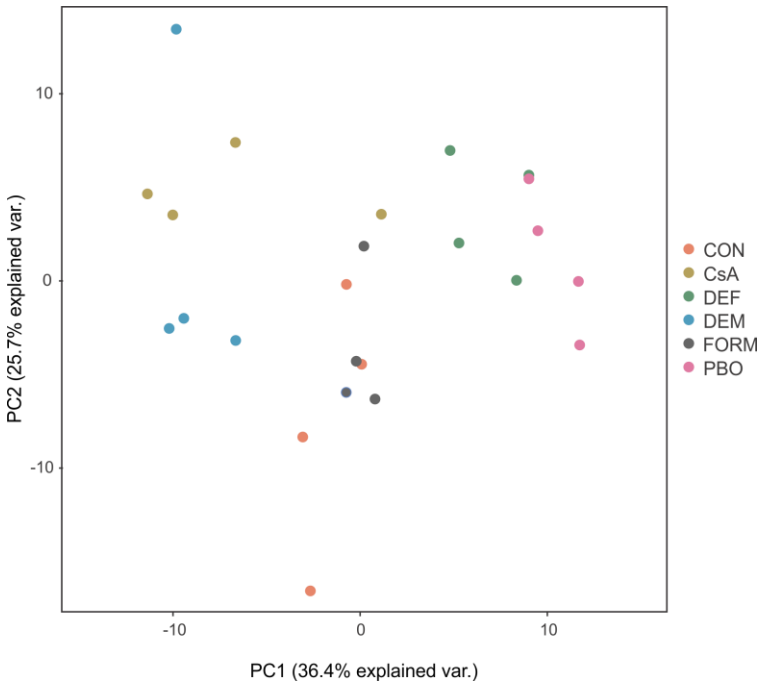

Figure 1 - Gene expression relationships among synergist treatments and controls. PCA plot of gene expression levels in untreated adult *T. urticae* females (CON), adult *T. urticae* females sprayed with formulation only (FORM) or adult *T. urticae* females exposed to synergist compounds CsA, DEF, DEM or PBO.

Leeuwen *et al.*, 2006; Van Pottelberge *et al.*, 2009a). Mortality for each treatment was scored, and found to be in line with those of previous reports for that strain (Khalighi *et al.*, 2014). Mites alive at 24 hours were collected for each treatment (PBO, DEF, DEM, CsA) and the controls (CON, FORM) and used for RNA extraction and RNA-seq library generation. Illumina sequencing generated ~82-92 million strand-specific paired end reads per sample. Alignment of RNA-seq reads against the *T. urticae* annotation resulted in an overall mapping rate of uniquely mapped reads of 83.01 ± 0.19 SE% across samples (Supplementary Table S1).

4.2. Principal component analysis (PCA)

A PCA revealed that about forty percent (36.8%) of the total variation could be explained by PC1 while PC2 accounted for 25.7 % of the variation (Figure 1). Except for replicate 4 of the CsA treatment, biological replicates clustered by treatment on PC1 relatively well. On the other hand, all replicates of the CsA treatment clustered relatively well on PC2. Interestingly, in the PCA the expression data of PBO treatments clustered most closely with those of the DEF treatments, those of the FORM treatments grouped with those of unsprayed mites (CON), and those of the CsA treatments grouped with those of the DEM treatments.

4.3. Gene-set enrichment analysis

We used DESeq2 to perform differential gene expression (DEG) analyses between treatments and controls (fold change (FC) ≥ 1.5 and a Benjamini-Hochberg adjusted p-value < 0.05)

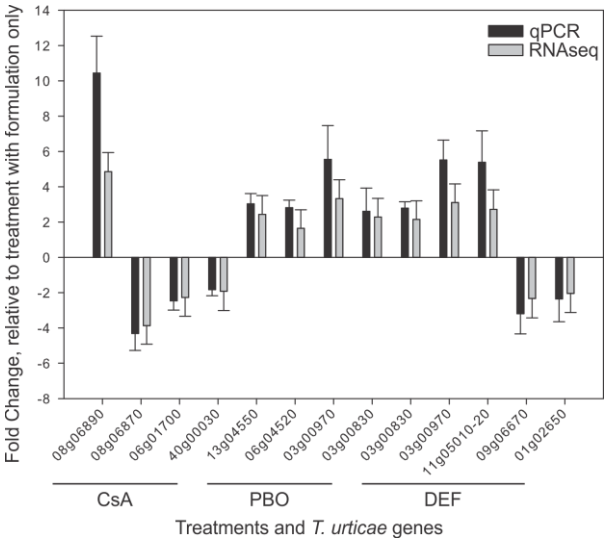

Figure 2 - qPCR validation of differentially expressed genes in adult *T. urticae* females after PBO, DEF or CsA treatment. Eight up- and five downregulated genes as assessed by differential gene expression (DESeq2) analysis of RNA-seq data were selected for qPCR analysis. Error bars represent the standard error of the calculated mean. Except for *tetur40g00030* (CsA treatment), each gene was significantly differentially expressed (based on an unpaired t-test) compared to the reference condition (FORM).

(Wang *et al.*, 2014). Between mites sprayed with formulation and unsprayed mites, only one gene (*tetur13g00990*, coding for an "orphan secreted protein") was differentially expressed (FC of 1.53), indicating that the formulation on its own had no significant effect on gene expression. Next, we compared gene expression levels between mites treated with one of the synergists and mites that were treated with formulation only. One hundred and sixty-two genes were differentially expressed between mites treated with PBO and mites treated with formulation, of which 77 were downregulated and 85 upregulated (Supplementary Table S2). The top twenty down- and upregulated genes had a FC of -2.11 to -1.74 and 1.86 to 3.33 respectively. For the DEF treatment, 174 genes were differentially expressed, of which 69 were downregulated and 105 were upregulated (Supplementary Table S3). The expression level of the 20 most down- and upregulated genes varied from a FC of -2.33 to -1.73 and 1.88 to 3.10, respectively. For the DEM treatment, 78 genes were differentially expressed, with 17 genes being downregulated and 61 upregulated and the expression level of the 20 most down- and upregulated genes varied from a FC of -2.3 to -1.5 and 1.7 to 2.1, respectively (Supplementary Table S4). Finally, for the CsA treatment, 58 genes were differentially expressed. Forty-two of them were downregulated, while 16 were upregulated and the expression level of the 20 most downregulated genes varied from -3.87 to -1.72 (Supplementary Table S5). For a selection of genes, the differential expression analyses based on RNA-seq were consistent with differential expression as validated independently by qPCR (Figure 2). As shown in Figure 3, the majority of DEGs were not shared between the different treatments. Only one upregulated gene was in common for all treatments (*tetur01g06580*, a sodium dependent glucose transporter), while two upregulated genes (*tetur16g03490* and *tetur11g05520*, coding for an antigen B membrane protein and CYP385C4, respectively) were shared between the PBO, DEF and CsA treatments. In contrast, 60 DEGs (37% and 35% of the total number of DEGs for the PBO and DEF

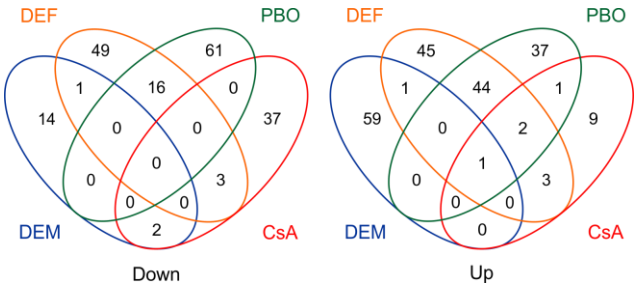

Figure 3 - Venn diagrams depicting overlap among differentially expressed genes of adult *T. urticae* females exposed to either PBO, DEF, DEM or CsA compared to adult *T. urticae* females treated with formulation only. Left panel: downregulated genes, right panel: upregulated genes.

treatment, respectively) were shared between PBO and the DEF treatment and had the same direction of fold change, with 44 genes being upregulated and 16 being downregulated.

4.4. GO enrichment and cluster analysis

We next performed GO enrichment analyses for the various differentially expressed gene sets. For the DEGs of the DEM treatment, no significantly (Benjamini-Hochberg adjusted p-value < 0.05) enriched GO terms were identified, while for the CsA treatment DEGs were significantly enriched in the GO terms “transmembrane transport” (GO:0055085) and “integral component of membrane” (GO:0016021) (Table 1). Inspecting the DEGs in more detail revealed that these GO terms were mainly present in genes coding for transporters of the major facilitator superfamily (MFS, InterPro domain IPR020846) (20 out of 58 DEGs, 34.5%), and the majority of these MFS genes (15 out of 20) were downregulated (Supplementary Table S5, Supplementary Table S6, Figure 4). Based on their best BLASTp hit in the Transporter Classification database (Saier *et al.*, 2014), these MFS genes belong to either the Oxalate:Formate Antiporter Family (1/20), Proton Coupled Folate Transporter/Heme Carrier Protein Family (4/20), Fucose H+ Symporter (5/20) or the Anion/Cation Symporter (10/20) MFS subfamily. The GO:0016021 term was also associated with genes coding for P450s (3 DEGs), UGTs (2 DEGs), cation-proton exchanger proteins (InterPro domain IPR018422, 2 DEGs) and a protein with an Apple-like domain (tetur25g02030, InterPro domain IPR003609). Interestingly, genes coding for ABC transporters, which are known to be inhibited by CsA (Qadir *et al.*, 2005), were not found among the DEGs of the CsA treatment.

DEGs of both the PBO and DEF treatment were significantly enriched in the GO terms “oxidoreductase activity, acting on paired donors, with incorporation or reduction of molecular oxygen” (GO:0016705), “heme binding” (GO:0020037), “monooxygenase activity” (GO:0004497), “iron ion binding” (GO:0005506), “oxidation-reduction process” (GO:0055114), “antibiotic metabolic process” (GO:0016999) and “transferase activity, transferring hexosyl groups” (GO:0016758). The first five GO terms were mainly present in genes coding for P450s (14 and 11 DEGs for the PBO and DEF treatments, respectively) while the latter two terms were found in UGTs (7 and 12 DEGs for the PBO and DEF treatments, respectively). Interestingly, almost all P450 and UGT genes (13/14 P450s and 7/7 UGTs (PBO treatment) and 10/11 P450s and 12/12 UGTs (DEF treatment))

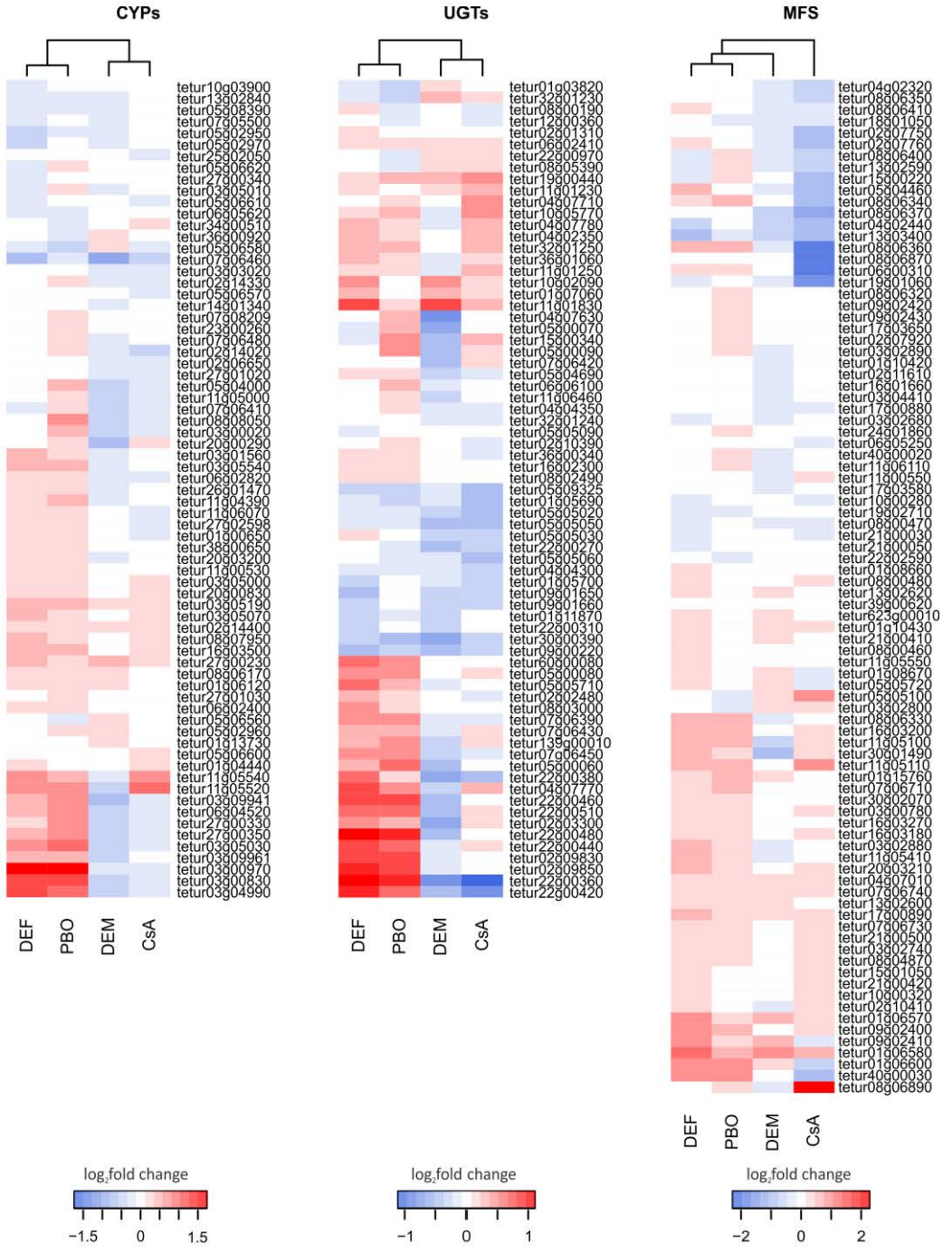

Figure 4 - Expression heatmaps of genes coding for P450s, UGTs or MFS members in adult *T. urticae* females exposed to either PBO, DEF, DEM or CsA. The $\log_2$ transformed fold changes are relative to adult *T. urticae* females treated with formulation only and were clustered using a Euclidean distance metric and Ward's method. *T. urticae* gene IDs are shown on the right.

Table 1 - GO enrichment analysis of differentially expressed genes (absolute fold change ≥ 1.5 and Benjamini-Hochberg adjusted p-value < 0.05) in adult *T. urticae* females of the JP-R strain exposed to either PBO, DEF or CsA compared to adult *T. urticae* females treated with formulation only.

Treatment	GO Category	Description	adjusted p-value	Subontology*
CsA	GO:0055085	transmembrane transport	0	BP
CsA	GO:0016021	integral component of membrane	6.72^{E}-05	CC
PBO	GO:0016705	oxidoreductase activity, acting on paired donors, with incorporation or reduction of molecular oxygen	2.68^{E}-09	MF
PBO	GO:0020037	heme binding	3.05^{E}-08	MF
PBO	GO:0004497	monooxygenase activity	3.05^{E}-08	MF
PBO	GO:0005506	iron ion binding	3.08^{E}-08	MF
PBO	GO:0055114	oxidation-reduction process	1.28^{E}-05	BP
PBO	GO:0016999	antibiotic metabolic process	8.83^{E}-04	BP
PBO	GO:0016758	transferase activity, transferring hexosyl groups	2.21^{E}-02	MF
DEF	GO:0016758	transferase activity, transferring hexosyl groups	2.86^{E}-05	MF
DEF	GO:0016999	antibiotic metabolic process	4.00^{E}-05	BP
DEF	GO:0005506	iron ion binding	1.45^{E}-04	MF
DEF	GO:0055114	oxidation-reduction process	3.43^{E}-04	BP
DEF	GO:0020037	heme binding	4.93^{E}-04	MF
DEF	GO:0016705	oxidoreductase activity, acting on paired donors, with incorporation or reduction of molecular oxygen	5.10^{E}-04	MF
DEF	GO:0004497	monooxygenase activity	7.96^{E}-04	MF
DEF	GO:0005179	hormone activity	1.18^{E}-03	MF
DEF	GO:0016021	integral component of membrane	1.66^{E}-03	CC

* BP, Biological Process; MF, Molecular Function; CC, Cellular Component

were upregulated for both the PBO and DEF treatment. The majority of the upregulated P450 genes (12/13 and 8/10 for the PBO and DEF treatments, respectively) belonged to the CYP392 family within the CYP2 clan for which several members were shown previously to respond strongly to acaricide selection and feeding on different hosts (Dermauw *et al.*, 2013b). GO:0055114 was also found in genes coding for short chain dehydrogenases (4 and 3 DEGs for the PBO and DEF treatments, respectively) and intradiol ring-cleavage dioxygenases (2 and 4 DEGs for the PBO and DEF treatments, respectively) while for the DEF treatment this term was also present in genes coding for a superoxide dismutase (*tetur02g11180*), a fatty acid synthase (*tetur04g02370*) and a glucose dehydrogenase (*tetur03g09330*). In addition, DEGs of the DEF treatment were also significantly enriched in the GO terms “hormone activity” (GO:0005179) and “integral component of membrane” (GO:0016021). The “hormone activity” term was present in four DEGs coding for neuropeptides (InterPro domain IPR001955 or IPR016179), while “integral component of membrane” was present in more than 45 DEGs, including, amongst others, genes coding for P450s (10 DEGs), MFS proteins (10 DEGs), UGTs (7 DEGs), ABC transporters (3 DEGs), neuropeptides

(2 DEGs), innexins (InterPro domain IPR000990, 2 DEGs) and proteins with a DUF3421 domain (InterPro domain IPR024518, 2 DEGs) (Table 1 and Supplementary Table S2 and S3). A cluster analysis of expression data of P450, UGT and MFS genes complemented the findings of our GO analyses. For both the P450 and UGT gene expression data the PBO and DEF treatment clustered together, while for MFS gene expression data, the CsA treatment fell outside the clade with all other treatments (Figure 4).

5. Discussion

Gene expression changes are a major component of stress responses, and contribute to or complement alterations in metabolism, cell cycle progression, protein homeostasis, cytoskeletal organization, vesicular trafficking and modification of enzymatic activities (de Nadal *et al.*, 2011). Expression changes can be grouped into generic responses shared by many stresses, and stress-specific adaptive responses. In contrast to post-translational effects, which provide immediate responses, regulation of gene expression is essential for the slower, long term acclimation to and recovery from a stress factor (de Nadal *et al.*, 2011). At present, our understanding of gene expression changes in arthropods to synergist exposure is very limited in spite of their importance in insecticide- and acaricide-mediated control. In fact, only two studies have investigated genome-wide transcriptional changes in an insect upon synergist exposure. Willoughby *et al.*, 2007 and Zimmer *et al.*, 2017 studied PBO induced gene expression changes in *D. melanogaster* and *B. tabaci*, respectively. Gene expression changes upon exposure to other synergist compounds have not yet been determined.

In this study, we examined transcriptional responses in a polyphagous arthropod pest, *T. urticae*, upon exposure to the synergist compounds PBO, DEF, DEM and CsA. The strain that was used for our experiments (JP-R, see Material & Methods) was shown to be resistant to the mitochondrial complex II inhibitors cyenopyrafen and cyflumetofen (both compounds are beta-keto nitrile derivatives belonging to IRAC Mode of Action Classification 25A, (IRAC, 2017; Sparks and Nauen, 2015)), with cyenopyrafen and cyflumetofen toxicity strongly synergized by PBO and DEM, respectively, while DEF moderately synergized cyenopyrafen toxicity (Khalighi *et al.*, 2015). Because acaricides are typically applied 24h after synergist treatment (Khalighi *et al.*, 2015, 2014; Van Leeuwen *et al.*, 2006; Van Pottelberge *et al.*, 2009c), transcriptional changes were captured 24h after exposure. In future, it would be interesting to also capture the transcription levels at those synergist exposure periods that have been used in previous synergism studies with *T. urticae* (1h and 4h) (Kim *et al.*, 2006, 2004; Rauch and Nauen, 2002; Stumpf and Nauen, 2002; Tsagkarakou *et al.*, 2002; Van Pottelberge *et al.*, 2009c; Yang *et al.*, 2001). Finally, the observed fold changes of up- and downregulated *T. urticae* genes (ranging from -3.8 to 3.3 across all synergist treatments) were in line with those observed for *B. tabaci* by Zimmer *et al.*, 2017. In contrast, fold changes of PBO induced *Drosophila* genes were considerably higher (ranging from 2 to 32) (Willoughby *et al.*, 2007). However, in our study a 24h synergist pretreatment was used, while in *Drosophila* expression measurements were taken after 4 hours of synergist exposure, and with the *Drosophila* 16K full genome array. Briefly, the *Drosophila* 16K full genome array contained only one 70mer probe per

gene (Willoughby *et al.*, 2007), confounding reliable estimation of fold changes (Chou *et al.*, 2004), while in our study and that of Zimmer *et al.*, 2017 gene-expression levels were captured by Illumina RNA-sequencing.

Stress responses can be induced by a variety of stressors such as extreme temperatures, elevated ion concentrations or toxic substances, all of which usually result in excessive amounts of denatured proteins (Stetler *et al.*, 2010). The general stress response typically consists of an increased production or activation of antioxidant proteins (e.g. Cu/Zn superoxide dismutase and GSTs) and chaperone proteins (e.g. heat shock proteins) (Santoro, 2000; Takeda *et al.*, 2008), together with an increased mobilization of energy from storage tissues (Vermetten and Bremner, 2002). The latter is associated with the overexpression of numerous genes involved in energy production or in cellular catabolism such as NADH dehydrogenase, ATP synthase, trypsin and lipases (David *et al.*, 2010). Only one GST gene was significantly upregulated in the PBO and DEF treatment while a gene coding for a superoxide dismutase was downregulated in the DEF treatment. A GO enrichment analysis did not reveal a GO category that was in common between the different synergist treatments and that was related to the above-mentioned proteins. Even more, only one upregulated gene, coding for a putative sodium-dependent glucose transporter (*tetur01g06580*, member of the MFS-gene family), was in common for all treatments. Hence, we assume that the observed gene expression changes are not general stress responses but rather specific for the synergist compounds to which the mites had been exposed. However, based on PC1 of our principal component analysis gene expression levels of PBO and DEF treatment replicates did cluster together (Figure 1). Even more, about 35% of the *T. urticae* DEGs that were identified for both these treatments were shared and had fold changes in the same direction (Figure 3). Interestingly, about one third (15/44) of the upregulated shared DEGs coded for members of the P450 and UGT gene families (Figure 4, Supplementary Table S2). For *D. melanogaster*, it has been shown that the transcription factor CncC plays an important role in xenobiotic-inducible gene expression of P450s, GSTs, UGTs and membrane transporters (Misra *et al.*, 2011). However, none of the *T. urticae* orthologs of *D. melanogaster CncC* (*tetur07g06850* and *tetur07g04600* (Dermauw *et al.*, 2013b)) were differentially expressed after 24h (Supplementary Table S2, S3, S4 and S5). In addition, *T. urticae* genes related to the gene coding for *Drosophila* Keap1 (Kelch-associated protein 1), a negative regulator of CncC, and that are downregulated in acaricide resistant and host plant adapted mite lines (OrthoMCL group 10254) (Dermauw *et al.*, 2013b; Wybouw *et al.*, 2015) were also not found among the DEGs of both the PBO and DEF treatment. However, expression changes of *T. urticae* transcription factors genes (Phuong, 2014) did correlate for these treatments (Supplementary Figure S1), suggesting a common transcriptional regulation. Ten of these transcription factor genes had a fold change of more than 1.25 in both the PBO and DEF treatments and had an opposite direction of fold change compared to the CsA and DEM treatments (Supplementary Table S7) and, hence, might be good candidates to be investigated for their role in xenobiotic resistance regulation in *T. urticae*.

The induction of P450s upon exposure by PBO has been reported by other groups (Chan *et al.*, 2014; Ellinger-Ziegelbauer *et al.*, 2005; Skrinjaric-Spoljar *et al.*, 1971; Watanabe *et al.*, 1998;

Willoughby *et al.*, 2007; Zimmer *et al.*, 2017). As hypothesized by Chan *et al.*, 2014, it might be a compensation strategy for an enzyme to be upregulated upon contact with an inhibitor in order to minimize the effect of reduced enzyme activity. In general, several studies have shown that xenobiotics are able to induce expression of arthropod P450s, (Bautista *et al.*, 2007; Dermauw *et al.*, 2013b; S. Liu *et al.*, 2014; Misra *et al.*, 2011; Poupardin *et al.*, 2010, 2008; Willoughby *et al.*, 2006; Wybouw *et al.*, 2015; Zimmer *et al.*, 2017). In *Drosophila* for example, about a third of the P450s can be induced following xenobiotic substance feeding or topical application (Giraudo *et al.*, 2010). For *T. urticae* it has been shown that the application of barbital, phenobarbital and geraniol does increase P450 activity in a dose-dependent way and that pretreatment with these inducers resulted in decreased acaricide toxicity (Van Pottelberge *et al.*, 2008). Willoughby *et al.*, 2007 suggested that the increase of detoxification enzymes by PBO might speed up insecticide tolerance if these detoxification enzymes could metabolize insecticides. Hence, one might question whether induction of *T. urticae* detoxification genes by synergist compounds could lead to a decreased toxicity of acaricides. In this study, *CYP392A11* and *CYP392A12* were both upregulated upon exposure of the JP-R strain by PBO. In 2015 it was shown that the upregulation of these genes was associated with cyenopyrafen resistance of the JP-R strain (Khalighi *et al.*, 2015) and that CYP392A11 could metabolize cyenopyrafen (Riga *et al.*, 2015). Similarly, only three carboxyl/choline esterase, *TuCCE06* (*tetur01g10800*), *TuCCE07* (*tetur01g010810*) and *TuCCE25* (*tetur04g06670*), were upregulated upon exposure of the JP-R strain by DEF and recently it was shown that TuCCE25 was highly upregulated in the JP-R strain and responded to cyenopyrafen selection (Khalighi *et al.*, 2015). In summary, both PBO and DEF seem to induce genes coding for detoxification enzymes that are strongly associated/implicated in cyenopyrafen resistance of the JP-R strain. On the other hand, both PBO and DEF, at the same concentration and exposure period that was used in this study, have previously been shown to synergize cyenopyrafen toxicity (Khalighi *et al.*, 2015). Hence, the direct inhibition of these P450s and CCEs by PBO and DEF, respectively, seems to outweigh the impact of the synergists on their induction. In contrast, in instances where P450s or CCEs may not be involved in acaricide resistance, PBO or DEF induction of genes encoding enzymes that are not inhibited by the synergist compound and that are capable of metabolizing acaricides, might interfere and lead to misinterpretation of synergism experiments (for example antagonism instead of synergism).

Both the PBO and DEF treatments resulted in an upregulation of *TuGSTd14* (*tetur29g00220*). Of particular note, *TuGSTd14* was also upregulated in multi-resistant *T. urticae* strains (Dermauw *et al.*, 2013b) and showed affinity toward abamectin and a competitive type of inhibition (Pavlidi *et al.*, 2015). In contrast, the DEM treatment did not result in the overexpression of GSTs. Even more, significantly enriched GO terms could not be identified for the DEM treatment. This result was somewhat unanticipated as it is known that depletion of GSH by DEM results in oxidative stress and destabilized proteins *in vitro* (Freeman *et al.*, 1997) and that the response to oxidative stress typically consists of highly coordinated changes in gene expression (for example, in human carcinoma cells (Casey *et al.*, 2002)). In the study by Casey *et al.*, 2002, exposure to DEM resulted in GSH depletion below control levels from 1h to 24h after DEM treatment. However,

although the expression of about 800 genes had a significant change (over two-fold at more than one time point) during this 24h time course experiment, $\log_2$ fold changes of almost all genes returned to near zero at the 24h time point (Casey *et al.*, 2002). Previously it was shown that a 24h treatment with DEM strongly synergized cyflumetofen toxicity in the JP-R strain (Khalighi *et al.*, 2015) and that a GST (TuGSTd05) that was upregulated in this strain could metabolize cyflumetofen. Hence, the 24h DEM exposure most likely resulted in depleted GSH levels in mites of the JP-R strain but the expression changes that are associated with the onset of depletion may not have been captured in our study.

The Major Facilitator Superfamily (MFS) is, along with ATP-binding cassette (ABC) transporters, one of the largest transporter families present in all living organisms. MFS transporters, as opposed to ABC transporters, use an existing electrochemical gradient instead of ATP to transport substrates (either by symport, uniport or antiport) across membranes (Dermauw and Van Leeuwen, 2014; Pao *et al.*, 1998). Numerous studies have pointed to the importance of ABC transporters in xenobiotic resistance in arthropods (Dermauw and Van Leeuwen, 2014; Merzendorfer, 2014). In the case of *T. urticae*, several of its 103 ABC transporter genes were differentially expressed in multi-pesticide resistant strains and/or in mites transferred to a more challenging host plant (Dermauw *et al.*, 2013a). MFS transporters, however, have been less studied in arthropods and it is only recently that evidence for their role in xenobiotic resistance in arthropods has been reported (De la Paz Celorio-Mancera *et al.*, 2013; Dermauw *et al.*, 2013b). Consistent with this, 37 *T. urticae* MFS genes (belonging to either OrthoMCL group arthro10032, arthro10082 or arthro10236), were differentially expressed upon long term transfer of mites from bean to tomato (Dermauw *et al.*, 2013b).

None of the 103 ABC *T. urticae* transporter genes were differentially expressed upon exposure to the ABC transporter modulator CsA. In contrast, about one third of the DEGs of the CsA treatment coded for MFS transporters, including five sugar transporters. The differential expression of these sugar transporters might be caused by interference of cyclosporine in glucose metabolism (Christians *et al.*, 2004; Dresner *et al.*, 1989). On the other hand, the majority of the remaining differentially expressed MFS genes showed similarity with members of the anion/cation superfamily that can transport a variety of substrates (Reimer, 2013). Finally, it should be mentioned that CsA inhibition of ABC transporters is not well characterized in arthropods compared to vertebrates (Dermauw and Van Leeuwen, 2014), and the transcriptional changes that were observed might not reflect those that are caused by the inhibition of ABC transporters but rather by inhibition of another target like calcineurin (the *T. urticae* subunits of this target are tetur04g07540, tetur04g07560 and tetur03g06410 as assessed by a blastp search, E-value between E-86 and 0 with human calcineurin subunits as queries), as occurs in the vertebrate immune system (Liu *et al.*, 1991).

To conclude, transcriptional changes in arthropod pests exposed to synergist compounds have only been marginally studied. In this work, we exposed a polyphagous arthropod pest, *T. urticae*, for 24 hours to four different synergist compounds PBO, DEF, DEM and CsA and measured genome-wide gene expression changes. The CsA treatment resulted primarily in the

downregulation of *T.urticae* MFS genes, while *T. urticae* DEGs of the DEM treatment were not significantly enriched for a GO term. Exposure to PBO and DEF resulted in a broad transcriptional response and about one third of the DEGs, including cytochrome P450 monooxygenases and UDP-glycosyltransferases, were shared between both treatments, suggesting modulation of a common transcriptional program. Moreover, both DEF and PBO induced genes that are strongly implicated in acaricide resistance of the strain used in this study. Based on previous synergism toxicity studies, however, the induction of these detoxification genes seems not to interfere with the outcome of synergism assays, although the effects of induction might be relatively more important when resistance is not synergized.

Funding information

W.D. is a postdoctoral fellow of the Research Foundation Flanders (FWO). R.G. was supported by the National Institutes of Health Genetics Training Grant TM32GM007464. This project was supported by the Research Foundation Flanders (FWO) (grant G009312N to L.T. and T.V.L. and grant G053815N to L.T., T.V.L. and W.D.).

Author contributions

TVL, WD and SS designed the experiment. SS conducted the experiments. Analysis and interpretation of the results was done by SS, RG, WD, RMC and TVL. The manuscript was written by SS and WD, all figures were prepared by SS and WD. All authors reviewed the manuscript.

Supplementary information

Supplementary data can be found at 10.1038/s41598-017-13397-x

Supplementary Figure S1 – Expression heatplot of *T. urticae* genes coding for transcription factors in adult *T urticae* females exposed to either PBO, DEF, DEM, or CsA. The log2 transformed fold changes are relative to adult *T.urticae* females treated with formulation only and were clustered using Euclidean distance metric and Ward's method. *T. urticae* gene IDs are shown on the right. Transcription factor genes with a fold change equal to zero in at least three out of four treatments were excluded from the heatplot.

Supplementary Table S1 - Number of strand-specific paired-end Illumina reads and their mapping rates against the *T. urticae* annotation for all treatments (CON, DEF, DEM, CsA, PBO and FORM).

Supplementary Table S2 - Differentially expressed genes (absolute fold change (FC) ≥ 1.5 and Benjamini-Hochberg adjusted p-value < 0.05) between adult *T. urticae* females of the JP-R strain treated with PBO compared to adult *T. urticae* females treated with formulation only.

Supplementary Table S3 - Differentially expressed genes (absolute fold change (FC) ≥ 1.5 and Benjamini-Hochberg adjusted p-value < 0.05) between adult *T. urticae* females of the JP-R strain treated with DEF compared to adult *T. urticae* females treated with formulation only.

Supplementary Table S4 - Differentially expressed genes (absolute fold change (FC) ≥ 1.5 and Benjamini-Hochberg adjusted p-value < 0.05) between adult *T. urticae* females of the JP-R strain treated with DEM compared to adult *T. urticae* females treated with formulation only.

Supplementary Table S5 - Differentially expressed genes (absolute fold change (FC) ≥ 1.5 and Benjamini-Hochberg adjusted p-value < 0.05) between adult *T. urticae* females of the JP-R strain treated with CsA compared to adult *T. urticae* females treated with formulation only.

Supplementary Table S6 - Differentially expressed genes (absolute fold change (FC) ≥ 1.5 and Benjamini-Hochberg adjusted p-value < 0.05) of the Major Facilitator Superfamily (MFS) in adult *T. urticae* females after exposure to cyclosporin A.

Supplementary Table S7 - Supplementary Table S6: *T. urticae* genes coding for transcription factors with an absolute fold change ≥ 1.25 in both the PBO and DEF treatment and with an opposite direction of fold change compared to the CsA and DEM treatment.

Supplementary Table S8 - Primers used in this study.

Chapter 4

Transcriptomic plasticity in the arthropod generalist *Tetranychus urticae* upon long-term acclimation to different host plants

This chapter has been partially redrafted from:

Snoeck*, S., Wybouw*, N., Van Leeuwen, T., Dermauw, W. (2018). Transcriptomic plasticity in the arthropod generalist *Tetranychus urticae* upon long-term acclimation to different host plants. G3: genes | genomes | genetics, 8(12), 3865-3879.

1. Abstract

The two-spotted spider mite *Tetranychus urticae* is an important pest with an exceptionally broad host plant range. This generalist rapidly acclimatizes and adapts to a new host, hereby overcoming nutritional challenges and a novel pallet of constitutive and induced plant defenses. Although recent studies reveal that a broad transcriptomic response upon host plant transfer is associated with a generalist life style in arthropod herbivores, it remains uncertain to what extent these transcriptional changes are general stress responses or host-specific. In the present study, we analyzed and compared the transcriptomic changes that occur in a single *T. urticae* population upon long-term transfer from *Phaseolus vulgaris* to a similar, but chemically defended, host (cyanogenic *Phaseolus lunatus)* and to multiple economically important crops (*Glycine max, Gossypium hirsutum*, *Solanum lycopersicum* and *Zea mays*). These long-term host plant transfers were associated with distinct transcriptomic responses with only a limited overlap in both specificity and directionality, suggestive of a fine-tuned transcriptional plasticity. Nonetheless, analysis at the gene family level uncovered overlapping functional processes, recruiting genes from both well-known and newly discovered detoxification families. Of note, our analyses highlighted a possible detoxification role for *Tetranychus*-specific short-chain dehydrogenases and single PLAT domain proteins, and manual genome annotation showed that both families are expanded in *T. urticae*. Our results shed new light on the molecular mechanisms underlying the remarkable adaptive potential for host plant use of generalist arthropods and set the stage for functional validation of important players in *T. urticae* detoxification of plant secondary metabolites.

2. Introduction

Host plant acceptance by a herbivore is influenced by the nutrient composition, with the protein/carbohydrate ratio being a critical characteristic (Behmer, 2009; Mattson, 1980). In addition to the nutrient composition of a potential host plant, plant defenses play a pivotal role in host plant acceptance. These defenses can either be chemical or physical (e.g. thorns, and trichomes). Chemical plant defense barriers include the production of toxic plant secondary metabolites and anti-digestive compounds as well as the attraction of enemies of the herbivore via the release of plant volatiles. Plants can also re-allocate their resources towards non-attacked tissues to minimize the negative fitness consequences of tissue loss due to herbivore feeding (Howe and Jander, 2008; Kant *et al.*, 2015).

Based on the timing of their production, plant secondary defense metabolites can be divided into two categories. Phytoanticipins are synthesized constitutively whereas phytoalexins are induced upon herbivore or pathogen attack via damage recognition and mediated by well-characterized plant hormone systems (Dixon, 2001; Kant *et al.*, 2015; Rioja *et al.*, 2017; Stahl *et al.*, 2018). Across the plant kingdom, a staggering diversity of phytoalexins and phytoanticipins have evolved in the co-evolutionary arms-race between plants and their attackers (Rosenthal and Berenbaum, 1991; Wink, 2010). Phytoanticipins with well-characterized effects on feeding herbivores include the glycoalkaloid tomatine in tomato, the benzoxazinoid DIMBOA-Glc in maize and related grasses and cyanogenic glucosides in cyanogenic plants, including cassava (DongSub

et al., 2014; Friedman, 2002; Glauser *et al.*, 2011; Pičmanová *et al.*, 2015). On the other hand, gossypol in cotton and isoflavonoids in legumes are examples of phytoalexins (Dakora and Phillips, 1996; McCormick, 1982). Another well-studied induced defense response upon herbivore feeding is the increased production of anti-digestive compounds such as proteinase inhibitors (PIs) that causes an amino acid deficiency in the attacking herbivore (Green and Ryan, 1972; Hartl *et al.*, 2010). Such increase of PIs has been observed in many plants upon attack of insects but also spider mite herbivores such as *Tetranychus urticae* and *Tetranychus evansi* (Kant *et al.*, 2004; Martel *et al.*, 2015).

Arthropod herbivores have developed several mechanisms to avoid, resist or suppress plant defenses. Two main mechanisms are thought to allow herbivores to cope with ingested plant secondary metabolites: (1) mechanisms that decrease sensitivity and (2) mechanisms that decrease exposure to plant metabolites, such as sequestration and increased metabolism (Kant *et al.*, 2015). With the exception of a number of biological systems such as herbivore resistance against plant cardenolides (Dobler *et al.*, 2012), the first mechanism has only been rarely documented. Probably, this is because plant secondary metabolites often have multiple or unspecific modes of action, in contrast to, for example, insecticides used to control insects and mites (for a review, see Feyereisen *et al.* 2015 and Van Leeuwen & Dermauw 2016). Mechanisms of decreased exposure, on the other hand, are far better documented and in many cases are mediated by genes that code for enzymes and transporters that typically belong to ubiquitous multi-gene families (Després *et al.*, 2007; Erb and Robert, 2016; Heckel, 2014; Heidel-Fischer and Vogel, 2015). Metabolic detoxification can be categorized into three phases based on the interaction with the ingested toxin. These interactions are: direct metabolism (phase I), conjugation (phase II) and translocation (phase III). Enzymes that operate during phase I are often cytochrome P450 monooxygenases (P450s) and carboxyl/choline esterases (CCEs), whereas enzymes such as glutathione-S-transferases (GSTs) and UDP-glycosyltransferases (UGTs) typically operate during phase II. Finally, transport of the toxins or the phase II metabolites out of the cell or into specialized cell compartments is often performed by ATP-binding cassette (ABC) transporters and solute carrier (SLC) family proteins (Brattsten, 1988; Dermauw and Van Leeuwen, 2014; Després *et al.*, 2007; Heckel, 2014; Kant *et al.*, 2015). Recently it was reviewed whether the genes encoding the above-mentioned enzymes and transporters are less abundant in the genomes of specialist herbivores (those restricted to one or a few related host plants) compared to generalist herbivores (able to feed on a diverse set of host plants) and whether generalist herbivores are genetically predisposed to rapidly develop pesticide resistance; so far, conclusive evidence is yet to be found for these relationships (Dermauw *et al.*, 2018; Hardy *et al.*, 2018; Rane *et al.*, 2016). Some studies also found that arthropod generalists exhibit a remarkably stronger transcriptional response upon host plant transfer compared to specialists and suggest that this activity is linked to the ability to cope with different host plants (Schweizer *et al.*, 2017; Wybouw *et al.*, 2015). More studies are however needed to establish the generality of these observations across the Arthropoda phylum.

Instead of coping with ingested plant secondary metabolites, some arthropod herbivores also evolved the ability to suppress the induced plant defenses, mostly via the secretion of

molecules directly into the plant tissue (named effectors, reviewed in Kant *et al.* 2015 and Felton *et al.* 2014) and expansion of salivary genes has been suggested to be important in the adaptation processes of generalist herbivores (Boulain *et al.*, 2018; Jonckheere, 2018). The relative importance of plant defense manipulation and detoxification in arthropod-plant interactions remains however to be determined (Blaazer *et al.*, 2018; Rioja *et al.*, 2017).

The two-spotted spider mite *T. urticae* is among the most polyphagous herbivores known, with a host range covering more than 1,100 different plant species, scattered over more than 140 different plant families. Together, these plants produce a staggering number of different plant defense metabolites (Migeon, Nouguier and Dorkeld, 2018; Grbić *et al.*, 2011). It is well known that *T. urticae* populations readily, but differentially, adapt to a novel plant (Agrawal *et al.*, 2002; Fry, 1989; Gould, 1979; Magalhães *et al.*, 2009, 2007). Analysis of the *T. urticae* genome revealed large, lineage-specific expansions of detoxification gene families including P450s, CCEs, GSTs, UGTs and ABCs (Ahn *et al.*, 2014; Dermauw *et al.*, 2013a; Grbić *et al.*, 2011). In addition, analysis of the spider mite salivome revealed a whole array of putative effectors (Jonckheere, 2018; Jonckheere *et al.*, 2016), of which two effectively suppress plant defenses and promote mite performance (Villarroel *et al.*, 2016).

In recent years, many of the “classical” detoxification genes (coding for P450s, CCEs, GSTs, UGTs and ABCs) were shown to be differentially expressed upon transfer of mite populations to different host plants, but also genes previously not known to be implicated in arthropod detoxification were uncovered (Ahn *et al.*, 2014; Dermauw *et al.*, 2013b; Grbić *et al.*, 2011; Wybouw *et al.*, 2015; Zhurov *et al.*, 2014). These include genes coding for binding/sequestering proteins such as lipocalins and transporters of the Major Facilitator Superfamily. Remarkably, spider mites have also acquired novel metabolic abilities via horizontal gene transfer. The horizontally transferred gene repertoire of *T. urticae* includes a family of 17 intradiol ring-cleavage dioxygenases (DOGs) capable of hydrolyzing aromatic ring structures (Dermauw *et al.*, 2013b; Wybouw *et al.*, 2015), but also a gene (*β-cyanoalanine synthase*) that was horizontally transferred from bacteria and of which its encoded enzyme detoxifies hydrogen cyanide (Wybouw *et al.*, 2014) (see Wybouw *et al.* 2016 and Wybouw *et al.* 2018 for the general role of horizontal gene transfer in the evolution of insect and mite herbivory).

The majority of these and other gene expression studies was however based on short-term transfer (less than or equal to 24 h) of plant-feeding mites to a new host (Dermauw *et al.*, 2013b; Grbić *et al.*, 2011; Zhurov *et al.*, 2014) and only few studies have assessed mite gene expression changes upon long-term acclimation (> 1 generation) or adaptation to a new host (Dermauw *et al.*, 2013b; Wybouw *et al.*, 2014, Wybouw 2015). Moreover, studies examining expression changes upon long-term acclimation in non-chelicerate arthropod herbivores are very scarce (Mathers *et al.*, 2017; Müller *et al.*, 2017; Xie *et al.*, 2014). In this study, we examined the transcriptomic responses of *T. urticae* to a long-term transfer from bean to five different host plants; lima bean, soybean, cotton, tomato, and maize. We assessed the host plant specificity and overlap of these transcriptomic changes and dissected the different gene families involved, including “unexpected” families such as short-chain dehydrogenases (SDRs) and single PLAT domain proteins.

3. Materials and methods

3.1. Plants and spider mites

The ancestral reference population ('London') originates from a wild-collected *T. urticae* population from the Vineland region (Ontario, Canada) and was previously described (Grbić *et al.*, 2011). The London laboratory population was maintained on potted common bean plants (*Phaseolus vulgaris* L. cv. 'Prelude') at a continuously high population density and served as the ancestral population for all host plant transfers in the current study. Lines were established on different host plants by transferring about 250 adult females to lima bean (*Phaseolus lunatus* L. genotype 8078), soybean (*Glycine max* cv. 'Merlin'), maize (*Zea mays* L. cv. 'Ronaldinio'), tomato (*Solanum lycopersicum* L. cv 'Moneymaker') and cotton (*Gossypium hirsutum* cv. 'upland cotton') (see Jonckheere *et al.*, 2016; Wybouw *et al.*, 2015, 2012 for a more detailed description of the experimental set-up). Three independent lines were generated on cotton and tomato, whereas four independent lines were obtained for lima bean, maize, and soybean. All lines were mass reared on their respective host plants at 26 °C (±0.5 °C), 60% relative humidity (RH) and 16/8 h light/dark photoperiod.

3.2. RNA isolation, gene expression microarray set-up and differential gene expression analysis

Samples were collected from the soybean, cotton, and maize lines three months (approximately five generations) after transfer to the new host (Jonckheere *et al.*, 2016), while the tomato and lima bean lines were collected after 18 months (approximately 30 generations) (Wybouw *et al.*, 2015, 2014). Per sample, RNA was extracted from a pool of 100-120 adult females using a RNeasy minikit (Qiagen, Belgium). Following DNase treatment (Turbo DN*ase*, Ambion), the concentration and integrity of the RNA samples were assessed by Nanodrop and by running 1µl on a 1% agarose gel. RNA was labelled using the Low Input Quick Amplification Kit (Agilent Technologies, Diegem, Belgium) following the manufacturer's instructions. RNA that was collected from mites of the ancestral London population on common bean and of mites that were transferred to a novel host were consistently dyed with cy3 and cy5, respectively. Cyanine-labelled RNA was hybridized to a custom-made gene-expression microarray (GEO Platform GPL16890, Bryon *et al.* 2013). Hybridization, washing and scanning protocols were identical as previously described (Dermauw *et al.*, 2013b). Raw intensity data were used as input for final processing and statistical analysis in limma of the Bioconductor framework (Smyth, 2004). Here, background correction was first performed by the 'normexp' method, using an offset of 50 (Ritchie *et al.*, 2007). Background-corrected data were within- and between-array normalized (global loess and Aquantile, respectively) and quality was subsequently assessed using arrayQualityMetrics (Kauffmann *et al.*, 2009). Prior to final differential gene expression analysis, the 55,469 probe sequences were remapped to the *T. urticae* genome annotation of August 11, 2016 (File S1) using Bowtie2-2.2.6 with default settings (Langmead and Salzberg, 2012). Only the 36,589 probes that uniquely aligned to the annotated genome were incorporated in the differential gene expression analysis. A linear model was fitted to

the processed data that treated the ancestral population as a common reference (cy3 channel in sample GSM1214964-GSM1214967, GSM2124774-GSM2124784 and GSM1679383-GSM1679385). Significant differential gene-expression was identified via empirical Bayesian statistics and in reference to the ancestral population on common bean. Significant differentially expressed genes (DEGs) were identified by applying a 0.05 and 0.585 cut-off for Benjamini-Hochberg corrected p-value and absolute $\log_2$FC, respectively. The DEG set of each replicated host plant population was tested for enrichment of multigene families (OrthoMCL groups with at least 10 members) using a Chi square test. A Principal Component Analysis (PCA) was performed using the relative gene expression levels of all genes present on the array platform and the prcomp function within the R environment. *T. urticae* gene expression data are accessible at the Gene Expression Omnibus with accession numbers GSE50162, GSE80337 and GSE68708.

3.3. *k*-means clustering

The optimal cluster number for the *k*-means clustering approach was assessed using the gap statistic (method="global max", seed set at 54,321, cluster number ranging from 1 to 10) (Tibshirani *et al.*, 2001). The centered Pearson's correlation was used as the distance metric for *k*-means clustering. The relative transcription levels of genes that were significantly differentially expressed in any transcriptomic comparison were used as input for *k*-means clustering. Venn-diagrams were created for both the upregulated and downregulated transcripts using the VennDiagram 1.6.20 package in the R environment.

3.4. GO enrichment of differentially expressed genes

Gene Ontology (GO)-terms were assigned to *T. urticae* proteins using Blast2GO. The complete *T. urticae* proteome (19,086 sequences, version of August 11, 2016) was first used as query in a blastp search against the non-redundant protein database in NCBI (version of March 12, 2018) using the following settings "-outfmt 5 -evalue 1e-5 -word_size 3 -sshow_gis -num_alignments 20 -max_hsps_per_subject 20". The resulting blastp output was then loaded into the Blast2GO (version 5.1) program and *T. urticae* proteins were annotated using the default parameters (Conesa *et al.*, 2005). InterProScan 5 and ANNEX were used to augment the annotation of GO terms. GO terms were condensed using the generic GO Slim subset. Gene set enrichment analyses were conducted using the Bioconductor package piano (Väremo *et al.*, 2013). The mite transcriptomic changes associated with the five host plant transfers (lima bean, soybean, cotton, tomato, and maize) were analyzed with the differential gene expression-associated statistics in a distinct directional gene set analysis (PAGE).

3.5. OrthoMCL grouping

OrthoMCL grouping of *T. urticae* proteins was derived from Jonckheere 2018. InterProScan 5.25-64, with an E-value threshold of E^{-3}, was used to identify PFAM domains in the *T. urticae* proteome (version of August 11, 2016) and PFAM domains were assigned to each

OrthoMCL group based on the presence of PFAM domains in *T. urticae* proteins contained within each group. Each OrthoMCL group was filtered for those proteins of which their corresponding genes did not had probes on the microarray. For each filtered OrthoMCL protein group (having at least 5 members), we determined the percentage of corresponding genes that was differentially expressed upon long-term transfer to a host plant using the package dplyr version 0.7.4 (Wickham and Francois, 2015) within the R-framework (R Developement Core Team, 2015). A two-sided Fisher's exact test in combination with the Benjamini-Hochberg procedure for multiple testing correction (FDR) using all *T. urticae* genes (having uniquely mapping probes on the array; 13,943 genes in total) as a reference was employed to identify significantly enriched OrthoMCL groups (FDR < 0.05) among the DEG sets of the different *T. urticae* host plant populations.

3.6. Phylogenetic analysis of short-chain dehydrogenases

Among the significantly enriched OrthoMCL groups we identified two groups containing SDRs. The *T. urticae* proteome was mined for proteins with SDR-related PFAM domains; PF00106, PF01073, PF01370 and PF13561 (Persson and Kallberg, 2013). Those *T. urticae* proteins with a SDR-related PFAM domain were used as query in a tblastn and blastp search (E-value threshold of E^{-3}) against the *T. urticae* genome (Grbić *et al.*, 2011) and proteome (version of August 11, 2018) respectively. *T. urticae* SDR gene models were modified when necessary or new SDR gene models were created using Genomeview (Abeel *et al.*, 2012). *H. sapiens* SDRs were derived from (Bray *et al.*, 2009), while those of *Drosophila melanogaster* and *Metaseiulus occidentalis* were identified by mining their proteomes (*M. occidentalis* 1.0 (GNOMON release, (Hoy *et al.*, 2016)) and *D. melanogaster* release 6.16 (FlyBase (Gramates *et al.*, 2017)), respectively) for the above-mentioned SDR-related PFAM domains (see File S2 for accession numbers). Full-length *T. urticae* SDRs were aligned with those of *M. occidentalis*, *D. melanogaster*, *Homo sapiens* and *T. urticae* using the online version of MAFFT 7 with the E-INS-i iterative refinement method strategy (Katoh *et al.*, 2002), 1,000 iterations and the option "reorder". The SDR alignment was trimmed using trimAl v1.4 with the "gappyout" option (Capella-Gutiérrez *et al.*, 2009) as SDR sequences are known to be highly divergent (Persson *et al.*, 2003). A phylogenetic analysis was performed on the Cipres web portal (Miller *et al.*, 2010) using RAxML v8 HPC2-XSEDE (Stamatakis, 2014) with the automatic protein model assignment algorithm using maximum likelihood criterion and 1,000 bootstrap replicates. The LG+G protein model was selected as the optimal model for maximum likelihood analysis. The resulting tree was midpoint rooted, visualized using MEGA6 (Tamura *et al.*, 2013) and edited in CorelDRAW Home & Student ×7.

3.7. Phylogenetic analysis of single PLAT domain proteins

OrthoMCL group Tetra_22 consisted of 20 proteins, of which three (tetur02g12320, tetur02g15207 and tetur22g02180) had a single PLAT (polycystin-1, lipoxygenase, alphatoxin) PFAM domain (PF01477) and eleven proteins belonged to the CATH/Gene3D Superfamily 2.60.60.20 (PLAT/LH2). Throughout this study, we refer to the proteins in Tetra_22 as *T. urticae*

single PLAT domain proteins. *T. urticae* single PLAT domain proteins were used as query in a blastp and tblastn search (E-value threshold of E^{-3}) against the *T. urticae* proteome (version of August 11, 2018) and genome (Grbić *et al.*, 2011), respectively. *T. urticae* single PLAT domain protein gene models were modified when necessary or new single PLAT domain protein gene models were created using Genomeview (Abeel *et al.*, 2012). The transcriptomes of related tetranychid species, *Tetranychus evansi, Panonychus ulmi* and *Panonychus citri* (Bajda *et al.*, 2015; Villarroel *et al.*, 2016) were mined for single PLAT domain protein genes using tblastn (with an E-value threshold E^{-5}) and *T. urticae* single PLAT domain proteins as query. Redundant tblastn transcript hits were filtered using the cd-hit-est software (Fu *et al.*, 2012) with the following settings "-c 0.95 -n 10". Those *T. evansi*, *P. ulmi* and *P. citri* tblastn hits of more than 100 amino acids long were retained for further analysis. In addition, we also mined the NCBI non-redundant protein database (version of May 1 2018) for the presence of these proteins in non-tetranychid species using blastp (with an E-value threshold E^{-5}) and *T. urticae* single PLAT domain proteins as query (see File S3 for accession numbers). Full-length *T. urticae* single PLAT domain proteins were aligned with those of *T. evansi*, *P. ulmi* and *P. citri* using the online version of MAFFT 7 with the E-INS-i iterative refinement method strategy (Katoh *et al.*, 2002), 1000 iterations and the option "reorder". A phylogenetic analysis was performed on the Cipres web portal (Miller *et al.*, 2010) using RAxML v8 HPC2-XSEDE (Stamatakis, 2014) with the automatic protein model assignment algorithm using maximum likelihood criterion and 1,000 bootstrap replicates. The LG+G protein model was selected as the optimal model for maximum likelihood analysis. The resulting tree was midpoint rooted, visualized using MEGA6 (Tamura *et al.*, 2013) and edited in CorelDRAW Home & Student ×7.

3.8. Detection and analysis of short-chain dehydrogenase and single PLAT domain protein clusters

A sliding window approach earlier described in Ngoc *et al.*, 2016 was used to identify clusters of both the SDR and single PLAT domain protein genes throughout the *T. urticae* genome. A 50-kb window, incremented in 10-kb steps, was used. Only complete SDR and single PLAT domain protein genes were included in the analysis. Genes were considered as a part of each sliding window cluster if any portion of them overlapped the 50-kb window. Neighboring clusters that shared at least one gene were considered to be part of the same cluster, and were merged into a single larger cluster (as described in Thomas, 2006). The midpoints of the final clusters and the number of genes within each cluster were used for plotting.

3.9. Data availability

File S1 contains the CDS sequences of the *T. urticae* genome annotation of August 11, 2016. File S2 contains the protein sequences of the SDRs of *T. urticae*, *M. occidentalis*, *D. melanogaster* and *H. sapiens* that were included in the phylogenetic analysis. File S3 contains the sequences of the full-length single PLAT domain proteins of *T. urticae*, *T. evansi*, *P. ulmi* and *P. citri* that were included in the phylogenetic analysis. Figure S1 shows the expression heatmaps of genes

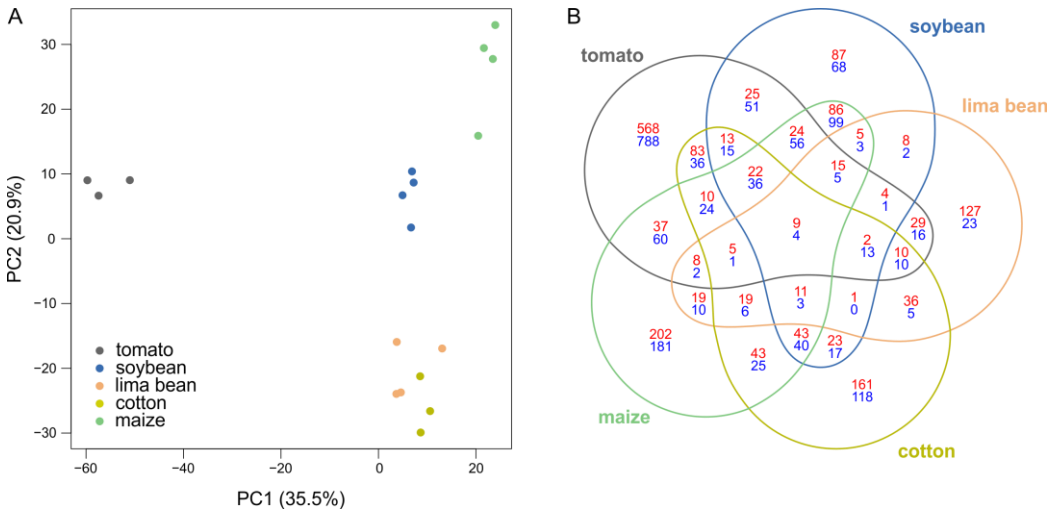

Figure 1 - Principal component analysis (PCA) and differential gene expression of the different host plant populations of *T. urticae.* (A) PCA plot of the relative gene expression levels in *T. urticae* populations after long-term transfer (≥ five generations) from common bean to different host plants: lima bean, soybean, cotton, tomato, and maize. (B) Venn-diagram depicting the overlap among the DEG sets of the populations after long-term transfer (≥ five generations) from common bean to different host plants. Red numbers: upregulated genes, blue numbers: downregulated genes.

coding for group I and II SDRs and of group I and II single PLAT domain protein genes across the replicated *T. urticae* host plant populations (lima bean, soybean, cotton, tomato and maize). Table S1 contains the differential gene expression results of the *T. urticae* host plant populations. Table S2 shows the overlap between DEGs of the different *T. urticae* host plant populations. Table S3 shows the *k*-means clustering of the DEGs identified in the different host plant populations of *T. urticae*. Table S4 shows the OrthoMCL grouping of the *T. urticae* proteome. Table S5 contains the OrthoMCL enrichment results of the DEG sets of each *T. urticae* host plant population. Table S6 contains the significantly enriched GO terms in the DEG sets of the different host plant populations of *T. urticae*. Table S7 contains the SDR genes annotated in the *T. urticae* genome. Table S8 contains the single PLAT domain protein genes annotated in the *T. urticae* genome. *T. urticae* gene expression data are available at the Gene Expression Omnibus with accession numbers GSE50162, GSE80337 and GSE68708. Supplemental material is available at Figshare: https://figshare.com/s/b99d2ba31a466a997998.

Table 1 - Differentially expressed genes in different host plant populations of *T. urticae* (lima bean, soybean, cotton, tomato and maize) compared to an ancestral population on common bean

	total number	upregulated	downregulated	specific upregulated	specific downregulated
lima bean	410	307	103	127 (41)	23 (22)
soybean	789	377	412	87 (23)	68 (17)
cotton	842	490	352	161 (33)	118 (34)
tomato	1,982	864	1,118	568 (66)	788 (70)
maize	1,111	557	554	202 (36)	181 (33)

4. Results

4.1. Effect of long-term acclimation to different host plants on the *T. urticae* transcriptome

Using a whole-genome gene expression microarray, we measured significant gene expression changes in *T. urticae* adult females upon long-term transfer from common bean to either lima bean, soybean, cotton, tomato or maize ($log_2FC \geq 0.585$ and Benjamini-Hochberg corrected p-value < 0.05). A PCA plot revealed that 35.5 and 20.9% of the total gene expression variation across host plant lines could be explained by PC1 and PC2, respectively (Figure 1A). Individual lines clustered by host plant on both PC1 and PC2, with PC1 clearly separating the three tomato lines from the other host plant lines. The lima bean and cotton lines clustered along PC1. Our statistical analysis showed that the host plant transfer from bean to tomato resulted in the highest number of DEGs, 1,982 DEGs in total, of which 864 were upregulated and 1,118 downregulated (Table 1). On the other hand, acclimation to lima bean resulted in the lowest amount of DEGs, 410 in total, containing 307 upregulated and 103 downregulated genes. Long-term transfer to soybean, cotton, and maize resulted in 789, 842 and 1,111 DEGs, respectively (Table 1, Table S1). In terms of amplitude, the replicated transfers to tomato and cotton plants resulted in the highest up- and downregulated DEGs. The DEG set of each replicated host plant population was enriched in multigene families (OrthoMCL groups ≥ 10 members), with 226/410, 304/789, 292/842, 479/1982 and 408/1111 of the DEGs of lima bean, soybean, cotton, tomato, and maize line belonging to multigene families, respectively (Chi-square test p-values less than E^{-30} for each DEG set). As shown in Figure 1B, the majority of DEGs was not shared between the different host plant populations, with only nine upregulated genes and four downregulated genes in common for all transfers. These common upregulated DEGs coded for an intradiol ring-cleavage dioxygenase (*tetur28g01250*), a short-chain dehydrogenase (*tetur32g01960*), two Major Facilitator Superfamily proteins (*tetur03g04330* and *tetur11g05100*), a serine protease homologue (*tetur16g03330*), a CCAAT/enhance binding protein alpha (*tetur06g04210*), a LIM-domain (PF00412) protein (*tetur06g00950*) and two hypothetical proteins (*tetur23g01600*, *tetur22g00690*). The common downregulated DEGs coded for a small secreted protein from family A (*tetur22g02750*), a viral nucleoprotein (*tetur22g01100*, which was acquired through horizontal gene transfer (Wybouw *et al.* 2018)), and two hypothetical proteins (*tetur01g09880* and *tetur13g01730*). Fifty-four genes were upregulated for four out of five transfers, while 57 were downregulated (Table S2). Of particular note, the tomato transfer resulted in the highest number of up- and downregulated genes that were not shared with the response of any other host plant population, and therefore appeared to be the most specific response (Table 1 and Figure 1).

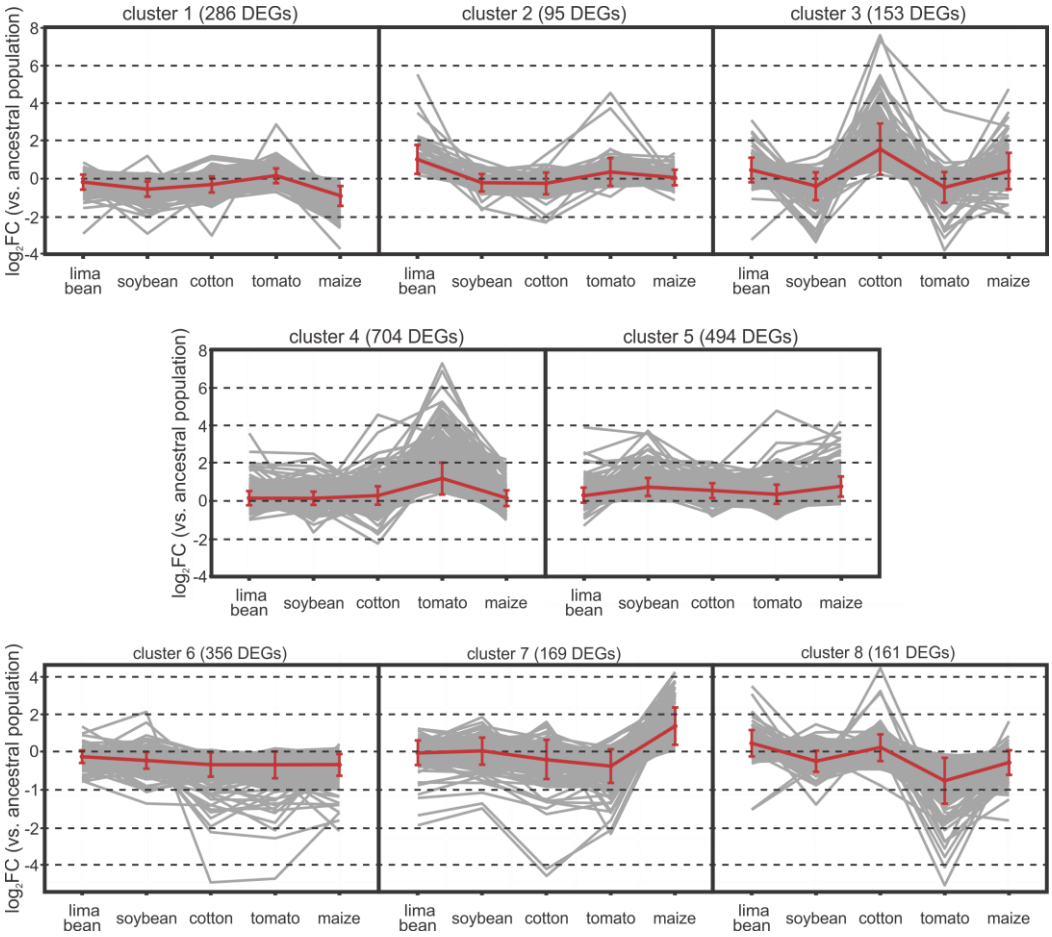

Figure 2 - *k*-means clustering of the *T. urticae* DEGs upon the different long-term host plant transfers. Mite transcriptomic responses to the long-term host plant transfers were categorized into eight clusters using centered Pearson's correlation as the distance metric. Clusters were arranged according to the magnitude of log_2FC of the DEGs. Red lines connect the averages of log_2FC of the different host plant populations within each cluster, with error bars representing the standard deviation.

4.2. *k*-means clustering of transcriptomic responses to long-term host plant transfer

To get more insight into the global transcriptomic patterns, we performed a *k*-means clustering of the mite transcriptomic responses to the long-term host plant transfers using eight clusters (cluster number identified using the gap-statistic, Figure 2). The identity of the DEGs in each of the eight groups is listed in Table S3. Three global transcriptomic patterns became apparent when focusing on these groups. Cluster 6 and 5, with a total of 850 DEGs, appeared to reflect a general response and did not exhibit any host plant specificity. Genes of clusters 1, 3, 7, and 8, with a total of 769 DEGs, were differentially up- and downregulated upon feeding to the different hosts of this study, hereby creating zig-zag patterns. Finally, clusters 2 and 4 appeared to reflect a host plant specific transcriptional response. Cluster 2 was assembled of DEGs (n=95) that were mainly specifically upregulated after long-term feeding on cyanogenic lima bean. This included *tetur10g01570,* a horizontally transferred gene of bacterial origin that codes for a functionally active β-cyanoalanine synthase that is able to detoxify cyanide, the main defense compound of lima bean

(Wybouw *et al.*, 2014). Cluster 4 consisted of the largest number of DEGs (n=704) and largely reflected a tomato-specific transcriptional response (Figure 2, Table S3).

4.3. Gene-set enrichment analysis

To look at gene family-wide patterns, we grouped *T. urticae* genes into OrthoMCL groups (Table S4, Figure 3), determined the percentage of DEGs for each OrthoMCL group for each replicated host plant population (Table S5) and subsequently performed an OrthoMCL enrichment analysis. Ten OrthoMCL groups were significantly enriched (FDR < 0.05) in all host plant populations: DOGs (OG5_134812), lipocalins (OG5_130527), cysteine proteases, papains (OG5_127800, OG5_126607), single PLAT domain proteins (Tetra_22), CCEs (OG5_126875), MFS proteins (OG5_138329), PAN domain proteins (Tetra_5) and hypothetical proteins (Tetra_9 (Small Secreted Protein Family A) and Tetra_24). A number of these gene groups (DOGs, lipocalins, CCEs, MFS, PAN-domain proteins, Tetra_9 (cluster 10066 in Dermauw *et al.*, 2013b) and Tetra_24 (cluster 10257 in Dermauw *et al.*, 2013b) were previously significantly enriched in DEG lists of both mite resistant strains and a tomato acclimatized (5 generations) mite line, while cysteine proteases and single PLAT domain proteins (cluster 10204 in Dermauw *et al.*, 2013b) were only enriched in the tomato acclimatized mite line (Dermauw *et al.*, 2013b). Among the remaining significantly enriched OrthoMCL groups we identified ten *T. urticae* specific gene clusters, including Tetra_19, Tetra_38, Tetra_54, Tetra_62, Tetra_73, Tetra_74, Tetra_85, Tetra_112, Tetra_116 and Tetra_195). Of particular note, members of OrthoMCL groups Tetra_19 (referred to as Tu_MCL_12 in Jonckheere *et al.* 2016), Tetra_54 (referred to as Tu_MCL_25 in Jonckheere *et al.* 2016), Tetra_62 (referred to as Tu_MCL_35 in Jonckheere *et al.* 2016, Small Secreted Protein Family F) were previously identified in the *T. urticae* salivary proteome and shown to be expressed in the salivary glands (Jonckheere *et al.*, 2016). In addition, members of Tetra_54 were also shown to be constitutively upregulated in tomato-adapted mites (Wybouw *et al.*, 2015). The replicated maize population had the highest number of significantly enriched OrthoMCLs (n=33), followed by the soybean (n=29), lima bean (n=28), cotton (n=24) and tomato (n=22) populations. Four significantly enriched OrthoMCLs were unique for the tomato-fed mites, including genes coding for BTB and C-terminal Kelch related proteins (OG5_184484), while three, one, one and three significantly enriched OrthoMCL groups were unique for the lima bean, soybean, cotton, and maize populations, respectively. As a next step in our functional characterization of the mite transcriptomic responses, we complemented our OrthoMCL analysis with GO enrichment analyses (Table S6). For the DEG sets upon the lima bean, soybean, cotton, and maize long-term transfer, only a few significantly enriched GO terms could be identified, as shown in Table S6. The highest number of significantly enriched GO terms (n=15) was found for the DEG list upon the long-term transfer to tomato, ranging from “perceiving signals” (GO:0007165) over transcription factor activity (GO:0003677 and GO:0003700) to “transmembrane transport” (GO:0055085).

4.4. Phylogenetic analysis of *T. urticae* short-chain dehydrogenases and single PLAT domain proteins

Among the OrthoMCL groups that were significantly enriched we identified two gene families that have not yet been associated with mite xenobiotic response to host transfer: short-chain dehydrogenases (OG5_126860 and OG5_128170, having PFAM domain PF00106 and/or PF13561) and single PLAT domain proteins (PFAM domain PF01477). Both families were annotated within the *T. urticae* Sanger-sequenced genome assembly and their phylogenetic relatedness was investigated using a maximum-likelihood phylogenetic approach. Eighty-eight full-length SDR genes and 24 SDR gene fragments/pseudogenes were annotated in the *T. urticae* genome (Table S7). Full-length *T. urticae* SDR proteins were, together with those of *M. occidentalis*, *D. melanogaster* and *H. sapiens,* used in a maximum-likelihood analysis. We identified clear 1:1:1:1 orthology between five SDRs of each arthropod species and human SDRs (HSD17B4, HSD17B8, KDSR, TSTA3, WWOX and DHRSX), verifying the validity of our phylogenetic approach. Furthermore, we identified several *T. urticae* specific expansions. Twenty-Five *T. urticae* SDRs (either belonging to OrthoMCl group OG5_128170 or OG5_136892) clustered with high bootstrap support with 5 SDRs of both *M. occidentalis* and *D. melanogaster* (group I and tetur08g02060 in Figure 4), while ten *T. urticae* SDRs (OG5_126860) clustered with high bootstrap support with a *Drosophila* SDR (FBtr0071183) (group II in Figure 4). The latter *Drosophila* SDR, named sniffer, is a carbonyl reductase and has been shown to prevent oxidative stress-induced neurodegeneration (Martin *et al.*, 2011). Remarkably, OG5_128170 was significantly enriched in the DEG sets of the bean, soybean, and maize populations whereas OG5_126860 was significantly enriched in DEGs of the tomato and maize populations (Figure 3). Finally, we also identified two smaller *T. urticae* SDR expansions, one with five SDRs in *T. urticae* (belonging to OrthoMCL group OG5_127561) compared to one in *M. occidentalis* (Mo_rna15492) and one with five SDRs in *T. urticae* (belonging to OrthoMCL group OG5_131031) compared to one in both *M. occidentalis* (Mo_rna12331)*, D. melanogaster* (FBtr0074654) and *H. sapiens* (DCXR). Genes encoding *T. urticae* SDRs seem to be dispersed across the genome with 61.4% of them being singletons. However, most of the genes within two *T. urticae* SDR specific expansions (Group I and II (Figure 4, panel B)) were found in clusters of scaffolds 6, 12 and 28. Within the SDR gene clusters on scaffolds 6 and 12, genes were not only found in a head-to-tail orientation but in both orientations. Moreover, the largest clusters (on scaffold 6 and scaffold 12) are rich in transposable elements (TE) sequences (see e.g. *tetur12g00570* at ORCAE (http://bioinformatics.psb.ugent.be/orcae/overview/Tetur/, Sterck *et al.*, 2012)), suggestive of multiple duplication events. However, features of genomic distribution will become clearer once a chromosome-wide assembly of the *T. urticae* genome will be available.

We also investigated *T. urticae* single PLAT domain proteins into more detail. Twenty-one single PLAT domain protein genes were found in the *T. urticae* genome (20 were considered as full-length genes and one as a pseudogene), and four single PLAT domain gene fragments were identified. Next, we also identified single PLAT domain protein genes in the transcriptomes of other

less polyphagous tetranychid mites such as *T. evansi* (n=8), *P. ulmi* (n=6) and *P. citri* (n=10) (Table S8). A blastp search against the non-redundant protein database in NCBI, revealed that tetranychid single PLAT domain proteins do not show sequence similarity with proteins of non-tetranychid eukaryotic species. A literature search, however, revealed that single PLAT domain proteins do occur in dicot and monocot plant species (Hyun *et al.*, 2015), but these do not show

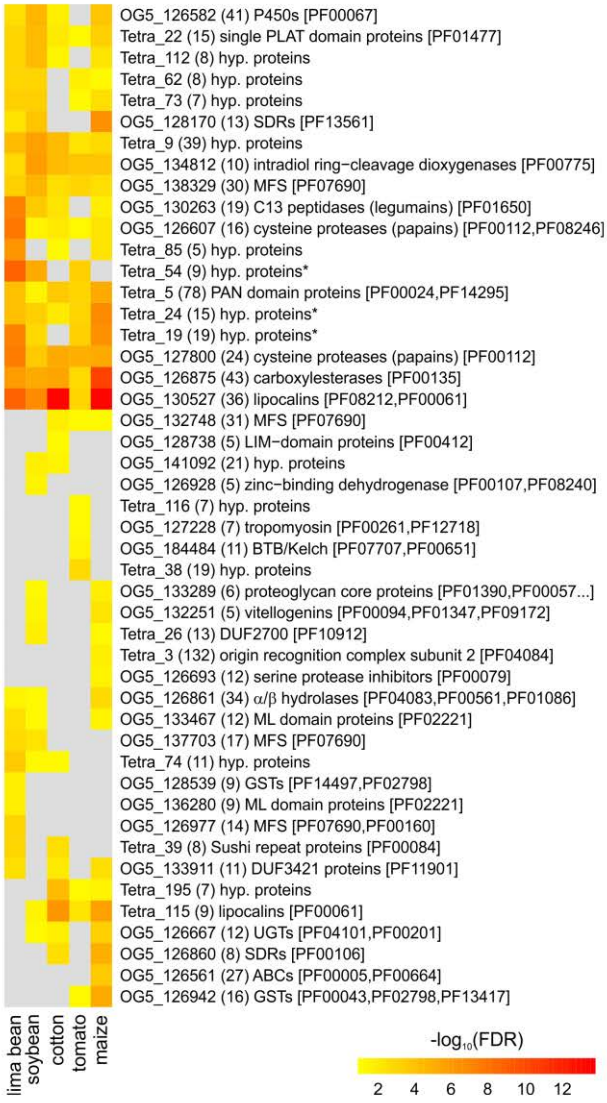

Figure 3 - OrthoMCL enrichment analysis of the DEGs identified in the different host plant populations of *T. urticae*. Heatmap showing the Benjamini-Hochberg corrected p-value (FDR) significance of OrthoMCL groups among DEGs of each host plant population. A grey colored cell indicates that the OrthoMCL group was not significantly enriched (FDR ≥ 0.05) for a certain host plant population. The number between parentheses represents the total number of *T. urticae* genes in an OrthoMCL group (corrected for those genes that have probes on the array), while PFAM accessions associated with any of the genes in a certain OrthoMCL group are shown between square brackets. An asterisk indicates that members of these hypothetical protein OrthoMCL groups were found in the salivary proteome of *T. urticae* (Jonckheere *et al.*, 2016).

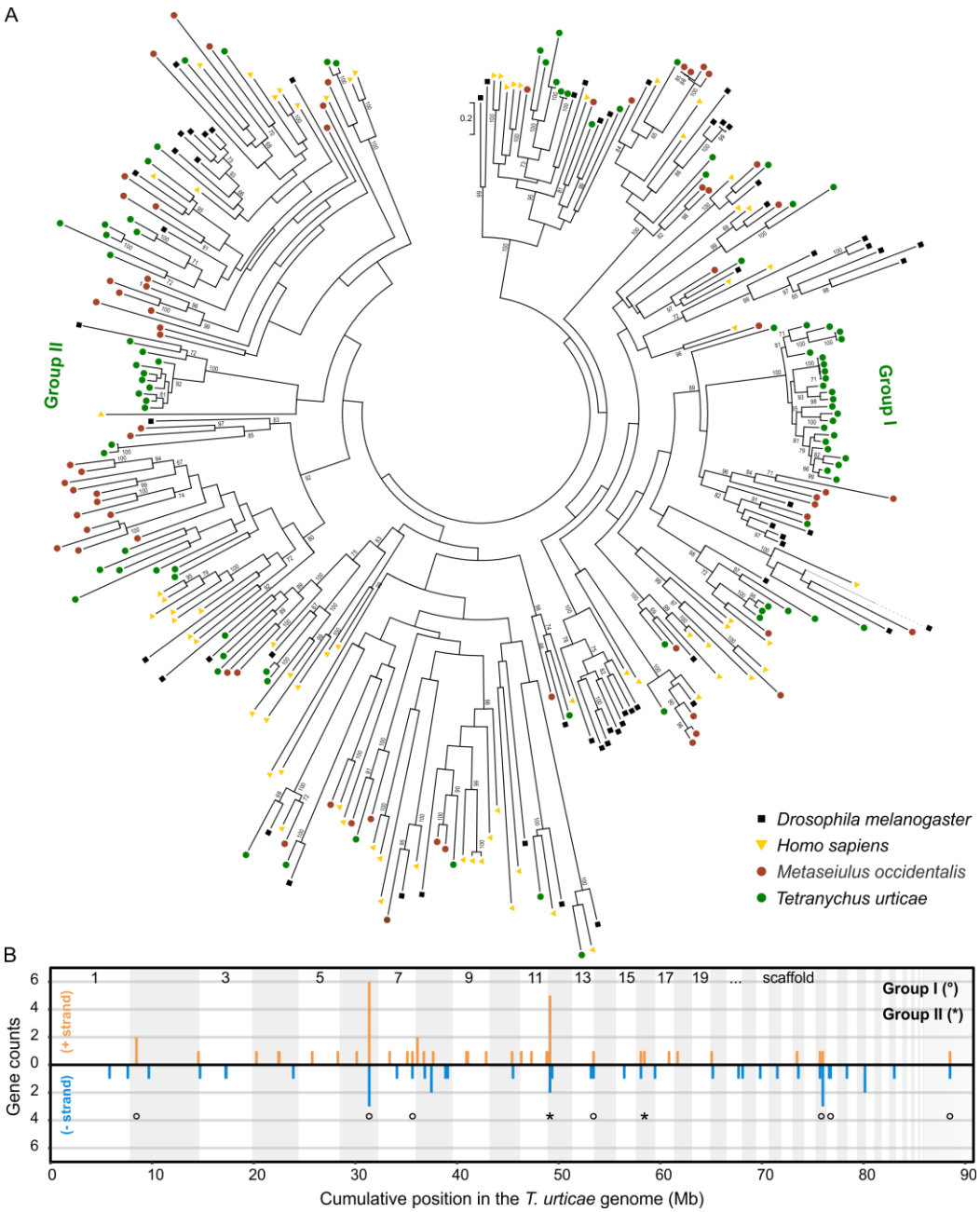

Figure 4 - (A) Maximum likelihood phylogenetic analysis of the SDRs of *Homo sapiens*, *Drosophila melanogaster*, *Metaseiulus occidentalis* and *Tetranychus urticae*. Only bootstrapping values higher than 65 are shown. The scale bar represents 0.2 amino acid substitutions per site. *T. urticae* SDR expansions containing members of OrthoMCL groups that were significantly enriched among one of the DEG sets of the host plant populations are indicated by green font and labeled as Group I (°) and Group II (*). Branches that were shortened for figure clarity are shown as dashed lines. Information and accession numbers of the used SDRs can be found in Table S7 and File S2. (B) Genomic distribution of *T. urticae* SDRs is shown with lengths of vertical line segments corresponding to counts in a gene cluster; gene counts for the forward (+, orange) and reverse (−, blue) strand orientations. Clusters of SDRs were calculated such that, for a given gene, its count contributes to only one vertical line segment. Only intact SDRs were included in the analysis. Genes of the expansions of Group I and II (see panel A) are marked with their respective symbol. The genome was concatenated from largest to smallest scaffolds for display, alternating scaffolds are indicated by shading. The original figure, including all gene names, can be found in Snoeck *et al.*, 2018.

sequence similarity with those of *T. urticae*. Nevertheless, both *T. urticae* and plant single PLAT domain proteins do share the same protein secondary structure, as they both have the PLAT domain, a β-sandwich composed of two sheets of four strands each (Bateman and Sandford, 1999). Finally, we performed a maximum likelihood phylogenetic analysis using tetranychid single PLAT domain proteins (Figure 5). We identified two clear expansions of single PLAT domain proteins in *T. urticae*, with one expansion consisting of six single PLAT domain proteins in *T. urticae* (group I) compared to one in *P. citri* and *T. evansi* and one expansion consisting of seven single PLAT domain proteins in *T. urticae* (group II) compared to one in *P. citri* and *T. evansi*. Interestingly, *tetur11g05720* and *tetur11g05730* of group I showed the strongest expression changes (log_2FC between -7 and 3) of all *T. urticae* single PLAT domain protein genes upon long-term transfer to any of the host plant lines (Table S1, Figure S1). Only 20% of the genes encoding single PLAT domain proteins in the *T. urticae* genome are singletons. The remaining single PLAT domain proteins (n=16) are found in clusters on scaffolds 6, 11, 15 and 22 (Figure 5, panel B). Similar as for the SDR genome distribution, single PLAT domain protein gene clusters contained genes in both orientations and were rich in TE sequences (see e.g. *tetur11g05730* at the ORCAE database (Sterck *et al.*, 2012)), suggestive of multiple duplication events.

5. Discussion

Arthropod herbivores are important crop pests, and the last decade has seen an unprecedented increase in our understanding of the evolutionary mechanisms associated with resistance development to insecticides and acaricides used for their control. Given the wealth of knowledge on the molecular genetic mechanisms of pesticide resistance in mites and insects (Li *et al.* 2007; Feyereisen *et al.* 2015; Van Leeuwen and Dermauw 2016), it is surprising that mechanisms that allow broad plant use have remained elusive. In the last few years, an increasing number of transcriptomic studies have revealed that short-term exposure or within-generation transfer to novel hosts in polyphagous arthropod herbivores is associated with large transcriptional responses (e.g. Govind *et al.* 2010; Grbić *et al.* 2011; Dermauw *et al.* 2013b; de la Paz Celorio-Mancera *et al.* 2013; Vogel *et al.* 2014; Zhurov *et al.* 2014; Roy *et al.* 2016). Fewer studies have addressed changes in gene expression upon long-term exposure and adaptation, especially in comparison to an ancestral genetic background (feeding on original host). For spider mites, Wybouw *et al.* 2015 revealed that the number of DEGs and the extent of transcriptional change increases over time and generations, and based on the functional prediction of the DEGs upon short- and long-term exposure, it was postulated that these transcriptional responses are adaptive, enabling the herbivore to survive a shift in dietary nutrients and toxins. However, the few studies addressing these important evolutionary processes looked at the transfer to a single or very few

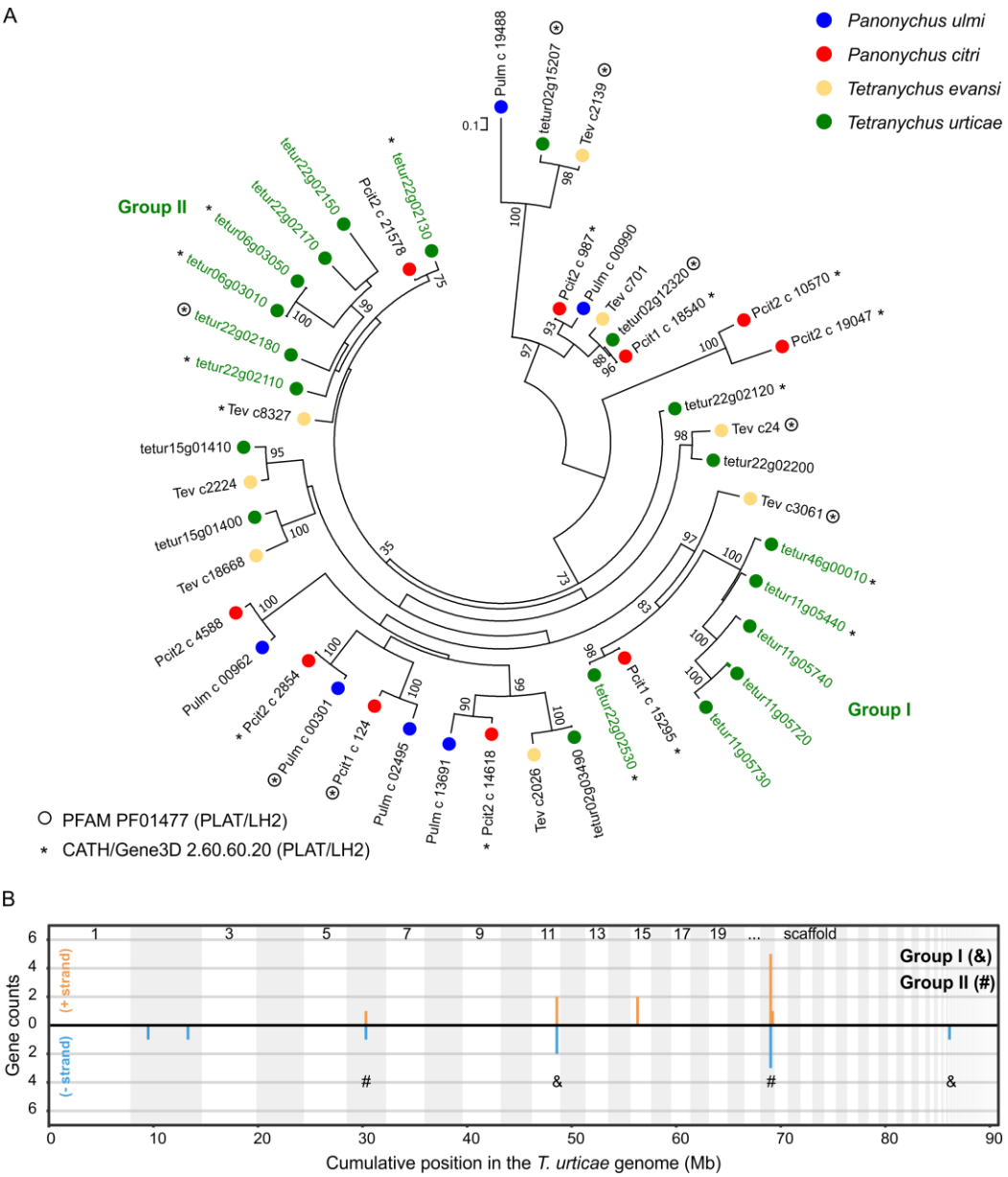

Figure 5 - (A) Maximum likelihood phylogenetic analysis of the single PLAT domain proteins of *Panonychus ulmi*, *Panonychus citri*, *Tetranychus evansi* and *Teteranychus urticae*. Only bootstrapping values higher than 65 are shown. The scale bar represents 0.1 amino acid substitutions per site. *T. urticae* single PLAT domain protein expansions are indicated by green font and labeled Group I (&) and Group II (#). Information and accession numbers of the tetranychid single PLAT domain proteins can be found in Table S8 and File S3. Those proteins with the PFAM PLAT domain (PF01477) or belonging to the CATH/Gene3D PLAT/LH2 Superfamily (2.60.60.20) are indicated with a circle and an asterisk, respectively (B) Genomic distribution of *Tetranychus urticae* single PLAT domain protein genes is shown with lengths of vertical line segments corresponding to counts in a gene cluster; gene counts for the forward (+, orange) and reverse (−, blue) strand orientations. Clusters of single PLAT domain protein genes were calculated such that a given gene its count contributes to only one vertical line segment. Only intact single PLAT domain protein genes were included in the analysis. Genes of the expansions of Group I and II (see panel A) are marked with their respective symbol. The genome was concatenated from largest to smallest scaffolds for display, alternating scaffolds are indicated by shading.

new hosts (Dermauw *et al.*, 2013b; Mathers *et al.*, 2017; Müller *et al.*, 2017; Wybouw *et al.*, 2015, 2014; Xie *et al.*, 2014). Therefore, we have addressed in the current study to what extent the long-term transcriptional responses are host plant specific, using spider mites as a model. In addition, we investigated which multi-gene families were associated with the different host plant transfers.

Mites were transferred from their ancestral host (common bean) to lima bean, soybean, cotton, tomato, and maize. These plant species were selected as many of these are economically important crops on which spider mites are reported as pests (Van Leeuwen *et al.* 2014). In addition, some of the metabolites that are produced by this selection of plants have been well-characterized as plant allelochemicals with a defensive role against attacking herbivores, including the cyanogenic glucosides of lima bean, the tomato alkaloid tomatine (DongSub *et al.*, 2014; Friedman, 2002), coumestrol in soybean leaves (Yuk *et al.*, 2011), the terpenoid gossypol produced by cotton (McCormick, 1982) and the benzoxazinoid DIMBOA-Glc in maize (Glauser *et al.*, 2011). Remarkably, although it is suggested that generalists have a less fine-tuned, host-specific regulation of gene expression compared to a specialist (Dermauw *et al.*, 2013b; Govind *et al.*, 2010; Voelckel and Baldwin, 2004), the majority of *T. urticae* DEGs were not shared between the different host plant populations in our study. Furthermore, the number of DEGs upon the different host plant transfers could also be related to the phylogenetic distance of the novel host plant to the ancestral host (common bean, Fabaceae) (Table 1). The host specificity of the mite transcriptomic response was also reflected in our *k*-means clustering analysis, where the majority of the DEGs were present in clusters that show a host-specific pattern (Figure 2). Such transcriptomic specificity was also observed recently in the oligophagous mustard leaf beetle (*Phaedon cochleariae*) (Müller *et al.* 2017). When this beetle is transferred from its original host *Brassica rapa* to *Nasturtium officinale* and *Sinapis alba* for 26 generations, transcriptomic analysis shows that most of the response is host plant specific, even though the two new hosts share the same classes of defensive metabolites as the ancestral host (glucosinolates, phenolics, and terpenoids – in different compositions).

Wybouw *et al.* 2015 showed that approximately half of the complete transcriptional response of *T. urticae* after a long-term exposure to tomato is genetically determined and thus evolves upon tomato adaptation. The genetic changes in tomato-adapted mites affect both constitutive transcription and within-generation transcriptional plasticity. Here, we did not investigate whether the long-term transfer resulted in adaptation and therefore cannot distinguish between genetic adaptation, environmental induction and an interaction between these factors as the cause of the transcriptomic changes. Nevertheless, as the ancestral population was genetically diverse and the PCA plot did not show any signs of genetic drift, a substantial part of the observed responses probably resulted from genetic adaptation. In corroboration, *T. urticae* populations have shown great adaptive potential to a diverse set of novel hosts in addition to tomato (Fry, 1989; Gould, 1979; Magalhães *et al.*, 2009, 2007; Wybouw *et al.*, 2012).

Although the overall response was very specific on the gene level, there was much less specificity on the gene family level, which does suggest the presence of common mechanisms of acclimation and adaptation. Indeed, the set of DEGs of each host plant population was significantly enriched for genes from multigene families (OrthoMCL groups ≥ 10 members) and many of the

multigene families that were significantly enriched, were previously shown to respond to xenobiotic pressure. These families were comprised of P450s and CCEs, involved in detoxification, cysteine proteases, involved in digestion, and previously unknown players in xenobiotic detoxification such as DOGs, lipocalins and MFS proteins (Dermauw *et al.*, 2013b; Santamaría *et al.*, 2015). The importance of the metabolic processes associated with their activities was also partially reflected in the GO enrichment analysis, where GO terms “peptidase activity”, “transferase activity” and “transmembrane transport" were enriched in the DEG sets of the host plant populations (Table S6). In addition to overall metabolic processes, these transcriptomic changes upon acclimation to different host plants also provide a first link between differential expression patterns of specific genes and known defense compounds of each host plant. Gossypol, for example, is a well-known phytoalexin in cotton and it has been shown that UGT-glycosylation and P450-oxygenation of gossypol are important for gossypol detoxification (Krempl *et al.*, 2016; Mao *et al.*, 2007). Interestingly, a *CYP* and *UGT* gene were among the most highly upregulated genes when feeding on cotton (log_2FC of 7.6 and 2.5 for *tetur07g06410* (*CYP392A1*) and *tetur04g02350* (*UGT203A2*), respectively, see Table S1). Similarly, a *UGT* (*tetur05g05020* (*UGT201B7*)) and *GST* (*tetur05g05270* (*TuGSTd15*)) were highly upregulated in the maize population (log_2FC of 3.6 and 3.7, respectively) while downregulated or not differentially expressed in all other host plants, and might thus be involved in the detoxification of benzoxazinoids, phytochemicals that are widespread in grasses (Loayza-Muro *et al.*, 2000; Wouters *et al.*, 2016).

Next to the overall implication of gene families known to be involved in arthropod xenobiotic metabolism, our analyses also revealed the prominent presence of a number of gene families that have only been marginally associated with arthropod detoxification (Figure 3 and Table S5). For example, OrthoMCL analysis revealed that SDRs were significantly enriched in the DEG sets of the *T. urticae* host plant populations (Table S1). The SDR superfamily is one of the largest and most highly divergent protein superfamilies found in all domains of life (Kallberg *et al.*, 2010). SDR enzymes are 250-300 amino acids long (see InterPro domain IPR020904) and are NAD(P)(H)-dependent oxidoreductases with low pairwise sequence identities. They contain at least 2 domains, a structurally conserved N-terminal region which binds NAD(H) or NADP(H) as a co-factor and a structurally variable C-terminal region that binds the substrate and contains the amino acids involved in catalysis (Bray *et al.*, 2009). In contrast to the P450 superfamily, functional insights on the SDR superfamily are very scarce (Škarydová and Wsól, 2012). Carbonyl-reducing enzymes (CDRs) from the SDR superfamily are known to be involved in the biosynthesis/metabolism of endogenous signaling molecules like steroid hormones and retinoids, but are as well involved in the detoxification of endobiotics and xenobiotics (Hoffmann and Maser, 2007; Oppermann, 2007; Škarydová and Wsól, 2012). In humans, SDRs have been shown to play a central role in phase I metabolism by converting aldehydes or ketones into the corresponding alcohols, thereby reducing the overall chemical activity of their substrates (Ebert *et al.*, 2016; Škarydová and Wsól, 2012). In insects, the best characterized SDRs are alcohol dehydrogenases (Figueroa-Teran *et al.*, 2016; Mayoral *et al.*, 2013; Zhang *et al.*, 2004). However, only few studies report upon the possible role of SDRs in arthropod-plant interactions. SDR genes are overexpressed in the Asian longhorn beetle

Anoplophora chinensis upon dietary changes (Mason *et al.*, 2016) and are present in the saliva of aphids, white flies and thrips (Stafford-Banks *et al.*, 2014; Su *et al.*, 2012). Reduction of quinone by a carbonyl reductases in the luna moth *Actias luna*, is presumably the best known example of an SDR that is involved in detoxification of a plant allelochemical (Lindroth, 1991). *Actias luna* larvae are able to feed on plants of the Juglandaceae family, which contain juglone, a compound toxic to a variety of insects. Feeding larvae exhibited high carbonyl reductase and glutathione transferase activity, and these activities have been linked to the metabolism of juglone and related quinones in the plant family of the Jungladaceae (Lindroth, 1989). Since SDRs have only been marginally described in both the context of host plant transfer as well as xenobiotic metabolism in mites, we have provided a survey of the SDR superfamily in *T. urticae* and identified eighty-eight full length SDRs in the genome of *T. urticae*, including several apparent species-specific expansions, which increased the diversity of the SDR repertoire. One of the expansions clustered together with a *Drosophila* SDR, named sniffer, a carbonyl reductase involved in the prevention of oxidative stress-induced neurodegeneration (Martin *et al.*, 2011). The production of reactive-oxygen species is an essential part of the plant response towards herbivore attack, including those of spider mites (Santamaria *et al.* 2018). Several *T. urticae* SDRs that clustered with *Drosophila* sniffer were differentially expressed upon acclimation of *T. urticae* to different host plants (Figure 3, Figure S1, Table S1) and, hence, might play a protective role during spider mite feeding.

Next to the SDR gene family, the presence of a remarkable set of proteins containing a single PLAT domain was also evident from the OrthoMCL enrichment analysis (Figure 3). Proteins with a PLAT domain are ubiquitously present across eukaryotic species (see species distribution of PF01477 at https://pfam.xfam.org/) and PLAT domains are for example present in pancreatic triglyceride lipases (cd01755 at Conserved Domain Database (CDD)). However, short single PLAT domain proteins (less than 200 amino acids) are to our knowledge only present in plants (see EOG09360P3N at OrthoDB v9.1 and cd01754 at the Conserved Domain Database for phylogenetic distribution of these plant PLAT proteins) and apparently tetranychid mites (this study). There is virtually nothing known about the possible role of these proteins in plants. Hyun *et al.* 2015,2014, showed that a single PLAT domain protein of *Arabidopsis* (PLAT1, *AT4G39730)* is involved in abiotic stress tolerance while in *Capsicum annuum* a single PLAT domain protein, named CaTin1, interferes with the redox balance of plants, leading to an altered response to ethylene and biotic/abiotic stress (Shin *et al.*, 2004). Coker *et al.* 2005, on the other hand, showed that a single PLAT domain protein gene (*FIT-6*) is upregulated upon fire damage. In *T. urticae,* several single PLAT domain protein genes were among the DEGs with the strongest transcriptional response upon long-term host transfer, with a single PLAT gene (*tetur11g05730*) being more than 100-fold lower expressed upon long-term cotton feeding while being about 10-fold overexpressed in the maize population. Although one must be cautious when comparing genomic and transcriptomic data (e.g. recent duplications and lowly expressed genes might be missed in transcriptomic data), a phylogenetic analysis using tetranychid single PLAT domain protein sequences derived from genomic (*T. urticae*) and transcriptomic data *(T. evansi*, *P. ulmi*, and *P. citri)* showed that single PLAT domain protein genes were expanded in the polyphagous *T. urticae* compared to

oligophagous tetranychid species (Figure 5). Overall, it can be speculated that single PLAT domain proteins are involved in the stress response of *T. urticae* and that their expansion might have contributed to the polyphagous nature of this species.

In summary, we investigated long-term acclimation to five novel host plants in the spider mite *T. urticae*. Using different analytical tools, we uncovered that responses were specific on the individual gene level, but that similar gene families and metabolic processes were involved in host plant use. A number of surprising new gene families have entered the stage, such as genes encoding single PLAT domain proteins and short-chain dehydrogenases. Our data set identified specific enzymes that likely underlie resistance to specific plant allelochemicals and now await *in vitro* functional validation by recombinant expression in model systems like insect cells or *E. coli* and/or *in vivo* functional validation by reverse and forward genetic approaches, once they become available as robust tools for spider mite research.

Funding information

NW and WD are postdoctoral fellows of the Research Foundation Flanders (FWO). This project was supported by NWO (the Netherlands) under the Joint Programming Initiative on Agriculture, Food Security and Climate Change (FACCEJPI) European Research Area Networks (ERA-NET) Plus framework (GENOMITE, project ID 137), the Research Foundation Flanders (FWO, Belgium) (grant G009312N to TVL and grant G053815N to TVL and WD).

Author contributions

TVL, WD and NW designed the experiment. Analysis and interpretation of the results was done by SS, NW and WD. The manuscript was written by SS, NW and WD, all figures were prepared by SS, NW and WD. All authors reviewed the manuscript.

Supplementary information

All supplementary data can be found at doi.org/10.25387/g3.7189412

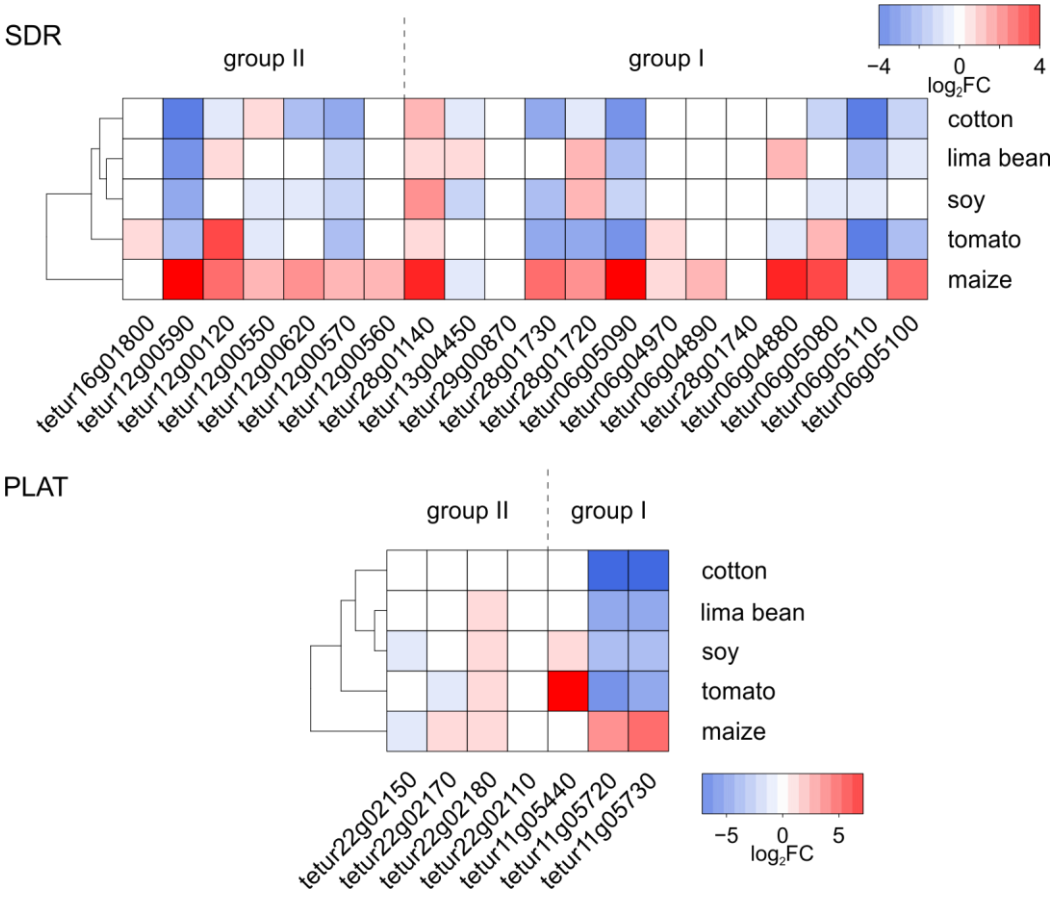

Figure S1 – Expression heatmaps of genes coding for group I and II SDRs and group I and II single PLAT domain protein genes for the different *T. urticae* host plant lines. The $\log_2$ transformed gene fold changes of adult *T. urticae* females transferred to new hostplants (lima bean, soybean, cotton, tomato, maize) relative to adult *T. urticae* females of the parental population on bean are shown. Host plants were clustered using a Euclidean distance metric and Ward's method. *T. urticae* genes are shown at the bottom.

Table S1 – Differential gene expression analysis of the different *T. urticae* host plant lines. DEGs (absolute fold change (FC) ≥ 1.5 and Benjamini-Hochberg adjusted p-value < 0.05) between populations of adult *T. urticae* females transferred to new hostplants (lima bean, soybean, cotton, tomato, maize) compared to adult *T. urticae* females of the parental population on bean.

Table S2 - Overlap between DEGs of the different *T. urticae* host plant lines. Overlap of upregulated/downregulated DEGs between the different *T. urticae* host plant lines, all in comparison to adult *T. urticae* females of the parental population on *Phaseolus vulgaris* (absolute fold change (FC) ≥ 1.5 and Benjamini-Hochberg adjusted p-value < 0.05)

Table S3 - k-means clustering of the DEGs identified in the different host plant lines of *T. urticae* (tomato, soybean, lima bean, maize and cotton). Mite transcriptomic responses to the long-term host plant transfers were categorized into eight clusters.

Table S4 - OrthoMCL clustering of the *T. urticae* proteome OrthoMCL clustering of the *T. urticae* proteome (version of August 11, 2016; see Jonckheere 2018, PhD dissertation, ISBN: 9789491407543). A summary of the number of *T. urticae* proteins in each OrthoMCL can be found in the worksheet 'OrthoMCL summary'.

Table S5 – OrthoMCL enrichment analysis of the DEG sets of each *T. urticae* host plant line

Table S6 - Significantly enriched GO terms in the DEGs of the different host plant lines of *T. urticae*

Table S7 - Short-chain dehydrogenase genes annotated in the *T. urticae* genome

Table S8 - Single PLAT domain protein genes annotated in the *T. urticae* genome

File S1 – FASTA-file containing the CDS sequences of the *T. urticae* genome annotation (version of August 11, 2016), compressed ZIP-file

File S2 – FASTA-file containing protein sequences of the short-chain dehydrogenases of *T. urticae*, *M. occidentalis*, *D. melanogaster* and *Homo sapiens* included in the phylogenetic analysis (Figure 4).

File S3 – FASTA-file containing sequences of the full-length single PLAT domain proteins of *T. urticae*, *T. evansi, P. ulmi* and *P. citri* included in the phylogenetic analysis (Figure 5).

Chapter 5

Substrate specificity and promiscuity of horizontally transferred UDP-glycosyltransferases in the generalist herbivore *Tetranychus urticae*

This chapter has been partially redrafted from:

Snoeck[*], S., Pavlidi[*], N., Pipini, D., Vontas, J., Dermauw, W., Van Leeuwen, T. (2019). Substrate specificity and promiscuity of horizontally transferred UDP-glycosyltransferases in the generalist herbivore *Tetranychus urticae*. Insect Biochemistry and Molecular Biology, 109, 116-127.

1. Abstract

Uridine diphosphate (UDP)-glycosyltransferases (UGTs) catalyze the addition of UDP-sugars to small hydrophobic molecules, turning them into more water-soluble metabolites. While their role in detoxification is well documented for vertebrates, arthropod UGTs have only recently been linked to the detoxification and sequestration of plant toxins and insecticides. The two-spotted spider mite *Tetranychus urticae* is a generalist herbivore notorious for rapidly developing resistance to insecticides and acaricides. We identified a set of eight UGT genes that were overexpressed in mites upon long-term acclimation or adaptation to a new host plant and/or in mite strains highly resistant to acaricides. Functional expression revealed that they were all catalytically active and that the majority preferred UDP-glucose as activated donor for glycosylation of model substrates. A high-throughput substrate screening of both plant secondary metabolites and pesticides revealed patterns of both substrate specificity and promiscuity. We further selected nine enzyme-substrate combinations for more comprehensive analysis and determined steady-state kinetic parameters. Among others, plant metabolites such as capsaicin and several flavonoids were shown to be glycosylated. The acaricide abamectin was also glycosylated by two UGTs and one of these was also overexpressed in an abamectin resistant strain. Our study corroborates the potential role of *T. urticae* UGTs in detoxification of both synthetic and natural xenobiotic compounds and paves the way for rapid substrate screening of arthropod UGTs.

2. Introduction

Glycosyltransferases catalyze the transfer of sugar moieties from activated donor molecules to an acceptor molecule and are ubiquitous across all kingdoms of life (Lairson *et al.*, 2008). Uridine diphosphate(UDP)-glycosyltransferases (UGTs) are the largest family of glycosyltransferases (Lombard *et al.*, 2014) and catalyze the addition of UDP-sugars to small hydrophobic molecules. Next to important roles in biosynthesis, storage and transport of secondary metabolites, UGTs are, together with glutathione-S-transferases, also well-known as phase II enzymes in the detoxification process (Jancova *et al.*, 2010). By catalyzing the conjugation of hydrophobic compounds with UDP sugars, more hydrophilic compounds are generated, that enhance excretion (Mackenzie *et al.*, 1997). In contrast to human UGTs, the glycosylation of small hydrophobic compounds by arthropod UGTs has been poorly studied. Only recently, biochemical and functional studies could specifically link arthropod UGTs to the detoxification and sequestration of plant allelochemicals and insecticides (Highfill *et al.*, 2017; Krempl *et al.*, 2016; Li *et al.*, 2017). Krempl *et al.*, 2016 detected glycosylated gossypol isomers in the feces of *Helicoverpa armigera* and *Heliothis virescens*, and showed that two UGTs were capable of glycosylating gossypol. Hence, they suggested that these UGTs might play a crucial role in gossypol detoxification in generalist herbivores utilizing cotton as a host plant.

The two-spotted spider mite *Tetranychus urticae* (Chelicerata: Acari: Trombidiformes), is able to feed on more than 1100 plant species which belong to more than 140 different plant families (Migeon *et al.*, 2010). Next to being extremely polyphagous*, T. urticae* is also considered as the ‘resistance champion’ among arthropods, as it has the most documented instances of resistance to

diverse pesticides (Van Leeuwen *et al.*, 2010; Van Leeuwen and Dermauw, 2016). Eighty UGT genes were earlier identified in the *T. urticae* genome, similar to *Bemisia tabaci* (81 UGTs), but a substantially larger number than any other arthropod species reported so far (Ahn *et al.*, 2014; Chen *et al.*, 2016). They are classified in seven distinct families (UGT201-207) and recent lineage-specific gene expansions have been reported for the subfamilies UGT201A, UGT201B and UGT202A. Moreover, it was shown that these *T. urticae* UGT genes were very likely acquired from bacteria through horizontal gene transfer (Ahn *et al.*, 2014; Bajda *et al.*, 2015; Van Leeuwen and Dermauw, 2016). As a consequence, similar to bacterial UGTs, *T. urticae* UGTs do not harbor a signal peptide and a transmembrane domain (TM), which indicates that they are cytosolic enzymes (Ahn *et al.*, 2014). This contrasts to other eukaryotes, were the N-terminal signal peptide is removed upon insertion of the UGT into the endoplasmic reticulum (ER), and a C-terminal TM domain anchors the protein to the ER (Ahn *et al.*, 2012, 2014; Erb *et al.*, 2009; Magdalou *et al.*, 2010).

In this study, we identified a set of eight UGTs that were overexpressed in *T. urticae* upon long term plant acclimation/adaptation and/or resistance against certain acaricides. Next, we recombinantly expressed this set of *T. urticae* UGTs in *Escherichia coli* and determined their catalytic properties against model substrates, as well as examined their potential to conjugate an array of secondary plant metabolites and acaricides. Nine enzyme-acceptor interactions were further characterized by determining their steady state kinetic parameters and their preferred UDP-donor substrate.

3. Materials and methods

3.1. *T. urticae* strains, chemicals and plant secondary metabolites

All *T. urticae* populations were described previously (Dermauw *et al.*, 2013a; Grbić *et al.*, 2011; Jonckheere *et al.*, 2016, Chapter 4) and mass reared on their respective host plants at 26 °C (±0.5 °C), 60% relative humidity (RH) and 16/8 h light/dark photoperiod. For a more detailed description of each population, see Supplementary Table 1. All chemicals, including pesticides, and plant secondary metabolites used in this study were of analytical grade. Detailed information about suppliers and purity of substrates can be found in Supplementary Table 2.

3.2. UGT gene expression analysis

The UGT metanalysis of existing microarray gene expression data was performed in three different batches. An analysis of A) microarrays run with RNA from adult *T. urticae* females and the 1st array design (GPL15756/Agilent-028213; Dermauw *et al.*, 2013), B) microarrays run with RNA from deutonymph *T. urticae* females and the 1st array design (GPL15756/Agilent-028213; Demaeght *et al.*, 2013) and C) microarrays run with RNA from adult *T. urticae* females and the 2nd array design (GPL16890/Agilent-033850; (Jonckheere *et al.*, 2016; Khalighi *et al.*, 2015; Pavlidi *et al.*, 2017; Wybouw *et al.*, 2015, 2014, Chapter 4)). For each analysis, raw intensity data were used as input for final processing and statistical analysis in limma (version 3.30.13) of the Bioconductor framework (Smyth, 2004). Prior to differential gene expression analysis, the probe sequences were

remapped to the *T. urticae* genome annotation (cDNA sequences) of August 11, 2016 using Bowtie2-2.3.4.3 and following setting "--norc -f -a" (Langmead and Salzberg, 2012). Only the probes that aligned uniquely and without mismatches (probes having "AS:i:0" in the 1st optional field of the SAM output of Bowtie2) to the annotated genome (42577 probes for analysis A and B while 39650 probes for analysis C) were incorporated in the differential expression analysis. Next, background correction was performed by the 'normexp' method, using an offset of 50 (Ritchie *et al.*, 2007). Background-corrected data were within- and between-array normalized (global loess and Aquantile, respectively) and quality was subsequently assessed using arrayQualityMetrics (Kauffmann *et al.*, 2009). A linear model (using "lmFit" in the limma R package) was fitted to the processed data that treated the London (analysis A and C) or LS-VL (analysis B) strain as a common reference (cy3 channel in sample GSM980545-GSM980555 for analysis A, cy3 channel in sample GSM1065002-GSM1065006 for analysis B and cy3 channel in sample GSM1214964-GSM1214967, GSM2124774-GSM2124784, GSM1679383-GSM1679385 and GSM1633888-GSM1633891 for analysis C). Empirical Bayes moderated t-statistics (using the "eBayes" function in the limma R package; Smyth, 2004) was used to determine differences in transcript expression levels in reference to the London (adult females, analysis A and C) or LS-VL (deutonymph females, analysis B) strain. UGT gene expression heatmaps were created in R (R Developement Core Team, 2015) using the relative transcript levels (log_2FC) and the R package gplots_3.0.1 (Warnes *et al.*, 2009).

3.3. Phylogenetic analysis

T. urticae UGT protein sequences were derived from the ORCAE genome portal while those of *Panonychus citri* and *Panonychus ulmi* were obtained from Bajda *et al.*, 2015 and Sterck *et al.*, 2012. *Tetranychus evansi* UGTs were identified by mining the *T. evansi* transcriptome (Villarroel *et al.*, 2016): *T. urticae* UGT protein sequences were used as query in a tblastn search (E-value threshold of E^{-3}, BLAST 2.2.31+) against the *T. evansi* transcriptome. In cases where *T. evansi* contigs showed more than 95% identity at the nucleotide level, they were considered as allelic variants and the longest transcript was retained for further analysis using cd-hit-est with sequence identity threshold (-c) of 0.95 (Fu *et al.*, 2012). Open reading frames (ORFs) of *T. evansi* were identified using "EMBOSS 6.6.0.0 getorf" integrated in the Mobyle portal framework (http://mobyle.pasteur.fr/). *T. evansi* contig sequences were manually corrected to contain the longest UGT encoding ORFs. Those ORFs that showed identical overlap and had the same blastx top-hit against the *T. urticae* proteome, were considered to be part of the same gene and were manually merged using BioEdit v7.2.5 (Hall, 2013). Subsequently, ORFs were once more filtered for allelic variants using cd-hit-est (sequence identity threshold (-c) 0.95) and the longest ORF was retained for further analysis (Fu *et al.*, 2012). Finally, only *T. evansi* ORFs longer than 150 AA were retained for phylogenetic analysis. *T. urticae* UGTs were aligned with those of *T. evansi*, *P. citri* and *P. ulmi* using the online version of MAFFT 7 with the E-INS-I iterative refinement method strategy, 1000 iterations and the option "reorder" (Katoh *et al.*, 2002). A phylogenetic analysis was performed on the Cipres web portal using RAxML v8.2.10 HPC2-XSEDE with the automatic protein model assignment algorithm using maximum likelihood criterion and 1,000 bootstrap replicates (Miller *et*

al., 2010; Stamatakis, 2014). The LG + G protein model was selected as the best scoring model for maximum likelihood analysis. The resulting tree was midpoint rooted, visualized using MEGA7 (Tamura *et al.*, 2013) and edited in Corel-DRAW Home & Student x7.

3.4. Cloning, functional expression and purification of recombinant UGTs

The cDNA sequences were amplified from the maize (*tetur05g09325, tetur01g05690 and tetur05g05050*), tomato (*tetur05g00060* and *tetur22g00270*) and cotton (*tetur04g02350*) lines as well as from the London (*tetur22g00440*) and the MAR-AB (*tetur02g09850*) strain (Supplementary Table 3). For cDNA preparation, total RNA of adult spider mites was extracted using RNeasy Plus Mini kit (Qiagen, Belgium) and reverse transcribed using Maxima first strand cDNA synthesis kit (Thermo Scientific, Belgium). One microliter of the prepared cDNAs was used as the PCR template using the blunt-end Phusion High-Fidelity DNA Polymerase (Thermo Scientific, Belgium) and specific primers (Supplementary Table 4). Conditions were 98 ºC for 2 min, followed by 30 cycles of 98 ºC for 15 sec, 60 ºC for 30 sec, 72 ºC for 30 sec. PCR product was purified using E.Z.N.A. Gel Extraction Kit (Omega Bio Tek, the Netherlands) and ligated into pET100/D-TOPO (Invitrogen Life Technologies, the Netherlands), which allows expression of recombinant protein with an N-terminal 6x His tag, following manufacturer's instructions. TOP10 competent *Escherichia coli* cells were transformed with the ligation reaction and the resulted colonies were screened by colony PCR using the cloning primers (Supplementary Table 4) for the presence of the inserts. At least 5 positive colonies were further grown on liquid cultures and the corresponding plasmids were extracted using E.Z.N.A. Plasmid Mini Kit I (Omega Bio Tek, the Netherlands) and sent for sequencing (Macrogen, The Netherlands). A clone of the correct DNA sequence was selected for heterologous expression. *Escherichia coli* BL21(DE3) STAR competent cells transformed with UGT-pET100/D-TOPO construct were grown over-night and used for the 1 to 50 inoculation of 2 L LB medium containing 100 mg/ml of ampicillin. The cultures were grown at 37 ºC with shaking (170 rpm), until the absorbance at 595 nm reached 0.8-1. Then, the expression was induced by the addition of isopropyl β-D-thiogalactoside (IPTG) to a final concentration of 0.5 mM. The cultures were further grown at 18 ºC overnight and subsequently the cells were harvested by centrifugation at 5000 g for 30 min. Cell pellets were re-suspended in 25 ml of sodium phosphate buffer pH 7.4 (containing 20 mM sodium phosphate, 40 mM imidazole and 500 mM NaCl). Cells were lysed by 2 rounds of freezing/thawing followed by incubation with 10 mg/ml of lysozyme (Sigma Aldrich, the Netherlands) on ice for 30 min and sonication. Cell lysate was centrifuged at 10,000 g at 4 ºC for 30 min and the supernatant was used for the purification of the recombinant enzymes. Supernatant was loaded in 0.2 ml of pre-equilibrated Ni-NTA resin (Qiagen, Belgium) following manufacturer's instructions. Unbound proteins were washed with 30 ml (15 bed volumes) of 160 mM sodium phosphate buffer pH 7.4 and the recombinant enzyme was eluted using 500 mM imidazole in 160 mM sodium phosphate buffer pH 7.4. Protein eluates were applied to PD-10 desalting columns (GE Healthcare, the Netherlands) following manufacturer's protocol to remove imidazole, proteins were eluted with 20 mM Tris-HCl, pH 7.4 and stored at -20 ºC in 25 mM DDT and 40% glycerol. Protein concentration was measured by Bradford assay (Bradford, 1976). Purified protein was run on a 12% SDS-PAGE

gel and subsequently a Western blot was performed using anti-His-tag primary antibodies (Bio-Rad, Belgium) to verify the purity and potential proteolytic degradation of the recombinant protein. As negative controls for the downstream activity assays fractions, of non-induced constructs for *tetur05g09325* and *tetur01g05690* were purified following the procedure as described above except that IPTG was not added.

3.5. Activity assays and determination of specificities for model substrates

UGT activity was determined against the model substrates p-nitrophenol (Leszczynski and Dixon, 1990), 1-naphthol and 2- naphthol (Sigma-Aldrich, Belgium). All reactions were performed at 25 °C in 0.1 M of sodium phosphate buffer pH 7.5 in the presence of 0.83 mM of UDP-glucose (Sigma-Aldrich, Belgium), 16.7 mM MgCl2 and 0.16 mM of the model substrate. The total reaction volume was 250 µl and the incubation time 20 min. Depletion of p-nitrophenol was detected spectrophotometrically at 400 nm, and depletion of 1- and 2-naphthol substrates was quantified after fast blue staining (55.6 mM Fast Blue RR crystalline, Sigma-Aldrich, Belgium) as the resulted azo-dyes were monitored at 570 nm.

In addition to depletion, formation of reaction product was also monitored for 20 min to calculate the specific activity against each model substrate. The formation of the corresponding glucoside was detected spectrophotometrically at 295 nm for p-nitrophenol, while the conjugates of 1-naphthol and 2-naphthol were quantified by fluorescence spectrophotometry, using excitation/emission wavelength of 287/335 nm and 283/341 nm respectively, with 1 nm slit widths. For all experiments, measurements were performed in three independent replicates in 96-well plates (Greiner Bio-One, Belgium) using a Bio-Tek Synergy H1 multimode microplate reader (Bio-Tek, Belgium). Reactions without recombinant enzyme were included as a negative control for non-enzymatic glycosylation.

3.6. Treatment with β-glucosidase

To further ensure that model substrates were glycosylated by *T. urticae* UGTs, a treatment with β-glucosidase (Sigma-Aldrich, Belgium) was conducted after incubation of the model substrates p-nitrophenol and 1-naphthol with the UGTs tetur05g09325 and tetur01g05690, respectively. UGT reactions were performed as described above (Section 3.5) and upon incubation of 20 min, the reaction mixture was boiled for 2 min to inactivate the UGT enzymes. Subsequently, 1 mg of β-glucosidase (Sigma-Aldrich, Belgium) was added and incubation was continued for 1 h. Negative control reaction mixtures without recombinant enzymes were included and measurements were performed in 9 replicates. Model substrate concentrations were measured spectrophotometrically (Section 2.5) before and after incubation with β-glucosidase. R and the R package ggplot2_2.2.1 were used to plot the results.

3.7. UDP-sugar preference

Ultra-pure UDP-glucose, UDP-glucuronic acid, UDP-galactose, UDP-N-acetylgalactosamine (UDP-GlcNAc) and UDP-N-acetylglycosamine (UDP-galNAc) were purchased

from the Promega corporation and were tested as potential UDP-sugar substrates for all functionally expressed enzymes by using either p-nitrophenol or 1-naphthol depending on the model substrate preference of each enzyme (Table 1). Model substrate depletion was monitored spectrophotometrically after 20 min of incubation as described above (Section 3.5). Measurements were performed in three independent replicates. Results were plotted in R with the R package ggplot2_2.2.1.

3.8. UGT incubation and UDP-glo glycosyltransferase assay

Incubation of 50 µM substrate, 0.1µg enzyme, 400µM UDP-sugar, in a total reaction volume of 125 µl containing 0.1M sodium phosphate buffer (pH 7.5) and 16.7 mM MgCl2 at 25 °C for 1 hour was performed. Enzyme reactions were stopped by the addition of the UDP Detection Reagent of the UDP-Glo™ glycosyltransferase assay (Promega, the Netherlands), and detection of free-UDP was performed as described below. Negative controls used for the calculations consisted of all reaction components except the substrates, all reaction components except the UDP-sugar and all reaction components except the enzyme. In addition, another incubation set-up was tested for two enzymes with a relatively lower activity (tetur04g02350 and tetur05g05050) similar to the former one, except for the amount of enzyme, which was elevated to 1 µg.

The formation of free-UDP by the glycosyltransferase reaction was quantified by using the UDP-Glo™ Glycosylotransferase assay (Promega, the Netherlands). This assay detects the UDP release by converting free-UDP to ATP which results in the generation of light in a luciferase reaction. Following the manufacturer's protocol, each glycosyltransferase reaction was combined in a ratio of 1:1 (25 µL:25 µL) with the UDP-Glo™ Detection Reagent (three technical replicates) in independent wells of a white, flat bottom 96-(chimney)-well lumitrac medium binding assay plate (Greiner, Belgium) and was allowed to incubate at room temperature for 1 hour. Subsequently, luminescence was measured in Relative Luminescence Units (RLU) with a Bio-Tek Synergy H1 multimode microplate reader (Bio-Tek, Belgium) in triplicates. For absolute quantification, a UDP standard curve was determined (0-25µM UDP) and plotted with SigmaPlot 12.0 software (Figure S1). The range of measurements was determined to be in the linear range of detection.

3.9. Substrate screening

The following potential substrates were tested in the substrate screening experiment with UDP-glucose as activated donor; 7-hydroxyflavone, abamectin, acequinocyl, atropine, azadirachtin, bifenazate, bifenthrin, caffeic acid, caffeine, capsaicin, catechol, chlorfenapyr, chlorogenic acid, chrysin, clofentezine, coumestrol, cyenopyrafen, cyflumetofen, DIMBOA, dopamine, eriodictyol, fenpyroximate, gossypol, hesperetin, hexythiazox, jasmonic acid, kaempferol, L-3,4-dihydroxyphenylalanine, l-canavanine, MBOA, methanol, naringenin, nicotinic acid, profenofos, pyflubumide, pyridaben, quercetin, rutin hydrate, salicylic acid, scopoletin, spirodiclofen and vanillin (Supplementary Table 5). All substrates were dissolved in methanol and glycosylation was quantified by using the UDP-Glo™ Glycosylotransferase assay (Promega, the Netherlands) as

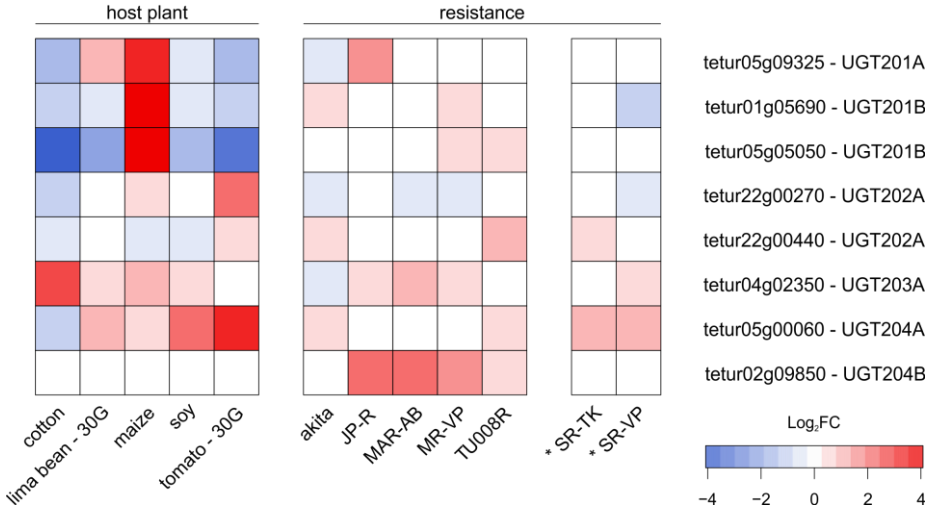

Figure 1 - Expression heatmap of a selection of *T.urticae* UGTs. Expression heatmap of the recombinant UGTs in adult (or deutonymph*) *T. urticae* females adapted to tomato and lima bean (≥ 30 generations), long-term acclimatized to soy, cotton and maize (≥ 5 generations) and resistant against acaricides (Supplementary Table 1). The log_2 transformed fold changes are relative to adult *T. urticae* females of the susceptible London strain or susceptible deutonymph *T. urticae* females of the LS-VL strain.

described above. Plots were created in R (R Developement Core Team, 2015) using R package ggplot2_2.2.1.

3.10. Image processing

CorelDRAW Home & Student ×7 was used for processing of images.

3.11. Kinetic studies of specific enzymes-substrate combinations (9) and UDP-sugar preference

Based on the substrate screening (indirect measurement of glycosylation by quantification of released free-UDP), steady-state kinetic parameters were determined for the UDP-glucose conjugation reaction of nine enzyme-acceptor combinations: tetur02g09850 – (capsaicin, kaempferol, abamectin), tetur22g00270 – (capsaicin, kaempferol), tetur22g00440 – (kaempferol), tetur04g02350 – (DIMBOA, kaempferol) and tetur05g0060 – (abamectin). Initial velocities were determined by using a constant concentration of UDP-glucose (400 µM) while acceptors were used in the concentration range of 0-400 µM, using UDP-Glo assay protocol and the reaction set-up described above. The Michaelis-Menten or Hill equation was fitted to the obtained data to define K_m and V_{max} parameters using OriginLab (OriginLab Corporation, USA) (see Table 2 for the type of equation that was fitted). Subsequently, ultra-pure UDP-glucose, UDP-glucuronic acid, UDP-galactose, UDP-N-acetylgalactosamine and UDP-N-acetylglycosamine (Promega, the Netherlands) were tested as sugar donor using acceptor substrates in a final concentration of 200 µM. A Wilcoxon rank sum test (pairwise comparison – $p < 0.05$) was performed in R using the R package pgirmess (version 1.6.9) and the data was plotted using the R package gplots_3.0.1 (Giraudoux *et al.*, 2018; Warnes *et al.*, 2009).

Table 1 - Specific activities of the recombinant enzymes for the model substrates. Enzyme characteristics were measured at 25°C and calculated as ΔOD/min/mg for the model substrate p-nitrophenol and ΔRFU/min/mg for the model substrates 1-naphthol and 2-naphthol.

enzyme	p- nitrophenol (ΔOD/min/mg)	1-naphthol ((ΔRFU/min/mg)*10^5)	2-naphthol ((ΔRFU/min/mg)*10^5)
tetur05g09325	18.92 ± 4.40	4 ± 0.12	0.15 ± 0.02
tetur01g05690	9.48 ± 1.23	350 ± 70	27 ± 2.00
tetur02g09850	8.30 ± 0.99	100 ± 10	20 ± 6.45
tetur05g05050	0.01 ± 0.00	n.d.	0.005 ± 0.001
tetur04g02350	0.02 ± 0.00	0.40 ± 0.05	0.02 ± 0.01
tetur22g00270	5.78 ± 0.88	120 ± 17	21 ± 8.00
tetur22g00440	1.25 ± 0.42	5 ± 0.47	0.64 ± 0.08
tetur05g00060	0.04 ± 0.01	0.02 ± 0.001	0.04 ± 0.008

4. Results

4.1. Selection of glycosyltransferases

T. urticae UGTs were selected based on their expression profile in acaricide resistant strains or in mite lines acclimatized or adapted to a challenging host (Figure 1, Figure S2, Supplementary Table 6). Next to gene expression data, a phylogenetic analysis was used to select UGT genes that belonged to diverse UGT clades/subfamilies, including those of lineage-specific subfamilies (Figure 2). *Tetur05g00060* and *tetur22g00270* were selected based on their high expression in the *T. urticae* line adapted to tomato. *Tetur01g05690, tetur05g05050* and *tetur05g09325* were highly expressed in a mite population acclimatized to maize. *Tetur04g02350* was highly expressed in a cotton acclimatized population. Finally, *tetur02g09850* and *tetur22g00440* were chosen because of their high expression in acaricide resistant strains MAR-AB, JP-R and MR-VP, and TU008R, respectively.

4.2. Cloning, heterologous expression and purification of *T. urticae* UGTs

Coding sequences of selected UGTs were successfully cloned into the pET100/D-TOPO expression vector and inspection of cloned sequences did not reveal any sequencing errors. IPTG induction of expression resulted in good levels of protein production. Although the majority of the expressed protein was found in the insoluble fraction, the remaining yield in the soluble fraction was sufficient to allow efficient metal affinity purification of recombinant enzymes. The overall amount of recombinant UGTs ranged from 4-10 mg derived from 2 L bacterial cultures. All UGTs were successfully purified close to homogeneity, as verified by obtaining a main band of the expected size after both SDS-PAGE as well as a Western-blot with anti-His-tag primary antibodies (Figure S3, panel A and B).

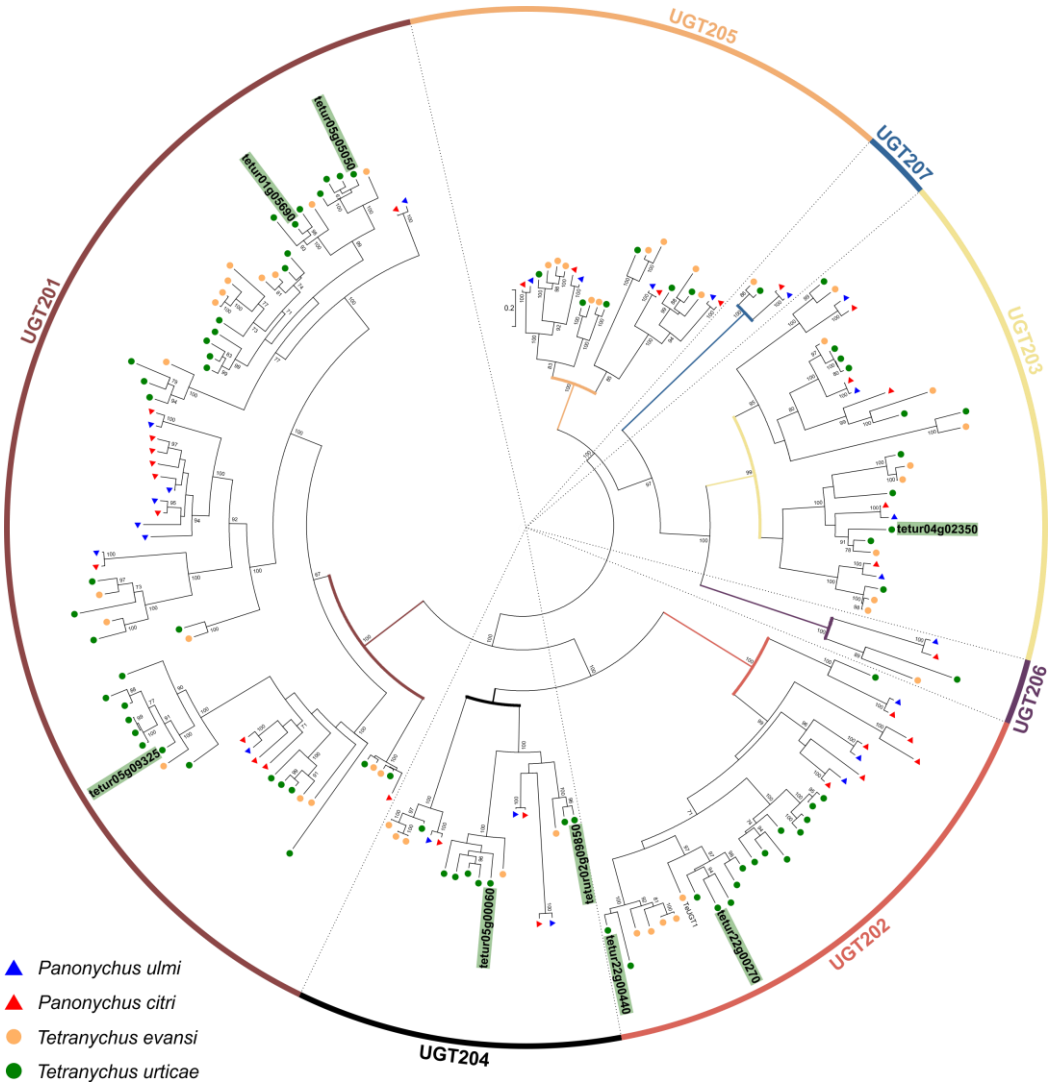

Figure 2 - Phylogenetic analysis of UGTs. Maximum likelihood phylogenetic analysis of the UGTs of *P. citri*, *P. ulmi*, *T. evansi* and *T. urticae*. UGT families (UGT201-UGT207) are labelled in the phylogenetic tree. Functionally expressed enzymes are highlighted in green. Only bootstrap values higher than or equal to 65 are shown. The scale bar represents 0.2 amino acid substitutions per site. Information and accession numbers of the used UGT sequences can be found in Supplementary Table 2. The original figure, including all gene names, can be found in Snoeck *et al.*, 2019.

4.3. Kinetic properties of recombinant *T. urticae* UGTs

The recombinant UGTs were assayed towards the model substrates p-nitrophenol, 1-naphthol and 2-naphthol to investigate whether they exhibited UDP glycosyltransferase activity (Table 1). All recombinant UGTs were capable of conjugating at least one of the model substrates. Nevertheless, for all model substrates tested, tetur05g05050, tetur05g00060 and tetur04g02350 showed low activity compared to the other recombinant UGTs. As a negative control, incubation was also performed with a recombinant glutathione S-transferase, GSTd05. Model substrates were

not glycosylated by the recombinant GSTd05 (Fig S4, panel A and B), strongly indicating that the above measured activities are the result of recombinant *T. urticae* UGT enzymes and not from *E. coli* background proteins. Elutions from non-induced constructs of tetur01g05690 and tetur05g09325 were also included as a control and resulted in a relatively low glycosylation of the model substrates compared to the induced constructs. A sign of leakage in expression which increased when the elution volume was increased from 12.5 to 25 µl (Figure S4, panel A and B). Finally, as beta-glucosidase is known to remove the glucose group of a glycosylated model substrate, we added this enzyme after incubation of model substrates with tetur01g05690 and tetur05g09325. The amount of non-glycosylated model substrate increased after incubation with beta-glucosidase in comparison to the amount of non-glycosylated model substrate before incubation with beta-glucosidase (Figure S4, panel C).

4.4. Sugar selectivity of the recombinant UGTs

The model substrates p-nitrophenol and 1-naphthol were used to determine the sugar selectivity of the functionally expressed UGTs, depending on the acceptor preference of each enzyme (Table 1). Most enzymes were able to use multiple UDP-sugars as activated donor although five out of eight enzymes clearly preferred UDP-glucose (Figure 3). For those UGTs that showed the lowest activity against any of the model substrates, tetur04g02350, tetur05g05050 and tetur05g00060, the preferred UDP-sugar could not be clearly determined. Interestingly, tetur22g0440 could only use UDP-glucose as an activated donor molecule. Based on the sugar selectivity experiment, UDP-glucose was chosen as UDP-sugar for the subsequent experiments (Section 3.5 and 3.6).

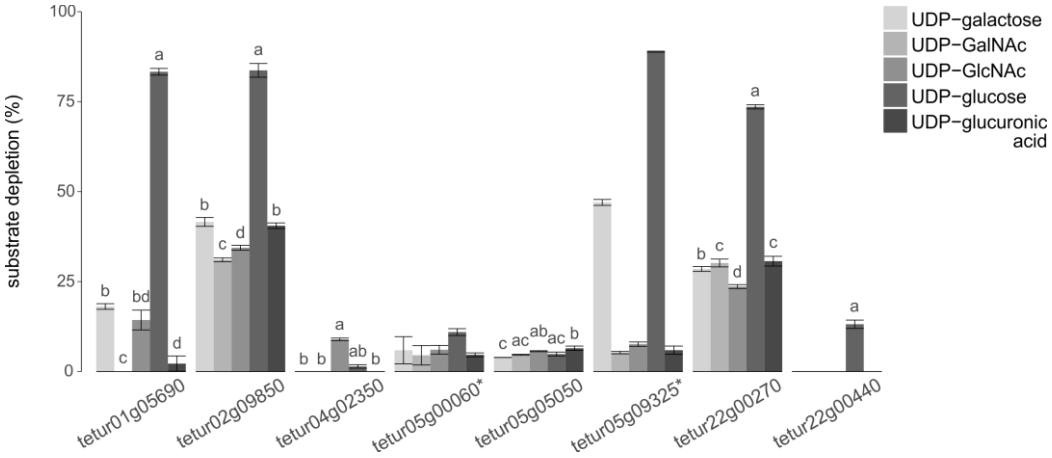

Figure 3 - Sugar-preference for model substrates. Model substrate depletion after incubation with the respective recombinant *T. urticae* UGT enzyme and the activated donors (UDP-galactose, UDP-GalNAc, UDP-GlcNAc, UDP-glucose and UDP-glucuronic acid). The model substrate p-nitrophenol or 1-naphthol was used depending on the model substrate preference of the enzyme (Table 1). Error bars represent the standard deviation of the calculated mean of three to four independent replicates. Statistical differences were analyzed using the Wilcoxon rank sum test (pairwise comparison), and are indicated as different letters (p <0.05). Two enzymes were marked with an asterisk (*) since they only had three replicates, which was insufficient to detect statistical differences.

4.5. Substrate/acceptor specificity

The substrate promiscuity of selected *T. urticae* UGT enzymes was evaluated towards a diverse set of 44 substrates (3 model substrates, 27 plant secondary metabolites and 14 acaricides) using the UDP-Glo™ glycosyltransferase assay (Promega, the Netherlands) as a quick qualitative screening method. Methanol was used as a substrate solvent for all assays.

Assays with tetur05g09325 caused very high (RLU) background values in the negative control (solvent without substrate), and this issue could not be overcome by using a different solvent (aceton, acetonitrile, DMSO or ethanol). Hence, this recombinant *T. urticae* UGT was excluded from the substrate screening.

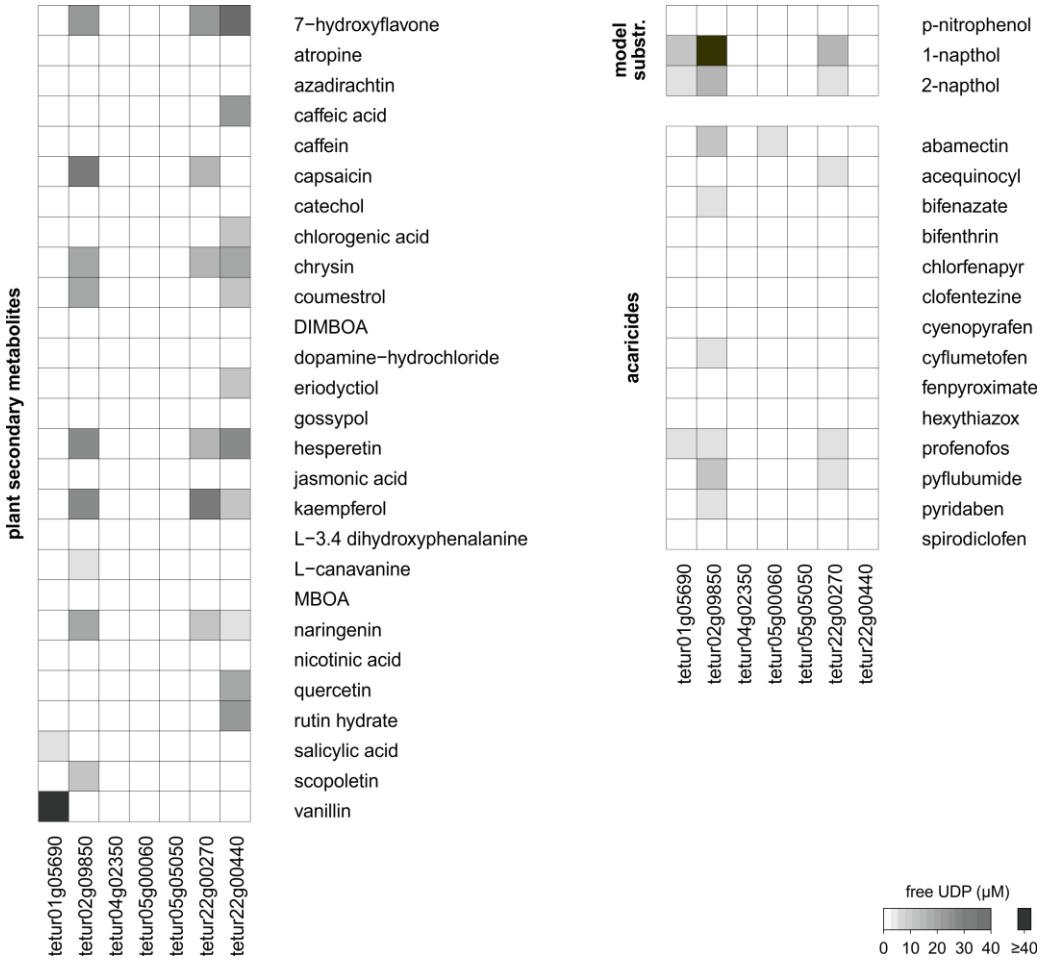

Figure 4 - Substrate screening assay. Endpoint measurement of the release of free-UDP (µM) after incubation of the respective recombinant *T. urticae* UGT enzyme (0.1µg) with 44 substrates (3 model substrates, 27 plant secondary metabolites and 14 acaricides) and UDP-glucose (Table S6). Release of free-UDP is directly linked with the activity of glycosyltransferases.

enzyme	substrate	equation	kinetic parameters			
			K_m (µM)	V_{max} (nmol UDP min^{-1} ml^{-1})	k_{cat} (min^{-1})	k_{cat}/ K_m (μM^{-1} min^{-1})
tetur02g09850	capsaicin	Michaelis-Menten	6.20 ± 0.54	0.22 ± 0.008	14.90	2.40
	kaempferol	Michaelis-Menten	34.45 ± 6.17	0.44 ± 0.02	29.81	0.86
	abamectin	Hills (n= 2.97 ± 0.29)	1.83 ± 0.06	1.83 ± 0.05	12.40	6.77
tetur22g00270	capsaicin	Michaelis-Menten	690.53 ± 180.77	0.90 ± 0.18	59.62	0.08
	kaempferol	Michaelis-Menten	31.69 ± 7.18	0.33 ± 0.02	21.86	0.68
tetur22g00440	kaempferol	Hills (n= 2.12 ± 0.23)	14.95 ± 2.36	0.33 ± 0.04	21.98	1.47
tetur04g02350	DIMBOA	Hills (n= 1.59 ± 0.08)	128.46 ± 18.28	0.13 ± 0.01	0.85	0.006
	kaempferol	Hills (n= 2.15 ± 0.11)	48.55 ± 1.38	0.26 ± 0.005	1.71	0.03
tetur05g00060	abamectin	Hills (n= 2.20 ± 0.07)	7.91 ± 0.13	0.96 ± 0.009	63.84	0.87

Table 2 - Steady-state kinetics. Steady-state kinetic parameters of recombinant *T. urticae* UGT enzymes for the conjugation of UDP-glucose to selected substrates. Results were determined by varying the concentration of substrates (1.5-200 µM) at fixed concentration of UDP-glucose (400 µM). All values are means ± SD of three independent experiments.

Some common features emerged regarding substrate specificity of the recombinant UGTs, at least for the parameters of the set-up of this high-throughput screening (Figure 4, Supplementary Table 7). (1) Three UGTs (tetur02g09850, tetur22g00270 and tetur22g00440) could glycosylate multiple substrates of the flavonoid class of secondary plant metabolites. The flavonoids included in our screening were: 7-hydroxyflavone, chrysin, coumestrol, eriodictyol, hesperitin, kaempferol, naringenin, quercetin and rutin hydrate. (2) The latter three UGTs and tetur02g09850 in particular also glycosylated a broad spectrum of acaricides. (3) In contrast with the broad spectra of the earlier mentioned UGTs, the other recombinant UGT enzymes had a narrower substrate spectrum. Tetur05g00060 glycosylated three substrates (capsaicin, abamectin and cyenopyrafen) while tetur04g02350 and tetur05g05050 showed no activity towards any of the substrates.

Specific enzyme-substrate combinations of potential interest included: (1) tetur01g05690 and the substrate vanillin, which resulted in the highest amount of released free-UDP (~glycosylation) of all combinations tested (2) next to flavonoids, tetur02g09850 and tetur22g00270 also glycosylated capsaicin (3) the plant secondary metabolite DIMBOA was not glycosylated by any of the recombinant enzymes at the default parameters of our screening assay. However, upon augmentation of the enzyme amount from 0.1 µg to 1 µg for two enzymes with a relatively lower activity (Table 1), both DIMBOA and kaempferol were glycosylated by tetur04g02350 (Figure S5).

4.6. Enzymatical characterization of the recombinant UGTs

Based on the results of the high-throughput screening, a subset of enzyme-acceptor combinations was further enzymatically characterized by determination of the steady-state kinetic parameters and presented in Table 2. Tetur02g09850 and abamectin had the highest affinity (K_m) of all enzyme-substrate combinations tested (K_m 1.83 ± 0.06 µM). Additionally, tetur02g09850 had

a high affinity for capsaicin (K_m 6.20 ± 0.54 µM). Abamectin and tetur05g00060 also resulted in a relatively good K_m and the highest turnover number (k_{cat}) observed of all enzyme-substrate combinations (K_m 7.91 ± 0.13 µM and k_{cat} 63.84 min^{-1}). Tetur22g00440 had the highest affinity of all four enzymes that were characterized with kaempferol (K_m 14.95 ± 2.36 µM). Finally, tetur04g02350 had a rather low affinity for DIMBOA (128.46 ± 18.28 µM).

Additionally, sugar selectivity of the recombinant UGTs was re-determined with the substrates from the selected subset of enzyme-acceptor combinations, instead of with the preferred model substrates as in Section 4.4. Out of the UDP-sugars tested (UDP-glucose, UDP-glucuronic acid, UDP-galactose, UDP-galNAc and UDP-GlcNAc), UDP-glucose was the preferred activated sugar donor for all enzyme-substrate combinations (Figure S6).

5. Discussion

In arthropods, cytochrome P450 monooxygenases (P450s), glutathione-S-transferases (GSTs) and carboxyl/cholinesterases (CCEs) are well-known players in the detoxification process of noxious compounds (Bajda *et al.*, 2017; Després *et al.*, 2007; Feyereisen *et al.*, 2015; Li *et al.*, 2007; Pavlidi *et al.*, 2018). UGTs, like GSTs, act in phase II of the detoxification process and catalyze the glycosylation of compounds, making them more water soluble and resulting in more rapid excretion. However, in contrast to human UGTs, the role of arthropod UGTs in detoxification has been overlooked for many years. Recently, a number of UGT genes were found to be overexpressed in insecticide resistant and host plant acclimatized/adapted populations (Faucon *et al.*, 2015; Kaplanoglu *et al.*, 2017; Li *et al.*, 2018; Tian *et al.*, 2018; Zhang *et al.*, 2017, Chapter 4) and the role of UGTs in detoxification of pesticides was investigated using inhibitors such as sulfinpyrazone and 5-nitrouracil (Li *et al.*, 2017; Pan *et al.*, 2018; Tian *et al.*, 2018; M. Y. Wang *et al.*, 2018). In addition, glycosylated plant toxins were detected in either feces or after incubation with homogenates of arthropods as UGT enzyme source (Ahn *et al.*, 2011; Kojima *et al.*, 2010; Krempl *et al.*, 2016; Maag *et al.*, 2014; Sasai *et al.*, 2009; Wouters *et al.*, 2014) and in some cases specific insect UGTs could be linked with detoxification of toxic compounds (Highfill *et al.*, 2017; Krempl *et al.*, 2016; Li *et al.*, 2017). In the genome of the spider mite *T. urticae*, 80 UGT genes were identified. Although their pattern of diversification as well as the observed plasticity of gene expression strongly suggests an important role in detoxification (Ahn *et al.*, 2014, Chapter 4), specific associations between *T. urticae* UGTs and the glycosylation of a certain compound are scarce. At present only one UGT (UGT201D3, corresponding to tetur04g02350) from the red morph of *T. urticae* has been partially characterized and was shown to be inhibited by the acaricide abamectin (M. Y. Wang *et al.*, 2018). In this study, we functionally expressed and characterized eight UGT genes that were highly expressed in *T. urticae* populations acclimatized/adapted to host plants or resistant to acaricides and that belonged to diverse UGT subfamilies, including lineage-specific UGT expansions (Figure 2). In contrast to both insect and vertebrate UGTs, which are anchored in the endoplasmic reticulum, *T. urticae* UGTs are, like bacterial UGTs, cytosolic enzymes (Ahn *et al.*, 2014). Hence, *T. urticae* UGTs could be readily functionally expressed in *E. coli* and all showed catalytic activity against at least one of the tested model substrates (p-nitrophenol, 1-naphthol and

2-naphthol, Table 1). Nevertheless, this does not rule out that eukaryotic expression systems (such as insect cells) could generate proteins with different properties. Except for tetur22g00440, recombinant *T. urticae* UGT enzymes were able to use multiple UDP-sugars for glycosylation. Interestingly, all recombinant *T. urticae* UGTs could use UDP-glucose, with five out of eight enzymes having a distinct preference for UDP-glucose (Figure 3). Hence, UDP-glucose was used as activated donor for all further glycosylation experiments. Biochemical studies in insects have shown that insect UGT enzymes also typically use UDP-glucose as the main activated donor for glycosylation (Ahn *et al.*, 2012). Likewise, plant UGTs typically use UDP-glucose next to other donors such as UDP-rhamnose, UDP-arabinose, UDP-galactose, UDP-xylose, and UDP-glucuronic acid (Bowles *et al.*, 2006; Kim *et al.*, 2013). In contrast, vertebrate UGTs mainly utilize UDP-glucuronic acid (Bock, 2003).

A high-throughput substrate screening was performed to examine the substrate breadth of *T. urticae* UGTs by testing a diverse array of 44 substrates, comprising both plant metabolites and acaricides. To our knowledge, solely Luque *et al.*, 2002 performed a similar experiment for a *Bombyx mori* UGT. While in the latter study, the amount of conjugated radio-labelled sugar was quantified after thin layer chromatography (TLC), we measured the release of free-UDP upon glycosylation spectrophotometrically, making a high-throughput set-up more feasible. In our substrate screening assay, detected free-UDP values ranged from 0.1 to 40 µM. In several cases, none or a very low level of free-UDP was detected. However, this does not necessarily imply that glycosylation is absent or very low as evidenced by enzyme activity measurements with model substrates. For example, tetur01g05690, tetur02g09850 and tetur22g00270 showed low enzyme activity towards the model substrate p-nitrophenol (Table 1), but only for one of these UGTs (tetur22g00270) free-UDP was detected in the substrate screening assay (Supplementary Table 7). Likewise, only for those UGTs that had a relatively high specific activity for the model substrates 1-naphthol and 2-naphthol, free-UDP was detected in the screening assay, suggesting that our screening assay is rather conservative. The low amount of conjugation in the high-throughput screening could be a consequence of substrate inhibition when acceptor concentrations are higher than optimal (Chaplin and Bucke, 1990), or UDP-glucose might not be the preferred activated donor for a specific UGT-acceptor combination (Figure 3). In general, the parameters of our UGT screening assay were not optimal for all enzyme-substrate combinations included in the screening. However, this cannot be expected since we tested 44 different potential acceptors against seven recombinant enzymes. Hence, the magnitude of released UDP (µM) should not be interpreted/used as an absolute predictor of affinities for enzyme-substrate combinations. Although tetur02g09850 was able to glycosylate capsaicin > kaempferol > abamectin in the screening assay, 20.1µM, 16.5 µM and 6.7µM (out of 50µM) respectively, enzyme characterization showed that tetur02g09850 had the highest affinity for abamectin (Table 2). Nevertheless, all acceptor-enzyme combinations that were selected based on the screening assay for detailed kinetic studies showed affinities in the micromolar range. Hence, the substrate screening assay showed its value as a high-throughput method to test potential substrates for glycosylation.

Flavonoids are one of the major classes of plant secondary metabolites and are widely distributed in the plant kingdom. Most of them are present in the form of a glycoside under natural conditions (Bohm, 1998) and the majority of functions of flavonoids result from their strong anti-oxidative properties. They participate in plant protection against both biotic (herbivores and pathogens) and abiotic (UV, radiation and heat) stress (Dakora and Phillips, 1996; Mierziak *et al.*, 2014). Furthermore, they are able to influence the behavior, growth and development of insects (Falcone Ferreyra *et al.*, 2012; Mierziak *et al.*, 2014; War *et al.*, 2012). Nine flavonoids (7-hydroxyflavone, chrysin, coumestrol, eriodictyol, hesperitin, kaempferol, naringenin, quercetin and rutin hydrate) were included in our screening assay and all were glycosylated by at least one of the following recombinant *T. urticae* UGTs (tetur02g09850, tetur22g00270 and tetur22g00440) (Figure 4). In arthropods, two *B. mori* UGTs were shown to glycosylate quercetin and/or naringenin (Daimon *et al.*, 2010; Luque *et al.*, 2002), but broad flavonoid substrate spectra like for *T. urticae* UGTs were not reported before. Nevertheless, such spectra have previously been described for certain plant, microbial and human UGTs too (Hyung Ko *et al.*, 2006; Jones *et al.*, 2003; Kim *et al.*, 2007; Modolo *et al.*, 2007; Su *et al.*, 2017; Xie *et al.*, 2007). Kaempferol was selected for further detailed kinetic analysis since it is omnipresent in plants and fruits (Robards and Antolovich, 1997) and because this flavonoid was glycosylated by the afore mentioned UGT enzymes. From the characterized enzymes, tetur22g00440 had the highest affinity and catalytic efficiency for kaempferol (Table 2).

Tetur22g00440 was also able to glycosylate chlorogenic acid, which contributes to the physiological defenses of maize. Other major players in the plant defense of maize are protein inhibitors, the flavonoid maysin and benzoxazinoids (BXs) (Meihls *et al.*, 2012). BXs are synthesized constitutively and stored as an inactive form (BX-glucosides) in the plant cell. Upon tissue disruption, unstable aglycone BXs are released which are highly reactive and toxic to a wide range of arthropod herbivores including *T. urticae* (Bui *et al.*, 2018; Morant *et al.*, 2008; Niemeyer, 2009; Wouters *et al.*, 2016). DIMBOA is the more prevalent BX in maize (Niemeyer, 2009), and a relatively slow, perhaps non-enzymatic breakdown of DIMBOA results in the formation of MBOA, another toxic BX (Grambow *et al.*, 1986). Glycosylation of DIMBOA has been detected for *Mythimna separata*, *Spodoptera exigua, S. littoralis* and *S. frugiperda* (Glauser *et al.*, 2011; Sasai *et al.*, 2009; Wouters *et al.*, 2014) and glycosylation of MBOA for *S. littoralis* and *S. frugiperda* (Maag *et al.*, 2014). Although six of the recombinant UGT enzymes were upregulated in *T. urticae* upon long-term acclimation to maize (Figure 1), none of them glycosylated DIMBOA or MBOA at the default parameters of the screening. Since two of our enzymes had shown lower activity against the model substrates (Table 1), all substrates were additionally screened after incubation with a ten-times higher amount of both enzymes. This resulted in glycosylation of DIMBOA by tetur04g02350, but both the affinity and turnover rate were rather low (Table 2). Additionally, tetur04g02350 was only marginally upregulated after long-term acclimation to maize (log_2FC 1.33). Hence, no strong conclusions can be made considering the involvement of tetur04g02350 in hostplant acclimation to maize.

The plant secondary metabolite capsaicin was glycosylated upon incubation with four recombinant UGTs: tetur01g05690, tetur05g00060, tetur02g09850 and tetur22g00270

(Supplementary Table 7). Capsaicin (capsaicinoids) is found solely in hot peppers (*Capsicum spp.*) and is known to deter oviposition (Cowles *et al.*, 1989), inhibit feeding (Hori *et al.*, 2011) and delay larval growth (Weissenberg *et al.*, 1986) in insects. Glycosylation has been linked with the detoxification of capsaicin by the Lepidopteran species *Helicoverpa armigera*, *H. zea* and *H. assulta*, resulting in capsaicin glucoside, a more water-soluble compound than its aglycone and subsequently easier to excrete (Ahn *et al.*, 2011). The enzyme characteristics of tetur02g09850 and tetur22g00270 in combination with capsaicin were determined since they resulted in a higher amount of glycosylation in the substrate screening assay. In contrast to tetur22g00270, tetur02g09850 had a strong affinity for capsaicin (Table 2) and although this might suggest a functional role in adaption, a more dedicated study is needed to draw any further conclusions.

The highest amount of glycosylation detected in the substrate screening assay resulted from the incubation of tetur01g05690 with vanillin (Figure 4). Tetur02g09850 and tetur22g00270 were able to glycosylate vanillin too but at a lower rate under the default parameters of the screening assay. Vanillin is one of the most widely used flavors and aromas worldwide. Since multiple UGTs from different plants possess a high *in vitro* catalytic activity towards vanillin (Hansen *et al.*, 2009; Jones, 1998; Jones *et al.*, 1999; Song *et al.*, 2016), vanillin has been suggested to be an ubiquitous metabolite that is easily converted by a number of plant UGTs (Song *et al.*, 2016). This statement seems not to be constrained to the plant kingdom as nine human UGTs were able to glucuronidate vanillin (Yu *et al.*, 2013) and in arthropods, a recombinant UGT of *Bombyx mori* was able to glycosylate vanillin (Luque *et al.*, 2002). However, in the scope of this study, detoxification of toxic compounds by *T. urticae* UGTs, we decided to not analyze the latter enzyme-substrate combination in depth.

Tetur04g02350 was the highest upregulated UGT after long-term host plant acclimation on cotton (Figure S2), and the most highly overexpressed UGT of all comparisons made in this study (Figure 1). The major defense compound of cotton is the toxic sesquiterpene dimer, gossypol (Dodou, 2005), which was metabolized by UGTs via glycosylation in *Helicoverpa armigera* and *Heliothis* virescens (Krempl *et al.*, 2016). However, gossypol was not glycosylated by tetur04g02350 or any of the other recombinant *T. urticae* UGTs in this study.

Next to plant secondary metabolites, we also tested whether our set of recombinant *T. urticae* UGTs could glycosylate a selection of pesticides. The acetylcholinesterase inhibitor profenofos was glycosylated by tetur01g05690, tetur02g09850 and tetur22g0270. Profenofos is just like pyraclofos an organophosphate (Mode of Action (MoA) 1b, (IRAC, 2017)), and previously it was shown that glycosylation plays a role in pyraclofos resistance in *Musca domestica* (Lee *et al.*, 2006). Besides profenofos, tetur02g09850 glycosylated abamectin, bifenazate, cyflumetofen, pyflubumide and pyridaben. In contrast, tetur05g00060 only glycosylated abamectin. The chloride channel activator abamectin (MoA 6 (IRAC, 2017)), has been and is still widely used to control *T. urticae* and other phytophagous mite species and field resistance has been reported (Brown *et al.*, 2017; Ferreira *et al.*, 2015; Ilias *et al.*, 2017; Memarizadeh *et al.*, 2013; Riga *et al.*, 2014). Glutamate-gated chloride channel target-site mutations have been associated with abamectin resistance in *T. urticae* (Dermauw *et al.*, 2012; Kwon *et al.*, 2010d; F. Liu *et al.*, 2014; Mermans *et al.*, 2017; Wolstenholme

and Rogers, 2005) as well as metabolic resistance by a P450 mono-oxygenase (CYP392A16), capable of metabolizing abamectin (Riga *et al.*, 2014). Most recently, UGT201D3 (corresponding to *T. urticae* tetur04g02350, UGT 201 family) was specifically linked to abamectin resistance (M. Y. Wang *et al.*, 2018). In the latter study, the inhibition of 1-naphthol glycosylation was inhibited by abamectin (K_i = 9.9 ± 6.2 µmol/l), but the glycosylated product was not detected. Here, we performed detailed kinetic analysis for tetur02g09850 and tetur05g00060 with abamectin and both recombinant enzymes were able to glycosylate the acaricide. Tetur02g09850 had the highest affinity and tetur05g00060 the highest turnover number. Tetur02g09850 was also overexpressed (log_2FC 2.20) in the abamectin resistant strain MAR-AB (Dermauw *et al.*, 2013b) (Figure1). Noteworthy, tetur02g09850 and tetur05g00060 both cluster in the UGT204 family, in contrast to UGT201D3 of Wang *et al.* 2018 (UGT 201 family, Figure 2). In conclusion, these results suggest a potential contribution of glycosylation to abamectin resistance in *T. urticae*.

6. Conclusion

Eight *T. urticae* UGTs were functionally expressed and all could use UDP-glucose as activated donor for the glycosylation of model substrates. A high-throughput substrate screening comprising both toxic plant metabolites and pesticides led to the selection of nine enzyme-substrate combinations which were further enzymatically characterized. Strong affinities of the recombinant enzymes with both plant secondary metabolites as wells as an acaricide corroborate the potential role of *T. urticae* UGTs in detoxification.

Funding information

This work was supported by the Research Foundation Flanders (FWO) [grant G009312N to TVL and grant G053815N to TVL and WD] and the Research Council (ERC) under the European Union's Horizon 2020 research and innovation program [grant 772026-POLYADAPT to TVL and 773902-SuperPest to TVL and JV]. WD is a post-doctoral fellow of the Research Foundation Flanders.

Author contributions

TVL and NP designed the experiment. NP, DP and SS conducted the experiments. Analysis and interpretation of the results was done by SS, NP and WD. The manuscript was written by SS, WD and NP, all figures were prepared by SS. All authors reviewed the manuscript.

Supplementary information

All supplementary data can be found at https://doi.org/10.1016/j.ibmb.2019.04.010

Figure S1 Standard curve glycosyltransferase assay. Free-UDP standard curve, Relative Luminescence Units (RLU) in function of free-UDP (range of 0-25µM). Values represent the mean of five replicates ± SD. The regression line (R^2 0.9844) was added to the plot as well as the 99% confidence interval.

Figure S2 Expression heatmap of a selection of *T. urticae* UGTs. Expression heatmap of all completely annotated *T. urticae* UGTs in adult (or deutonymph*) *T. urticae* females adapted to tomato and lima bean (≥ 30

generations), long-term acclimatized to soy, cotton and maize (≥ 5 generations) and resistant against certain acaricides (Supplementary Table 1). The $\log_2$ transformed fold changes are relative to adult *T. urticae* females of the susceptible London strain or the susceptible deutonymph *T. urticae* females of the LS-VL strain. NA values were colored in grey, functionally expressed UGT enzymes were underlined. **(next page)**

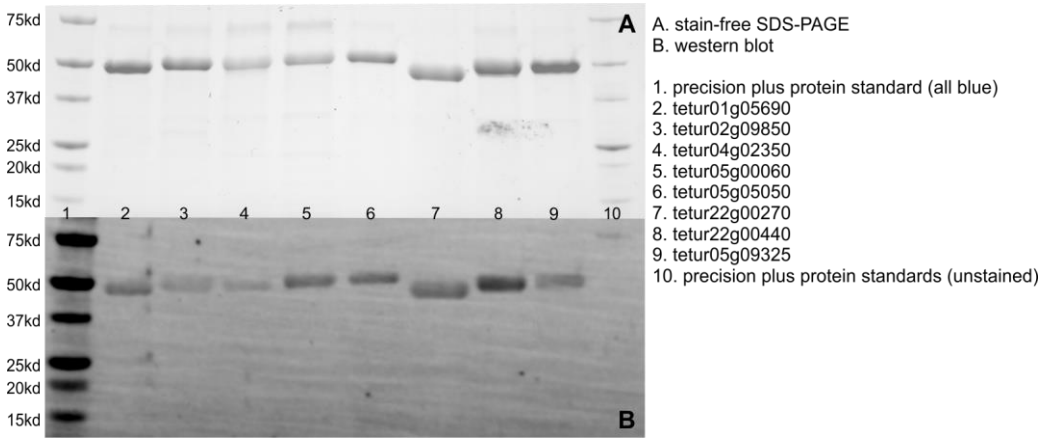

Figure S3 SDS-PAGE and western blot of the purified fractions of the recombinantly expressed *T. urticae* UGTs. Panel **(A)** contains SDS-PAGE result, Western blot is shown in panel **(B)**. Lane 1: molecular weight marker (Precision Plus Protein™ All Blue Prestained Protein Standard, Bio-Rad, Belgium). Lane 2-9: purified His-tagged *T. urticae* recombinant UGTs. Lane 10: molecular weight marker (Precision Plus Protein™ Unstained Protein Standards, *Strep*-tagged recombinant, Bio-Rad, Belgium). 10 µg protein diluted in PBS was loaded for each recombinant enzyme.

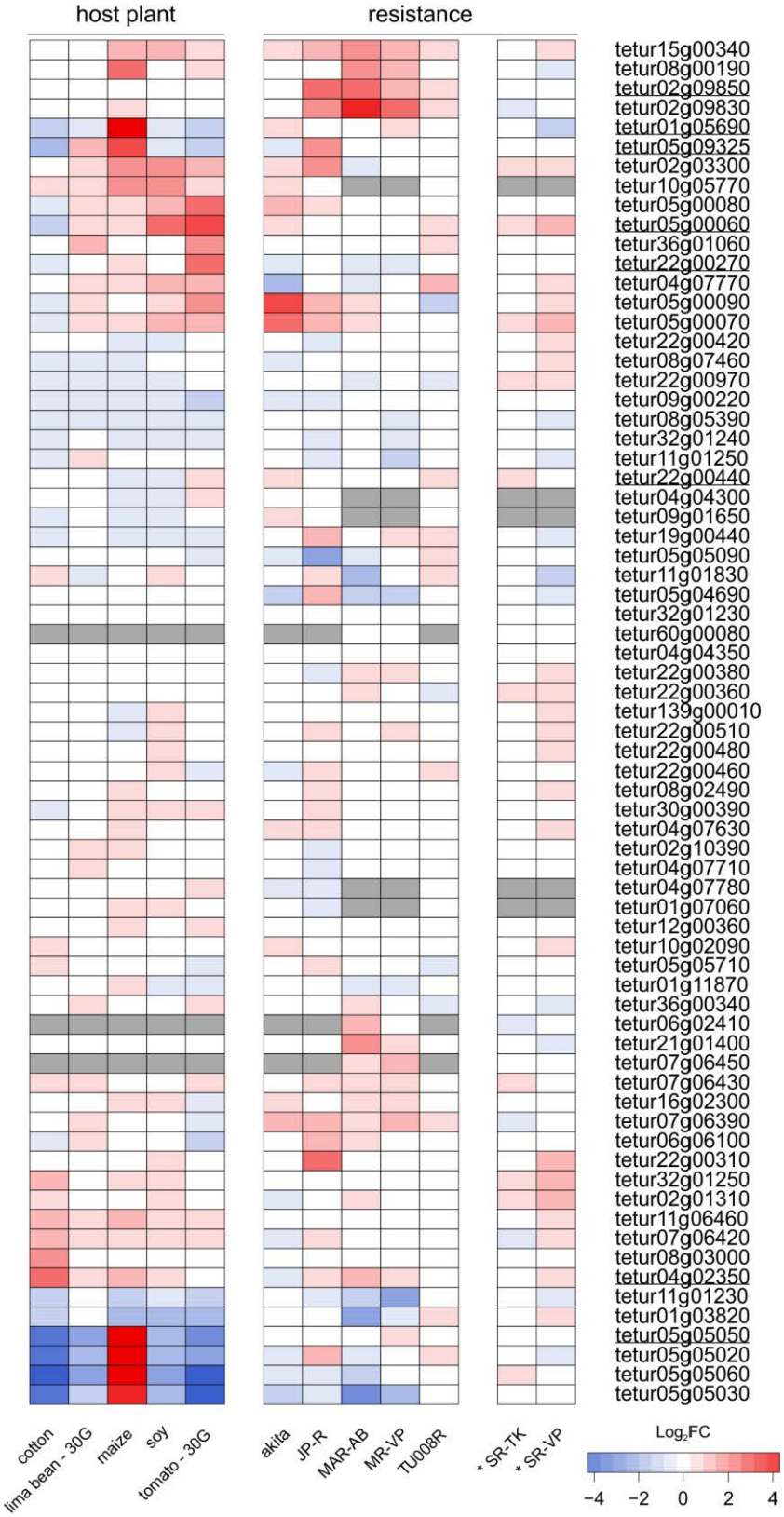
host plant
resistance
tetur15g00340
tetur08g00190
tetur02g09850
tetur02g09830
tetur01g05690
tetur05g09325
tetur02g03300
tetur10g05770
tetur05g00080
tetur05g00060
tetur36g01060
tetur22g00270
tetur04g07770
tetur05g00090
tetur05g00070
tetur22g00420
tetur08g07460
tetur22g00970
tetur09g00220
tetur08g05390
tetur32g01240
tetur11g01250
tetur22g00440
tetur04g04300
tetur09g01650
tetur19g00440
tetur05g05090
tetur11g01830
tetur05g04690
tetur32g01230
tetur60g00080
tetur04g04350
tetur22g00380
tetur22g00360
tetur139g00010
tetur22g00510
tetur22g00480
tetur22g00460
tetur08g02490
tetur30g00390
tetur04g07630
tetur02g10390
tetur04g07710
tetur04g07780
tetur01g07060
tetur12g00360
tetur10g02090
tetur05g05710
tetur01g11870
tetur36g00340
tetur06g02410
tetur21g01400
tetur07g06450
tetur07g06430
tetur16g02300
tetur07g06390
tetur06g06100
tetur22g00310
tetur32g01250
tetur02g01310
tetur11g06460
tetur07g06420
tetur08g03000
tetur04g02350
tetur11g01230
tetur01g03820
tetur05g05050
tetur05g05020
tetur05g05060
tetur05g05030
cotton
lima bean - 30G
maize
soy
tomato - 30G
akita
JP-R
MAR-AB
MR-VP
TU008R
* SR-TK
* SR-VP
Log2FC
−4
−2
0
2
4

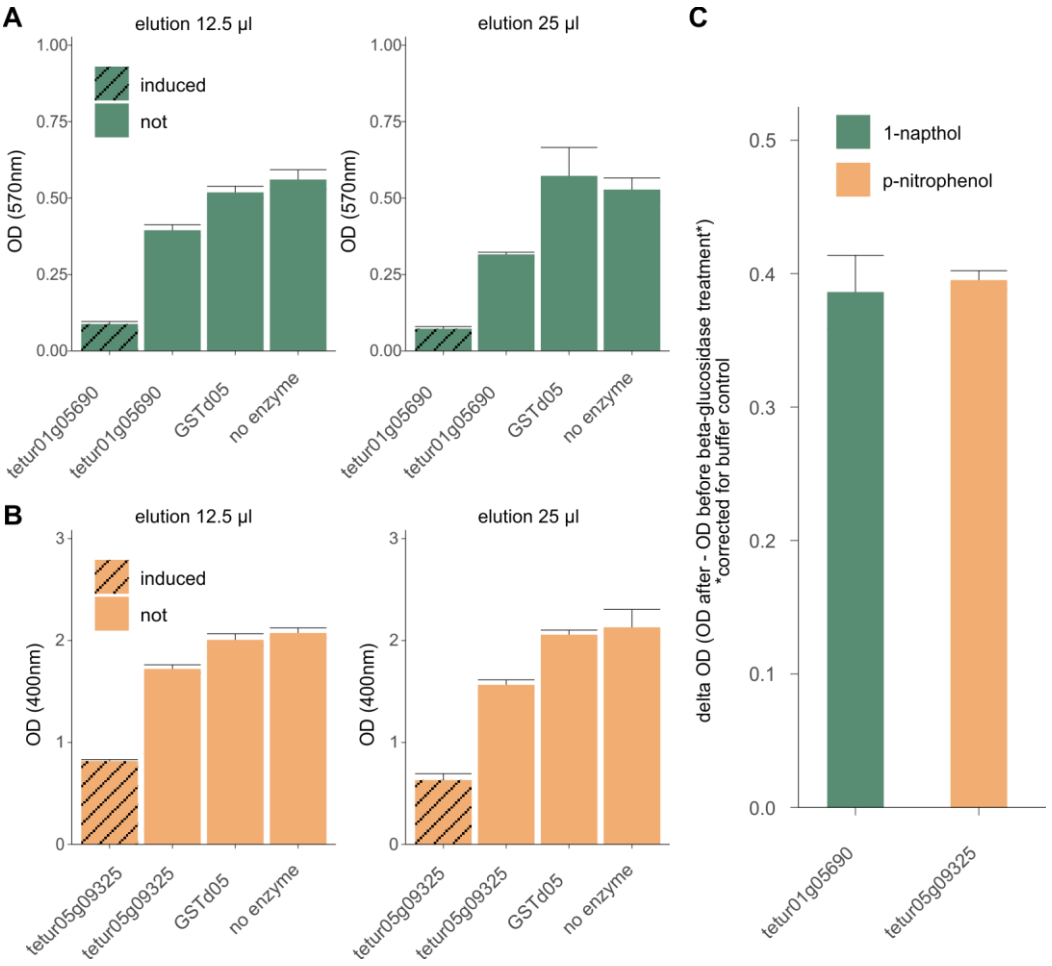

Figure S4 Validation UGT activity. (A) 1-naphthol (OD 570 nm) spectrophotometrical measurement after incubation with the elution's (left 12.5 µl, right 25µl) of the (not-) induced constructs of tetur01g05690, elution's of the construct GSTd05 (*E. coli* enzyme activity, control), and elution buffer (no enzyme construct/*E. coli*, control). **(B)** p-nitrophenol (OD 400 nm) spectrophotometrical measurement after incubation with the elution's (left 12.5 µl, right 25µl) of the (not-) induced constructs of tetur05g09325, elution's of the construct GSTd05 used as control, and control elution's (no enzyme construct). **(C)** Model substrate was measured spectrophotometrically after incubation with the respective recombinant *T. urticae* UGT enzyme and was subtracted with the substrate measurement after an additional incubation step with beta-glucosidase after incubation with the UGT enzyme. P-nitrophenol or 1-naphthol was used depending on the model substrate preference of the enzyme (Table 1). Values represent the mean of nine replicates ± SD.

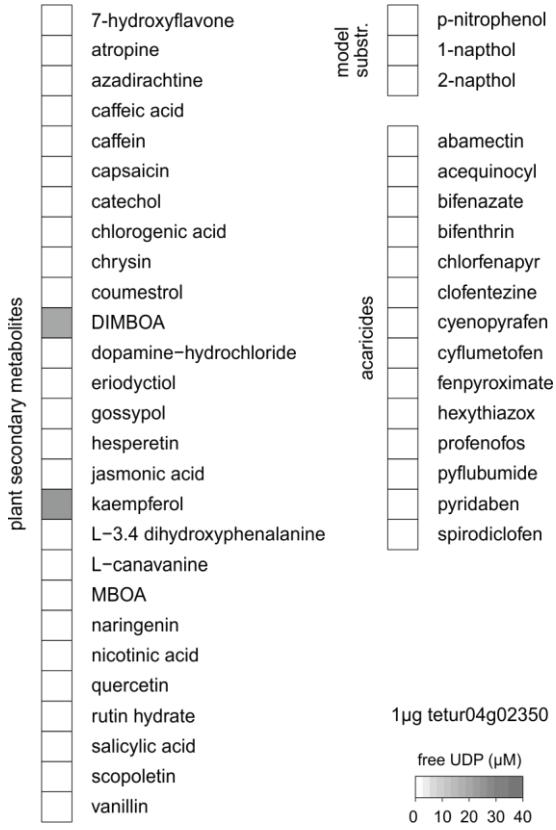

Figure S5 Enzyme-substrate screening assay. Endpoint measurement of the release of free-UDP (µM) after incubation of the recombinant *T. urticae* UGT enzyme tetur04g02350 (1µg) with 44 substrates (3 model substrates, 27 plant secondary metabolites and 14 acaricides) and UDP-glucose. Release of free-UDP is directly linked with the activity of glycosyltransferases.

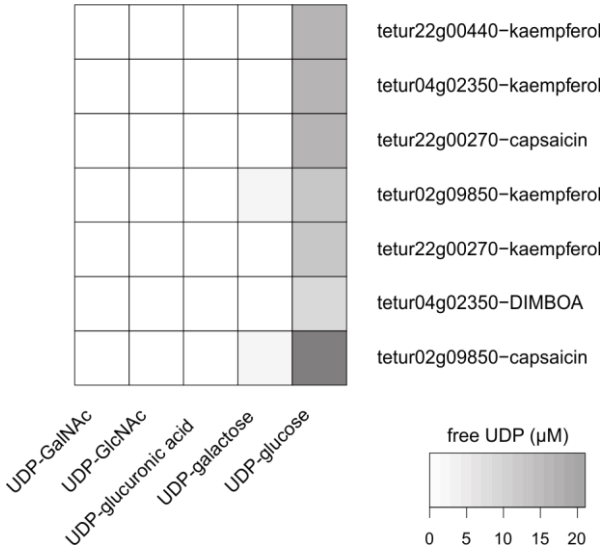

Figure S6 Sugar-preference for specific substrates. Endpoint measurement of the release of free-UDP (µM) after incubation with different activated donors (UDP-galactose, UDP-GalNAc, UDP-GlcNAc, UDP-glucose and UDP-glucuronic acid) and all enzyme-substrate combinations selected for steady-state kinetic analysis. Release of free-UDP is directly linked with the activity of glycosyltransferases.

Supplementary Table 1 Detailed information of the strains used for the transcriptomic analysis of *T. urticae* UGTs (Figure 1 and Figure S2)

Supplementary Table 2 Sequence information and accession numbers of UGTs used in the phylogenetic analysis (Figure 2)

Supplementary Table 3 Nucleotide sequences of the recombinant *T. urticae* UGT genes used in this study

Supplementary Table 4 Primers used in this study

Supplementary Table 5 Compounds used in this study

Supplementary Table 6 Gene expression differences between the different *T. urticae* populations/strains and the London or LS-VL strain

Supplementary Table 7 Endpoint measurement of the release of free-UDP (µM) after incubation of the respective recombinant *T. urticae* UGT enzyme with 41 different substrates (27 plant secondary metabolites and 14 acaricides) and UDP-glucose. Release of free-UDP is directly linked with the activity of glycosyltransferases. Values represent the mean of three replicates ± SD.

Chapter 6

Discussion

This chapter has been partially redrafted from:

Kurlovs*, A., Snoeck*, S., Kosterlitz, O., Van Leeuwen, T., Clark, R.M. (2019) Trait mapping in diverse arthropods by bulked segregant analysis. Current Opinion in Insect Science, 36.

1. Abstract

During my PhD work, I used a variety of approaches to study the molecular and genetic mechanisms underlying resistance and acclimation to xenobiotic compounds, in the spider mite *T. urticae*. These approaches included QTL mapping, gene expression profiling, and enzyme characterization.

BSAs in *T. urticae* helped elucidating the target-site of the mite growth inhibitors (clofentezine, hexythiazox and etoxazole) affecting chitin synthase 1 (CHS1) (Demaeght *et al.*, 2014; Van Leeuwen *et al.*, 2012). Moreover, a BSA that aimed to reveal resistance mechanisms contributing to spirodiclofen (acetyl-CoA carboxylase inhibitor) resistance resulted in a QTL-peak containing the target-site *CoA carboxylase* among two other QTL-peaks (Wybouw *et al.*, 2019). Most recently (Chapter 3), a BSA that aimed to reveal resistance mechanisms for three different METI-I pesticides validated the importance of an earlier discovered target-site mutation in the PSST subunit of complex I (H92R). Hence, QTL-mapping by BSA has shown its potential to reveal MoA of pesticides and could be used as a strategy to reveal unknown MoA of other compounds. Knowledge of the MoA is of utmost importance in the light of pesticide cross-resistance and multiple resistance. Since our ability to manage xenobiotic resistance, i.e. to prevent the further spread of resistance, relies on the 'alteration' of classes of compounds with different mode of actions. Such a strategy assumes that resistance to compound A will decline during the subsequent use of compound B. Additionally, in the light of our results in Chapter 2, bioassays and molecular diagnostics could be used to monitor the H92R target-site mutation in the field. In combination with toxicity assays, this molecular marker could help predict the efficacy of METI-I pesticides against *T. urticae* infestations.

In Chapter 3, RNAseq analysis revealed that the synergists PBO and DEF induced genes that code for detoxification enzymes. Based on previous synergisms toxicity studies, in a standardized set-up in the lab, the induction of these detoxification genes seems not to interfere with the outcome of synergisms assays. Since direct inhibition of P450s and CCEs (by PBO and DEF respectively) most likely outweighed the induction of detoxification enzymes. However, one might wonder if synergists are applied in the field and the pest is only exposed to a low dosage of synergist (e.g. due to unequal spray coverage or degradation of the synergist) which is insufficient to inhibit P450s and CCEs on the protein level, would detoxification genes still be induced? If so, this could speed up pesticide tolerance. Hence, to study the potential impact of synergist usage in the field, further experiments are needed to reveal the impact of synergist application on both the transcriptomic level as well as the protein level (synergist assays) while using different dosages of synergists.

Chapter 5 corroborates the predicted role of UGTs in arthropod detoxification. So far, only a few enzymes were partially studied in insects, mainly due to technical obstacles and the fact that these enzymes are membrane bound and difficult to express. We functionally expressed a wide collection of *T. urticae* UGT genes belonging to diverse UGT subfamilies. Subsequently, a high-throughput substrate screening comprising both toxic plant metabolites and pesticides was

performed, revealing that some of these enzymes have both remarkable specificity as well as substrate promiscuity. Spider mite UGTs may hence lead to new biotechnical applications, out of the scope of this fundamental research project.

In the subsequent section, the potential of trait/QTL mapping by using bulked segregant analysis in *T. urticae* and other arthropods will be discussed. Finally, an overview of common validation approaches and recent breakthroughs is provided, while highlighting potential future strategies for the validation of hypotheses brought forward in this thesis.

2. Bulked segregant analysis

Bulked segregant analysis (BSA) is a cross-based method for genetic mapping in sexually reproducing organisms. The method's use of bulked (pooled) samples markedly reduces the genotyping effort associated with traditional linkage mapping studies. Further, it can be applied to species with life histories or physical attributes (as for micro-insects) that render genetic mapping with other methods impractical. Recent studies in both insects and mites have revealed that advanced BSA experimental designs can resolve causal loci to narrow genomic intervals, facilitating follow-up investigations. As high-quality genomes become more widely available, BSA methods are poised to become an increasingly important tool for the rapid mapping of both monogenic and polygenic traits in diverse arthropod species.

The ultimate goal of BSA mapping is to identify loci responsible for variation in traits of interest. In accomplishing this goal, many genotyping methods have been employed, with high-throughput, short-read sequencing (e.g., Illumina sequencing (Bentley *et al.*, 2008)) emerging as a dominant approach. By sequencing genomic DNA from pools (Bastide *et al.*, 2016; Bryon *et al.*, 2017a; Demaeght *et al.*, 2014; Jagadeesan *et al.*, 2013; Van Leeuwen *et al.*, 2012; Wybouw *et al.*, 2019), or in some cases cDNA (RNA-seq) (Park *et al.*, 2014), marker discovery and genotyping can be performed simultaneously at comparatively low cost where reference genomes are available (genetic variation is inferred from read alignments to a known genome sequence). Exploiting this data type, Pool (2016) developed a particularly elegant approach for QTL detection in BSA studies, although the method was tailored for *Drosophila* species. More recently, Mansfeld and Grumet (2017) released the QTLseqr package, which implements or elaborates several proposed methods to detect QTL in BSA data (Magwene *et al.*, 2011; Takagi *et al.*, 2013). Further, Wybouw *et al.* (2019) recently developed a permutation-based approach for QTL detection applicable to BSA designs, although this method requires moderate-to-high replication of segregating populations. An advantage of the latter two approaches is that only a single input file in the Variant Call Format (VCF) is required for an analysis. Pipelines of well supported programs, as well as best practice guidelines for their use in generating VCF files, are now robustly established and lower the informatic barrier to entry for BSA studies (see Wybouw *et al.*, 2019 for example pipelines with the respective software and citations).

2.1. Beyond theory and simulations: lessons from experimental studies in insects and mites

Apart from the genetic architecture (monogenic versus polygenic) and species-specific characteristics (short life cycle, haplodiploidy, maintenance in the lab, recombination frequency…) that can impact the practical implementation of BSA experimental designs, factors that affect power and resolution include the sizes of bulks, generation number, and marker density (Bazakos *et al.*, 2017; Pool, 2016; Schneeberger, 2014; C. Zou *et al.*, 2016). For these parameters, theory and lessons from simulated data suggest that more is usually better than less (e.g., Pool, 2016), and recent experimental work in arthropods reflects this. To date, most BSA studies in insects have focused on traits that are easy to score, like pigmentation, and have started with parental strains with large phenotypic differences (i.e., susceptible and highly pesticide-resistant strains). Despite some notable exceptions, small- to modestly-sized F2 or backcross populations have often been used. Mirroring initial studies in plants, BSA studies in insects have often used sparse genetic data; examples of marker types used to date include simple sequence repeat (microsatellite) markers (Behrens *et al.*, 2011; Chandrakanth *et al.*, 2015; Jairin *et al.*, 2017), amplified fragment length polymorphism markers (Baxter *et al.*, 2008; Heckel *et al.*, 1999; Henniges-Janssen *et al.*, 2011), restriction fragment length polymorphism markers (Morlais and Severson, 2001), restriction-site associated DNA markers (Kunte *et al.*, 2014), single feature polymorphisms ascertained from microarrays (Desjardins *et al.*, 2013; Lai *et al.*, 2007; Ocorr *et al.*, 2007; Zhang *et al.*, 2013), random amplified DNA fingerprinting (Schlipalius *et al.*, 2002), a combination of random amplified polymorphic DNA and microsatellite markers (Gadau *et al.*, 2001), and in a few cases dense marker data obtained from resequencing (e.g., (Jagadeesan *et al.*, 2013; Park *et al.*, 2014)). The number of genetic markers used in these studies varied greatly, with sparsely (and unevenly) distributed markers likely contributing to low QTL mapping resolution in some cases. Nevertheless, in the beet armyworm *Spodoptera exigua,* BSA mapping that used RNA-seq data for genotyping, aided by knowledge of potential candidate genes and their characterization with RNAi, led to the identification of ATP-binding cassette (ABC) transporters as underlying insensitivity to *Bacillus thuringiensis* (Bt) toxin in a resistant strain (Park *et al.*, 2014). In several other studies, genes in BSA peak regions have been proposed as candidates, such as *doublesex* in the control of sex-related mimicry in the butterfly *Papilio polytes* (Kunte *et al.*, 2014). In many instances, however, only broad regions of chromosomes harboring many genes were associated with phenotypes. Notwithstanding the introduction of methods like genome editing to a growing number of insect species (Trible *et al.*, 2017), which will facilitate functional assessment of candidates, characterizing long lists of genes in broad QTL intervals remains a daunting task.

A small set of studies have now illustrated how more advanced BSA designs, in concert with the effectively saturating genotypic data afforded by high-throughput sequencing, can resolve causal loci to much narrower chromosome regions. A number of these studies have been performed with the two-spotted spider mite, *Tetranychus urticae*, an agricultural pest known for its rapid evolution of pesticide resistance and host plant use (Gould, 1979; Van Leeuwen *et al.*, 2010; Wybouw *et al.*, 2019). These mites are small, ~600 µm in length for females, with males substantially smaller. Although single *T. urticae* individuals can be genotyped at a moderate number of loci by

PCR (Bajda *et al.*, 2017; Bryon *et al.*, 2017a; Riga *et al.*, 2017; Van Leeuwen *et al.*, 2012), marker-based genotyping at a genome-wide scale is challenging, hindering QTL identification by traditional linkage mapping approaches that have been successful in larger-bodied insects. However, *T. urticae* strains can be crossed, and segregating populations can be expanded to thousands of individuals on detached leaves or on whole plants (Bryon *et al.*, 2017a; Demaeght *et al.*, 2014; Van Leeuwen *et al.*, 2012; Wybouw *et al.*, 2019, Chapter 2). In two studies that started with crosses of *T. urticae* strains susceptible or resistant to mite growth inhibitor compounds, narrow BSA peaks for recessive, monogenic resistance were resolved to a single tiny chromosome region (Demaeght *et al.*, 2014; Van Leeuwen *et al.*, 2012). Both studies used large segregating populations that were expanded over ~6 generations; in the larger and more powered of these studies, peaks of haplotype fixation were either within or less than 20 kb from *chitin synthase 1* (*CHS1*) (Demaeght *et al.*, 2014), which was subsequently demonstrated by a genome editing approach in *D. melanogaster* to encode the target-site for the growth inhibitor compounds used for selection (Douris *et al.*, 2016). With a conceptually similar design, Bryon *et al.* 2017a also used BSA mapping, in concert with follow-up studies, to identify mutations in a horizontally transferred gene, *phytoene desaturase*, as causal for the absence of carotenoid-based pigmentation in albino *T. urticae* strains. A reanalysis of Bryon *et al.*'s data with the methods used in Wybouw *et al.*, 2019 and Chapter 2 revealed that the BSA peak, as assessed with replicate populations used in that study, was ~95 kb from the causal gene.

Similar designs have also elucidated the genetic basis of polygenic traits. For example, in *D. melanogaster,* Bastide *et al.* 2016 used multigeneration, long-term segregant populations and sequencing of bulks to identify 19 distinct QTL for high-altitude melanism in multiple crosses. The BSA peaks for QTL were localized to small genomic intervals that included candidate pigmentation genes. This finding, along with follow-up analyses of allele frequencies in wild populations, suggested that at least many of the QTL are valid. Two studies in 2019 in *T. urticae* have also highlighted the promise of continuous selection over many generations, followed by the isolation and sequencing of bulks, to unravel the genetic architecture of complex modes of inheritance (Wybouw *et al.*, 2019, Chapter 2). In each study, replicated segregant populations derived from pesticide-susceptible and -resistant strains were selected with discriminating pesticide doses for ~25-50 generations. In these cases, resistance phenotypes were known to be polygenic, and multiple resistance QTL were identified, as shown by reproducible shifts toward alleles contributed by resistant parents that were observed in selected as compared to unselected populations. Although new candidate loci identified in this work have yet to be investigated in follow-up studies, the identity of genes near BSA peaks suggests that the QTL are likely real. For instance, several BSA peaks fell within a mere tens of kb from genes encoding known target sites of the pesticides used for selection (Figure 1). Further, major QTL were also resolved to tiny chromosome regions harboring genes with suspected or known roles in xenobiotic detoxification, a major route to resistance (Feyereisen *et al.*, 2015). These genes encode a potential xenobiotic receptor, copy variable CYPs, and also cytochrome P450 reductase, which is required for CYP activity, and that

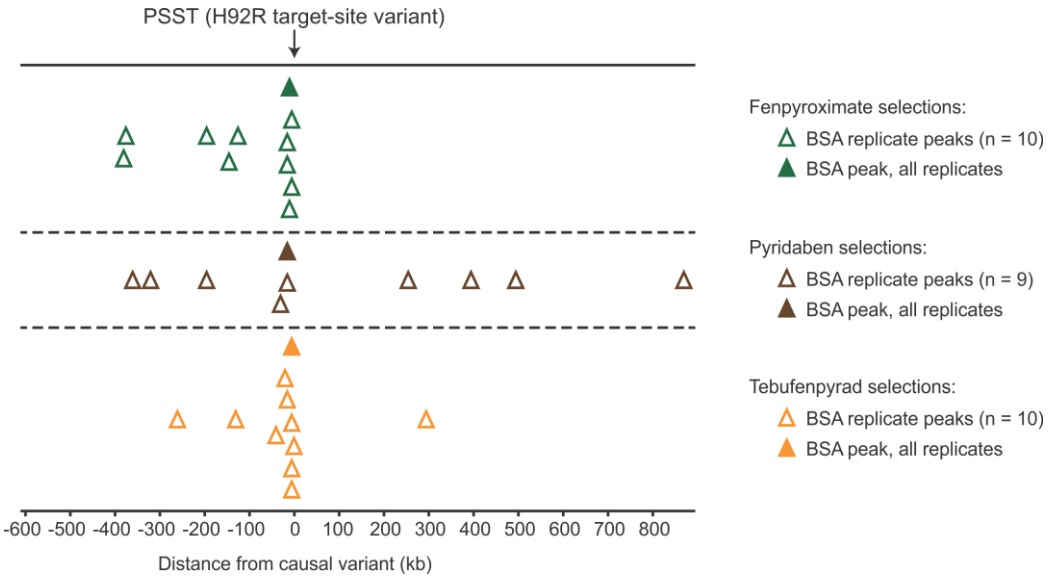

Figure 1 - BSA mapping resolution for a pesticide resistance QTL. Data from nine or ten selected populations from Chapter 3 in *T. urticae* for each of three pesticides (fenpyroximate, pyridaben, and tebufenpyrad) was reanalyzed along with control populations (75 kb windows were used with 5 kb offsets). The three pesticides are Mitochondrial Electron Transport Inhibitors of complex I (METI-Is), for which the H92R change in the gene encoding the PSST subunit associates with target-site resistance (Bajda *et al.* 2017). For each pesticide, BSA averages (solid triangles) were within tens of kb of the causal variant; this was true for some replicates also (open triangles), but in a moderate number of cases, peaks were much farther from the causal variant (especially for selection by pyridaben, for which the populations may have undergone a bottleneck during the propagation steps (Chapter 3)). Therefore, while BSA approaches can provide high mapping resolution, relying on a small number of replicates can potentially be misleading.

was identified as a candidate for resistance to multiple compounds in independent crosses (Wybouw *et al.*, 2019, Chapter 2).

2.2. Concluding remarks BSA

For most arthropods, the genetic tools that have enabled model-organism geneticists to link genes and alleles to phenotypic variation are poorly developed, if not even entirely absent. For many species, however, strains with contrasting phenotypes – including for pesticide resistance, pigmentation or other visual features, or variation in life history traits – are available or can be readily isolated. Where strains can be crossed, BSA genetic mapping holds great promise for the identification of causal loci. Nevertheless, given the species richness of insects and their relatives, and high levels of intraspecific phenotypic and genotypic variation, the method has been relatively little used to date. We believe this is poised to change rapidly. The emergence of cost-effective, high-throughput short-read sequencing for simultaneous marker discovery and dense genotyping has recently revolutionized BSA studies. However, assembled genomes are nonetheless needed to fully exploit short-read sequence data, and currently limit broader adoption of the method (or for that matter, other genetic approaches as well) (Wybouw *et al.*, 2019). The extent of this limitation was starkly revealed in BSA studies with *T. urticae*, as assembly incompleteness hampered QTL detection. Even though the *T. urticae* draft genome had a scaffold N50 of 2.99 Mb (Grbić *et al.*, 2011), it was only after allele frequency data from BSA populations was used to order scaffolds into

a chromosome-level assembly that comprehensive QTL detection was possible (Wybouw *et al.*, 2019). Paving the way for the elucidation of other *T. urticae* polygenic resistant cases, such as resistance against abamectin, chlorfenapyr, cyhexatin and pyflubumide. In the context of Chapter 5, it would be interesting to perform a BSA revealing QTL linked to abamectin resistance. Next to metabolism by UGTs, abamectin resistance has been linked to *in vitro* P450 metabolism (Riga *et al.*, 2014), and two target-site mutations (Dermauw *et al.*, 2012; Kwon *et al.*, 2010e; Mermans *et al.*, 2017). However, introgression of the latter target-site mutations did not lead to high resistance levels, as are often reported in abamectin resistant strains (Riga *et al.*, 2017).

While the *T. urticae* genome sequence was produced with the high-quality Sanger method, *de novo* assemblies with short-read data are typically far more fragmented. However, newer single-molecule, long-read sequencing technologies, like PacBio and Oxford Nanopore (Jain *et al.*, 2016; Rhoads and Au, 2015), are now poised to overcome the genome assembly challenge, as they enable assemblies with scaffold sizes in the many Mb range, and potentially ones of chromosome lengths. These disruptive technologies are already in use for technically challenging genome assembly projects in insects (Kingan *et al.*, 2019). Given the success of recent BSA studies in insects and mites, coupled with the evolving potential to rapidly generate high-quality genome assemblies, BSA approaches should be considered as a prominent tool for the rapid elucidation of the genetic architecture of trait variation in both model and non-model arthropod species.

3. Validation of candidate genes linked to pesticide resistance or host plant acclimation in *T. urticae*

In Chapter 2, QTL-mapping revealed that a locus containing a *CPR* variant underlies *T. urticae* resistance against the METI-I acaricides pyridaben and tebufenpyrad, possibly by improving the efficiency of P450 metabolic detoxification of certain METI-Is. In Chapter 4 we identified *T. urticae* genes that could potentially be involved in the detoxification of plant defense compounds. For example, CYP392A1 and UGT203A2 were both highly upregulated on cotton, and UGT201B7 and TuGSTd15 were highly upregulated on maize. Similarly, arthropod P450s, UGTs and GSTs have previously been linked to detoxification of plant defense compounds (Krempl *et al.*, 2016; Mao *et al.*, 2007; Schramm *et al.*, 2012; H. Wang *et al.*, 2018; Wouters *et al.*, 2016; X. Zou *et al.*, 2016). Additionally, among the highly upregulated genes in mites acclimatized to plants, we also identified certain gene families such as short-chain dehydrogenases and single PLAT domain proteins that were previously marginally associated with arthropod detoxification. In the following sections, I will discuss how the role of these enzymes/proteins could be functionally validated.

3.1. *In vitro* validation

3.1.1. Functional expression

Functional expression is a powerful tool for the validation of candidate genes involved in resistance or acclimation to xenobiotic compounds. Proteins are recombinantly expressed using heterologous systems such as *Escherichia coli*, insect cells and yeast, and are subsequently used in downstream protein assays. The catalytic activity of these recombinant enzymes is usually

determined using model substrates. Steady-state kinetics can be determined and compared to other enzymes from the same family. Additionally, if the preferred model substrate has been determined for a recombinant enzyme, a screening can be performed with other potential and relevant substrates, by determining their potential to inhibit the enzymatic metabolism of the model substrate (*T. urticae* examples: (Pavlidi *et al.*, 2015; Riga *et al.*, 2014; M. Y. Wang *et al.*, 2018; Wei *et al.*, 2019b)). For example, five insecticides were screened for their ability to inhibit activity of CYP392A16 with the model substrate Luciferin-ME EGE (L-ME EGE), revealing a strong inhibition potential of abamectin (Riga *et al.*, 2014). However, inhibition enzyme activity assays cannot distinguish inhibition caused by direct competition for the active site or binding to regions adjacent to the active site (Pavlidi *et al.*, 2015). Hence, additional experiments should be performed to confirm the findings found in this type of assay. For example, by detection of potential metabolites after incubation of enzyme and substrate.

In Chapter 5, UGT metabolism was followed-up indirectly, having the advantage that any (soluble) compound can be tested as a potential substrate for the UGT enzyme, without using model substrates in an inhibition assay. The formation of free-UDP by the glycosyltransferase reaction was quantified using the UDP-Glo™ Glycosyltransferase assay (Promega, the Netherlands). This assay detects the UDP release by converting free-UDP to ATP which results in the generation of light in a luciferase reaction. Hence, the release of free-UDP upon glycosylation can be detected spectrophotometrically, making a high-throughput set-up feasible. However, detailed studies, optimized for specific enzyme-substrate combinations, can also be performed and have a higher sensitivity (Chapter 5). *T. urticae* UGTs have the advantage of being cytosolic enzymes, facilitating the production of recombinant enzymes. Although more challenging, functional expression of insect UGTs is also possible, by infecting insect cells with a baculovirus expressing the desired UGT (Luque *et al.*, 2002). Hence, we paved the way for high-throughput UGT substrate screenings and enzyme characterization of insect UGTs. A HPLC-MS approach might be used to validate promising enzyme-substrate combinations. However, because of its relative high cost, this technique cannot be used for high-throughput assays, emphasizing the importance of inhibition enzyme activity assays (see above) for other detoxification gene families (e.g. P450s, CCEs, GSTs). Nevertheless, HPLC-MS analysis has been successfully used to validate the *in vitro* metabolism of certain acaricides by *T. urticae* detoxification enzymes: P450s (Demaeght *et al.*, 2013; Riga *et al.*, 2015, 2014), GSTs (Pavlidi *et al.*, 2017) and CCEs (Wei *et al.*, 2019a). On the other hand, LC-MS also aided in identifying a *T. urticae* enzyme involved in the detoxification of HCN to β-cyanoalanine, a conversion of utmost importance for mites living on cyanogenic plants (Wybouw *et al.*, 2014).

In Chapter 2, QTL-mapping revealed that a locus containing a *CPR* variant was underlying *T. urticae* resistance against the METI-I acaricides pyridaben and tebufenpyrad. CPR is an obligatory electron donor for microsomal P450s (Murataliev *et al.*, 2004). Hence, to study recombinant P450s, CPR needs to be co-expressed. CYP392E10 and CYP392E7 were co-expressed with CPR from *Anopheles gambiae* (Demaeght *et al.*, 2013), CYP392A11, CYP392A12 and CYP392A16 were co-expressed with *T. urticae* CPR (Riga *et al.*, 2015, 2014). Although the P450 reductase activity was higher for the *T. urticae* CPR, both approaches were successful. Based

on homology modelling, it was suggested that the D384Y mutation of CPR potentially could have an influence on the electron transfer from the FMN domain of CPRs to P450s (Chapter 2, section 3.1.1). This hypothesis could be validated by expressing both the wild type and the mutant CPR for METI-I resistance and compare the cytochrome P450 reductase activity, which can be measured by monitoring cytochrome c reduction (Strobel and Dignam, 1978).

In Chapter 4, several short-chain dehydrogenase (SDR) genes were overexpressed upon long-term host plant transfer and/or in pesticide resistant strains (Figure 2). For example, *tetur12g00120* was strongly upregulated in tomato-adapted *T. urticae* populations, and adaptation to maize resulted in a strong upregulation of multiple SDR genes. Next, three different *T. urticae* pesticide resistant strains showed strong upregulation of *tetur06g04970* (Figure 2). All three populations are resistant against pyridaben. Hence, *tetur06g04970* is a top candidate gene to study the potential role of (*T. urticae*) SDR genes in pesticide resistance. In arthropods, *E. coli* was successfully used to express *Aedes aegypti* SDRs and *Drosophila melanogaster* SDRs (Mayoral *et al.*, 2013, 2009; Rivera-Perez *et al.*, 2013; Zhang *et al.*, 2010, 2004). In contrast, an Sf9 (insect) cell culture was used to express an SDR from the bark beetle *Ips pini* (Figueroa-Teran *et al.*, 2016, 2012). Since SDRs are NAD(P)(H)-dependent oxidoreductases, the enzymatic activity and kinetic properties of SDRs for potential substrates can be determined spectrophotometrically, based on the different optical properties of nicotinamide adenine dinucleotide phosphate ($NADP^+$) and its reduced from (NADPH) at 340nm (Decker, 1977; Mayoral *et al.*, 2009). Most recently, a faster and more sensitive assay (WTS-8 assay) was published to measure NAD(P)H concentrations and dehydrogenase enzyme activity (Chamchoy *et al.*, 2019). The tetrazolium salt WST-8 reacts with NAD(P)H resulting in the formation of formazan, which can be followed by measuring absorbance at 450nm. Optimization and limitations of the assay are discussed by Chamchoy *et al.*, 2019. Both assays follow up enzyme activity indirectly, like the UDP-Glo™ Glycosyltransferase assay used in Chapter 5, and can be used in (high-throughput) substrate screening assays. Additionally, HPLC-MS could also be used to validate the *in vitro* metabolism of a substrate by an SDR.

3.2. *In vivo* validation

In *T. urticae*, recombinant expression has been the main tool to validate candidate mutations and genes related to resistance or host plant acclimation/adaptation. These approaches can provide strong evidence on the affinity of a substrate (pesticide or plant toxin) to the target-site of the recombinant protein, but are less suitable to assess relative phenotypic consequences *in vivo* (Cully *et al.*, 1994; Ludmerer *et al.*, 2002). Additionally, *in vitro* approaches using recombinant protein expression are not always feasible, such as for large oligomeric integral protein complexes, especially when interactions are pre-or postcatalytic or involve the oligomerization of the complex (Douris *et al.*, 2016; Merzendorfer, 2013; Van Leeuwen *et al.*, 2012).

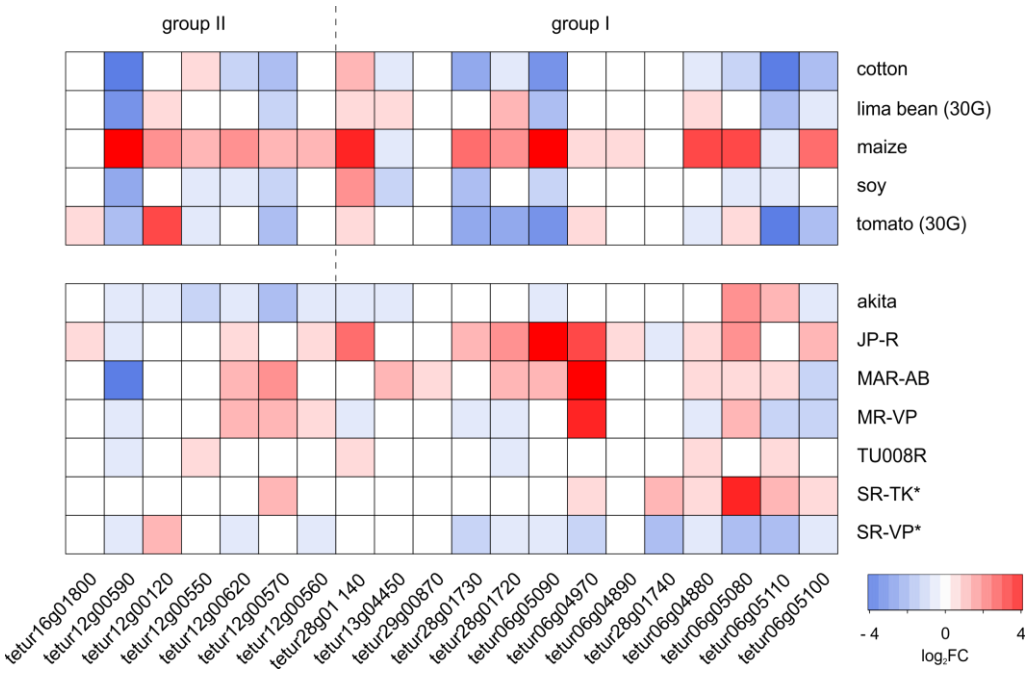

Figure 2 - Expression heatmap of genes coding for group I and II SDRs for adult *T. urticae* females adapted to tomato and lima bean (≥ 30 generations), long-term acclimatized to soy, cotton and maize (≥5 generations) and resistant against acaricides (see below). The $\log_2$ transformed gene fold changes are relative to adult *T. urticae* females of the susceptible London strain or susceptible deutonymph *T. urticae* females of the LS-VL strain. Deutonymph strains are indicated with an asterisks (*), and *T. urticae* genes are shown at the bottom.

strain	resistance status
akita	METIs
JP-R	cyenopyrafen and pyridaben
MAR-AB	abamectin, bifenthrin, clofentezine, hexythiazox, fenbutatin oxide and pyridaben
MR-VP	METIs, cyflumetofen, cyenopyrafen
TU008R	cyflumetofen
SR-TK	spirodiclofen
SR-VP	spirodiclofen

For example, the A1017F target-site mutation in *T. urticae* chitin synthase (*CHS1*) was linked to resistance against chitin biosynthesis inhibitors in 2012 (Van Leeuwen *et al.*, 2012). However, as a heterologous expression system for a completely functional arthropod chitin synthase (catalysis and translocation) is currently lacking, this mutation was only functionally validated in arthropods when a new genome editing technique, CRISPR/Cas9, became available (Douris *et al.*, 2016). In addition to CRISPR/Cas9, introgression can also be used to introduce a specific trait in a defined genetic background that lacks the trait/phenotype. Finally, post-transcriptional gene silencing by RNAi can also be used for *in vivo* functional genomics in insects.

3.2.1. CRISPR/Cas9

Clustered, regularly interspaced, short palindromic repeat (CRISPR)/Cas9, a bacterial adaptive immune system, was developed as a powerful and highly specific genome editing tool. CRISPR/Cas9-mediated gene editing has been used in a multitude of organisms and cells. However, current common approaches rely upon delivering the Cas9 ribonucleoprotein (RNP)

complex by embryonic microinjection, limiting the number of species where CRISPR/Cas9 was successful, and inefficient even when successful (Chaverra-Rodriguez *et al.*, 2018).

Although CRISPR/Cas9 success has been achieved for multiple insects, with *D. melanogaster* taking a leading role (including genome engineered fly lines expressing Cas9 themselves), no convincing studies were published yet with mites. Recently, Bryon *et al.* 2017, aimed at disrupting the *T. urticae phytoene desaturase* gene, which was predicted to have a role in carotenoid accumulation and diapause. Out of 20,000 F1 male progeny, 15 males were identified that either lacked all pigmentation, or were partially albino. However, further experiments revealed that the latter phenotypes were unrelated to the CRISPR/Cas9 editing event. Most likely, the phenotypes were caused by rare alleles segregating at very low frequencies in the original population (Bryon *et al.*, 2017a). Adult *T. urticae* females were injected in the proximity of the ovaria, because of the limited size of the eggs (ø ± 150µm). A challenge to efficient delivery of genome-editing proteins into target cells is their proteolytic instability and poor membrane permeability (Fu *et al.*, 2014). Hence, the development of delivery vehicles to transport active protein is essential to increase the efficiency of protein-based genome editing.

Wang *et al.*, 2016 reported that delivery of the anionic Cas9:sgRNA complex in combination with bioreducible lipids enhanced functional protein delivery and gene recombination efficiencies in human cells and the mouse brain. In Hemiptera, it was shown that BAPC-assisted delivery of CRISPR/Cas9 component also increased efficiency of gene editing (Hunter *et al.*, 2018). Lastly, another technology was developed that helped with the delivery of Cas9 ribonucleoprotein (RNP) complex, named Receptor-Mediated Ovary Transduction of Cargo (ReMOT Control). A peptide (P2C) was identified that mediates transduction of Cas9 RNP from the hemolymph to developing oocytes, bypassing the requirement for embryonic microinjection. ReMOT Control resulted in heritable gene editing of the offspring in six different mosquito species, with efficiencies as high as 0.3 mutants per injected mosquito (Chaverra-Rodriguez *et al.*, 2018). If a successful CRISPR/Cas9 protocol would be developed for *T. urticae*, this would facilitate the study of the expanded DBD-lacking NHR96-like genes (Chapter 2), starting with the validation of the role of *tetur06g04270* by gene knockout in tebufenpyrad resistance.

Although CRISPR/Cas9 was not yet successful in mites, it can already be used to validate *T. urticae* resistance mutations. If the mutation is located in a highly conserved arthropod single-copy gene, standardized assays for *D. melanogaster* can be performed to investigate mutations across species boundaries. CRISPR/Cas9-mediated gain-of-function in *D. melanogaster* was used for example to validate target-site mutations at the exact same position for *Plutella xylostella* (I1024M) and *Tetranychus urticae* (I1017F) (Douris *et al.*, 2016). As suggested in Chapter 2, since the strong conservation of the CPR sequence in arthropods, a reverse genetic approach using *D. melanogaster* may be suitable for studying the effect of the *T. urticae* D384Y CPR mutation on METI-I resistance. However, it should be noted that this approach has also unpredictable pitfalls. Although modified fly lines were successfully created by introducing the *T. urticae* H92R mutation in the *D. melanogaster* PSST homologue by CRISPR/Cas9 (Bajda *et al.*, 2017), the mutation could

unfortunately not be brought to homozygosity, most likely because the mutation was lethal in *D. melanogaster* in contrast to *T. urticae.*

3.2.2. Introgression

Since genome editing tools such as CRISPR/Cas9 are not (yet) available for certain species, introgression of a mutation can be a feasible alternative (Georghiou, 1969; McCart *et al.*, 2005; Roush and McKenzie, 1987). Introgression, i.e. marker assisted backcrossing, is an approach that produces near-isogenic sister lines. In short, a haploid male of the resistant strain is crossed with a virgin female of the susceptible strain. Resulting heterozygous virgin females are backcrossed to susceptible males and heterozygote genotypes are identified, after they had laid a sufficient amount of eggs. The latter process is repeated for six to nine generations. Finally, in the last generation, a cross is carried out between the backcrossed heterozygous virgin females and their first-born sons representing either a susceptible (absence of mutation) or the resistant (presence of mutation) genotype. This results in congenic homozygous lines for the mutation and the wild type allele. Introgression provides a straight-forward and relative precise method to untangle a mutation of interest from other mechanisms that might have been co-selected in the resistant population. Introgressed strains can be analyzed by comparison with the genetically identical susceptible strain that only differs in a small region, which harbors the resistant locus of interest (Bajda *et al.*, 2017; Brito *et al.*, 2013; Riga *et al.*, 2017).

Although a possible effect of closely linked loci cannot be excluded (Hospital, 2001), resulting *T. urticae* populations are believed to be near-isogenic, since high recombination rates have been reported previously in BSA studies (Bryon *et al.*, 2017; Demaeght *et al.*, 2014; Van Leeuwen *et al.*, 2012; Wybouw *et al.*, 2019 and Chapter 2). Introgression was first used in *T. urticae* by Bajda *et al.* 2017, to confirm the involvement of the H92R target site mutation in the PSST homologue of complex I in METI-I resistant *T. urticae*, and its contribution to the total resistance phenotype. The study suggested that other factors were also at play, as was later confirmed by the BSA performed in Chapter 2. More recently, introgression was used to study the relative contribution of nine known target-site mutations conferring resistance to abamectin, pyrethroids or bifenazate (Riga *et al.*, 2017). To conclude, introgression in *T. urticae* is a well-established approach, and can be used to validate mutations, reveal their relative contribution to the resistance phenotype, and discover synergistic effects between multiple mechanisms. Additionally, introgression can be used to study the potential fitness costs/advantages of mutations, and reveal pleiotropic effects of a gene (Arnaud *et al.*, 2002; Brito *et al.*, 2013; ffrench-Constant and Bass, 2017; Wang and Wu, 2014).

In Chapter 2, it was hypothesized that the D384Y mutation in the CPR potentially has a fitness cost to mites not exposed to the pesticides pyridaben and tebufenpyrad as the BSA peak (difference in allele frequencies between selected and unselected population) centering on the mutation did not result from elevated allele frequencies in the selected populations, but from low allele frequencies in the control population (i.e. the absence of selection). The same pattern was observed in a BSA that linked the CPR mutant to spirodiclofen resistance in a different *T. urticae* strain (Wybouw *et al.*, 2019). Hence, creating a near-isogenic line containing the CPR mutation

could be interesting, to validate the hypothesis of the fitness cost, and to study the relative importance of the CPR mutant in pyridaben- and tebufenpyrad resistance.

3.2.3. RNA interference

RNA interference (RNAi), or post-transcriptional gene silencing, was first discovered in animals in the nematode worm *Caenorhabditis elegans* (Fire *et al.*, 1998). Sequence-specific gene silencing was observed as a response to the injection of double-stranded RNA (dsRNA). Subsequently, RNAi became an important tool for functional genomics in insects, and interest arose in the use of RNAi to protect plants from herbivory. But, RNAi efficiencies are known to variate strongly in arthropods, due to species-specific variation in dsRNA uptake, non-cell-autonomous RNAi, nucleases (dsRNases) and virus-load (reviewed by Joga *et al.*, 2016). The current status and future perspectives of RNAi in mite pests was recently reviewed by (Niu *et al.*, 2018).

A genome-wide screen revealed that the complete RNAi machinery is present in *T. urticae* (Dicer, Argonautes and RISC components) (Grbić *et al.*, 2011). Moreover, fluorescently labelled double stranded RNA (dsRNA) and short interfering RNA (siRNA) injected into the abdomen of an adult female distributed throughout the abdominal cavity and was incorporated in the eggs, where the expected phenotype was observed in developing embryos (Khila and Grbić, 2007). Subsequently, RNAi through oral delivery was successful, by allowing *T. urticae* or *T. cinnabarinus* to feed on leaves floating on, or soaked in dsRNA (e.g.(Kwon *et al.*, 2016, 2013; Shi *et al.*, 2016a, 2016b, 2015; Wei *et al.*, 2019b, 2019a)). The efficiency of the latter and other dsRNA delivery approaches was compared in *T. urticae*. dsRNA-coated leaves and mite soaking in dsRNA solution appeared to be the most efficient RNAi approaches, and also required the lowest amount of dsRNA input. Artificial diet supplemented with dsRNA and dsRNA-expressing plants had an intermediate efficiency, and leaves floating on a dsRNA solution the lowest (Suzuki *et al.*, 2017). However, in contrast to RNAi sensitive coleopterans, were only small doses of dsRNA result in 90% gene knockdown or higher, and result in a long lasting and even hereditary effect (Baum *et al.*, 2007; Bolognesi *et al.*, 2012; Rangasamy and Siegfried, 2012; Zhu *et al.*, 2011), *T. urticae* gene knockdown using RNAi is only around 60% or lower, and silencing often temporary. This is similar to other RNAi recalcitrant species, limiting the usability of RNAi for *in vivo* validation in *T. urticae* so far (Joga *et al.*, 2016; Li *et al.*, 2013). Optimization of RNAi was reported in other arthropod species such as for example *Spodoptera exigua* (Lepidoptera), by improving the stability of dsRNA in their alkaline gut environment, due to the formulation of dsRNA with guanidine-containing polymers (Christiaens *et al.*, 2018).

Next to the validation of candidate detoxification genes, RNAi could be used to study functions of nuclear receptor and co-regulators, if persistent and specific knockdown of target genes can be realized (Ashrafi *et al.*, 2003; Zhou *et al.*, 2003). Hence, if gene knockdown levels by RNAi in *T. urticae* would improve, this approach could also be used to validate the role of the DBD-lacking NHR96-like gene in tebufenpyrad resistance.

3.3. X-ray crystallography and homology modelling

Three-dimensional (3D) protein structures can help providing important information about the proteins biochemical function and its interaction properties. Recently, an x-ray crystallography was made of a *T. urticae* intradiol ring-cleavage dioxygenase (DOG), the first structurally characterized DOG of an eukaryote (Schlachter *et al.*, 2019). The acquired protein model showed to be very distinct from its bacterial homologs, and the enzyme had some unusual structural properties. As part of the same collaboration, protein structure models will be created for the seven recombinant UGTs of Chapter 5 that were used in the high-throughput substrate screening.

Since structural information is not available for the vast majority of proteins, 3D homology modeling (a.k.a. comparative modeling or fold recognition) can be a good alternative. Based on experimentally determined structures of related family members, computational methods (e.g. SWISS-MODEL, IntFOLD and Phyre2) can be used to predict protein structures (Kelley *et al.*, 2015; Roche *et al.*, 2011; Schwede *et al.*, 2003). This approach was used in a study that explored the association of *T. urticae* GSTs with insecticide resistance (Pavlidi *et al.*, 2015). By predicting the three-dimensional structure, key structural characteristics were identified, providing insights into the substrate specificity and the catalytic mechanism of the enzyme.

References

Abeel, T., Van Parys, T., Saeys, Y., Galagan, J., Van De Peer, Y., 2012. GenomeView: a next-generation genome browser. Nucleic Acids Res. 40, e12. https://doi.org/10.1093/nar/gkr995

Afschar, S., Toivonen, J.M., Hoffmann, J.M., Tain, L.S., Wieser, D., Finlayson, A.J., Driege, Y., Alic, N., Emran, S., Stinn, J., Froehlich, J., Piper, M.D., Partridge, L., 2016. Nuclear hormone receptor DHR96 mediates the resistance to xenobiotics but not the increased lifespan of insulin-mutant *Drosophila*. Proc. Natl. Acad. Sci. 113, 1321–1326. https://doi.org/10.1073/pnas.1515137113

Agrawal, A.A., Vala, F., Sabelis, M.W., 2002. Induction of preference and performance after acclimation to novel hosts in a phytophagous spider mite: adaptive plasticity? Am. Nat. 159, 553–565. https://doi.org/10.1086/339463

Ahmad, S., 1986. Enzymatic adaptations of herbivorous insects and mites to phytochemicals. J. Chem. Ecol. 12, 533–560. https://doi.org/10.1007/BF01020571

Ahn, S.-J., Badenes-Pérez, F.R., Reichelt, M., Svatoš, A., Schneider, B., Gershenzon, J., Heckel, D.G., 2011. Metabolic detoxification of capsaicin by UDP-glycosyltransferase in three *Helicoverpa* species. Arch. Insect Biochem. Physiol. 78, 104–18. https://doi.org/10.1002/arch.20444

Ahn, S.-J., Vogel, H., Heckel, D.G., 2012. Comparative analysis of the UDP-glycosyltransferase multigene family in insects. Insect Biochem. Mol. Biol. 42, 133–47. https://doi.org/10.1016/j.ibmb.2011.11.006

Ahn, S.J., Dermauw, W., Wybouw, N., Heckel, D.G., Van Leeuwen, T., 2014. Bacterial origin of a diverse family of UDP-glycosyltransferase genes in the *Tetranychus urticae* genome. Insect Biochem. Mol. Biol. 50, 43–57. https://doi.org/10.1016/j.ibmb.2014.04.003

Aigrain, L., Pompon, D., Moréra, S., Truan, G., 2009. Structure of the open conformation of a functional chimeric NADPH cytochrome P450 reductase. EMBO Rep. 10, 742–747. https://doi.org/10.1038/embor.2009.82

Alba, J.M., Schimmel, B.C.J., Glas, J.J., Ataide, L.M.S., Pappas, M.L., Villarroel, C.A., Schuurink, R.C., Sabelis, M.W., Kant, M.R., 2015. Spider mites suppress tomato defenses downstream of jasmonate and salicylate independently of hormonal crosstalk. New Phytol. 205, 828–840. https://doi.org/10.1111/nph.13075

Ali, J.G., Agrawal, A.A., 2012. Specialist versus generalist insect herbivores and plant defense. Trends Plant Sci. 17, 293–302. https://doi.org/10.1016/j.tplants.2012.02.006

Anazawa, Y., Tomita, T., Aiki, Y., Kozaki, T., Kono, Y., 2003. Sequence of a cDNA encoding acetylcholinesterase from susceptible and resistant two-spotted spider mite, *Tetranychus urticae*. Insect Biochem. Mol. Biol. 33, 509–14.

Anders, S., McCarthy, D.J., Chen, Y., Okoniewski, M., Smyth, G.K., Huber, W., Robinson, M.D., 2013. Count-based differential expression analysis of RNA sequencing data using R and Bioconductor. Nat. Protoc. 8, 1765–1786. https://doi.org/10.1038/nprot.2013.099\rhttp://www.nature.com/nprot/journal/v8/n9/abs/nprot.2013.099.html#supplementary-information

Anders, S., Pyl, P.T., Huber, W., 2015. HTSeq-A Python framework to work with high-throughput sequencing data. Bioinformatics 31, 166–169. https://doi.org/10.1093/bioinformatics/btu638

Andrews, S., 2010. FastQC: A quality control tool for high throughput sequence data. [WWW Document].

Angerer, H., Nasiri, H.R., Niedergesäß, V., Kerscher, S., Schwalbe, H., Brandt, U., 2012. Tracing the tail of ubiquinone in mitochondrial complex I. Biochim. Biophys. Acta - Bioenerg. 1817, 1776–1784. https://doi.org/10.1016/j.bbabio.2012.03.021

Arnaud, L., Brostaux, Y., Assié, L.K., Gaspar, C., Haubruge, E., 2002. Increased fecundity of malathion-specific resistant beetles in absence of insecticide pressure. Heredity (Edinb). 89, 425–429. https://doi.org/10.1038/sj.hdy.6800167

Arnold, C.N., Xia, Y., Lin, P., Ross, C., Schwander, M., Smart, N.G., Müller, U., Beutler, B., 2011. Rapid identification of a disease allele in mouse through whole genome sequencing and bulk segregation analysis. Genetics 187, 633–641. https://doi.org/10.1534/genetics.110.124586

Ashrafi, K., Chang, F.Y., Watts, J.L., Fraser, A.G., Kamath, R.S., Ahringer, J., Ruvkun, G., 2003. Genome-wide RNAi analysis of *Caenorhabditis elegans* fat regulatory genes. Nature 421, 268–272. https://doi.org/10.1038/nature01279

Auger, P., Migeon, A., Ueckermann, E.A., Tiedt, L., Navajas, M., 2013. Evidence for synonymy between *Tetranychus urticae* and *Tetranychus cinnabarinus* (Acari, Prostigmata, Tetranychidae): review and new data. Acarologia 53, 383–415. https://doi.org/10.1051/acarologia/20132102

Bailey, S.F., Keifer, H.H., 1943. The tomato russet mite, *Phyllocoptes destructor* Keifer: its present status. J. Econ. Entomol. 36, 706–712. https://doi.org/10.1093/jee/36.5.706

Bajda, S., Dermauw, W., Greenhalgh, R., Nauen, R., Tirry, L., Clark, R.M., Van Leeuwen, T., 2015. Transcriptome profiling of a spirodiclofen susceptible and resistant strain of the European red mite *Panonychus ulmi* using strand-specific RNA-seq. BMC Genomics 16, 974. https://doi.org/10.1186/s12864-015-2157-1

Bajda, S., Dermauw, W., Panteleri, R., Sugimoto, N., Douris, V., Tirry, L., Osakabe, M., Vontas, J., Van Leeuwen, T., 2017. A mutation in the PSST homologue of complex I (NADH:ubiquinone oxidoreductase) from *Tetranychus urticae* is associated with resistance to METI acaricides. Insect Biochem. Mol. Biol. 80, 79–90. https://doi.org/10.1016/j.ibmb.2016.11.010

Balabanidou, V., Grigoraki, L., Vontas, J., 2018. Insect cuticle: a critical determinant of insecticide resistance. Curr. Opin. Insect Sci. 27, 68–74. https://doi.org/10.1016/j.cois.2018.03.001

Barrero, R.A., Guerrero, F.D., Black, M., McCooke, J., Chapman, B., Schilkey, F., Pérez de León, A.A., Miller, R.J., Bruns, S., Dobry, J., Mikhaylenko, G., Stormo, K., Bell, C., Tao, Q., Bogden, R., Moolhuijzen, P.M., Hunter, A., Bellgard, M.I., 2017. Gene-enriched draft genome of the cattle tick *Rhipicephalus microplus*: assembly by the hybrid Pacific Biosciences/Illumina approach enabled analysis of the highly repetitive genome. Int. J. Parasitol. 47, 569–583. https://doi.org/10.1016/J.IJPARA.2017.03.007

Barrett, L.G., Heil, M., 2012. Unifying concepts and mechanisms in the specificity of plant-enemy interactions. Trends Plant Sci. 17, 282–292. https://doi.org/10.1016/j.tplants.2012.02.009

Bartley, K., Wright, H.W., Bull, R.S., Huntley, J.F., Nisbet, A.J., 2015. Characterisation of *Dermanyssus gallinae* glutathione S-transferases and their potential as acaricide detoxification proteins. Parasit. Vectors 8, 350. https://doi.org/10.1186/s13071-015-0960-9

Bass, C., Puinean, A.M., Zimmer, C.T., Denholm, I., Field, L.M., Foster, S.P., Gutbrod, O., Nauen, R., Slater, R., Williamson, M.S., 2014. The evolution of insecticide resistance in the peach potato aphid, *Myzus persicae*. Insect Biochem. Mol. Biol. 51, 41–51. https://doi.org/10.1016/j.ibmb.2014.05.003

Bast, J., Schaefer, I., Schwander, T., Maraun, M., Scheu, S., Kraaijeveld, K., 2016. No accumulation of transposable elements in asexual arthropods. Mol. Biol. Evol. 33, 697–706. https://doi.org/10.1093/molbev/msv261

Bastide, H., Lange, J.D., Lack, J.B., Yassin, A., Pool, J.E., 2016. A variable genetic architecture of melanic evolution in *Drosophila melanogaster*. Genetics 204, 1307–1319. https://doi.org/10.1534/genetics.116.192492

Bateman, A., Martin, M.J., O'Donovan, C., Magrane, M., Apweiler, R., Alpi, E., Antunes, R., Arganiska, J., Bely, B., Bingley, M., Bonilla, C., Britto, R., Bursteinas, B., Chavali, G., Cibrian-Uhalte, E., Da Silva, A., De Giorgi, M., Dogan, T., Fazzini, F., Gane, P., Castro, L.G., Garmiri, P., Hatton-Ellis, E., Hieta, R., Huntley, R., Legge, D., Liu, W., Luo, J., Macdougall, A., Mutowo, P., Nightingale, A., Orchard, S., Pichler, K., Poggioli, D., Pundir, S., Pureza, L., Qi, G., Rosanoff, S., Saidi, R., Sawford, T., Shypitsyna, A., Turner, E., Volynkin, V., Wardell, T., Watkins, X., Zellner, H., Cowley, A., Figueira, L., Li, W., McWilliam, H., Lopez, R., Xenarios, I., Bougueleret, L., Bridge, A., Poux, S., Redaschi, N., Aimo, L., Argoud-Puy, G., Auchincloss, A., Axelsen, K., Bansal, P., Baratin, D., Blatter, M.C., Boeckmann, B., Bolleman, J., Boutet, E., Breuza, L., Casal-Casas, C., De Castro, E., Coudert, E., Cuche, B., Doche, M., Dornevil, D., Duvaud, S., Estreicher, A., Famiglietti, L., Feuermann, M., Gasteiger, E., Gehant, S., Gerritsen, V., Gos, A., Gruaz-Gumowski, N., Hinz, U., Hulo, C., Jungo, F., Keller, G., Lara, V., Lemercier, P., Lieberherr, D., Lombardot,

T., Martin, X., Masson, P., Morgat, A., Neto, T., Nouspikel, N., Paesano, S., Pedruzzi, I., Pilbout, S., Pozzato, M., Pruess, M., Rivoire, C., Roechert, B., Schneider, M., Sigrist, C., Sonesson, K., Staehli, S., Stutz, A., Sundaram, S., Tognolli, M., Verbregue, L., Veuthey, A.L., Wu, C.H., Arighi, C.N., Arminski, L., Chen, C., Chen, Y., Garavelli, J.S., Huang, H., Laiho, K., McGarvey, P., Natale, D.A., Suzek, B.E., Vinayaka, C.R., Wang, Q., Wang, Y., Yeh, L.S., Yerramalla, M.S., Zhang, J., 2015. UniProt: a hub for protein information. Nucleic Acids Res. 43, D204–D212. https://doi.org/10.1093/nar/gku989

Bateman, A., Sandford, R., 1999. The PLAT domain: a new piece in the PKD1 puzzle. Curr. Biol. 9, R588-90.

Bates, D., Mächler, M., Bolker, B., Walker, S., 2015. Fitting linear mixed-effects models using lme4. J. Stat. Softw. 67, 51. https://doi.org/10.18637/jss.v067.i01

Baum, J.A., Bogaert, T., Clinton, W., Heck, G.R., Feldmann, P., Ilagan, O., Johnson, S., Plaetinck, G., Munyikwa, T., Pleau, M., Vaughn, T., Roberts, J., 2007. Control of coleopteran insect pests through RNA interference. Nat. Biotechnol. 25, 1322–1326. https://doi.org/10.1038/nbt1359

Bautista, M.A.M., Tanaka, T., Miyata, T., 2007. Identification of permethrin-inducible cytochrome P450s from the diamondback moth, *Plutella xylostella* (L.) and the possibility of involvement in permethrin resistance. Pestic. Biochem. Physiol. 87, 85–93. https://doi.org/10.1016/j.pestbp.2006.06.004

Baxter, S.W., Papa, R., Chamberlain, N., Humphray, S.J., Joron, M., Morrison, C., Ffrench-Constant, R.H., McMillan, W.O., Jiggins, C.D., 2008. Convergent evolution in the genetic basis of Müllerian mimicry in *Heliconius* butterflies. Genetics 180, 1567–1577. https://doi.org/10.1534/genetics.107.082982

Bazakos, C., Hanemian, M., Trontin, C., Jiménez-Gómez, J.M., Loudet, O., 2017. New strategies and tools in quantitative genetics: how to go from the phenotype to the genotype. Annu. Rev. Plant Biol. 68, 435–455. https://doi.org/10.1146/annurev-arplant-042916-040820

Beaver, L.M., Hooven, L.A., Butcher, S.M., Krishnan, N., Sherman, K.A., Chow, E.S.Y., Giebultowicz, J.M., 2010. Circadian clock regulates response to pesticides in *Drosophila* via conserved Pdp1 pathway. Toxicol. Sci. 115, 513–520. https://doi.org/10.1093/toxsci/kfq083

Beck, B., Steurbaut, W., Spanoghe, P., 2012. How to define green adjuvants. Pest Manag. Sci. 68, 1107–1110. https://doi.org/10.1002/ps.3308

Behmer, S.T., 2009. Insect herbivore nutrient regulation. Annu. Rev. Entomol. 54, 165–187. https://doi.org/10.1146/annurev.ento.54.110807.090537

Behrens, D., Huang, Q., Geßner, C., Rosenkranz, P., Frey, E., Locke, B., Moritz, R.F.A., Kraus, F.B., 2011. Three QTL in the honey bee *Apis mellifera* L. suppress reproduction of the parasitic mite *Varroa destructor*. Ecol. Evol. 1, 451–458. https://doi.org/10.1002/ece3.17

Benjamini, Y., Hochberg, Y., 1995. Controlling the false discovery rate: A practical and powerful approach to multiple testing. J. R. Stat. Soc. Ser. B 57, 289–300. https://doi.org/10.2307/2346101

Bensoussan, N., Santamaria, M.E., Zhurov, V., Diaz, I., Grbić, M., Grbić, V., 2016. Plant-herbivore interaction: dissection of the cellular pattern of *Tetranychus urticae* feeding on the host plant. Front. Plant Sci. 7, 1105. https://doi.org/10.3389/fpls.2016.01105

Bentley, D.R., Balasubramanian, S., Swerdlow, H.P., Smith, G.P., Milton, J., Brown, C.G., Hall, K.P., Evers, D.J., Barnes, C.L., Bignell, H.R., Boutell, J.M., Bryant, J., Carter, R.J., Keira Cheetham, R., Cox, A.J., Ellis, D.J., Flatbush, M.R., Gormley, N.A., Humphray, S.J., Irving, L.J., Karbelashvili, M.S., Kirk, S.M., Li, H., Liu, X., Maisinger, K.S., Murray, L.J., Obradovic, B., Ost, T., Parkinson, M.L., Pratt, M.R., Rasolonjatovo, I.M.J., Reed, M.T., Rigatti, R., Rodighiero, C., Ross, M.T., Sabot, A., Sankar, S. V., Scally, A., Schroth, G.P., Smith, M.E., Smith, V.P., Spiridou, A., Torrance, P.E., Tzonev, S.S., Vermaas, E.H., Walter, K., Wu, X., Zhang, L., Alam, M.D., Anastasi, C., Aniebo, I.C., Bailey, D.M.D., Bancarz, I.R., Banerjee, S., Barbour, S.G., Baybayan, P.A., Benoit, V.A., Benson, K.F., Bevis, C., Black, P.J., Boodhun, A., Brennan, J.S., Bridgham, J.A., Brown, R.C., Brown, A.A., Buermann, D.H., Bundu, A.A., Burrows, J.C., Carter, N.P., Castillo, N., Chiara E. Catenazzi, M., Chang, S., Neil Cooley, R., Crake, N.R., Dada, O.O., Diakoumakos, K.D., Dominguez-Fernandez, B., Earnshaw, D.J., Egbujor, U.C., Elmore, D.W., Etchin, S.S., Ewan, M.R., Fedurco, M., Fraser, L.J., Fuentes Fajardo, K. V., Scott Furey, W., George, D.,

Gietzen, K.J., Goddard, C.P., Golda, G.S., Granieri, P.A., Green, D.E., Gustafson, D.L., Hansen, N.F., Harnish, K., Haudenschild, C.D., Heyer, N.I., Hims, M.M., Ho, J.T., Horgan, A.M., Hoschler, K., Hurwitz, S., Ivanov, D. V., Johnson, M.Q., James, T., Huw Jones, T.A., Kang, G.-D., Kerelska, T.H., Kersey, A.D., Khrebtukova, I., Kindwall, A.P., Kingsbury, Z., Kokko-Gonzales, P.I., Kumar, A., Laurent, M.A., Lawley, C.T., Lee, S.E., Lee, X., Liao, A.K., Loch, J.A., Lok, M., Luo, S., Mammen, R.M., Martin, J.W., McCauley, P.G., McNitt, P., Mehta, P., Moon, K.W., Mullens, J.W., Newington, T., Ning, Z., Ling Ng, B., Novo, S.M., O'Neill, M.J., Osborne, M.A., Osnowski, A., Ostadan, O., Paraschos, L.L., Pickering, L., Pike, Andrew C., Pike, Alger C., Chris Pinkard, D., Pliskin, D.P., Podhasky, J., Quijano, V.J., Raczy, C., Rae, V.H., Rawlings, S.R., Chiva Rodriguez, A., Roe, P.M., Rogers, John, Rogert Bacigalupo, M.C., Romanov, N., Romieu, A., Roth, R.K., Rourke, N.J., Ruediger, S.T., Rusman, E., Sanches-Kuiper, R.M., Schenker, M.R., Seoane, J.M., Shaw, R.J., Shiver, M.K., Short, S.W., Sizto, N.L., Sluis, J.P., Smith, M.A., Ernest Sohna Sohna, J., Spence, E.J., Stevens, K., Sutton, N., Szajkowski, L., Tregidgo, C.L., Turcatti, G., vandeVondele, S., Verhovsky, Y., Virk, S.M., Wakelin, S., Walcott, G.C., Wang, J., Worsley, G.J., Yan, J., Yau, L., Zuerlein, M., Rogers, Jane, Mullikin, J.C., Hurles, M.E., McCooke, N.J., West, J.S., Oaks, F.L., Lundberg, P.L., Klenerman, D., Durbin, R., Smith, A.J., 2008. Accurate whole human genome sequencing using reversible terminator chemistry. Nature 456, 53–59. https://doi.org/10.1038/nature07517

Bernard, C.B., Philogène, B.J., 1993. Insecticide synergists: role, importance, and perspectives. J. Toxicol. Environ. Health 38, 199–223. https://doi.org/10.1080/15287399309531712

Bernays, E., Graham, M., 1988. On the evolution of host specificity in phytophagous arthropods. Ecology 69, 886–892. https://doi.org/10.2307/1941237

Blaazer, C.J.H., Villacis-Perez, E.A., Chafi, R., Van Leeuwen, T., Kant, M.R., Schimmel, B.C.J., 2018. Why do herbivorous mites suppress plant defenses? Front. Plant Sci. 9, 1057. https://doi.org/10.3389/fpls.2018.01057

Bock, K.W., 2003. Vertebrate UDP-glucuronosyltransferases: functional and evolutionary aspects. Biochem. Pharmacol. 66, 691–696. https://doi.org/10.1016/S0006-2952(03)00296-X

Bohm, B.A., 1998. Introduction to flavonoids, Chemistry and Biochemistry of Organic Natural Products. https://doi.org/10.1017/CBO9781107415324.004

Bolognesi, R., Ramaseshadri, P., Anderson, J., Bachman, P., Clinton, W., Flannagan, R., Ilagan, O., Lawrence, C., Levine, S., Moar, W., Mueller, G., Tan, J., Uffman, J., Wiggins, E., Heck, G., Segers, G., 2012. Characterizing the mechanism of action of double-stranded RNA activity against western corn rootworm (*Diabrotica virgifera* virgifera LeConte). PLoS One 7, e47534. https://doi.org/10.1371/journal.pone.0047534

Boulain, H., Legeai, F., Guy, E., Morlière, S., Douglas, N.E., Oh, J., Murugan, M., Smith, M., Jaquiéry, J., Peccoud, J., White, F.F., Carolan, J.C., Simon, J.-C., Sugio, A., 2018. Fast evolution and lineage-specific gene family expansions of aphid salivary effectors driven by interactions with host-plants. Genome Biol. Evol. 10, 1554–1572. https://doi.org/10.1093/gbe/evy097

Bowen, M.E., Henke, K., Siegfried, K.R., Warman, M.L., Harris, M.P., 2012. Efficient mapping and cloning of mutations in zebrafish by low-coverage whole-genome sequencing. Genetics 190, 1017–1024. https://doi.org/10.1534/genetics.111.136069

Bowles, D., Lim, E.-K., Poppenberger, B., Vaistij, F.E., 2006. Glycosyltransferases of lipophilic small molecules. Annu. Rev. Plant Biol. 57, 567–597. https://doi.org/10.1146/annurev.arplant.57.032905.105429

Boyland, E., Chasseaud, L.F., 1970. The effect of some carbonyl compounds on rat liver glutathione levels. Biochem. Pharmacol. 19, 1526–1528. https://doi.org/10.1016/0006-2952(70)90075-4

Bradford, M.M., 1976. A rapid and sensitive method for the quantitation of microgram quantities of protein utilizing the principle of protein-dye binding. Anal. Biochem. 72, 248–254. https://doi.org/10.1016/0003-2697(76)90527-3

Brattsten, L.B., 1988. Enzymic adaptations in leaf-feeding insects to host-plant allelochemicals. J. Chem. Ecol.

14, 1919–1939. https://doi.org/10.1007/BF01013486

Bray, J., Marsden, B., Oppermann, U., 2009. The human short-chain dehydrogenase/reductase (SDR) superfamily: A bioinformatics summary. Chem. Biol. Interact. 178, 99–109. https://doi.org/10.1016/j.cbi.2008.10.058

Brito, L.P., Linss, J.G.B., Lima-Camara, T.N., Belinato, T.A., Peixoto, A.A., Lima, J.B.P., Valle, D., Martins, A.J., 2013. Assessing the effects of *Aedes aegypti* kdr mutations on pyrethroid resistance and its fitness cost. PLoS One 8, e60878. https://doi.org/10.1371/journal.pone.0060878

Brown, S., Kerns, D.L., Gore, J., Lorenz, G., Stewart, S., 2017. Susceptibility of twospotted spider mites (*Tetranychus urticae*) to abamectin in Midsouth cotton. Crop Prot. 98, 179–183. https://doi.org/10.1016/J.CROPRO.2017.04.002

Bryon, A., Kurlovs, A.H., Dermauw, W., Greenhalgh, R., Riga, M., Grbić, M., Tirry, L., Osakabe, M., Vontas, J., Clark, R.M., Van Leeuwen, T., 2017a. Disruption of a horizontally transferred phytoene desaturase abolishes carotenoid accumulation and diapause in *Tetranychus urticae*. Proc. Natl. Acad. Sci. 114, E5871–E5880. https://doi.org/10.1073/pnas.1706865114

Bryon, A., Kurlovs, A.H., Van Leeuwen, T., Clark, R.M., 2017b. A molecular-genetic understanding of diapause in spider mites: current knowledge and future directions. Physiol. Entomol. 42, 211–224. https://doi.org/10.1111/phen.12201

Bryon, A., Wybouw, N., Dermauw, W., Tirry, L., Van Leeuwen, T., 2013. Genome wide gene-expression analysis of facultative reproductive diapause in the two-spotted spider mite *Tetranychus urticae*. BMC Genomics 14, 815. https://doi.org/10.1186/1471-2164-14-815

Bui, H., Greenhalgh, R., Ruckert, A., Gill, G.S., Lee, S., Ramirez, R.A., Clark, R.M., 2018. Generalist and specialist mite herbivores induce similar defense responses in maize and barley but differ in susceptibility to benzoxazinoids. Front. Plant Sci. 9, 1222. https://doi.org/10.3389/fpls.2018.01222

Bumgarner, R., 2013. Overview of dna microarrays: types, applications, and their future. Curr. Protoc. Mol. Biol. 22, 1–11. https://doi.org/10.1002/0471142727.mb2201s101

Burgess, Stewart T.G., Bartley, K., Marr, E.J., Wright, H.W., Weaver, R.J., Prickett, J.C., Hughes, M., Haldenby, S., Thi Le, P., Rombauts, S., Van Leeuwen, T., Van de Peer, Y., Nisbet, A.J., Burgess STG, C., Le, T.P., 2018. Draft genome assembly of the sheep scab mite, Psoroptes ovis. genome Announc. 6, 265–283. https://doi.org/10.1128/genomeA.00265-18

Burgess, Stewart T. G., Bartley, K., Nunn, F., Wright, H.W., Hughes, M., Gemmell, M., Haldenby, S., Paterson, S., Rombauts, S., Tomley, F.M., Blake, D.P., Pritchard, J., Schicht, S., Strube, C., Øines, Ø., Van Leeuwen, T., Van de Peer, Y., Nisbet, A.J., 2018. Draft genome assembly of the poultry red mite, Dermanyssus gallinae. Microbiol. Resour. Announc. 30, 59–59. https://doi.org/10.1128/MRA.01221

Burke, M.K., Dunham, J.P., Shahrestani, P., Thornton, K.R., Rose, M.R., Long, A.D., 2010. Genome-wide analysis of a long-term evolution experiment with *Drosophila*. Nature 467, 587–590. https://doi.org/10.1038/nature09352

Burkhard, F.Z., Parween, S., Udhane, S.S., Flück, C.E., Pandey, A. V., 2017. P450 Oxidoreductase deficiency: analysis of mutations and polymorphisms. J. Steroid Biochem. Mol. Biol. 165, 38–50. https://doi.org/10.1016/J.JSBMB.2016.04.003

Butterworth, J.H., Morgan, E.D., 1968. Isolation of a substance that suppresses feeding in locusts. Chem. Commun. 23. https://doi.org/10.1039/c19680000023

Capella-Gutiérrez, S., Silla-Martínez, J.M., Gabaldón, T., 2009. trimAl: A tool for automated alignment trimming in large-scale phylogenetic analyses. Bioinformatics 25, 1972–1973. https://doi.org/10.1093/bioinformatics/btp348

Carlini, C.R., Grossi-De-Sá, M.F., 2002. Plant toxic proteins with insecticidal properties. A review on their potentialities as bioinsecticides. Toxicon 40, 1515–1539. https://doi.org/10.1016/S0041-0101(02)00240-4

Carrière, Y., 2003. Haplodiploidy, sex, and the evolution of pesticide resistance. J. Econ. Entomol. 96, 1626–40.

Casey, W., Anderson, S., Fox, T., Dold, K., Colton, H., Morgan, K., 2002. Transcriptional and physiological responses of HepG2 cells exposed to diethyl maleate: time course analysis. Physiol. Genomics 8, 115–122. https://doi.org/10.1152/physiolgenomics.00064.2001

Casida, J.E., 1970. Mixed-function oxidase involvement in the biochemistry of insecticide synergists. J. Agric. Food Chem. 18, 753–772.

Chaisson, M.J., Tesler, G., 2012. Mapping single molecule sequencing reads using basic local alignment with successive refinement (BLASR): application and theory. BMC Bioinformatics 13, 238. https://doi.org/10.1186/1471-2105-13-238

Chamchoy, K., Pakotiprapha, D., Pumirat, P., Leartsakulpanich, U., Boonyuen, U., 2019. Application of WST-8 based colorimetric NAD(P)H detection for quantitative dehydrogenase assays. BMC Biochem. 20, 4. https://doi.org/10.1186/s12858-019-0108-1

Chan, H.H. ao, Wajidi, M.F. adzil F., Zairi, J., 2014. Molecular cloning and xenobiotic induction of seven novel cytochrome P450 monooxygenases in *Aedes albopictus*. J. Insect Sci. 14, 163. https://doi.org/10.1093/jisesa/ieu025

Chandrakanth, N., Moorthy, S.M., Ponnuvel, K.M., Sivaprasad, V., 2015. Identification of microsatellite markers linked to thermotolerance in silkworm by bulk segregant analysis and in silico mapping. Genetika 47, 1063–1078. https://doi.org/10.2298/GENSR1503063C

Chaplin, M.F., Bucke, C., 1990. Enzyme technology. Cambridge University Press.

Chaverra-Rodriguez, D., Macias, V.M., Hughes, G.L., Pujhari, S., Suzuki, Y., Peterson, D.R., Kim, D., McKeand, S., Rasgon, J.L., 2018. Targeted delivery of CRISPR-Cas9 ribonucleoprotein into arthropod ovaries for heritable germline gene editing. Nat. Commun. 9, 3008. https://doi.org/10.1038/s41467-018-05425-9

Che-Mendoza, A., Penilla, R., Rodríguez, D., 2009. Insecticide resistance and glutathione S-transferases in mosquitoes: A review. African J. Biotechnol. 8, 1386–1397.

Chen, W., Hasegawa, D.K., Kaur, N., Kliot, A., Pinheiro, P.V., Luan, J., Stensmyr, M.C., Zheng, Y., Liu, W., Sun, H., Xu, Y., Luo, Y., Kruse, A., Yang, X., Kontsedalov, S., Lebedev, G., Fisher, T.W., Nelson, D.R., Hunter, W.B., Brown, J.K., Jander, G., Cilia, M., Douglas, A.E., Ghanim, M., Simmons, A.M., Wintermantel, W.M., Ling, K.S., Fei, Z., 2016. The draft genome of whitefly *Bemisia tabaci* MEAM1, a global crop pest, provides novel insights into virus transmission, host adaptation, and insecticide resistance. BMC Biol. 14, 110. https://doi.org/10.1186/s12915-016-0321-y

Cheng, D., Xia, Q., Duan, J., Wei, L., Huang, C., Li, Z., Wang, G., Xiang, Z., 2008. Nuclear receptors in *Bombyx mori*: insights into genomic structure and developmental expression. Insect Biochem. Mol. Biol. 38, 1130–1137. https://doi.org/10.1016/j.ibmb.2008.09.013

Cho, J.B., Kim, Y.J., Ahn, Y.J., Yoo, J.K., Lee, J.O., 1995. Monitoring of acaricide resistance in field-collected populations of *Tetranychus urticae* (Acari: Tetranychidae) in Korea. Korean J. Appl. Entomol. 34, 40–45.

Chou, C.-C., Chen, C.-H., Lee, T.-T., Peck, K., 2004. Optimization of probe length and the number of probes per gene for optimal microarray analysis of gene expression. Nucleic Acids Res. 32, e99. https://doi.org/10.1093/nar/gnh099

Christiaens, O., Tardajos, M.G., Martinez Reyna, Z.L., Dash, M., Dubruel, P., Smagghe, G., 2018. Increased RNAi efficacy in *Spodoptera exigua* via the formulation of dsRNA with guanylated polymers. Front. Physiol. 9, 316. https://doi.org/10.3389/fphys.2018.00316

Christians, U., Gottschalk, S., Miljus, J., Hainz, C., Benet, L.Z., Leibfritz, D., Serkova, N., 2004. Alterations in glucose metabolism by cyclosporine in rat brain slices link to oxidative stress: interactions with mTOR inhibitors. Br. J. Pharmacol. 143, 388–396. https://doi.org/10.1038/sj.bjp.0705939

Cingolani, P., Platts, A., Wang, L.L., Coon, M., Nguyen, T., Wang, L., Land, S.J., Lu, X., Ruden, D.M., 2012. A program for annotating and predicting the effects of single nucleotide polymorphisms, SnpEff: SNPs in the genome of *Drosophila melanogaster* strain w 1118; iso-2; iso-3. Fly (Austin). 6, 80–92.

https://doi.org/10.4161/fly.19695

Clark, A.G., Shamaan, N.A., 1984. Evidence that DDT-dehydrochlorinase from the house fly is a glutathione S-transferase. Pestic. Biochem. Physiol. 22, 249–261. https://doi.org/10.1016/0048-3575(84)90018-X

Claudianos, C., Ranson, H., Johnson, R.M., Biswas, S., Schuler, M.A., Berenbaum, M.R., Feyereisen, R., Oakeshott, J.G., 2006. A deficit of detoxification enzymes: pesticide sensitivity and environmental response in the honeybee. Insect Mol. Biol. 15, 615–636. https://doi.org/10.1111/j.1365-2583.2006.00672.x

Clotuche, G., Deneubourg, J.L., Mailleux, A.C., Detrain, C., Hance, T., 2012. Discrimination through silk recognition: the case of the two-spotted spider mite *Tetranychus urticae*. Comptes Rendus - Biol. 335, 535–40. https://doi.org/10.1016/j.crvi.2012.07.001

Clotuche, G., Mailleux, A.C., Fernández Astudillo, A., Deneubourg, J.L., Detrain, C., Hance, T., 2011. The formation of collective silk balls in the spider mite *Tetranychus urticae* Koch. PLoS One 6, e18854. https://doi.org/10.1371/journal.pone.0018854

Clotuche, G., Mailleux, A.C., Yano, S., Detrain, C., Deneubourg, J.L., Hance, T., 2013. Settlement decisions by the two-spotted spider mite *Tetranychus urticae*. Comptes Rendus - Biol. 336, 93–101. https://doi.org/10.1016/j.crvi.2013.02.006

Coker, J.S., Vian, A., Davies, E., 2005. Identification, accumulation, and functional prediction of novel tomato transcripts systemically upregulated after fire damage. Physiol. Plant. 124, 311–322. https://doi.org/10.1111/j.1399-3054.2005.00488.x

Conesa, A., Götz, S., García-Gómez, J.M., Terol, J., Talón, M., Robles, M., 2005. Blast2GO: A universal tool for annotation, visualization and analysis in functional genomics research. Bioinformatics 21, 3674–3676. https://doi.org/10.1093/bioinformatics/bti610

Correia, M.A., Ortiz de Montellano, P.R., 2005. Inhibition of Cytochrome P450 Enzymes, in: Cytochrome P450: Structure, Mechanism, and Biochemistry. pp. 247–322.

Cowles, R.S., Keller, J.E., Miller, J.R., 1989. Pungent spices, ground red pepper, and synthetic capsaicin as onion fly ovipositional deterrents. J. Chem. Ecol. 15, 719–730. https://doi.org/10.1007/BF01014714

Cramaro, W.J., Revets, D., Hunewald, O.E., Sinner, R., Reye, A.L., Muller, C.P., 2015. Integration of *Ixodes ricinus* genome sequencing with transcriptome and proteome annotation of the naïve midgut. BMC Genomics 16, 871. https://doi.org/10.1186/s12864-015-1981-7

Crozier, R.H., 1985. Adaptive consequences of male-haploidy, in: Helle, W., Sabelis, M.W. (Eds.), Spider Mites: Their Biology, Natural Anemies and Control. Elsevier, Amsterdam, the Netherlands, pp. 201–222.

Cully, D.F., Vassilatis, D.K., Liu, K.K., Paress, P.S., Van der Ploeg, L.H.T., Schaeffer, J.M., Arena, J.P., 1994. Cloning of an avermectin-sensitive glutamate-gated chloride channel from *Caenorhabditis elegans*. Nature 371, 707–711. https://doi.org/10.1038/371707a0

Daborn, P.J., Yen, J.L., Bogwitz, M.R., Le Goff, G., Feil, E., Jeffers, S., Tijet, N., Perry, T., Heckel, D., Batterham, P., Feyereisen, R., Wilson, T.G., Ffrench-Constant, R.H., 2002. A single P450 allele associated with insecticide resistance in *Drosophila*. Science (80-.). 297, 2253–2256. https://doi.org/10.1126/science.1074170

Daimon, T., Hirayama, C., Kanai, M., Ruike, Y., Meng, Y., Kosegawa, E., Nakamura, M., Tsujimoto, G., Katsuma, S., Shimada, T., 2010. The silkworm Green b locus encodes a quercetin 5-O-glucosyltransferase that produces green cocoons with UV-shielding properties. Proc. Natl. Acad. Sci. U. S. A. 107, 11471–6. https://doi.org/10.1073/pnas.1000479107

Dakora, F.D., Phillips, D.A., 1996. Diverse functions of isoflavonoids in legumes transcend anti-microbial definitions of phytoalexins. Physiol. Mol. Plant Pathol. 49, 1–20. https://doi.org/10.1006/pmpp.1996.0035

David, J.-P., Coissac, E., Melodelima, C., Poupardin, R., Riaz, M., Chandor-Proust, A., Reynaud, S., 2010. Transcriptome response to pollutants and insecticides in the dengue vector *Aedes aegypti* using next-generation sequencing technology. BMC Genomics 11, 216. https://doi.org/10.1186/1471-2164-11-216

De la Paz Celorio-Mancera, M., Wheat, C.W., Vogel, H., Söderlind, L., Janz, N., Nylin, S., 2013. Mechanisms of macroevolution: polyphagous plasticity in butterfly larvae revealed by RNA-Seq. Mol. Ecol. 22, 4884–4895. https://doi.org/10.1111/mec.12440

de Moraes, G.J., McMurtry, J.A., Baker, E.W., 1987. Redescription and distribution of the spider mites *T. evansi* and *T. marianae*. Acarologia 28, 333–343.

de Nadal, E., Ammerer, G., Posas, F., 2011. Controlling gene expression in response to stress. Nat. Rev. Genet. 12, 833–45. https://doi.org/10.1038/nrg3055

Decker, L.A., 1977. Worthington enzyme manual. Worthingt. Biochem. Corp.

Degli Esposti, M., 1998. Inhibitors of NADH-ubiquinone reductase: an overview. Biochim. Biophys. Acta - Bioenerg. 1364, 222–235. https://doi.org/10.1016/S0005-2728(98)00029-2

Demaeght, P., 2015. A genomic approach to investigate resistance mechanims in the two-spotted spider mite *Tetranychus urticae* . Ghent university.

Demaeght, P., Dermauw, W., Tsakireli, D., Khajehali, J., Nauen, R., Tirry, L., Vontas, J., Lümmen, P., Van Leeuwen, T., 2013. Molecular analysis of resistance to acaricidal spirocyclic tetronic acids in *Tetranychus urticae*: CYP392E10 metabolizes spirodiclofen, but not its corresponding enol. Insect Biochem. Mol. Biol. 43, 544–554. https://doi.org/10.1016/j.ibmb.2013.03.007

Demaeght, P., Osborne, E.J., Odman-Naresh, J., Grbić, M., Nauen, R., Merzendorfer, H., Clark, R.M., Van Leeuwen, T., 2014. High resolution genetic mapping uncovers chitin synthase-1 as the target-site ofthe structurally diverse mite growth inhibitors clofentezine, hexythiazox and etoxazole in *Tetranychus urticae*. Insect Biochem. Mol. Biol. 51, 52–61. https://doi.org/10.1016/j.ibmb.2014.05.004

Dermauw, W., Ilias, A., Riga, M., Tsagkarakou, A., Grbić, M., Tirry, L., Van Leeuwen, T., Vontas, J., 2012. The cys-loop ligand-gated ion channel gene family of *Tetranychus urticae*: implications for acaricide toxicology and a novel mutation associated with abamectin resistance. Insect Biochem. Mol. Biol. 42, 455–465. https://doi.org/10.1016/j.ibmb.2012.03.002

Dermauw, W., Osborne, E.J., Clark, R.M., Grbić, M., Tirry, L., Van Leeuwen, T., 2013a. A burst of ABC genes in the genome of the polyphagous spider mite *Tetranychus urticae*. BMC Genomics 14, 317. https://doi.org/10.1186/1471-2164-14-317

Dermauw, W., Pym, A., Bass, C., Van Leeuwen, T., Feyereisen, R., 2018. Does host plant adaptation lead to pesticide resistance in generalist herbivores? Curr. Opin. Insect Sci. 26, 25–33. https://doi.org/10.1016/J.COIS.2018.01.001

Dermauw, W., Van Leeuwen, T., 2014. The ABC gene family in arthropods: comparative genomics and role in insecticide transport and resistance. Insect Biochem. Mol. Biol. 45, 89–110. https://doi.org/10.1016/j.ibmb.2013.11.001

Dermauw, W., Wybouw, N., Rombauts, S., Menten, B., Vontas, J., Grbic, M., Clark, R.M., Feyereisen, R., Van Leeuwen, T., 2013b. A link between host plant adaptation and pesticide resistance in the polyphagous spider mite *Tetranychus urticae*. Proc. Natl. Acad. Sci. U. S. A. 110, E113-22. https://doi.org/10.1073/pnas.1213214110

Desjardins, C.A., Gadau, J., Lopez, J.A., Niehuis, O., Avery, A.R., Loehlin, D.W., Richards, S., Colbourne, J.K., Werren, J.H., 2013. Fine-scale mapping of the *Nasonia* genome to chromosomes using a high-density genotyping microarray. G3 (Bethesda). 3, 205–215. https://doi.org/10.1534/g3.112.004739

Després, L., David, J.-P., Gallet, C., 2007. The evolutionary ecology of insect resistance to plant chemicals. Trends Ecol. Evol. 22, 298–307. https://doi.org/10.1016/j.tree.2007.02.010

Devine, G.J., Barber, M., Denholm, I., 2001. Incidence and inheritance of resistance to METI-acaricides in European strains of the two-spotted spider mite (*Tetranychus urticae*) (Acari: Tetranychidae). Pest Manag. Sci. 57, 443–448. https://doi.org/10.1002/ps.307

Devonshire, A.L., Moores, G.D., 1982. A carboxylesterase with broad substrate specificity causes organophosphorus, carbamate and pyrethroid resistance in peach-potato aphids (*Myzus persicae*).

Pestic. Biochem. Physiol. 18, 235–246. https://doi.org/10.1016/0048-3575(82)90110-9

Devorshak, C., Roe, R.M., 1998. The role of esterases in insecticide resistance. Rev. Toxicol. 2, 501–537.

Díaz-Riquelme, J., Zhurov, V., Rioja, C., Pérez-Moreno, I., Torres-Pérez, R., Grimplet, J., Carbonell-Bejerano, P., Bajda, S., Van Leeuwen, T., Martínez-Zapater, J.M., Grbic, M., Grbic, V., 2016. Comparative genome-wide transcriptome analysis of vitis vinifera responses to adapted and non-adapted strains of two-spotted spider mite, *Tetranyhus urticae*. BMC Genomics 17, 74. https://doi.org/10.1186/s12864-016-2401-3

Dixon, R.A., 2001. Natural products and plant disease resistance. Nature 411, 843–847. https://doi.org/10.1038/35081178

Dobin, A., Davis, C.A., Schlesinger, F., Drenkow, J., Zaleski, C., Jha, S., Batut, P., Chaisson, M., Gingeras, T.R., 2013. STAR: Ultrafast universal RNA-seq aligner. Bioinformatics 29, 15–21. https://doi.org/10.1093/bioinformatics/bts635

Dobler, S., Dalla, S., Wagschal, V., Agrawal, A.A., 2012. Community-wide convergent evolution in insect adaptation to toxic cardenolides by substitutions in the Na,K-ATPase. Proc. Natl. Acad. Sci. 109, 13040–13045. https://doi.org/10.1073/pnas.1202111109

Dodou, K., 2005. Investigations on gossypol: past and present developments. Expert Opin. Investig. Drugs 14, 1419–1434. https://doi.org/10.1517/13543784.14.11.1419

Doitsidou, M., Poole, R.J., Sarin, S., Bigelow, H., Hobert, O., 2010. *C. elegans* mutant identification with a one-step whole-genome-sequencing and SNP mapping strategy. PLoS One 5, e15435. https://doi.org/10.1371/journal.pone.0015435

Dong, X., Armstrong, S.D., Xia, D., Makepeace, B.L., Darby, A.C., Kadowaki, T., 2017. Draft genome of the honey bee ectoparasitic mite, *Tropilaelaps mercedesae*, is shaped by the parasitic life history. Gigascience 6, 1–17. https://doi.org/10.1093/gigascience/gix008

Dong, X., Chaisiri, K., Xia, D., Armstrong, S.D., Fang, Y., Donnelly, M.J., Kadowaki, T., McGarry, J.W., Darby, A.C., Makepeace, B.L., 2018. Genomes of trombidid mites reveal novel predicted allergens and laterally transferred genes associated with secondary metabolism. Gigascience 7, 1–33. https://doi.org/10.1093/gigascience/giy127

DongSub, K., HaeYoung, N., Kwack, Y., ChangHoo, C., 2014. Secondary metabolite profiling in various parts of tomato plants. Korean J. Hortic. Sci. & Technol. 32, 252–260.

Douris, V., Steinbach, D., Panteleri, R., Livadaras, I., Pickett, J.A., Van Leeuwen, T., Nauen, R., Vontas, J., 2016. Resistance mutation conserved between insects and mites unravels the benzoylurea insecticide mode of action on chitin biosynthesis. Proc. Natl. Acad. Sci. 113, 14692–14697. https://doi.org/10.1073/pnas.1618258113

Dresner, L.S., Andersen, D.K., Kahng, K.U., Munshi, I.A., Wait, R.B., 1989. Effects of cyclosporine on glucose metabolism. Surgery 106, 163–9; discussion 170.

Duarte, M., Pópulo, H., Videira, A., Friedrich, T., Schulte, U., 2002. Disruption of iron-sulphur cluster N2 from NADH: ubiquinone oxidoreductase by site-directed mutagenesis. Biochem. J. 364, 833–839. https://doi.org/10.1042/BJ20011750

Dussourd, D.E., 2016. Behavioral sabotage of plant defenses by insect folivores. Annu. Rev. Entomol. 62, 15–34. https://doi.org/10.1146/annurev-ento-031616-035030

Ebert, B., Kisiela, M., Maser, E., 2016. Transcriptional regulation of human and murine short-chain dehydrogenase/reductases (SDRs) – an in silico approach. Drug Metab. Rev. https://doi.org/10.3109/03602532.2016.1167902

Ehrenreich, I.M., Torabi, N., Jia, Y., Kent, J., Martis, S., Shapiro, J.A., Gresham, D., Caudy, A.A., Kruglyak, L., 2010. Dissection of genetically complex traits with extremely large pools of yeast segregants. Nature 464, 1039. https://doi.org/10.1038/nature08923

Ellinger-Ziegelbauer, H., Stuart, B., Wahle, B., Bomann, W., Ahr, H.J., 2005. Comparison of the expression profiles induced by genotoxic and nongenotoxic carcinogens in rat liver. Mutat. Res. Mol. Mech. Mutagen.

575, 61–84. https://doi.org/10.1016/j.mrfmmm.2005.02.004

Elliott, M., Farnham, A.W., Janes, N.F., Needham, P.H., Pulman, D.A., Stevenson, J.H., 1973. A photostable pyrethroid. Nature 246, 169–170. https://doi.org/10.1038/246169a0

Erb, A., Weiss, H., Härle, J., Bechthold, A., 2009. A bacterial glycosyltransferase gene toolbox: generation and applications. Phytochemistry 70, 1812–21. https://doi.org/10.1016/j.phytochem.2009.05.019

Erb, M., Robert, C.A.M., 2016. Sequestration of plant secondary metabolites by insect herbivores: molecular mechanisms and ecological consequences. Curr. Opin. Insect Sci. 14, 8–11. https://doi.org/10.1016/j.cois.2015.11.005

Espinosa, P.J., Contreras, J., Quinto, V., Grávalos, C., Fernández, E., Bielza, P., 2005. Metabolic mechanisms of insecticide resistance in the western flower thrips, *Frankliniella occidentalis* (Pergande). Pest Manag. Sci. 61, 1009–1015. https://doi.org/10.1002/ps.1069

Evans, G.O., 1992. Principles of acarology. CAB International, Oxon, UK.

Fahrbach, S.E., Smagghe, G., Velarde, R.A., 2012. Insect nuclear receptors. Annu. Rev. Entomol. 57, 83–106. https://doi.org/10.1146/annurev-ento-120710-100607

Falcone Ferreyra, M.L., Rius, S.P., Casati, P., Ferreyra, M.L.F., Rius, S.P., Casati, P., 2012. Flavonoids: biosynthesis, biological functions, and biotechnological applications. Front. Plant Sci. 3, 1–15. https://doi.org/10.3389/fpls.2012.00222

Faucon, F., Dusfour, I., Gaude, T., Navratil, V., Boyer, F., Chandre, F., Sirisopa, P., Thanispong, K., Juntarajumnong, W., Poupardin, R., Chareonviriyaphap, T., Girod, R., Corbel, V., Reynaud, S., David, J.P., 2015. Identifying genomic changes associated with insecticide resistance in the dengue mosquito *Aedes aegypti* by deep targeted sequencing. Genome Res. 25, 1347–1359. https://doi.org/10.1101/gr.189225.115

Felton, G.W., Chung, S.H., Hernandez, M.G.E., Louis, J., Peiffer, M., Tian, D., 2014. Herbivore oral secretions are the first line of protection against plant-induced defences, in: Annual Plant Reviews. John Wiley & Sons, Ltd, Chichester, UK, pp. 37–76. https://doi.org/10.1002/9781118829783.ch2

Fendel, U., Tocilescu, M.A., Kerscher, S., Brandt, U., 2008. Exploring the inhibitor binding pocket of respiratory complex I. Biochim. Biophys. Acta - Bioenerg. 1777, 660–665. https://doi.org/10.1016/j.bbabio.2008.04.033

Feng, K., Yang, Y., Wen, X., Ou, S., Zhang, P., Yu, Q., Zhang, Y., Shen, G., Xu, Z., Li, J., He, L., 2019. Stability of cyflumetofen resistance in *Tetranychus cinnabarinus* and its correlation with glutathione-S-transferase gene expression. Pest Manag. Sci. ps.5392. https://doi.org/10.1002/ps.5392

Feng, Y. ning, Yan, J., Sun, W., Zhao, S., Lu, W.C., Li, M., He, L., 2011. Transcription and induction profiles of two esterase genes in susceptible and acaricide-resistant *Tetranychus cinnabarinus*. Pestic. Biochem. Physiol. 100, 70–73. https://doi.org/10.1016/j.pestbp.2011.02.007

Ferreira, C.B.S., Andrade, F.H.N., Rodrigues, A.R.S., Siqueira, H.A.A., Gondim Jr., M.G.C., 2015. Resistance in field populations of *Tetranychus urticae* to acaricides and characterization of the inheritance of abamectin resistance. Crop Prot. 67, 77–83. https://doi.org/10.1016/J.CROPRO.2014.09.022

Feuer, H., Lawrence, J.P., 1969. Alkyl nitrate nitration of active methylene compounds. VI. Synthesis of .alpha.-nitroalkyl heterocyclics. J. Am. Chem. Soc. 91, 1856–1857. https://doi.org/10.1021/ja01035a049

Feyereisen, R., 2015. Insect P450 inhibitors and insecticides: challenges and opportunities. Pest Manag. Sci. 71, 793–800. https://doi.org/10.1002/ps.3895

Feyereisen, R., 2012. Insect CYP Genes and P450 Enzymes, in: Insect Molecular Biology and Biochemistry. pp. 236–316. https://doi.org/10.1016/B978-0-12-384747-8.10008-X

Feyereisen, R., 1999. Insect P450 enzymes. Annu. Rev. Entomol. 44, 507–33. https://doi.org/10.1146/annurev.ento.44.1.507

Feyereisen, R., Dermauw, W., Van Leeuwen, T., 2015. Genotype to phenotype, the molecular and physiological dimensions of resistance in arthropods. Pestic. Biochem. Physiol. 121, 61–77.

https://doi.org/10.1016/j.pestbp.2015.01.004

Feyereisen, R., Langry, K.C., Ortiz de Montellano, P.R., 1984. Self-catalyzed destruction of insect cytochrome P-450. Insect Biochem. 14, 19–26. https://doi.org/10.1016/0020-1790(84)90079-9

ffrench-Constant, R.H., Bass, C., 2017. Does resistance really carry a fitness cost? Curr. Opin. Insect Sci. 21, 39–46. https://doi.org/10.1016/j.cois.2017.04.011

Fiedorczuk, K., Letts, J.A., Degliesposti, G., Kaszuba, K., Skehel, M., Sazanov, L.A., 2016. Atomic structure of the entire mammalian mitochondrial complex I. Nature 538, 406–410. https://doi.org/10.1038/nature19794

Figueroa-Teran, R., Pak, H., Blomquist, G.J., Tittiger, C., 2016. High substrate specificity of ipsdienol dehydrogenase (IDOLDH), a short-chain dehydrogenase from *Ips pini* bark beetles. J. Biochem. 160, 141–151. https://doi.org/10.1093/jb/mvw019

Figueroa-Teran, R., Welch, W.H., Blomquist, G.J., Tittiger, C., 2012. Ipsdienol dehydrogenase (IDOLDH): a novel oxidoreductase important for *Ips pini* pheromone production. Insect Biochem. Mol. Biol. 42, 81–90. https://doi.org/10.1016/J.IBMB.2011.10.009

Finn, R.D., Coggill, P., Eberhardt, R.Y., Eddy, S.R., Mistry, J., Mitchell, A.L., Potter, S.C., Punta, M., Qureshi, M., Sangrador-Vegas, A., Salazar, G.A., Tate, J., Bateman, A., 2016. The Pfam protein families database: towards a more sustainable future. Nucleic Acids Res. 44, D279–D285. https://doi.org/10.1093/nar/gkv1344

Fire, A., Xu, S., Montgomery, M.K., Kostas, S.A., Driver, S.E., Mello, C.C., 1998. Potent and specific genetic interference by double-stranded RNA in *Caenorhabditis elegans*. Nature 391, 806–811. https://doi.org/10.1038/35888

Foxwell, B.M., Mackie, A., Ling, V., Ryffel, B., 1989. Identification of the multidrug resistance-related P-glycoprotein as a cyclosporine binding protein. Mol. Pharmacol. 36, 543–6.

Freeman, M.L., Huntley, S.A., Meredith, M.J., Senisterra, G.A., Lepock, J., 1997. Destabilization and denaturation of cellular protein by glutathione depletion. Cell Stress Chaperones 2, 191–8.

Friedman, M., 2002. Tomato glycoalkaloids: role in the plant and in the diet. J. Agric. Food Chem. https://doi.org/10.1021/jf020560c

Friedrich, T., 1998. The NADH:ubiquinone oxidoreductase (complex I) from *Escherichia coli*. Biochim. Biophys. Acta - Bioenerg. 1364, 134–146. https://doi.org/10.1016/S0005-2728(98)00024-3

Fry, J.D., 1989. Evolutionary adaptation to host plants in a laboratory population of the phytophagous mite *Tetranychus urticae* Koch. Oecologia 81, 559–565. https://doi.org/10.1007/BF00378969

Fu, A., Tang, R., Hardie, J., Farkas, M.E., Rotello, V.M., 2014. Promises and pitfalls of intracellular delivery of proteins. Bioconjug. Chem. 25, 1602–1608. https://doi.org/10.1021/bc500320j

Fu, L., Niu, B., Zhu, Z., Wu, S., Li, W., 2012. CD-HIT: Accelerated for clustering the next-generation sequencing data. Bioinformatics 28, 3150–3152. https://doi.org/10.1093/bioinformatics/bts565

Fujioka, K., Casida, J.E., 2007. Glutathione S -transferase conjugation of organophosphorus pesticides yields S -phospho-, S -aryl-, and S -alkylglutathione derivatives. Chem. Res. Toxicol. 20, 1211–1217. https://doi.org/10.1021/tx700133c

Gadau, J., Gerloff, C.U., Krüger, N., Chan, H., Schmid-Hempel, P., Wille, A., Page, R.E., 2001. A linkage analysis of sex determination in *Bombus terrestris* (L.) (Hymenoptera: Apidae). Heredity (Edinb). 87, 234–242. https://doi.org/10.1046/j.1365-2540.2001.00919.x

Gasteiger, E., Gattiker, A., Hoogland, C., Ivanyi, I., Appel, R.D., Bairoch, A., 2003. ExPASy: the proteomics server for in-depth protein knowledge and analysis. Nucleic Acids Res. 31, 3784–3788. https://doi.org/10.1093/nar/gkg563

Georghiou, G.P., 1969. Genetics of resistance to insecticides in houseflies and mosquitoes. Exp. Parasitol. 26, 224–255. https://doi.org/10.1016/0014-4894(69)90116-7

Ghadamyari, M., Sendi, J.J., 2008. Resistance mechanisms to oxydemeton-methyl in *Tetranychus urticae* Koch

(Acari: Tetranychidae). Invertabrate Surviv. J. 5, 97.

Giovannoni, J.J., Wing, R.A., Ganal, M.W., Tanksley, S.D., 1991. Isolation of molecular markers from specific chromosomal intervals using DNA pools from existing mapping populations. Nucleic Acids Res. 19, 6553. https://doi.org/10.1093/NAR/19.23.6553

Giraudo, M., Unnithan, G.C., Le Goff, G., Feyereisen, R., 2010. Regulation of cytochrome P450 expression in *Drosophila*: Genomic insights. Pestic. Biochem. Physiol. 97, 115–122. https://doi.org/10.1016/j.pestbp.2009.06.009

Giraudoux, P., Antonietti, J.-P., Beale, C., Pleydell, D., Treglia, M., 2018. Package pgirmess; spatial analysis and data mining for field ecologists [WWW Document]. URL http://giraudoux.pagesperso-orange.fr/

Glauser, G., Marti, G., Villard, N., Doyen, G. a., Wolfender, J.L., Turlings, T.C.J., Erb, M., 2011. Induction and detoxification of maize 1,4-benzoxazin-3-ones by insect herbivores. Plant J. 68, 901–911. https://doi.org/10.1111/j.1365-313X.2011.04740.x

Gotoh, T., Bruin, J., Sabelis, M.W., Menken, S.B.J., 1993. Host race formation in *Tetranychus urticae*: genetic differentiation, host plant preference, and mate choice in a tomato and a cucumber strain. Entomol. Exp. Appl. 68, 171–178. https://doi.org/10.1111/j.1570-7458.1993.tb01700.x

Gould, F., 1979. Rapid host range evolution in a population of the phytophagous mite *Tetranychus urticae* Koch. Evolution (N. Y). 33, 791–802. https://doi.org/10.2307/2407646

Govind, G., Mittapalli, O., Griebel, T., Allmann, S., Böcker, S., Baldwin, I.T., 2010. Unbiased transcriptional comparisons of generalist and specialist herbivores feeding on progressively defenseless *Nicotiana attenuata* plants. PLoS One 5, e8735. https://doi.org/10.1371/journal.pone.0008735

Gramates, L.S., Marygold, S.J., Dos Santos, G., Urbano, J.M., Antonazzo, G., Matthews, B.B., Rey, A.J., Tabone, C.J., Crosby, M.A., Emmert, D.B., Falls, K., Goodman, J.L., Hu, Y., Ponting, L., Schroeder, A.J., Strelets, V.B., Thurmond, J., Zhou, P., Perrimon, N., Gelbart, S.R., Extavour, C., Broll, K., Zytkovicz, M., Brown, N.H., Attrill, H., Costa, M., Fexova, S., Jones, T., Larkin, A., Millburn, G.H., Staudt, N., Kaufman, T., Grumbling, G.B., Cripps, R., Werner-Washburne, M., Baker, P., 2017. FlyBase at 25: looking to the future. Nucleic Acids Res. 45, D663–D671. https://doi.org/10.1093/nar/gkw1016

Grambow, H.J., Lückge, J., Klausener, A., Müller, E., 1986. Occurrence of 2-(2-hydroxy-4,7-dimethoxy-2H-1,4-benzoxazin-3-one)-β-D-glucopyranoside in *Triticum aestivum* leaves and its conversion into 6-methoxy-benzoxazolinone. Zeitschrift für Naturforsch. C 41, 684–690. https://doi.org/10.1515/znc-1986-7-804

Grbic, M., Khila, A., Lee, K.Z., Bjelica, A., Grbic, V., Whistlecraft, J., Verdon, L., Navajas, M., Nagy, L., 2007. Mity model: *Tetranychus urticae*, a candidate for chelicerate model organism. BioEssays 29, 489–496. https://doi.org/10.1002/bies.20564

Grbić, M., Van Leeuwen, T., Clark, R.M., Rombauts, S., Rouzé, P., Grbić, V., Osborne, E.J., Dermauw, W., Ngoc, T., Cao, P., Ortego, F., Hernández-Crespo, P., Diaz, I., Martinez, M., Navajas, M., Sucena, É., Magalhães, S., Nagy, L., Pace, R.M., Djuranović, S., Smagghe, G., Iga, M., Christiaens, O., Veenstra, J. a., Ewer, J., Villalobos, R.M., Hutter, J.L., Hudson, S.D., Velez, M., Yi, S. V., Zeng, J., Pires-daSilva, A., Roch, F., Cazaux, M., Navarro, M., Zhurov, V., Acevedo, G., Bjelica, A., Fawcett, J. a., Bonnet, E., Martens, C., Baele, G., Wissler, L., Sanchez-Rodriguez, A., Tirry, L., Blais, C., Demeestere, K., Henz, S.R., Gregory, T.R., Mathieu, J., Verdon, L., Farinelli, L., Schmutz, J., Lindquist, E., Feyereisen, R., Van de Peer, Y., Ngoc, P.C.T., Ortego, F., Hernández-Crespo, P., Diaz, I., Martinez, M., Navajas, M., Sucena, É., Magalhães, S., Nagy, L., Pace, R.M., Djuranović, S., Smagghe, G., Iga, M., Christiaens, O., Veenstra, J. a., Ewer, J., Villalobos, R.M., Hutter, J.L., Hudson, S.D., Velez, M., Yi, S. V., Zeng, J., Pires-daSilva, A., Roch, F., Cazaux, M., Navarro, M., Zhurov, V., Acevedo, G., Bjelica, A., Fawcett, J. a., Bonnet, E., Martens, C., Baele, G., Wissler, L., Sanchez-Rodriguez, A., Tirry, L., Blais, C., Demeestere, K., Henz, S.R., Gregory, T.R., Mathieu, J., Verdon, L., Farinelli, L., Schmutz, J., Lindquist, E., Feyereisen, R., Van de Peer, Y., 2011. The genome of *Tetranychus urticae* reveals herbivorous pest adaptations. Nature 479, 487–92. https://doi.org/10.1038/nature10640

Green, T.R., Ryan, C.A., 1972. Wound-induced proteinase inhibitor in plant leaves: a possible defense

mechanism against insects. Science (80-.). 175, 776–777. https://doi.org/10.1126/science.175.4023.776

Groen, S.C., Whiteman, N.K., 2016. Using Drosophila to study the evolution of herbivory and diet specialization. Curr. Opin. Insect Sci. 14, 66–72. https://doi.org/10.1016/j.cois.2016.01.004

Gunning, R.V., Devonshire, A.L., Moores, G.D., 1995. Metabolism of Esfenvalerate by Pyrethroid-Susceptible and -Resistant Australian *Helicoverpa armigera* (Lepidoptera: Noctuidae). Pestic. Biochem. Physiol. 51, 205–213. https://doi.org/10.1006/pest.1995.1020

Gunning, R. V., Moores, G.D., Devonshire, A.L., 1998. Inhibition of Resistance-related Esterases by Piperonyl Butoxide in Helicoverpa armigera (Lepidoptera: Noctuidae) and Aphis gossypii (Hemiptera: Aphididae), in: Piperonyl Butoxide. Academic Press, London.

Habig, W.H., Pabst, M.J., Jakoby, W.B., 1974. Glutathione S-transferases. The first enzymatic step in mercapturic acid formation. J. Biol. Chem. 249, 7130–9.

Hales, K.G., Korey, C.A., Larracuente, A.M., Roberts, D.M., 2015. Genetics on the fly: a primer on the drosophila model system. Genetics 201, 815–842. https://doi.org/10.1534/genetics.115.183392

Hall, T., 2013. BioEdit version 7.2.5. Ibis Biosci. Carlsbad, CA, USA. https://doi.org/10.1016/j.ifset.2004.06.001

Hamdane, D., Xia, C., Im, S.C., Zhang, H., Kim, J.J.P., Waskell, L., 2009. Structure and function of an NADPH-cytochrome P450 oxidoreductase in an open conformation capable of reducing cytochrome P450. J. Biol. Chem. 284, 11374–11384. https://doi.org/10.1074/jbc.M807868200

Hansen, E.H., Møller, B.L., Kock, G.R., Bünner, C.M., Kristensen, C., Jensen, O.R., Okkels, F.T., Olsen, C.E., Motawia, M.S., Hansen, J., 2009. De novo biosynthesis of vanillin in fission yeast (*Schizosaccharomyces pombe*) and baker's yeast (*Saccharomyces cerevisiae*). Appl. Environ. Microbiol. 75, 2765–2774. https://doi.org/10.1128/AEM.02681-08

Hardy, N.B., Peterson, D.A., Ross, L., Rosenheim, J.A., 2018. Does a plant-eating insect's diet govern the evolution of insecticide resistance? Comparative tests of the pre-adaptation hypothesis. Evol. Appl. 11, 739–747. https://doi.org/10.1111/eva.12579

Hartl, D.L., 1972. A fundamental theorem of natural selection for sex linkage or arrhenotoky on JSTOR. Am. Nat. 106, 516–524.

Hartl, M., Giri, A.P., Kaur, H., Baldwin, I.T., 2010. Serine protease inhibitors specifically defend *Solanum nigrum* against generalist herbivores but do not influence plant growth and development. Plant Cell 22, 4158–4175. https://doi.org/10.1105/tpc.109.073395

Hashimshony, T., Wagner, F., Sher, N., Yanai, I., 2012. CEL-seq: single-cell RNA-seq by multiplexed linear amplification. Cell Rep. 2, 666–673. https://doi.org/10.1016/J.CELREP.2012.08.003

Hawkins, N.J., Bass, C., Dixon, A., Neve, P., 2019. The evolutionary origins of pesticide resistance. Biol. Rev. 94, 135–155. https://doi.org/10.1111/brv.12440

Heckel, D.G., 2014. Insect detoxification and sequestration strategies, in: Annual Plant Reviews: Insect-Plant Interactions. Wiley-Blackwell, Chichester, UK, pp. 77–114. https://doi.org/10.1002/9781118829783.ch3

Heckel, D.G., Gahan, L.J., Liu, Y.B., Tabashnik, B.E., 1999. Genetic mapping of resistance to *Bacillus thuringiensis* toxins in diamondback moth using biphasic linkage analysis. Proc. Natl. Acad. Sci. U. S. A. 96, 8373–7377. https://doi.org/10.1073/pnas.96.15.8373

Heidel-Fischer, H.M., Vogel, H., 2015. Molecular mechanisms of insect adaptation to plant secondary compounds. Curr. Opin. Insect Sci. 8, 8–14. https://doi.org/10.1016/j.cois.2015.02.004

Helle, W., Sabelis, M.W., 1985. Spider mites their biology, natural enemies and control. Elsevier Amsterdam. https://doi.org/10.1111/j.1570-7458.1987.tb03606.x

Hellemans, J., Mortier, G., De, P.A., Speleman, F., Vandesompele, J., 2007. qBase relative quantification framework and software for management and automated analysis of real-time quantitative PCR data. Genome Biol. 8, R19.

Henniges-Janssen, K., Reineke, A., Heckel, D.G., Groot, A.T., 2011. Complex inheritance of larval adaptation in *Plutella xylostella* to a novel host plant. Heredity (Edinb). 107, 421–432.

https://doi.org/10.1038/hdy.2011.27

Herron, G.A., Rophail, J., 1998. Tebufenpyrad (Pyranica®) resistance detected in two-spotted spider mite *Tetranychus urticae* Koch (Acari: Tetranychidae) from apples in Western Australia. Exp. Appl. Acarol. 22, 633–641. https://doi.org/10.1023/A:1006058705429

Highfill, C.A., Tran, J.H., Nguyen, S.K.T., Moldenhauer, T.R., Wang, X., Macdonald, S.J., 2017. Naturally segregating variation at ugt86dd contributes to nicotine resistance in *Drosophila melanogaster*. Genetics 207, 311–325. https://doi.org/10.1534/genetics.117.300058

Hill, N., 2008. A novel plant-based synergist for pyrethrum and pyrethroids against urban public health pests, in: Sixth International Conference on Urban Pests.

Hill, R.L., O'Donnell, D.J., 1991. The host range of *Tetranychus lintearius* (Acarina: Tetranychidae). Exp. Appl. Acarol. 11, 253–269. https://doi.org/10.1007/BF01202874

Hoffmann, F., Maser, E., 2007. Carbonyl reductases and pluripotent hydroxysteroid dehydrogenases of the short-chain dehydrogenase/reductase superfamily. Drug Metab. Rev. https://doi.org/10.1080/03602530600969440

Hollingworth, R.M., Ahammadsahib, K.I., 1995. Inhibitors of respiratory complex I. Mechanisms, pesticidal actions and toxicology. Rev. Pestic. Toxicol. 3, 277–302.

Hollingworth, R.M., Ahammadsahib, K.I., Gadelhak, G., McLaughlin, J.L., 1994. New inhibitors of complex I of the mitochondrial electron transport chain with activity as pesticides. Biochem. Soc. Trans. 22, 230–233. https://doi.org/10.1042/BST0220230

Hori, M., Nakamura, H., Fujii, Y., Suzuki, Y., Matsuda, K., 2011. Chemicals affecting the feeding preference of the Solanaceae-feeding lady beetle *Henosepilachna vigintioctomaculata* (Coleoptera: Coccinellidae). J. Appl. Entomol. 135, 121–131. https://doi.org/10.1111/j.1439-0418.2010.01519.x

Hospital, F., 2001. Size of donor chromosome segments around introgressed loci and reduction of linkage drag in marker-assisted backcross programs. Genetics 158, 1363–79.

Howe, G., Jander, G., 2008. Plant immunity to insect herbivores. Annu. Rev. Plant Biol. 59, 41–66. https://doi.org/10.1146/annurev.arplant.59.032607.092825

Hoy, M.A., Waterhouse, R.M., Wu, K., Estep, A.S., Ioannidis, P., Palmer, W.J., Pomerantz, A.F., Simão, F.A., Thomas, J., Jiggins, F.M., Murphy, T.D., Pritham, E.J., Robertson, H.M., Zdobnov, E.M., Gibbs, R.A., Richards, S., 2016. Genome sequencing of the phytoseiid predatory mite *Metaseiulus occidentalis* reveals completely atomized Hox genes and superdynamic intron evolution. Genome Biol. Evol. 8, 1762–1775. https://doi.org/10.1093/gbe/evw048

Huang, W.C., Ellis, J., Moody, P.C.E., Raven, E.L., Roberts, G.C.K., 2013. Redox-linked domain movements in the catalytic cycle of cytochrome P450 reductase. Structure 21, 1581–1589. https://doi.org/10.1016/j.str.2013.06.022

Huchelmann, A., Boutry, M., Hachez, C., 2017. Plant glandular trichomes: natural cell factories of high biotechnological interest. Plant Physiol. 175, 6–22. https://doi.org/10.1104/pp.17.00727

Huerta-Cepas, J., Serra, F., Bork, P., 2016. ETE 3: reconstruction, analysis, and visualization of phylogenomic data. Mol. Biol. Evol. 33, 1635–1638. https://doi.org/10.1093/molbev/msw046

Hunter, W.B., Gonzalez, M.T., Tomich, J., 2018. BAPC-assisted CRISPR/Cas9 system: targeted delivery into adult ovaries for heritable germline gene editing (Arthropoda: Hemiptera). bioRxiv. https://doi.org/10.1101/478743

Hyun, T.K., Albacete, A., van der Graaff, E., Eom, S.H., Großkinsky, D.K., Böhm, H., Janschek, U., Rim, Y., Ali, W.W., Kim, S.Y., Roitsch, T., 2015. The Arabidopsis PLAT domain protein1 promotes abiotic stress tolerance and growth in tobacco. Transgenic Res. 24, 651–653. https://doi.org/10.1007/s11248-015-9868-6

Hyun, T.K., Van Der Graaff, E., Albacete, A., Eom, S.H., Großkinsky, D.K., Böhm, H., Janschek, U., Rim, Y., Ali, W.W., Kim, S.Y., Roitsch, T., 2014. The Arabidopsis PLAT domain protein1 is critically involved in abiotic

stress tolerance. PLoS One 9, e112946. https://doi.org/10.1371/journal.pone.0112946

Hyung Ko, J., Gyu Kim, B., Joong-Hoon, A., 2006. Glycosylation of flavonoids with a glycosyltransferase from *Bacillus cereus*. FEMS Microbiol. Lett. 258, 263–268. https://doi.org/10.1111/j.1574-6968.2006.00226.x

Ilias, A., Vassiliou, V.A., Vontas, J., Tsagkarakou, A., 2017. Molecular diagnostics for detecting pyrethroid and abamectin resistance mutations in *Tetranychus urticae*. Pestic. Biochem. Physiol. 135, 9–14. https://doi.org/10.1016/j.pestbp.2016.07.004

Ioannidis, P., Simao, F.A., Waterhouse, R.M., Manni, M., Seppey, M., Robertson, H.M., Misof, B., Niehuis, O., Zdobnov, E.M., 2017. Genomic features of the damselfly *Calopteryx splendens* representing a sister clade to most insect orders. Genome Biol. Evol. 9, evx006. https://doi.org/10.1093/gbe/evx006

IRAC, 2017. IRAC Mode of Action Classification Scheme.

Jagadeesan, R., Fotheringham, A., Ebert, P.R., Schlipalius, D.I., 2013. Rapid genome wide mapping of phosphine resistance loci by a simple regional averaging analysis in the red flour beetle, *Tribolium castaneum*. BMC Genomics 14, 650. https://doi.org/10.1186/1471-2164-14-650

Jain, M., Olsen, H.E., Paten, B., Akeson, M., 2016. The Oxford Nanopore MinION: delivery of nanopore sequencing to the genomics community. Genome Biol. 17, 239. https://doi.org/10.1186/s13059-016-1103-0

Jairin, J., Leelagud, P., Pongmee, A., Srivilai, K., Jairin, J., Leelagud, P., Pongmee, A., Srivilai, K., 2017. Chromosomal location of a recessive red-eye mutant gene in the brown planthopper *Nilaparvata lugens* (Stål) (Insecta: Hemiptera). Adv. Entomol. 05, 33–39. https://doi.org/10.4236/ae.2017.51003

Jancova, P., Anzenbacher, P., Anzenbacherova, E., 2010. Phase II drug metabolizing enzymes. Biomed. Pap. 154, 103–116. https://doi.org/10.5507/bp.2010.017

Jeppson, L.R., Keifer, H.H., Baker, E.W., 1975. Mites injurious to economic plants, Florida Entomologist.

Jeschke, P., Nauen, R., 2008. Neonicotinoids-from zero to hero in insecticide chemistry. Pest Manag. Sci. 64, 1084–1098. https://doi.org/10.1002/ps.1631

Joffe, T., Gunning, R. V, Allen, G.R., Kristensen, M., Alptekin, S., Field, L.M., Moores, G.D., 2012. Investigating the potential of selected natural compounds to increase the potency of pyrethrum against houseflies *Musca domestica* (Diptera: Muscidae). Pest Manag. Sci. 68, 178–184. https://doi.org/10.1002/ps.2241

Joga, M.R., Zotti, M.J., Smagghe, G., Christiaens, O., 2016. RNAi efficiency, systemic properties, and novel delivery methods for pest insect control: what we know so far. Front. Physiol. 7, 553. https://doi.org/10.3389/fphys.2016.00553

Jonckheere, W., 2018. The salivary proteome of *Tetranychus urticae*: key to its polyphagous nature? University of Amsterdam, Amsterdam, The Netherlands.

Jonckheere, W., Dermauw, W., Khalighi, M., Pavlidi, N., Reubens, W., Baggerman, G., Tirry, L., Menschaert, G., Kant, M.R., Vanholme, B., Van Leeuwen, T., 2018. A gene family coding for salivary proteins (SHOT) of the polyphagous spider mite *Tetranychus urticae* exhibits fast host-dependent transcriptional plasticity. Mol. Plant-Microbe Interact. 31, 112–124. https://doi.org/10.1094/MPMI-06-17-0139-R

Jonckheere, W., Dermauw, W., Zhurov, V., Wybouw, N., Van den Bulcke, J., Villarroel, C.A., Greenhalgh, R., Grbić, M., Schuurink, R.C., Tirry, L., Baggerman, G., Clark, R.M., Kant, M.R., Vanholme, B., Menschaert, G., Van Leeuwen, T., 2016. The salivary protein repertoire of the polyphagous spider mite *Tetranychus urticae*: a quest for effectors. Mol. Cell. Proteomics 15, 3594–3613. https://doi.org/10.1074/mcp.M116.058081

Jones, D.A., 1998. Why are so many food plants cyanogenic? Phytochemistry 47, 155–162. https://doi.org/10.1016/S0031-9422(97)00425-1

Jones, P., Messner, B., Nakajima, J.I., Schäffner, A.R., Saito, K., 2003. UGT73C6 and UGT78D1, glycosyltransferases involved in flavonol glycoside biosynthesis in *Arabidopsis thaliana*. J. Biol. Chem. 278, 43910–43918. https://doi.org/10.1074/jbc.M303523200

Jones, P.R., Møller, B.L., Høj, P.B., 1999. The UDP-glucose:p-hydroxymandelonitrile-O-glucosyltransferase that

catalyzes the last step in synthesis of the cyanogenic glucoside dhurrin in *Sorghum bicolor*. Isolation, cloning, heterologous expression, and substrate specificity. J. Biol. Chem. 274, 35483–35491. https://doi.org/10.1074/jbc.274.50.35483

Kallberg, Y., Oppermann, U., Persson, B., 2010. Classification of the short-chain dehydrogenase/reductase superfamily using hidden Markov models. FEBS J. 277, 2375–2386. https://doi.org/10.1111/j.1742-4658.2010.07656.x

Kang, L., Aggarwal, D.D., Rashkovetsky, E., Korol, A.B., Michalak, P., 2016. Rapid genomic changes in *Drosophila melanogaster* adapting to desiccation stress in an experimental evolution system. BMC Genomics 17, 233. https://doi.org/10.1186/s12864-016-2556-y

Kant, M.R., Ament, K., Sabelis, M.W., Haring, M.A., Schuurink, R.C., 2004. Differential timing of spider mite-induced direct and indirect defenses in tomato plants. Plant Physiol. 135, 483–495. https://doi.org/10.1104/pp.103.038315

Kant, M.R., Jonckheere, W., Knegt, B., Lemos, F., Liu, J., Schimmel, B.C.J., Villarroel, C.A., Ataide, L.M.S., Dermauw, W., Glas, J.J., Egas, M., Janssen, A., Van Leeuwen, T., Schuurink, R.C., Sabelis, M.W., Alba, J.M., 2015. Mechanisms and ecological consequences of plant defence induction and suppression in herbivore communities. Ann. Bot. 115, 1015–1051. https://doi.org/10.1093/aob/mcv054

Kant, M.R., Sabelis, M.W., Haring, M.A., Schuurink, R.C., 2008. Intraspecific variation in a generalist herbivore accounts for differential induction and impact of host plant defences. Proc. R. Soc. B Biol. Sci. 275, 443–452. https://doi.org/10.1098/rspb.2007.1277

Kaplanoglu, E., Chapman, P., Scott, I.M., Donly, C., 2017. Overexpression of a cytochrome P450 and a UDP-glycosyltransferase is associated with imidacloprid resistance in the Colorado potato beetle, *Leptinotarsa decemlineata*. Sci. Rep. 7, 1762. https://doi.org/10.1038/s41598-017-01961-4

Karp, G., 2008. Cell and molecular Biology, fifth ed. ed. Wiley.

Katoh, K., Misawa, K., Kuma, K., Miyata, T., 2002. MAFFT: a novel method for rapid multiple sequence alignment based on fast Fourier transform. Nucleic Acids Res. 30, 3059–3066. https://doi.org/10.1093/nar/gkf436

Kauffmann, A., Gentleman, R., Huber, W., 2009. arrayQualityMetrics - a bioconductor package for quality assessment of microarray data. Bioinformatics 25, 415–416. https://doi.org/10.1093/bioinformatics/btn647

Kelley, L.A., Mezulis, S., Yates, C.M., Wass, M.N., Sternberg, M.J.E., 2015. The Phyre2 web portal for protein modeling, prediction and analysis. Nat. Protoc. 10, 845–858. https://doi.org/10.1038/nprot.2015.053

Kennaugh, L., Pearce, D., Daly, J.C., Hobbs, A.A., 1993. A piperonyl butoxide synergizable resistance to permethrin in *Helicoverpa armigera* which is not due to increased detoxification by cytochrome P450. Pestic. Biochem. Physiol. https://doi.org/10.1006/pest.1993.1026

Kessler, A., Baldwin, I.T., 2002. Plant responses to insect herbivory: the emerging molecular analysis. Annu Rev Plant Biol 53, 299–328. https://doi.org/10.1146/annurev.arplant.53.100301.135207

Khajehali, J., van Leeuwen, T., Grispou, M., Morou, E., Alout, H., Weill, M., Tirry, L., Vontas, J., Tsagkarakou, A., 2010. Acetylcholinesterase point mutations in European strains of *Tetranychus urticae* (Acari: Tetranychidae) resistant to organophosphates. Pest Manag. Sci. 66, 220–228. https://doi.org/10.1002/ps.1884

Khalighi, M., Dermauw, W., Wybouw, N., Bajda, S., Osakabe, M., Tirry, L., Van Leeuwen, T., 2015. Molecular analysis of cyenopyrafen resistance in the two-spotted spider mite *Tetranychus urticae*. Pest Manag. Sci. 72, 103–112. https://doi.org/10.1002/ps.4071

Khalighi, M., Tirry, L., Van Leeuwen, T., 2014. Cross-resistance risk of the novel complex II inhibitors cyenopyrafen and cyflumetofen in resistant strains of the two-spotted spider mite *Tetranychus urticae*. Pest Manag. Sci. 70, 365–368. https://doi.org/10.1002/ps.3641

Khila, A., Grbić, M., 2007. Gene silencing in the spider mite Tetranychus urticae: dsRNA and siRNA parental silencing of the Distal-less gene. Dev. Genes Evol. 217, 241–51. https://doi.org/10.1007/s00427-007-

0132-9

Kim, H.S., Kim, B.G., Sung, S., Kim, M., Mok, H., Chong, Y., Ahn, J.H., 2013. Engineering flavonoid glycosyltransferases for enhanced catalytic efficiency and extended sugar-donor selectivity. Planta 238, 683–693. https://doi.org/10.1007/s00425-013-1922-0

Kim, J.H., Kim, B.G., Kim, J.A., Park, Y., Lee, Y.J., Lim, Y., Ahn, J.H., 2007. Glycosylation of flavonoids with *E. coli* expressing glycosyltransferase from *Xanthomonas campestris*. J. Microbiol. Biotechnol. 17, 539–542.

Kim, Y.-J., Lee, S.-H., Lee, S.-W., Ahn, Y.-J., 2004. Fenpyroximate resistance in *Tetranychus urticae* (Acari: Tetranychidae): cross-resistance and biochemical resistance mechanisms. Pest Manag. Sci. 60, 1001–1006. https://doi.org/10.1002/ps.909

Kim, Y.-J., Park, H.-M., Cho, J.-R., Ahn, Y.-J., 2006. Multiple resistance and biochemical mechanisms of pyridaben resistance in *Tetranychus urticae* (Acari: Tetranychidae). J. Econ. Entomol. 99, 954–8. https://doi.org/10.1603/0022-0493-99.3.954

King-Jones, K., Horner, M.A., Lam, G., Thummel, C.S., 2006. The DHR96 nuclear receptor regulates xenobiotic responses in *Drosophila*. Cell Metab. 4, 37–48. https://doi.org/10.1016/j.cmet.2006.06.006

King-Jones, K., Thummel, C.S., 2005. Nuclear receptors - a perspective from *Drosophila*. Nat. Rev. Genet. 6, 311–323. https://doi.org/10.1038/nrg1581

Kingan, S., Heaton, H., Cudini, J., Lambert, C., Baybayan, P., Galvin, B., Durbin, R., Korlach, J., Lawniczak, M., 2019. A high-quality de novo genome assembly from a single mosquito using PacBio sequencing. Genes (Basel). 10, 62. https://doi.org/10.3390/genes10010062

Kofler, R., Schlötterer, C., 2014. A guide for the design of evolve and resequencing studies. Mol. Biol. Evol. 31, 474–483. https://doi.org/10.1093/molbev/mst221

Kojima, W., Fujii, T., Suwa, M., Miyazawa, M., Ishikawa, Y., 2010. Physiological adaptation of the Asian corn borer *Ostrinia furnacalis* to chemical defenses of its host plant, maize. J. Insect Physiol. 56, 1349–55. https://doi.org/10.1016/j.jinsphys.2010.04.021

Kostaropoulos, I., Papadopoulos, A.I., Metaxakis, A., Boukouvala, E., Papadopoulou-Mourkidou, E., 2001. Glutathione S-transferase in the defence against pyrethroids in insects. Insect Biochem. Mol. Biol. 31, 313–9. https://doi.org/10.1016/S0965-1748(00)00123-5

Krainacker, D.A., Carey, J.R., 1990. Male demographic constraints to extreme sex ratio in the twospotted spider mite. Oecologia 82, 417–423. https://doi.org/10.1007/BF00317492

Krantz, G.W., Lindquist, E.E., 1979. Evolution of phytophagous mites (Acari). Annu. Rev. Entomol. 24, 121–158. https://doi.org/10.1146/annurev.en.24.010179.001005

Krempl, C., Sporer, T., Reichelt, M., Ahn, S.-J., Heidel-Fischer, H., Vogel, H., Heckel, D.G., Joußen, N., 2016. Potential detoxification of gossypol by UDP-glycosyltransferases in the two Heliothine moth species *Helicoverpa armigera* and *Heliothis virescens*. Insect Biochem. Mol. Biol. 71, 49–57. https://doi.org/10.1016/j.ibmb.2016.02.005

Kretschmer, M., Leroch, M., Mosbach, A., Walker, A.S., Fillinger, S., Mernke, D., Schoonbeek, H.J., Pradier, J.M., Leroux, P., De Waard, M.A., Hahn, M., 2009. Fungicide-driven evolution and molecular basis of multidrug resistance in field populations of the grey mould fungus *Botrytis cinerea*. PLoS Pathog. 5, e1000696. https://doi.org/10.1371/journal.ppat.1000696

Kunte, K., Zhang, W., Tenger-Trolander, A., Palmer, D.H., Martin, A., Reed, R.D., Mullen, S.P., Kronforst, M.R., 2014. Doublesex is a mimicry supergene. Nature 507, 229–232. https://doi.org/10.1038/nature13112

Kwon, D.H., Clark, J.M., Lee, S.H., 2010a. Cloning of a sodium channel gene and identification of mutations putatively associated with fenpropathrin resistance in Tetranychus urticae. Pestic. Biochem. Physiol. 97, 93–100. https://doi.org/10.1016/j.pestbp.2009.07.009

Kwon, D.H., Clark, J.M., Lee, S.H., 2010b. Extensive gene duplication of acetylcholinesterase associated with organophosphate resistance in the two-spotted spider mite. Insect Mol. Biol. 19, 195–204. https://doi.org/10.1111/j.1365-2583.2009.00958.x

Kwon, D.H., Im, J.S., Ahn, J.J., Lee, J.H., Marshall Clark, J., Lee, S.H., 2010c. Acetylcholinesterase point mutations putatively associated with monocrotophos resistance in the two-spotted spider mite. Pestic. Biochem. Physiol. 96, 36–42. https://doi.org/10.1016/j.pestbp.2009.08.013

Kwon, D.H., Park, J.H., Ashok, P.A., Lee, U., Lee, S.H., 2016. Screening of target genes for RNAi in *Tetranychus urticae* and RNAi toxicity enhancement by chimeric genes. Pestic. Biochem. Physiol. 130, 1–7. https://doi.org/10.1016/J.PESTBP.2015.11.005

Kwon, D.H., Park, J.H., Lee, S.H., 2013. Screening of lethal genes for feeding RNAi by leaf disc-mediated systematic delivery of dsRNA in Tetranychus urticae. Pestic. Biochem. Physiol. 105, 69–75. https://doi.org/10.1016/j.pestbp.2012.12.001

Kwon, D.H., Seong, G.M., Kang, T.J., Lee, S.H., 2010d. Multiple resistance mechanisms to abamectin in the two-spotted spider mite. J. Asia. Pac. Entomol. 13, 229–232. https://doi.org/10.1016/j.aspen.2010.02.002

Kwon, D.H., Yoon, K.S., Clark, J.M., Lee, S.H., 2010e. A point mutation in a glutamate-gated chloride channel confers abamectin resistance in the two-spotted spider mite, *Tetranychus urticae* Koch. Insect Mol. Biol. 19, 583–591. https://doi.org/10.1111/j.1365-2583.2010.01017.x

Lai, C.Q., Leips, J., Zou, W., Roberts, J.F., Wollenberg, K.R., Parnell, L.D., Zeng, Z.B., Ordovas, J.M., Mackay, T.F.C., 2007. Speed-mapping quantitative trait loci using microarrays. Nat. Methods 4, 839–841. https://doi.org/10.1038/nmeth1084

Lairson, L.L., Henrissat, B., Davies, G.J., Withers, S.G., 2008. Glycosyltransferases: structures, functions, and mechanisms. Annu. Rev. Biochem. 77, 521–55. https://doi.org/10.1146/annurev.biochem.76.061005.092322

Langmead, B., Salzberg, S.L., 2012. Fast gapped-read alignment with Bowtie 2. Nat. Methods 9, 357–359. https://doi.org/10.1038/nmeth.1923

Larkin, M.A., Blackshields, G., Brown, N.P., Chenna, R., Mcgettigan, P.A., McWilliam, H., Valentin, F., Wallace, I.M., Wilm, A., Lopez, R., Thompson, J.D., Gibson, T.J., Higgins, D.G., 2007. Clustal W and clustal X version 2.0. Bioinformatics 23, 2947–2948. https://doi.org/10.1093/bioinformatics/btm404

Laursen, T., Jensen, K., Møller, B.L., 2011. Conformational changes of the NADPH-dependent cytochrome P450 reductase in the course of electron transfer to cytochromes P450. Biochim. Biophys. Acta - Proteins Proteomics 1814, 132–138. https://doi.org/10.1016/j.bbapap.2010.07.003

Lee, S.-W., Ohta, K., Tashiro, S., Shono, T., 2006. Metabolic resistance mechanisms of the housefly (*Musca domestica*) resistant to pyraclofos. Pestic. Biochem. Physiol. 85, 76–83. https://doi.org/10.1016/j.pestbp.2005.10.005

Leszczynski, B., Dixon, A.F.G., 1990. Resistance of cereals to aphids: interaction between hydroxamic acids and the aphid *Sitobion avenae* (Homoptera: Aphididae). Ann. Appl. Biol. 18, 1189–1200. https://doi.org/10.1111/j.1744-7348.1990.tb04191.x

Li, H., Durbin, R., 2009. Fast and accurate short read alignment with Burrows-Wheeler transform. Bioinformatics 25, 1754–1760. https://doi.org/10.1093/bioinformatics/btp324

Li, H., Handsaker, B., Wysoker, A., Fennell, T., Ruan, J., Homer, N., Marth, G., Abecasis, G., Durbin, R., 2009. The sequence alignment/map format and SAMtools. Bioinformatics 25, 2078–2079. https://doi.org/10.1093/bioinformatics/btp352

Li, J., Wang, X.-P., Wang, M.-Q., Ma, W.-H., Hua, H.-X., 2013. Advances in the use of the RNA interference technique in *Hemiptera*. Insect Sci. 20, 31–39. https://doi.org/10.1111/j.1744-7917.2012.01550.x

Li, W.H., Graur, D., 1991. Fundamentals of molecular evolution, Sunderland, Massachusetts. Sinauer Associates.

Li, X., Schuler, M. a, Berenbaum, M.R., 2007. Molecular mechanisms of metabolic resistance to synthetic and natural xenobiotics. Annu. Rev. Entomol. 52, 231–253. https://doi.org/10.1146/annurev.ento.51.110104.151104

Li, X., Shi, H., Gao, X., Liang, P., 2018. Characterization of UDP-glucuronosyltransferase genes and their

possible roles in multi-insecticide resistance in *Plutella xylostella* (L.). Pest Manag. Sci. 74, 695–704. https://doi.org/10.1002/ps.4765

Li, X., Zhu, B., Gao, X., Liang, P., 2017. Over-expression of UDP-glycosyltransferase gene *UGT2B17* is involved in chlorantraniliprole resistance in *Plutella xylostella* (L.). Pest Manag. Sci. 73, 1402–1409. https://doi.org/10.1002/ps.4469

Lindquist, E.E., 1998. Evolution of phytophagy in trombidiform mites. Exp. Appl. Acarol. 22, 81–100. https://doi.org/10.1023/A:1006041609774

Lindroth, R.L., 1991. Differential toxicity of plant allelochemicals to insects: roles of enzymatic detoxication systems, in: Insect-Plant Interactions. CRC Press, pp. 1–34. https://doi.org/10.1201/9780203711699-1

Lindroth, R.L., 1989. Chemical ecology of the luna moth - Effects of host plant on detoxification enzyme activity. J. Chem. Ecol. 15, 2019–2029. https://doi.org/10.1007/BF01207434

Linnen, C.R., O'Quin, C.T., Shackleford, T., Sears, C.R., Lindstedt, C., 2018. Genetic basis of body color and spotting pattern in redheaded pine sawfly larvae (*Neodiprion lecontei*). Genetics 209, 291–305. https://doi.org/10.1534/genetics.118.300793

Litman, T., Zeuthen, T., Skovsgaard, T., Stein, W.D., 1997. Competitive, non-competitive and cooperative interactions between substrates of P-glycoprotein as measured by its ATPase activity. Biochim. Biophys. Acta - Mol. Basis Dis. 1361, 169–176. https://doi.org/10.1016/S0925-4439(97)00027-6

Liu, F., Shi, X., Liang, Y., Wu, Q., Xu, B., Xie, W., Wang, S., Zhang, Y., Liu, N., 2014. A 36-bp deletion in the alpha subunit of glutamate-gated chloride channel contributes to abamectin resistance in *Plutella xylostella*. Entomol. Exp. Appl. 153, 85–92. https://doi.org/10.1111/eea.12232

Liu, J., Farmer, J.D., Lane, W.S., Friedman, J., Weissman, I., Schreiber, S.L., 1991. Calcineurin is a common target of cyclophilin-cyclosporin A and FKBP-FK506 complexes. Cell 66, 807–815. https://doi.org/10.1016/0092-8674(91)90124-H

Liu, S., Scott, I., Pelletier, Y., Kramp, K., Durst, T., Sims, S., Arnasson, J., 2014. Dillapiol: a pyrethrum synergist for control of the Colorado potato beetle. J. Econ. Entomol. 107, 797–805. https://doi.org/10.1603/ec13440

Loayza-Muro, R., Figueroa, C.C., Niemeyer, H.M., 2000. Effect of two wheat cultivars differing in hydroxamic acid concentration on detoxification metabolism in the aphid Sitobion avenae. J. Chem. Ecol. 26, 2725–2736.

Lombard, V., Golaconda Ramulu, H., Drula, E., Coutinho, P.M., Henrissat, B., 2014. The carbohydrate-active enzymes database (CAZy) in 2013. Nucleic Acids Res. 42, D490–D495. https://doi.org/10.1093/nar/gkt1178

López-Soler, N., Cervera, A., Quinto, V., Abellán, J., Bielza, P., Martínez-Pardo, R., Garcerá, M.D., 2011. Esterase inhibition by synergists in the western flower thrips *Frankliniella occidentalis*. Pest Manag. Sci. 67, 1549–56. https://doi.org/10.1002/ps.2211

Love, M.I., Anders, S., Kim, V., Huber, W., 2015. RNA-Seq workflow: gene-level exploratory analysis and differential expression. F1000Research 4, 1070. https://doi.org/10.12688/f1000research.7035.1

Lowe, R., Shirley, N., Bleackley, M., Dolan, S., Shafee, T., 2017. Transcriptomics technologies. PLoS Comput. Biol. 13, e1005457. https://doi.org/10.1371/journal.pcbi.1005457

Lucier, G.W., McDaniel, O.S., Matthews, H.B., 1971. Microsomal rat liver UDP glucuronyltransferase: Effects of piperonyl butoxide and other factors on enzyme activity. Arch. Biochem. Biophys. 145, 520–530. https://doi.org/10.1016/S0003-9861(71)80012-7

Ludmerer, S.W., Warren, V.A., Williams, B.S., Zheng, Y., Hunt, D.C., Ayer, M.B., Wallace, M.A., Chaudhary, A.G., Egan, M.A., Meinke, P.T., Dean, D.C., Garcia, M.L., Cully, D.F., Smith, M.M., 2002. Ivermectin and nodulisporic acid receptors in Drosophila melanogaster contain both gamma-aminobutyric acid-gated Rdl and glutamate-gated GluCl alpha chloride channel subunits. Biochemistry 41, 6548–60. https://doi.org/10.1021/bi015920o

Lümmen, P., 2007. Mitochondrial electron transport complexes as biochemical target sites for insecticides and acaricids, in: Insecticides Design Using Advanced Technologies. Springer, Berlin, Heidelberg, pp. 197–215. https://doi.org/10.1007/978-3-540-46907-0_8

Lümmen, P., 1998. Complex I inhibitors as insecticides and acaricides. Biochim. Biophys. Acta - Bioenerg. 1364, 287–296. https://doi.org/10.1016/S0005-2728(98)00034-6

Luo, L., Sun, Y.-J., Yang, L., Huang, S., Wu, Y.-J., 2013. Avermectin induces P-glycoprotein expression in S2 cells via the calcium/calmodulin/NF-κB pathway. Chem. Biol. Interact. 203, 430–9. https://doi.org/10.1016/j.cbi.2013.03.009

Luque, T., Okano, K., O'Reilly, D.R., 2002. Characterization of a novel silkworm (*Bombyx mori*) phenol UDP-glucosyltransferase. Eur. J. Biochem. 269, 819–825. https://doi.org/10.1046/j.0014-2956.2001.02723.x

Maag, D., Dalvit, C., Thevenet, D., Köhler, A., Wouters, F.C., Vassão, D.G., Gershenzon, J., Wolfender, J.L., Turlings, T.C.J., Erb, M., Glauser, G., 2014. 3-β-d-Glucopyranosyl-6-methoxy-2-benzoxazolinone (MBOA-N-Glc) is an insect detoxification product of maize 1,4-benzoxazin-3-ones. Phytochemistry 102, 97–105. https://doi.org/10.1016/j.phytochem.2014.03.018

Mackenzie, P.I., Owens, I.S., Burchell, B., Bock, K.W., Bairoch, A., Bélanger, A., Fournel-Gigleux, S., Green, M., Hum, D.W., Iyanagi, T., Lancet, D., Louisot, P., Magdalou, J., Chowdhury, J.R., Ritter, J.K., Schachter, H., Tephly, T.R., Tipton, K.F., Nebert, D.W., 1997. The UDP glycosyltransferase gene superfamily: recommended nomenclature update based on evolutionary divergence. Pharmacogenetics 7, 255–69. https://doi.org/10.1097/00008571-199708000-00001

Magalhães, S., Blanchet, E., Egas, M., Olivieri, I., 2009. Are adaptation costs necessary to build up a local adaptation pattern? BMC Evol. Biol. 9, 182. https://doi.org/10.1186/1471-2148-9-182

Magalhães, S., Fayard, J., Janssen, A., Carbonell, D., Olivieri, I., 2007. Adaptation in a spider mite population after long-term evolution on a single host plant. J. Evol. Biol. 20, 2016–2027. https://doi.org/10.1111/j.1420-9101.2007.01365.x

Magdalou, J., Fournel-Gigleux, S., Ouzzine, M., 2010. Insights on membrane topology and structure/function of UDP-glucuronosyltransferases. Drug Metab. Rev. 42, 159–166. https://doi.org/10.3109/03602530903209270

Magnitsky, S., Toulokhonova, L., Yano, T., Sled, V.D., Hägerhäll, C., Grivennikova, V.G., Burbaev, D.S., Vinogradov, A.D., Ohnishi, T., 2002. EPR characterization of ubisemiquinones and iron-sulfur cluster N2, central components of the energy coupling in the NADH-ubiquinone oxidoreductase (complex I) in situ. J. Bioenerg. Biomembr. 34, 193–208. https://doi.org/10.1023/A:1016083419979

Magwene, P.M., Willis, J.H., Kelly, J.K., 2011. The statistics of bulk segregant analysis using next generation sequencing. PLoS Comput. Biol. 7. https://doi.org/10.1371/journal.pcbi.1002255

Mannervik, B., 1985. The isoenzymes of glutathione transferase. Adv. Enzymol. Relat. Areas Mol. Biol. 57, 357–417.

Mannervik, B., Danielson, U.H., 1988. Glutathione transferases--structure and catalytic activity. CRC Crit. Rev. Biochem. 23, 283–337.

Mansfeld, B.N., Grumet, R., 2017. QTLseqr: an R package for bulk segregant analysis with next-generation sequencing. Plant Genome 11, 180006. https://doi.org/10.1093/bioinformatics/xxxxx

Mao, Y.B., Cai, W.J., Wang, J.W., Hong, G.J., Tao, X.Y., Wang, L.J., Huang, Y.P., Chen, X.Y., 2007. Silencing a cotton bollworm P450 monooxygenase gene by plant-mediated RNAi impairs larval tolerance of gossypol. Nat. Biotechnol. 25, 1307–1313. https://doi.org/10.1038/nbt1352

Martel, C., Zhurov, V., Navarro, M., Martinez, M., Cazaux, M., Auger, P., Migeon, A., Santamaria, M.E., Wybouw, N., Diaz, I., Van Leeuwen, T., Navajas, M., Grbic, M., Grbic, V., 2015. Tomato whole genome transcriptional response to *Tetranychus urticae* identifies divergence of spider mite-induced responses between Tomato and Arabidopsis. Mol Plant-Microbe Interact 28, 343–361. https://doi.org/10.1094/MPMI-09-14-0291-FI

Martin, H.J., Ziemba, M., Kisiela, M., Botella, J.A., Schneuwly, S., Maser, E., 2011. The Drosophila carbonyl reductase sniffer is an efficient 4-oxonon-2-enal (4ONE) reductase. Chem. Biol. Interact. 193, 48–54. https://doi.org/10.1016/j.cbi.2010.12.006

Mason, C.J., Scully, E.D., Geib, S.M., Hoover, K., 2016. Contrasting diets reveal metabolic plasticity in the tree-killing beetle, *Anoplophora glabripennis* (Cerambycidae: Lamiinae). Sci. Rep. 6, 33813. https://doi.org/10.1038/srep33813

Mathers, T.C., Chen, Y., Kaithakottil, G., Legeai, F., Mugford, S.T., Baa-Puyoulet, P., Bretaudeau, A., Clavijo, B., Colella, S., Collin, O., Dalmay, T., Derrien, T., Feng, H., Gabaldón, T., Jordan, A., Julca, I., Kettles, G.J., Kowitwanich, K., Lavenier, D., Lenzi, P., Lopez-Gomollon, S., Loska, D., Mapleson, D., Maumus, F., Moxon, S., Price, D.R.G., Sugio, A., van Munster, M., Uzest, M., Waite, D., Jander, G., Tagu, D., Wilson, A.C.C., van Oosterhout, C., Swarbreck, D., Hogenhout, S.A., 2017. Rapid transcriptional plasticity of duplicated gene clusters enables a clonally reproducing aphid to colonise diverse plant species. Genome Biol. 18, 27. https://doi.org/10.1186/s13059-016-1145-3

Matsumura, F., 1985. Metabolism of Insecticides by Animals and Plants, in: Toxicology of Insecticides. Springer US, Boston, MA, pp. 203–298.

Mattson, W.J., 1980. Herbivory in relation to plant nitrogen content. Annu. Rev. Ecol. Syst. 11, 119–161. https://doi.org/10.1146/annurev.es.11.110180.001003

Maumus, F., Fiston-Lavier, A.-S., Quesneville, H., 2015. Impact of transposable elements on insect genomes and biology. Curr. Opin. Insect Sci. 7, 30–36. https://doi.org/10.1016/j.cois.2015.01.001

Mayoral, J.G., Leonard, K.T., Nouzova, M., Noriega, F.G., Defelipe, L.A., Turjanski, A.G., 2013. Functional analysis of a mosquito short-chain dehydrogenase cluster. Arch. Insect Biochem. Physiol. 82, 96–115. https://doi.org/10.1002/arch.21078

Mayoral, J.G., Nouzova, M., Navare, A., Noriega, F.G., 2009. NADP+-dependent farnesol dehydrogenase, a corpora allata enzyme involved in juvenile hormone synthesis. Proc. Natl. Acad. Sci. U. S. A. 106, 21091–6. https://doi.org/10.1073/pnas.0909938106

McCart, C., Buckling, A., ffrench-Constant, R.H., 2005. DDT resistance in flies carries no cost. Curr. Biol. 15, R587–R589. https://doi.org/10.1016/j.cub.2005.07.054

McCormick, J.P., 1982. Secondary metabolites of Gossypium - a biogenetic analysis. Acs Symp. Ser. 189, 275–300. https://doi.org/10.1021/bk-1982-0189.ch018

McGaughey, G.B., Gagne, M., Rappe, A.K., 1998. Pi-stacking interactions. J. Biol. Chem. 273, 15458–15463. https://doi.org/10.1074/jbc.273.25.15458

McKenna, A., Hanna, M., Banks, E., Sivachenko, A., Cibulskis, K., Kernytsky, A., Garimella, K., Altshuler, D., Gabriel, S., Daly, M., DePristo, M.A., 2010. The genome analysis toolkit: a MapReduce framework for analyzing next-generation DNA sequencing data. Genome Res. 20, 1297–1303. https://doi.org/10.1101/gr.107524.110

Meihls, L.N., Kaur, H., Jander, G., 2012. Natural variation in maize defense against insect herbivores. Cold Spring Harb. Symp. Quant. Biol. 77, 269–283. https://doi.org/10.1101/sqb.2012.77.014662

Melander, A.L., 1914. Can insects become resistant to sprays? J. Econ. Entomol. 7, 167–173. https://doi.org/10.1093/jee/7.2.167

Memarizadeh, N., Ghadamyari, M., Zamani, P., Sajedi, R.H., 2013. Resistance mechanisms to abamectin in Iranian populations of the two-spotted spider mite, *Tetranychus urticae* Koch (Acari: Tetranychidae). Acarologia 53, 235–246. https://doi.org/10.1051/acarologia/20132093

Mermans, C., Dermauw, W., Geibel, S., Van Leeuwen, T., 2017. A G326E substitution in the glutamate-gated chloride channel 3 (GluCl3) of the two-spotted spider mite *Tetranychus urticae* abolishes the agonistic activity of macrocyclic lactones. Pest Manag. Sci. 73, 2413–2418. https://doi.org/10.1002/ps.4677

Merzendorfer, H., 2014. ABC transporters and their role in protecting insects from pesticides and their metabolites. Adv. In Insect Phys. 46, 1–72. https://doi.org/10.1016/B978-0-12-417010-0.00001-X

Merzendorfer, H., 2013. Chitin synthesis inhibitors: old molecules and new developments. Insect Sci. 20, 121–138. https://doi.org/10.1111/j.1744-7917.2012.01535.x

Michelmore, R.W., Paran, I., Kesseli, R. V., 1991. Identification of markers linked to disease-resistance genes by bulked segregant analysis: a rapid method to detect markers in specific genomic regions by using segregating populations. Proc. Natl. Acad. Sci. 88, 9828–9832. https://doi.org/10.1073/pnas.88.21.9828

Mierziak, J., Kostyn, K., Kulma, A., 2014. Flavonoids as important molecules of plant interactions with the environment. Molecules 19, 16240–16265. https://doi.org/10.3390/molecules191016240

Migeon, A., Nouguier, E., Dorkeld, F., 2010. Spider mites web: a comprehensive database for the Tetranychidae, in: Trends in Acarology. Springer, Dordrecht, The Netherlands, Dordrecht, pp. 557–560. https://doi.org/10.1007/978-90-481-9837-5_96

Miller, J.R., Koren, S., Dilley, K.A., Harkins, D.M., Stockwell, T.B., Shabman, R.S., Sutton, G.G., 2018. A draft genome sequence for the *Ixodes scapularis* cell line, ISE6. F1000Research 7, 297. https://doi.org/10.12688/f1000research.13635.1

Miller, M.A., Pfeiffer, W., Schwartz, T., 2010. Creating the CIPRES science gateway for inference of large phylogenetic trees, in: 2010 Gateway Computing Environments Workshop, GCE 2010. IEEE, New Orleans, LA, USA, pp. 1–8. https://doi.org/10.1109/GCE.2010.5676129

Misra, J.R., Horner, M.A., Lam, G., Thummel, C.S., 2011. Transcriptional regulation of xenobiotic detoxification in *Drosophila*. Genes Dev. 25, 1796–1806. https://doi.org/10.1101/gad.17280911

Mitchell, R., 1973. Growth and population dynamics of a spider mite (*Tetranychus Urticae* K., Acarina: Tetranychidae). Ecology 54, 1349–1355. https://doi.org/10.2307/1934198

Mo, Y.-D., Yang, S.-X., Zhao, J.-Y., Jin, P.-Y., Hong, X.-Y., 2017. Comparative transcriptomes and reciprocal best hit analysis revealed potential pigment genes in two color forms of *Tetranychus urticae*. Exp. Appl. Acarol. 73, 159–176. https://doi.org/10.1007/s10493-017-0188-9

Modolo, L. V., Blount, J.W., Achnine, L., Naoumkina, M.A., Wang, X., Dixon, R.A., 2007. A functional genomics approach to (iso)flavonoid glycosylation in the model legume *Medicago truncatula*. Plant Mol. Biol. 64, 499–518. https://doi.org/10.1007/s11103-007-9167-6

Montagne, J., Lecerf, C., Parvy, J.P., Bennion, J.M., Radimerski, T., Ruhf, M.L., Zilbermann, F., Vouilloz, N., Stocker, H., Hafen, E., Kozma, S.C., Thomas, G., 2010. The nuclear receptor DHR3 modulates ds6 kinase- dependent growth in *Drosophila*. PLoS Genet. 6, e1000937. https://doi.org/10.1371/journal.pgen.1000937

Morant, A.V., Jørgensen, K., Jørgensen, C., Paquette, S.M., Sánchez-Pérez, R., Møller, B.L., Bak, S., 2008. β-Glucosidases as detonators of plant chemical defense. Phytochemistry 69, 1795–1813. https://doi.org/10.1016/j.phytochem.2008.03.006

Morgan, M.S., Rider, S.D., Arlian, L.G., 2017. A draft genome of Euroglyphus Maynei with predicted allergens (ABSTRACT). J. Allergy Clin. Immunol. 139, AB118. https://doi.org/10.1016/j.jaci.2016.12.380

Morlais, I., Severson, D.W., 2001. Identification of a polymorphic mucin-like gene expressed in the midgut of the mosquito, *Aedes aegypti*, using an integrated bulked segregant and differential display analysis. Genetics 158, 1125–1136.

Mota-Sanchez, R.M., Wise, J.C., 2019. Arthropod pesticide resistance database [WWW Document]. URL https://www.pesticideresistance.org

Müller, C., Vogel, H., Heckel, D.G., 2017. Transcriptional responses to short-term and long-term host plant experience and parasite load in an oligophagous beetle. Mol. Ecol. 26, 6370–6383. https://doi.org/10.1111/mec.14349

Murataliev, M.B., Feyereisen, R., 2000. Interaction of NADP(H) with oxidized and reduced P450 reductase during catalysis. Studies with nucleotide analogues. Biochemistry 39, 5066–5074. https://doi.org/10.1021/bi992917k

Murataliev, M.B., Feyereisen, R., Walker, F.A., 2004. Electron transfer by diflavin reductases. Biochim. Biophys.

Acta - Proteins Proteomics 1698, 1–26. https://doi.org/10.1016/j.bbapap.2003.10.003

Murataliev, M.B., Guzov, V.M., Walker, F.A., Feyereisen, R., 2008. P450 reductase and cytochrome b5 interactions with cytochrome P450: effects on house fly CYP6A1 catalysis. Insect Biochem. Mol. Biol. 38, 1008–1015. https://doi.org/10.1016/j.ibmb.2008.08.007

Navajas, M., 1998. Host plant associations in the spider mite *Tetranychus urticae* (Acari: Tetranychidae): insights from molecular phylogeography. Exp. Appl. Acarol. 22, 201–214. https://doi.org/10.1023/A:1006062214318

Navia, D., Novelli, V.M., Rombauts, S., Astúa-Freitas, J., Santos de Mendonça, R., Nunes, M.A., Machado, M.A., Lin, Y.-C., Le, P., Zhang, Z., Grbić, M., Wybouw, N., Breeuwer, J.A.J., Van Leeuwen, T., Van de Peer, Y., 2019. Draft genome assembly of the false spider mite *Brevipalpus yothersi*. Microbiol. Resour. Announc. 8, e01563-18. https://doi.org/10.1128/MRA.01563-18

Ngoc, P.C.T., Greenhalgh, R., Dermauw, W., Rombauts, S., Bajda, S., Zhurov, V., Grbić, M., Van de Peer, Y., Van Leeuwen, T., Rouzé, P., Clark, R.M., 2016. Complex evolutionary dynamics of massively expanded chemosensory receptor families in an extreme generalist chelicerate herbivore. Genome Biol. Evol. 8, 3323–3339. https://doi.org/10.1093/gbe/evw249

Niemeyer, H.M., 2009. Hydroxamic acids derived from 2-hydroxy-2h-1,4-benzoxazin-3(4h)-one: key defense chemicals of cereals. J. Agric. Food Chem. 57, 1677–1695. https://doi.org/10.1021/jf8034034

Niranjan Reddy, B.P., Prasad, G.B.K.S., Raghavendra, K., 2011. In silico analysis of glutathione S-transferase supergene family revealed hitherto unreported insect specific δ- and ε-GSTs and mammalian specific μ-GSTs in *Ixodes scapularis* (Acari: Ixodidae). Comput. Biol. Chem. 35, 114–120. https://doi.org/10.1016/j.compbiolchem.2011.03.004

Niu, J., Shen, G., Christiaens, O., Smagghe, G., He, L., Wang, J., 2018. Beyond insects: current status and achievements of RNA interference in mite pests and future perspectives. Pest Manag. Sci. 74, 2680–2687. https://doi.org/10.1002/ps.5071

Nosil, P., 2002. Transition rates between specialization and generalization in phytophagous insects. Evolution (N. Y). 56, 1701–1706. https://doi.org/10.1111/j.0014-3820.2002.tb01482.x

Oakeshott, J.G., Claudianos, C., Campbell, P.M., Newcomb, R.D., Russell, R.J., 2005. Biochemical genetics and genomics of insect esterases, in: Comprehensive Molecular Insect Science. pp. 309–381. https://doi.org/10.1016/B0-44-451924-6/00073-9

Ocorr, K.A., Crawley, T., Gibson, G., Bodmer, R., 2007. Genetic variation for cardiac dysfunction in *Drosophila*. PLoS One 2, e601. https://doi.org/10.1371/journal.pone.0000601

Okoniewski, M.J., Miller, C.J., 2006. Hybridization interactions between probesets in short oligo microarrays lead to spurious correlations. BMC Bioinformatics 7, 276. https://doi.org/10.1186/1471-2105-7-276

Okun, J.G., Lümmen, P., Brandt, U., 1999. Three classes of inhibitors share a common binding domain in mitochondrial complex I (NADH:Ubiquinone oxidoreductase). J. Biol. Chem. 274, 2625–2630. https://doi.org/10.1074/jbc.274.5.2625

Oppermann, U., 2007. Carbonyl reductases: The complex relationships of mammalian carbonyl- and quinone-reducing enzymes and their role in physiology. Annu. Rev. Pharmacol. Toxicol. 47, 293–322. https://doi.org/10.1146/annurev.pharmtox.47.120505.105316

Ozawa, A., 1994. Acaricides susceptibility of Kanzawa spider mite, *Tetranychus kanzawai* KISHIDA (Acarina; Tetranychidae) collected from tea fields in Chuuen and Ogasa district in Shizuoka prefecture. Chagyo Kenkyu Hokoku (Tea Res. Journal) 1994, 1–14. https://doi.org/10.5979/cha.1994.1

Pan, Y., Tian, F., Wei, X., Wu, Y., Gao, X., Xi, J., Shang, Q., 2018. Thiamethoxam resistance in *Aphis gossypii* glover relies on multiple UDP-glucuronosyltransferases. Front. Physiol. 3, 322. https://doi.org/10.3389/fphys.2018.00322

Pao, S.S., Paulsen, I.T., Saier, M.H., 1998. Major facilitator superfamily. Microbiol. Mol. Biol. Rev. 62, 1–34.

Park, Y.-L., Lee, J.-H., 2002. Leaf Cell and Tissue Damage of Cucumber Caused by Twospotted Spider Mite

(Acari: Tetranychidae). J. Econ. Entomol. 95, 952–957. https://doi.org/10.1603/0022-0493-95.5.952

Park, Y., González-Martínez, R.M., Navarro-Cerrillo, G., Chakroun, M., Kim, Y., Ziarsolo, P., Blanca, J., Cañizares, J., Ferré, J., Herrero, S., 2014. ABCC transporters mediate insect resistance to multiple Bt toxins revealed by bulk segregant analysis. BMC Biol. 12, 46. https://doi.org/10.1186/1741-7007-12-46

Pavlidi, N., Khalighi, M., Myridakis, A., Dermauw, W., Wybouw, N., Tsakireli, D., Stephanou, E.G., Labrou, N.E., Vontas, J., Van Leeuwen, T., 2017. A glutathione-S-transferase (TuGSTd05) associated with acaricide resistance in *Tetranychus urticae* directly metabolizes the complex II inhibitor cyflumetofen. Insect Biochem. Mol. Biol. 80, 101–115. https://doi.org/10.1016/j.ibmb.2016.12.003

Pavlidi, N., Tseliou, V., Riga, M., Nauen, R., Van Leeuwen, T., Labrou, N.E., Vontas, J., 2015. Functional characterization of glutathione S-transferases associated with insecticide resistance in *Tetranychus urticae*. Pestic. Biochem. Physiol. 121, 53–60. https://doi.org/10.1016/j.pestbp.2015.01.009

Pavlidi, N., Vontas, J., Van Leeuwen, T., 2018. The role of glutathione S-transferases (GSTs) in insecticide resistance in crop pests and disease vectors. Curr. Opin. Insect Sci. 27, 97–102. https://doi.org/10.1016/j.cois.2018.04.007

Pemberton, R.W., Lee, J.H., 1996. The influence of extrafloral nectaries on parasitism of an insect herbivore. Am. J. Bot. 83, 1187–1194. https://doi.org/10.2307/2446203

Pentzold, S., Zagrobelny, M., Roelsgaard, P.S., Møller, B.L., Bak, S., 2014. The multiple strategies of an insect herbivore to overcome plant cyanogenic glucoside defence. PLoS One 9, e91337. https://doi.org/10.1371/journal.pone.0091337

Perry, T., Batterham, P., Daborn, P.J., 2011. The biology of insecticidal activity and resistance. Insect Biochem. Mol. Biol. https://doi.org/10.1016/j.ibmb.2011.03.003

Persson, B., Kallberg, Y., 2013. Classification and nomenclature of the superfamily of short-chain dehydrogenases/reductases (SDRs). Chem. Biol. Interact. 202, 111–115. https://doi.org/10.1016/j.cbi.2012.11.009

Persson, B., Kallberg, Y., Oppermann, U., Jörnvall, H., 2003. Coenzyme-based functional assignments of short-chain dehydrogenases/reductases (SDRs). Chem. Biol. Interact. 143–144, 271–278. https://doi.org/10.1016/S0009-2797(02)00223-5

Philippou, D., Borzatta, V., Capparella, E., Moroni, L., Field, L., Moores, G., 2013. The interactions between piperonyl butoxide and E4, a resistance-associated esterase from the peach-potato aphid, *Myzus persicae* Sulzer (Hemiptera: Aphididae). Pest Manag. Sci. 69, 499–506. https://doi.org/10.1002/ps.3400

Phillips, A.H., Langdon, R.G., 1962. Hepatic triphosphopyridine nucleotide-cytochrome c reductase: isolation, characterization, and kinetic studies. J. Biol. Chem. 237, 2652–60.

Phuong, C.T.N., 2014. Genome annotation and evolution of chemosensory receptors in spider mites Cao Thi Ngoc Phuong. Ghent university.

Pičmanová, M., Neilson, E.H., Motawia, M.S., Olsen, C.E., Agerbirk, N., Gray, C.J., Flitsch, S., Meier, S., Silvestro, D., Jørgensen, K., Sánchez-Pérez, R., Møller, B.L., Bjarnholt, N., 2015. A recycling pathway for cyanogenic glycosides evidenced by the comparative metabolic profiling in three cyanogenic plant species. Biochem. J. 469, 375–389. https://doi.org/10.1042/BJ20150390

Pimentel, D., 2005. 'Environmental and economic costs of the application of pesticides primarily in the United States.' Environ. Dev. Sustain. 7, 229–252. https://doi.org/10.1007/s10668-005-7314-2

Pimentel, D., Peshin, R., 2014. Integrated pest management: pesticide problems, Vol. 3. ed. Springer, Dordrecht. https://doi.org/10.1007/978-94-007-7796-5

Plapp, F.W., Bigley, W.S., Chapmen, G.A., Eddy, G.W., 1963. Synergism of malathion against resistant house flies and mosquitoes. J. Econ. Entomol. 56, 643–649. https://doi.org/10.1093/jee/56.5.643

Polilov, A.A., 2015. Small is beautiful: features of the smallest insects and limits to miniaturization. Annu. Rev. Entomol. 60, 103–121. https://doi.org/10.1146/annurev-ento-010814-020924

Pool, J.E., 2016. Genetic mapping by bulk segregant analysis in *Drosophila*: experimental design and simulation-

based inference. Genetics 204, 1295–1306. https://doi.org/10.1534/genetics.116.192484

Potter, D.A., Wrensch, D.L., Johnston, D.E., 2015. Guarding, aggressive behavior, and mating success in male twospotted spider mites. Ann. Entomol. Soc. Am. 69, 707–711. https://doi.org/10.1093/aesa/69.4.707

Poupardin, R., Reynaud, S., Strode, C., Ranson, H., Vontas, J., David, J.P., 2008. Cross-induction of detoxification genes by environmental xenobiotics and insecticides in the mosquito *Aedes aegypti*: Impact on larval tolerance to chemical insecticides. Insect Biochem. Mol. Biol. 38, 540–551. https://doi.org/10.1016/j.ibmb.2008.01.004

Poupardin, R., Riaz, M.A., Vontas, J., David, J.P., Reynaud, S., 2010. Transcription profiling of eleven cytochrome p450s potentially involved in xenobiotic metabolism in the mosquito *aedes aegypti*. Insect Mol. Biol. 19, 185–193. https://doi.org/10.1111/j.1365-2583.2009.00967.x

Qadir, M., O'Loughlin, K.L., Fricke, S.M., Williamson, N.A., Greco, W.R., Minderman, H., Baer, M.R., 2005. Cyclosporin A is a broad-spectrum multidrug resistance modulator. Clin. Cancer Res. 11, 2320–2326. https://doi.org/10.1158/1078-0432.CCR-04-1725

R Developement Core Team, 2015. R: a language and environment for statistical computing. R Found. Stat. Comput. 1, 409. https://doi.org/10.1007/978-3-540-74686-7

Raffa, K., Priester, T., 1985. Synergists as research tools and control agents in agriculture. J. Agric. Entomol 2, 27–45.

Rane, R. V, Walsch, T.K., Pearce, S.L., Jermiin, L.S., Gordon, K.H., Richards, S., Oakeshott, J.G., 2016. Are feeding preferences and insecticide resistance associated with the size of detoxifying enzyme families in insect herbivores? Curr. Opin. Insect Sci. 13, 70–76. https://doi.org/10.1016/J.COIS.2015.12.001

Rangasamy, M., Siegfried, B.D., 2012. Validation of RNA interference in western corn rootworm *Diabrotica virgifera* virgifera LeConte (Coleoptera: Chrysomelidae) adults. Pest Manag. Sci. 68, 587–591. https://doi.org/10.1002/ps.2301

Rauch, N., Nauen, R., 2002. Spirodiclofen resistance risk assessment in *Tetranychus urticae* (Acari: Tetranychidae): A biochemical approach. Pestic. Biochem. Physiol. 74, 91–101. https://doi.org/10.1016/S0048-3575(02)00150-5

Reddy, V.S., Shlykov, M.A., Castillo, R., Sun, E.I., Saier, M.H., 2012. The major facilitator superfamily (MFS) revisited. FEBS J. 279, 2022–2035. https://doi.org/10.1111/j.1742-4658.2012.08588.x

Reimer, R.J., 2013. SLC17: A functionally diverse family of organic anion transporters. Mol. Aspects Med. 34, 350–359. https://doi.org/10.1016/j.mam.2012.05.004

Reinking, J., Lam, M.M.S., Pardee, K., Sampson, H.M., Liu, S., Yang, P., Williams, S., White, W., Lajoie, G., Edwards, A., Krause, H.M., 2005. The *Drosophila* nuclear receptor E75 contains heme and is gas responsive. Cell 122, 195–207. https://doi.org/10.1016/j.cell.2005.07.005

Rhoads, A., Au, K.F., 2015. PacBio sequencing and its applications. Genomics. Proteomics Bioinformatics 13, 278–289. https://doi.org/10.1016/j.gpb.2015.08.002

Richards, S., Gibbs, R.A., Gerardo, N.M., Moran, N., Nakabachi, A., Stern, D., Tagu, D., Wilson, A.C.C., Muzny, D., Kovar, C., Cree, A., Chacko, J., Chandrabose, M.N., Dao, M.D., Dinh, H.H., Gabisi, R.A., Hines, S., Hume, J., Jhangian, S.N., Joshi, V., Lewis, L.R., Liu, Y.S., Lopez, J., Morgan, M.B., Nguyen, N.B., Okwuonu, G.O., Ruiz, S.J., Santibanez, J., Wright, R.A., Fowler, G.R., Hitchens, M.E., Lozado, R.J., Moen, C., Steffen, D., Warren, J.T., Zhang, J., Nazareth, L. V., Chavez, D., Davis, C., Lee, S.L., Patel, B.M., Pu, L.L., Bell, S.N., Johnson, A.J., Vattathil, S., Williams, R.L., Shigenobu, S., Dang, P.M., Morioka, M., Fukatsu, T., Kudo, T., Miyagishima, S.Y., Jiang, H., Worley, K.C., Legeai, F., Gauthier, J.P., Collin, O., Zhang, L., Chen, H.C., Ermolaeva, O., Hlavina, W., Kapustin, Y., Kiryutin, B., Kitts, P., Maglott, D., Murphy, T., Pruitt, K., Sapojnikov, V., Souvorov, A., Thibaud-Nissen, F., Câmara, F., Guigó, R., Stanke, M., Solovyev, V., Kosarev, P., Gilbert, D., Gabaldón, T., Huerta-Cepas, J., Marcet-Houben, M., Pignatelli, M., Moya, A., Rispe, C., Ollivier, M., Quesneville, H., Permal, E., Llorens, C., Futami, R., Hedges, D., Robertson, H.M., Alioto, T., Mariotti, M., Nikoh, N., McCutcheon, J.P., Burke, G., Kamins, A., Latorre, A., Ashton, P., Calevro, F., Charles, H., Colella, S., Douglas, A.E., Jander, G., Jones, D.H., Febvay, G.,

Kamphuis, L.G., Kushlan, P.F., Macdonald, S., Ramsey, J., Schwartz, J., Seah, S., Thomas, G., Vellozo, A., Cass, B., Degnan, P., Hurwitz, B., Leonardo, T., Koga, R., Altincicek, B., Anselme, C., Atamian, H., Barribeau, S.M., De Vos, M., Duncan, E.J., Evans, J., Ghanim, M., Heddi, A., Kaloshian, I., Vincent-Monegat, C., Parker, B.J., Pérez-Brocal, V., Rahbé, Y., Spragg, C.J., Tamames, J., Tamarit, D., Tamborindeguy, C., Vilcinskas, A., Bickel, R.D., Brisson, J.A., Butts, T., Chang, C.C., Christiaens, O., Davis, G.K., Duncan, E., Ferrier, D., Iga, M., Janssen, R., Lu, H.L., McGregor, A., Miura, T., Smagghe, G., Smith, J., Van Der Zee, M., Velarde, R., Wilson, M., Dearden, P., Edwards, O.R., Gordon, K., Hilgarth, R.S., Rider, S.D., Srinivasan, D., Walsh, T.K., Ishikawa, A., Jaubert-Possamai, S., Fenton, B., Huang, W., Rizk, G., Lavenier, D., Nicolas, J., Smadja, C., Zhou, J.J., Vieira, F.G., He, X.L., Liu, R., Rozas, J., Field, L.M., Campbell, P., Carolan, J.C., Fitzroy, C.I.J., Reardon, K.T., Reeck, G.R., Singh, K., Wilkinson, T.L., Huybrechts, J., Abdel-Latief, M., Robichon, A., Veenstra, J.A., Hauser, F., Cazzamali, G., Schneider, M., Williamson, M., Stafflinger, E., Hansen, K.K., Grimmelikhuijzen, C.J.P., Price, D.R.G., Caillaud, M., Van Fleet, E., Ren, Q., Gatehouse, J.A., Brault, V., Monsion, B., Diaz, J., Hunnicutt, L., Ju, H.J., Pechuan, X., Aguilar, J., Cortés, T., Ortiz-Rivas, B., Martínez-Torres, D., Dombrovsky, A., Dale, R.P., Davies, T.G.E., Williamson, M.S., Jones, A., Sattelle, D., Williamson, S., Wolstenholme, A., Cottret, L., Sagot, M.F., Heckel, D.G., Hunter, W., 2010. Genome sequence of the pea aphid *Acyrthosiphon pisum*. PLoS Biol. 8, e1000313. https://doi.org/10.1371/journal.pbio.1000313

Richards, S., Murali, S.C., 2015. Best practices in insect genome sequencing: what works and what doesn't. Curr. Opin. Insect Sci. 7, 1–7. https://doi.org/10.1016/j.cois.2015.02.013

Rider, S.D., Morgan, M.S., Arlian, L.G., 2015. Draft genome of the scabies mite. Parasites and Vectors 8, 585. https://doi.org/10.1186/s13071-015-1198-2

Riga, M., Bajda, S., Themistokleous, C., Papadaki, S., Palzewicz, M., Dermauw, W., Vontas, J., Leeuwen, T. Van, 2017. The relative contribution of target-site mutations in complex acaricide resistant phenotypes as assessed by marker assisted backcrossing in *Tetranychus urticae*. Sci. Rep. 7, 9202. https://doi.org/10.1038/s41598-017-09054-y

Riga, M., Myridakis, A., Tsakireli, D., Morou, E., Stephanou, E.G., Nauen, R., Van Leeuwen, T., Douris, V., Vontas, J., 2015. Functional characterization of the *Tetranychus urticae* CYP392A11, a cytochrome P450 that hydroxylates the METI acaricides cyenopyrafen and fenpyroximate. Insect Biochem. Mol. Biol. 65, 91–99. https://doi.org/10.1016/j.ibmb.2015.09.004

Riga, M., Tsakireli, D., Ilias, A., Morou, E., Myridakis, A., Stephanou, E.G., Nauen, R., Dermauw, W., Van Leeuwen, T., Paine, M., Vontas, J., 2014. Abamectin is metabolized by CYP392A16, a cytochrome P450 associated with high levels of acaricide resistance in *Tetranychus urticae*. Insect Biochem. Mol. Biol. 46, 43–53. https://doi.org/10.1016/j.ibmb.2014.01.006

Rioja, C., Zhurov, V., Bruinsma, K., Grbic, M., Grbic, V., 2017. Plant-herbivore interactions: a case of an extreme generalist, the two-spotted spider mite, *Tetranychus urticae*. Mol. Plant-Microbe Interact. 30, 935–945. https://doi.org/10.1094/MPMI-07-17-0168-CR

Ritchie, M.E., Silver, J., Oshlack, A., Holmes, M., Diyagama, D., Holloway, A., Smyth, G.K., 2007. A comparison of background correction methods for two-colour microarrays. Bioinformatics 23, 2700–2707. https://doi.org/10.1093/bioinformatics/btm412

Rivera-Perez, C., Nouzova, M., Clifton, M.E., Garcia, E.M., LeBlanc, E., Noriega, F.G., 2013. Aldehyde dehydrogenase 3 converts farnesal into farnesoic acid in the corpora allata of mosquitoes. Insect Biochem. Mol. Biol. 43, 675–682. https://doi.org/10.1016/J.IBMB.2013.04.002

Robards, K., Antolovich, M., 1997. Analytical chemistry of fruit bioflavonoids. A review. Analyst 122, 11R-34R. https://doi.org/10.1039/a606499j

Robinson-Rechavi, M., Escriva, H., Laudet, V., 2003. The nuclear receptor superfamily. J. Cell Sci. 116, 585–586. https://doi.org/10.1242/jcs.00247

Robinson, J.T., Thorvaldsdóttir, H., Winckler, W., Guttman, M., Lander, E.S., Getz, G., Mesirov, J.P., 2011. Integrative genomics viewer. Nat. Biotechnol. 29, 24–26. https://doi.org/10.1038/nbt.1754

Roche, D.B., Buenavista, M.T., Tetchner, S.J., McGuffin, L.J., 2011. The IntFOLD server: an integrated web resource for protein fold recognition, 3D model quality assessment, intrinsic disorder prediction, domain prediction and ligand binding site prediction. Nucleic Acids Res. 39, W171-176. https://doi.org/10.1093/nar/gkr184

Rosenthal, G.A., Berenbaum, M., 1991. Herbivores: their interactions with secondary plant metabolites. Elsevier Science.

Roush, R.T., McKenzie, J.A., 1987. Ecological genetics of insecticide and acaricide resistance. Annu. Rev. Entomol. 32, 361–380. https://doi.org/10.1146/annurev.en.32.010187.002045

Roy, A., Walker, W.B., Vogel, H., Chattington, S., Larsson, M.C., Anderson, P., Heckel, D.G., Schlyter, F., 2016. Diet dependent metabolic responses in three generalist insect herbivores *Spodoptera* spp. Insect Biochem. Mol. Biol. 71, 91–105. https://doi.org/10.1016/j.ibmb.2016.02.006

Rozen, S., Skaletsky, H., 2000. Primer3 on the WWW for general users and for biologist programmers. Methods Mol. Biol. 132, 365–386. https://doi.org/10.1385/1-59259-192-2:365

Sabelis, M.W., Dicke, M., 1988. How plants obtain predatory mites as bodyguards. Netherlands J. Zool. 38, 148–165. https://doi.org/10.1163/156854288X00111

Saha, S., 2019. Long range sequencing and validation of insect genome assemblies, in: Brown, S.J., Pfrender, M.E. (Eds.), Insect Genomics. Humana Press, New York, NY, pp. 33–44. https://doi.org/10.1007/978-1-4939-8775-7_4

Saidijam, M., Benedetti, G., Ren, Q., Xu, Z., Hoyle, C.J., Palmer, S.L., Ward, A., Bettaney, K.E., Szakonyi, G., Meuller, J., Morrison, S., Pos, M.K., Butaye, P., Walravens, K., Langton, K., Herbert, R.B., Skurray, R.A., Paulsen, I.T., O'reilly, J., Rutherford, N.G., Brown, M.H., Bill, R.M., Henderson, P.J.F., 2006. Microbial drug efflux proteins of the major facilitator superfamily. Curr. Drug Targets 7, 793–811.

Saier, M.H., Reddy, V.S., Tamang, D.G., Västermark, Å., 2014. The transporter classification database. Nucleic Acids Res. 42. https://doi.org/10.1093/nar/gkt1097

Sanchez-Arroyo, H., Koehler, P.G., Valles, S.M., 2001. Effects of the synergists piperonyl butoxide and S,S,S-tributyl phosphorotrithioate on propoxur pharmacokinetics in *Blattella germanica* (Blattodea: Blattellidae). J. Econ. Entomol. 94, 1209–16. https://doi.org/10.1603/0022-0493-94.5.1209

Santamaría, M.E., González-Cabrera, J., Martínez, M., Grbic, V., Castañera, P., Díaz, L., Ortego, F., 2015. Digestive proteases in bodies and faeces of the two-spotted spider mite, *Tetranychus urticae*. J. Insect Physiol. 78, 69–77. https://doi.org/10.1016/j.jinsphys.2015.05.002

Santoro, M.G., 2000. Heat shock factors and the control of the stress response. Biochem. Pharmacol. 59, 55–63. https://doi.org/10.1016/S0006-2952(99)00299-3

Sarmento, R.A., Lemos, F., Bleeker, P.M., Schuurink, R.C., Pallini, A., Oliveira, M.G.A., Lima, E.R., Kant, M., Sabelis, M.W., Janssen, A., 2011. A herbivore that manipulates plant defence. Ecol. Lett. 14, 229–236. https://doi.org/10.1111/j.1461-0248.2010.01575.x

Sasai, H., Ishida, M., Murakami, K., Tadokoro, N., Ishihara, A., Nishida, R., Mori, N., 2009. Species-specific glucosylation of DIMBOA in larvae of the rice Armyworm. Biosci. Biotechnol. Biochem. 73, 1333–8. https://doi.org/10.1271/bbb.80903

Schlachter, C.R., Daneshian, L., Amaya, J., Klapper, V., Wybouw, N., Borowski, T., Van Leeuwen, T., Grbic, V., Grbic, M., Makris, T.M., Chruszcz, M., 2019. Structural and functional characterization of an intradiol ring-cleavage dioxygenase from the polyphagous spider mite herbivore *Tetranychus urticae* Koch. Insect Biochem. Mol. Biol. 107, 19–30. https://doi.org/10.1016/j.ibmb.2018.12.001

Schlipalius, D.I., Cheng, Q., Reilly, P.E.B., Collins, P.J., Ebert, P.R., 2002. Genetic linkage analysis of the lesser grain borer *Rhyzopertha dominica* identifies two loci that confer high-level resistance to the fumigant phosphine. Genetics 8, e62909.

Schlötterer, C., Kofler, R., Versace, E., Tobler, R., Franssen, S.U., 2015. Combining experimental evolution with next-generation sequencing: A powerful tool to study adaptation from standing genetic variation. Heredity

(Edinb). 114, 431–440. https://doi.org/10.1038/hdy.2014.86

Schlötterer, C., Tobler, R., Kofler, R., Nolte, V., 2014. Sequencing pools of individuals-mining genome-wide polymorphism data without big funding. Nat. Rev. Genet. 15, 749–763. https://doi.org/10.1038/nrg3803

Schneeberger, K., 2014. Using next-generation sequencing to isolate mutant genes from forward genetic screens. Nat. Rev. Genet. 15, 662. https://doi.org/10.1038/nrg3745

Schneeberger, K., Ossowski, S., Lanz, C., Juul, T., Petersen, A.H., Nielsen, K.L., Jørgensen, J.-E., Weigel, D., Andersen, S.U., 2009. SHOREmap: simultaneous mapping and mutation identification by deep sequencing. Nat. Methods 6, 550. https://doi.org/10.1038/nmeth0809-550

Schoonhoven, L.M., Loon, J.J.A. van., Dicke, M., 2005. Insect-plant biology. Oxford University Press.

Schramm, K., Vassão, D.G., Reichelt, M., Gershenzon, J., Wittstock, U., 2012. Metabolism of glucosinolate-derived isothiocyanates to glutathione conjugates in generalist lepidopteran herbivores. Insect Biochem. Mol. Biol. 42, 174–182. https://doi.org/10.1016/J.IBMB.2011.12.002

Schuler, F., Casida, J.E., 2001. Functional coupling of PSST and ND1 subunits in NADH:ubiquinone oxidoreductase established by photoaffinity labeling. Biochim. Biophys. Acta - Bioenerg. 1506, 79–87. https://doi.org/10.1016/S0005-2728(01)00183-9

Schwede, T., Kopp, J., Guex, N., Peitsch, M.C., 2003. SWISS-MODEL: an automated protein homology-modeling server. Nucleic Acids Res. 31, 3381–3385. https://doi.org/10.1093/nar/gkg520

Schweizer, F., Heidel-Fischer, H., Vogel, H., Reymond, P., 2017. *Arabidopsis* glucosinolates trigger a contrasting transcriptomic response in a generalist and a specialist herbivore. Insect Biochem. Mol. Biol. 135, 561–573. https://doi.org/10.1016/j.ibmb.2017.04.004

Scott, J.G., 1990. Investigating Mechanisms of Insecticide Resistance: Methods, Strategies, and Pitfalls, in: Pesticide Resistance in Arthropods. Springer US, Boston, MA, pp. 39–57.

Segrè, A. V, Murray, A.W., Leu, J.-Y., 2006. High-resolution mutation mapping reveals parallel experimental evolution in yeast. PLoS Biol. 4, e256. https://doi.org/10.1371/journal.pbio.0040256

Sham, P., Bader, J.S., Craig, I., O'Donovan, M., Owen, M., 2002. DNA Pooling: a tool for large-scale association studies. Nat. Rev. Genet. 3, 862–871. https://doi.org/10.1038/nrg930

Sharom, F.J., 2011. The P-glycoprotein multidrug transporter. Essays Biochem. 50.

Shen, X., Zhou, M., Lu, W., Ohm, H., 2003. Detection of *Fusarium* head blight resistance QTL in a wheat population using bulked segregant analysis. Theor. Appl. Genet. 106, 1041–1047. https://doi.org/10.1007/s00122-002-1133-8

Shi, L., Wei, P., Wang, X., Shen, G., Zhang, J., Xiao, W., Xu, Z., Xu, Q., He, L., 2016a. Functional analysis of esterase TCE2 gene from *Tetranychus cinnabarinus* (Boisduval) involved in acaricide resistance. Sci. Rep. 6, 18646. https://doi.org/10.1038/srep18646

Shi, L., Zhang, J., Shen, G., Xu, Z., Wei, P., Zhang, Y., Xu, Q., He, L., 2015. Silencing NADPH-cytochrome P450 reductase results in reduced acaricide resistance in *Tetranychus cinnabarinus* (Boisduval). Sci. Rep. 5, 15581. https://doi.org/10.1038/srep15581

Shi, L., Zhang, J., Shen, G., Xu, Z., Xu, Q., He, L., 2016b. Collaborative contribution of six cytochrome P450 monooxygenase genes to fenpropathrin resistance in *Tetranychus cinnabarinus* (Boisduval). Insect Mol. Biol. 25, 653–665. https://doi.org/10.1111/imb.12251

Shin, R., An, J.M., Park, C.J., Kim, Y.J., Joo, S., Kim, W.T., Paek, K.H., 2004. *Capsicum annuum* tobacco mosaic virus-induced clone 1 expression perturbation alters the plant's response to ethylene and interferes with the redox homeostasis. Plant Physiol 135, 561–573. https://doi.org/10.1104/pp.103.035436

Shiraishi, Y., Murai, M., Sakiyama, N., Ifuku, K., Miyoshi, H., 2012. Fenpyroximate binds to the interface between PSST and 49 kDa subunits in mitochondrial NADH-Ubiquinone oxidoreductase. Biochemistry 51, 1953–1963. https://doi.org/10.1021/bi300047h

Škarydová, L., Wsól, V., 2012. Human microsomal carbonyl reducing enzymes in the metabolism of xenobiotics: well-known and promising members of the SDR superfamily. Drug Metab. Rev.

https://doi.org/10.3109/03602532.2011.638304

Skrinjaric-Spoljar, M., Matthews, H.B., Engel, J.L., Casida, J.E., 1971. Response of hepatic microsomal mixed-function oxidases to various types of insecticide chemical synergists administered to mice. Biochem. Pharmacol. 20, 1607–1618. https://doi.org/10.1016/0006-2952(71)90289-9

Smith, H.A., White, B.J., Kundert, P., Cheng, C., Romero-Severson, J., Andolfatto, P., Besansky, N.J., 2015. Genome-wide QTL mapping of saltwater tolerance in sibling species of *Anopheles* (malaria vector) mosquitoes. Heredity (Edinb). 115, 471–479. https://doi.org/10.1038/hdy.2015.39

Smyth, G.K., 2004. Linear models and empirical bayes methods for assessing differential expression in microarray experiments. Stat. Appl. Genet. Mol. Biol. 3, 1–25. https://doi.org/10.2202/1544-6115.1027

Snoeck, S., Kurlovs, A., Bajda, S., Feyereisen, R., Villacis-Perez, E., Kosterlitz, O., Dermauw, W., Clark, R.M., Van Leeuwen, T., 2019a. High-resolution QTL mapping in *Tetranychus urticae* reveals acaricide-specific responses and common target-site resistance after selection by different METI-I acaricides. Insect Biochem. Mol. Biol. 110, 19–33. https://doi.org/10.1016/J.IBMB.2019.04.011

Snoeck, S., Pavlidi, N., Pipini, D., Vontas, J., Dermauw, W., Van Leeuwen, T., 2019b. Substrate specificity and promiscuity of horizontally transferred UDP-glycosyltransferases in the generalist herbivore *Tetranychus urticae*. Insect Biochem. Mol. Biol. 109, 116–127. https://doi.org/10.1016/J.IBMB.2019.04.010

Snoeck, S., Wybouw, N., Van Leeuwen, T., Dermauw, W., 2018. Transcriptomic plasticity in the arthropod generalist *Tetranychus urticae* upon long-term acclimation to different host plants. G3 (Bethesda). 8, 3865–3879. https://doi.org/10.1534/g3.118.200585

Sogorb, M.A., Vilanova, E., 2002. Enzymes involved in the detoxification of organophosphorus, carbamate and pyrethroid insecticides through hydrolysis. Toxicol. Lett. 128, 215–228. https://doi.org/10.1016/S0378-4274(01)00543-4

Song, C., Hong, X., Zhao, S., Liu, J., Schulenburg, K., Huang, F.-C., Franz-Oberdorf, K., Schwab, W., 2016. Glucosylation of 4-hydroxy-2,5-dimethyl-3(2H)-furanone, the key strawberry flavor compound in strawberry fruit. Plant Physiol. 171, 139–151. https://doi.org/10.1104/pp.16.00226

Sparks, T.C., 2013. Insecticide discovery: an evaluation and analysis. Pestic. Biochem. Physiol. 107, 8–17. https://doi.org/10.1016/j.pestbp.2013.05.012

Sparks, T.C., Lockwood, J.A., Byford, R.L., Graves, J.B., Leonard, B.R., 1989. The role of behavior in insecticide resistance. Pestic. Sci. 26, 383–399. https://doi.org/10.1002/ps.2780260406

Sparks, T.C., Nauen, R., 2015. IRAC: Mode of action classification and insecticide resistance management. Pestic. Biochem. Physiol. 121, 122–128. https://doi.org/10.1016/j.pestbp.2014.11.014

Stafford-Banks, C.A., Rotenberg, D., Johnson, B.R., Whitfield, A.E., Ullman, D.E., 2014. Analysis of the salivary gland transcriptome of *Frankliniella occidentalis*. PLoS One 9, e94447. https://doi.org/10.1371/journal.pone.0094447

Stahl, E., Hilfiker, O., Reymond, P., 2018. Plant–arthropod interactions: who is the winner? Plant J. 93, 703–728. https://doi.org/10.1111/tpj.13773

Stamatakis, A., 2014. RAxML version 8: a tool for phylogenetic analysis and post-analysis of large phylogenies. Bioinformatics 30, 1312–3. https://doi.org/10.1093/bioinformatics/btu033

Sterck, L., Billiau, K., Abeel, T., Rouzé, P., Van de Peer, Y., 2012. ORCAE: online resource for community annotation of eukaryotes. Nat. Methods 9, 1041. https://doi.org/10.1038/nmeth.2242

Stetler, R.A., Gan, Y., Zhang, W., Liou, A.K., Gao, Y., Cao, G., Chen, J., 2010. Heat shock proteins: Cellular and molecular mechanisms in the central nervous system. Prog. Neurobiol. https://doi.org/10.1016/j.pneurobio.2010.05.002

Strobel, H.W., Dignam, J.D., 1978. Purification and properties of NADPH-cytochrome P-450 reductase. Methods Enzymol. 52, 89–96.

Strong, D., Lawton, J., Southwood, S., 1984. Insects on plants. Community patterns and mechanisms., Science. Harvard University Press.

Strycharz, J.P., Lao, A., Li, H., Qiu, X., Lee, S.H., Sun, W., Yoon, K.S., Doherty, J.J., Pittendrigh, B.R., Clark, J.M., 2013. Resistance in the highly DDT-resistant 91-R strain of *Drosophila melanogaster* involves decreased penetration, increased metabolism, and direct excretion. Pestic. Biochem. Physiol. 107, 207–217. https://doi.org/10.1016/j.pestbp.2013.06.010

Stumpf, N., Nauen, R., 2002. Biochemical markers linked to abamectin resistance in *Tetranychus urticae* (Acari: Tetranychidae). Pestic. Biochem. Physiol. 72, 111–121. https://doi.org/10.1006/pest.2001.2583

Su, X., Shen, G., Di, S., Dixon, R.A., Pang, Y., 2017. Characterization of UGT716A1 as a multi-substrate UDP:flavonoid glucosyltransferase gene in *Ginkgo biloba*. Front. Plant Sci. 8, 2085. https://doi.org/10.3389/fpls.2017.02085

Su, Y.L., Li, J.M., Li, M., Luan, J.B., Ye, X.D., Wang, X.W., Liu, S.S., 2012. Transcriptomic analysis of the salivary glands of an invasive whitefly. PLoS One 7, e39303. https://doi.org/10.1371/journal.pone.0039303

Sun, Y.P., Johnson, E.R., 1972. Quasi-synergism and penetration of insecticides. J. Econ. Entomol. 65, 349–53. https://doi.org/10.1093/jee/65.2.349

Suzuki, T., Nunes, M.A., España, M.U., Namin, H.H., Jin, P., Bensoussan, N., Zhurov, V., Rahman, T., Clercq, R. De, Hilson, P., Grbic, V., Grbic, M., 2017. RNAi-based reverse genetics in the chelicerate model *Tetranychus urticae*: a comparative analysis of five methods for gene silencing. PLoS One 12, e0180654. https://doi.org/10.1371/JOURNAL.PONE.0180654

Swinnen, S., Schaerlaekens, K., Pais, T., Claesen, J., Hubmann, G., Yang, Y., Demeke, M., Foulquié-Moreno, M.R., Goovaerts, A., Souvereyns, K., Clement, L., Dumortier, F., Thevelein, J.M., 2012. Identification of novel causative genes determining the complex trait of high ethanol tolerance in yeast using pooled-segregant whole-genome sequence analysis. Genome Res. 22, 975–84. https://doi.org/10.1101/gr.131698.111

Tabashnik, B.E., Mota-Sanchez, D., Whalon, M.E., Hollingworth, R.M., Carrière, Y., C., L., Y., Y., S., W., K., W., J., C., 2014. Defining terms for proactive management of resistance to Bt crops and pesticides. J. Econ. Entomol. 107, 496–507. https://doi.org/10.1603/EC13458

Taj, H.F. El, Hossain, K.F., Arifunnahar, M., Alim, M.A., Bachchu, M.A.A., 2016. Effects of host plants and seasons on the biology of the two-spotted spider mite, *Tetranychus urticae* (Koch). African Entomol. 24, 188–196. https://doi.org/10.4001/003.024.0188

Takagi, H., Abe, A., Yoshida, K., Kosugi, S., Natsume, S., Mitsuoka, C., Uemura, A., Utsushi, H., Tamiru, M., Takuno, S., Innan, H., Cano, L.M., Kamoun, S., Terauchi, R., 2013. QTL-seq: rapid mapping of quantitative trait loci in rice by whole genome resequencing of DNA from two bulked populations. Plant J. 74, 174–183. https://doi.org/10.1111/tpj.12105

Takeda, K., Noguchi, T., Naguro, I., Ichijo, H., 2008. Apoptosis signal-regulating kinase 1 in stress and immune response. Annu. Rev. Pharmacol. Toxicol. 48, 199–225. https://doi.org/10.1146/annurev.pharmtox.48.113006.094606

Tamura, K., Stecher, G., Peterson, D., Filipski, A., Kumar, S., 2013. MEGA6: molecular evolutionary genetics analysis version 6.0. Mol. Biol. Evol. 30, 2725–2729. https://doi.org/10.1093/molbev/mst197

Techer, M.A., Rane, R. V., Grau, M.L., Roberts, J.M.K., Sullivan, S.T., Liachko, I., Childers, A.K., Evans, J.D., Mikheyev, A.S., 2019. Genomic analyses of sibling honey bee ectoparasitic mite species show divergent strategies of adaptation. bioRxiv 512988. https://doi.org/10.1101/512988

Thomas, J.H., 2006. Analysis of homologous gene clusters in *Caenorhabditis elegans* reveals striking regional cluster domains. Genetics 172, 127–143. https://doi.org/10.1534/genetics.104.040030

Thomson, S.A., Baldwin, W.S., Wang, Y.H., Kwon, G., LeBlanc, G.A., 2009. Annotation, phylogenetics, and expression of the nuclear receptors in *Daphnia pulex*. BMC Genomics 10, 500. https://doi.org/10.1186/1471-2164-10-500

Tian, F., Wang, Z., Li, C., Liu, J., Zeng, X., 2018. UDP-glycosyltransferases are involved in imidacloprid resistance in the Asian citrus psyllid, *Diaphorina citri* (Hemiptera: Lividae). Pestic. Biochem. Physiol. 154, 23–31. https://doi.org/10.1016/J.PESTBP.2018.12.010

Tibshirani, R., Walther, G., Hastie, T., 2001. Estimating the number of clusters in a data set via the gap statistic. J. R. Stat. Soc. Ser. B, Stat. Methodol. 63, 411–423. https://doi.org/10.1111/1467-9868.00293

Tocilescu, M.A., Fendel, U., Zwicker, K., Dröse, S., Kerscher, S., Brandt, U., 2010. The role of a conserved tyrosine in the 49-kDa subunit of complex I for ubiquinone binding and reduction. Biochim. Biophys. Acta - Bioenerg. 1797, 625–632. https://doi.org/10.1016/j.bbabio.2010.01.029

Trible, W., Olivos-Cisneros, L., McKenzie, S.K., Saragosti, J., Chang, N.-C., Matthews, B.J., Oxley, P.R., Kronauer, D.J.C., 2017. Orco mutagenesis causes loss of antennal lobe glomeruli and impaired social behavior in ants. Cell 170, 727-735.e10. https://doi.org/10.1016/j.cell.2017.07.001

Tsagkarakou, A., Pasteur, N., Cuany, A., Chevillon, C., Navajas, M., 2002. Mechanisms of resistance to organophosphates in *Tetranychus urticae* (Acari: Tetranychidae) from Greece. Insect Biochem. Mol. Biol. 32, 417–24.

Tsagkarakou, A., Van Leeuwen, T., Khajehali, J., Ilias, A., Grispou, M., Williamson, M.S., Tirry, L., Vontas, J., 2009. Identification of pyrethroid resistance associated mutations in the para sodium channel of the two-spotted spider mite *Tetranychus urticae* (Acari: Tetranychidae). Insect Mol. Biol. 18, 583–593. https://doi.org/10.1111/j.1365-2583.2009.00900.x

Turner, T.L., Miller, P.M., 2012. Investigating natural variation in *Drosophila* courtship song by the evolve and resequence approach. Genetics 191, 633–642. https://doi.org/10.1534/genetics.112.139337

Turner, T.L., Stewart, A.D., Fields, A.T., Rice, W.R., Tarone, A.M., 2011. Population-based resequencing of experimentally evolved populations reveals the genetic basis of body size variation in *Drosophila melanogaster*. PLoS Genet. 7, e1001336. https://doi.org/10.1371/journal.pgen.1001336

Udhane, S.S., Parween, S., Kagawa, N., Pandey, A. V., 2017. Altered CYP19A1 and CYP3A4 activities due to mutations A115V, T142A, Q153R and P284L in the human P450 oxidoreductase. Front. Pharmacol. 25, 580. https://doi.org/10.3389/fphar.2017.00580

Valles, S., Koehler, P., Brenner, R., 1997. Antagonism of fipronil toxicity by piperonyl butoxide and S,S,S-tributyl phosphorotrithioate in the German cockroach (Dictyoptera: Blattellidae). J. Econ. Entomol. 90, 1254–1258. https://doi.org/10.1093/jee/90.5.1254

Van der Auwera, G.A., Carneiro, M.O., Hartl, C., Poplin, R., del Angel, G., Levy-Moonshine, A., Jordan, T., Shakir, K., Roazen, D., Thibault, J., Banks, E., Garimella, K. V., Altshuler, D., Gabriel, S., DePristo, M.A., 2013. From fastQ data to high-confidence variant calls: the genome analysis toolkit best practices pipeline. Curr. Protoc. Bioinforma. 43, 11.10.1-11.10.33. https://doi.org/10.1002/0471250953.bi1110s43

Van Leeuwen, T., Demaeght, P., Osborne, E.J., Dermauw, W., Gohlke, S., Nauen, R., Grbic, M., Tirry, L., Merzendorfer, H., Clark, R.M., 2012. Population bulk segregant mapping uncovers resistance mutations and the mode of action of a chitin synthesis inhibitor in arthropods. Proc. Natl. Acad. Sci. 109, 4407–4412. https://doi.org/10.1073/pnas.1200068109

Van Leeuwen, T., Dermauw, W., 2016. The molecular evolution of xenobiotic metabolism and resistance in chelicerate mites. Annu. Rev. Entomol. 61, 475–498. https://doi.org/10.1146/annurev-ento-010715-023907

Van Leeuwen, T., Stillatus, V., Tirry, L., 2004. Genetic analysis and cross-resistance spectrum of a laboratory-selected chlorfenapyr resistant strain of two-spotted spider mite (Acari: Tetranychidae). Exp. Appl. Acarol. 32, 249–261. https://doi.org/10.1023/B:APPA.0000023240.01937.6d

Van Leeuwen, T., Tirry, L., 2007. Esterase-mediated bifenthrin resistance in a multiresistant strain of the two-spotted spider mite, *Tetranychus urticae*. Pest Manag. Sci. 63, 150–156. https://doi.org/10.1002/ps.1314

Van Leeuwen, T., Tirry, L., Nauen, R., 2006. Complete maternal inheritance of bifenazate resistance in *Tetranychus urticae* Koch (Acari: Tetranychidae) and its implications in mode of action considerations. Insect Biochem. Mol. Biol. 36, 869–877. https://doi.org/10.1016/j.ibmb.2006.08.005

Van Leeuwen, T., Tirry, L., Yamamoto, A., Nauen, R., Dermauw, W., 2014. The economic importance of acaricides in the control of phytophagous mites and an update on recent acaricide mode of action research. Pestic. Biochem. Physiol. 121, 12–21. https://doi.org/10.1016/j.pestbp.2014.12.009

Van Leeuwen, T., Vanholme, B., Van Pottelberge, S., Van Nieuwenhuyse, P., Nauen, R., Tirry, L., Denholm, I., 2008. Mitochondrial heteroplasmy and the evolution of insecticide resistance: non-Mendelian inheritance in action. Proc. Natl. Acad. Sci. U. S. A. 105, 5980–5985. https://doi.org/10.1073/pnas.0802224105

Van Leeuwen, T., Vontas, J., Tsagkarakou, A., Dermauw, W., Tirry, L., 2010. Acaricide resistance mechanisms in the two-spotted spider mite *Tetranychus urticae* and other important Acari: a review. Insect Biochem. Mol. Biol. 40, 563–72. https://doi.org/10.1016/j.ibmb.2010.05.008

Van Nieuwenhuyse, P., Demaeght, P., Dermauw, W., Khalighi, M., Stevens, C. V., Vanholme, B., Tirry, L., Lümmen, P., Van Leeuwen, T., 2012. On the mode of action of bifenazate: new evidence for a mitochondrial target site. Pestic. Biochem. Physiol. 104, 88–95. https://doi.org/10.1016/j.pestbp.2012.05.013

Van Petegem, K., Moerman, F., Dahirel, M., Fronhofer, E.A., Vandegehuchte, M.L., Van Leeuwen, T., Wybouw, N., Stoks, R., Bonte, D., 2018. Kin competition accelerates experimental range expansion in an arthropod herbivore. Ecol. Lett. 21, 225–234. https://doi.org/10.1111/ele.12887

Van Pottelberge, S., Khajehali, J., Van Leeuwen, T., Tirry, L., 2009a. Effects of spirodiclofen on reproduction in a susceptible and resistant strain of Tetranychus urticae (Acari: Tetranychidae). Exp. Appl. Acarol. 47, 301–309. https://doi.org/10.1007/s10493-008-9226-y

Van Pottelberge, S., Van Leeuwen, T., Khajehali, J., Tirry, L., 2009b. Genetic and biochemical analysis of a laboratory-selected spirodiclofen-resistant strain of *Tetranychus urticae* Koch (Acari: Tetranychidae). Pest Manag. Sci. 65, 358–366. https://doi.org/10.1002/ps.1698

Van Pottelberge, S., Van Leeuwen, T., Nauen, R., Tirry, L., 2009c. Resistance mechanisms to mitochondrial electron transport inhibitors in a field-collected strain of *Tetranychus urticae* Koch (Acari: Tetranychidae). Bull. Entomol. Res. 99, 23–31. https://doi.org/10.1017/S0007485308006081

Van Pottelberge, S., Van Leeuwen, T., Van Amermaet, K., Tirry, L., 2008. Induction of cytochrome P450 monooxygenase activity in the two-spotted spider mite *Tetranychus urticae* and its influence on acaricide toxicity. Pestic. Biochem. Physiol. 91, 128–133. https://doi.org/10.1016/j.pestbp.2008.03.005

Väremo, L., Nielsen, J., Nookaew, I., 2013. Enriching the gene set analysis of genome-wide data by incorporating directionality of gene expression and combining statistical hypotheses and methods. Nucleic Acids Res. 41, 4378–4391.

Veerman, A., 1985. Diapause, in: Sabelis, M.W., Helle, W. (Eds.), Spider Mites: Their Biology, Natural Anemies and Control. Elsevier, Amsterdam, pp. 279–316. https://doi.org/10.1111/j.1570-7458.1987.tb03606.x

Vermetten, E., Bremner, J.D., 2002. Circuits and systems in stress. I. Preclinical studies. Depress. Anxiety 15, 126–147. https://doi.org/10.1002/da.10016

Villarroel, C.A., Jonckheere, W., Alba, J.M., Glas, J.J., Dermauw, W., Haring, M.A., Van Leeuwen, T., Schuurink, R.C., Kant, M.R., 2016. Salivary proteins of spider mites suppress defenses in *Nicotiana benthamiana* and promote mite reproduction. Plant J. 86, 119–131. https://doi.org/10.1111/tpj.13152

Vinothkumar, K.R., Zhu, J., Hirst, J., 2014. Architecture of mammalian respiratory complex I. Nature 515, 80–84. https://doi.org/10.1038/nature13686

Vinson, S.B., 1976. Host selection by insect parasitoids. Annu. Rev. Entomol. 21, 109–133. https://doi.org/10.1146/annurev.en.21.010176.000545

Voelckel, C., Baldwin, I.T., 2004. Generalist and specialist lepidopteran larvae elicit different transcriptional responses in *Nicotiana attenuata*, which correlate with larval FAC profiles. Ecol. Lett. 7, 770–775. https://doi.org/10.1111/j.1461-0248.2004.00633.x

Vogel, H., Musser, R.O., de la Paz Celorio-Mancera, M., 2014. Transcriptome responses in herbivorous insects towards host plant and toxin feeding, in: Annual Plant Reviews: Insect-Plant Interactions. Wiley-Blackwell, Chichester, UK, pp. 197–234. https://doi.org/10.1002/9781118829783.ch6

Vontas, J.G., Small, G.J., Hemingway, J., 2001. Glutathione S-transferases as antioxidant defence agents confer pyrethroid resistance in Nilaparvata lugens. Biochem. J. 357, 65–72.

Wada-Katsumata, A., Silverman, J., Schal, C., 2013. Changes in taste neurons support the emergence of an adaptive behavior in cockroaches. Science 340, 972–5. https://doi.org/10.1126/science.1234854

Waldron, R., McGowan, J., Gordon, N., McCarthy, C., Mitchell, E.B., Doyle, S., Fitzpatrick, D.A., 2017. Draft genome sequence of *Dermatophagoides pteronyssinus*, the european house dust mite. Parasit Vectors 8, 585. https://doi.org/10.1186/S13071-015-1198-2

Walter, D.E., 1996. Living on leaves: mites, tomenta, and leaf domatia. Annu. Rev. Entomol. 41, 101–114. https://doi.org/10.1146/annurev.ento.41.1.101

Walter, D.E., Proctor, H.C., 2013. Mites: ecology, evolution & behaviour. Life at microscale, 2nd ed. https://doi.org/10.1007/978-94-007-7164-2

Wang, C., Gong, B., Bushel, P.R., Thierry-Mieg, J., Thierry-Mieg, D., Xu, J., Fang, H., Hong, H., Shen, J., Su, Z., Meehan, J., Li, X., Yang, L., Li, H., ?abaj, P.P., Kreil, D.P., Megherbi, D., Gaj, S., Caiment, F., van Delft, J., Kleinjans, J., Scherer, A., Devanarayan, V., Wang, J., Yang, Y., Qian, H.-R., Lancashire, L.J., Bessarabova, M., Nikolsky, Y., Furlanello, C., Chierici, M., Albanese, D., Jurman, G., Riccadonna, S., Filosi, M., Visintainer, R., Zhang, K.K., Li, J., Hsieh, J.-H., Svoboda, D.L., Fuscoe, J.C., Deng, Y., Shi, L., Paules, R.S., Auerbach, S.S., Tong, W., 2014. The concordance between RNA-seq and microarray data depends on chemical treatment and transcript abundance. Nat. Biotechnol. 32, 926–932. https://doi.org/10.1038/nbt.3001

Wang, C., Scharf, M.E., Bennett, G.W., 2004. Behavioral and physiological resistance of the German cockroach to gel baits (Blattodea: Blattellidae). J. Econ. Entomol. 97, 2067–2072. https://doi.org/10.1093/jee/97.6.2067

Wang, H., Shi, Y., Wang, L., Liu, S., Wu, S., Yang, Y., Feyereisen, R., Wu, Y., 2018. CYP6AE gene cluster knockout in *Helicoverpa armigera* reveals role in detoxification of phytochemicals and insecticides. Nat. Commun. 9, 4820. https://doi.org/10.1038/s41467-018-07226-6

Wang, L., Zhang, Y.-J., Wu, Q.-J., Xie, W., Wang, S.-L., 2015. Establishment and application of the PASA technique of resistance detection to bifenthrin resis tance in Tetranychus urticae Koch(Acari: Tetranychidae). Chinese J. Appl. Entomol. 52, 510–518.

Wang, M., Roberts, D., 1997. Three-dimensional structure of NADPH–cytochrome P450 reductase: prototype for FMN-and FAD-containing enzymes. Proc. Natl. Acad. Sci. U. S. A. 94, 8411–8416. https://doi.org/10.1073/pnas.94.16.8411

Wang, M., Zuris, J.A., Meng, F., Rees, H., Sun, S., Deng, P., Han, Y., Gao, X., Pouli, D., Wu, Q., Georgakoudi, I., Liu, D.R., Xu, Q., 2016. Efficient delivery of genome-editing proteins using bioreducible lipid nanoparticles. Proc. Natl. Acad. Sci. U. S. A. 113, 2868–73. https://doi.org/10.1073/pnas.1520244113

Wang, M.Y., Liu, X.Y., Shi, L., Liu, J.L., Shen, G.M., Zhang, P., Lu, W.C., He, L., 2018. Functional analysis of UGT201D3 associated with abamectin resistance in Tetranychus cinnabarinus (Boisduval). Insect Sci. 00, 1–16. https://doi.org/10.1111/1744-7917.12637

Wang, R., Wu, Y., 2014. Dominant fitness costs of abamectin resistance in *Plutella xylostella*. Pest Manag. Sci. 70, 1872–1876. https://doi.org/10.1002/ps.3741

Wang, Z., Gerstein, M., Snyder, M., 2009. RNA-Seq: a revolutionary tool for transcriptomics. Nat. Rev. Genet. 10, 57–63. https://doi.org/10.1038/nrg2484

War, A.R., Paulraj, M.G., Ahmad, T., Buhroo, A.A., Hussain, B., Ignacimuthu, S., Sharma, H.C., 2012. Mechanisms of plant defense against insect herbivores. Plant Signal. Behav. 7, 1306–20. https://doi.org/10.4161/psb.21663

Warnes, G.R., Bolker, B., Bonebakker, L., Gentleman, R., Liaw, W.H.A., Lumley, T., Maechler, M., Magnusson, A., Moeller, S., Schwartz, M., Venables, B., 2009. Package “gplots”: Various R programming tools for plotting data. R Packag. version 2.17.0. 2, 1. https://doi.org/10.1111/j.0022-3646.1997.00569.x

Watanabe, T., Manabe, S., Ohashi, Y., Okamiya, H., Onodera, H., Mitsumori, K., 1998. Comparison of the induction profile of hepatic drug-metabolizing enzymes between piperonyl butoxide and phenobarbital in rats. J. Toxicol. Pathol. 11, 1–10. https://doi.org/10.1293/tox.11.1

Wei, P., Chen, M., Nan, C., Feng, K., Shen, G., Cheng, J., He, L., 2019a. Downregulation of carboxylesterase contributes to cyflumetofen resistance in *Tetranychus cinnabarinus* (Boisduval). Pest Manag. Sci. https://doi.org/10.1002/ps.5339

Wei, P., Li, J., Liu, X., Nan, C., Shi, L., Zhang, Y., Li, C., He, L., 2019b. Functional analysis of four upregulated carboxylesterase genes associated with fenpropathrin resistance in *Tetranychus cinnabarinus* (Boisduval). Pest Manag. Sci. 75, 252–261. https://doi.org/10.1002/ps.5109

Weissenberg, M., Klein, M., Meisner, J., Ascher, K.R.S., 1986. Larval growth inhibition of the spiny bollworm, *Earias insulana*, by some steroidal secondary plant compounds. Entomol. Exp. Appl. 42, 213–217. https://doi.org/10.1111/j.1570-7458.1986.tb01024.x

Whittaker, R.H., Feeny, P.P., 1971. Allelochemics: chemical interactions between species. Science (80-.). 171, 757–770. https://doi.org/10.1126/science.171.3973.757

Wickham, H., 2009. ggplot2 elegant graphics for data analysis. Media 35, 211. https://doi.org/10.1007/978-0-387-98141-3

Wickham, H., Francois, R., 2015. dplyr: a grammar of data manipulation. https://doi.org/10.18637/jss.v072.i07>.Depends

Willoughby, L., Batterham, P., Daborn, P.J., 2007. Piperonyl butoxide induces the expression of cytochrome P450 and glutathione S-transferase genes in *Drosophila melanogaster*. Pest Manag. Sci. 63, 803–808. https://doi.org/10.1002/ps.1391

Willoughby, L., Chung, H., Lumb, C., Robin, C., Batterham, P., Daborn, P.J., 2006. A comparison of *Drosophila melanogaster* detoxification gene induction responses for six insecticides, caffeine and phenobarbital. Insect Biochem. Mol. Biol. 36, 934–942. https://doi.org/10.1016/j.ibmb.2006.09.004

Wink, M., 2010. Annual plant reviews volume 40, biochemistry of plant secondary metabolism, second edition. Annu. Plant Rev. https://doi.org/10.1002/9781444320503

Wirth, C., Brandt, U., Hunte, C., Zickermann, V., Zick, V., 2016. Structure and function of mitochondrial complex I. BBA - Bioenerg. 1857, 902–914. https://doi.org/10.1016/j.bbabio.2016.02.013

Wolstenholme, A.J., Rogers, A.T., 2005. Glutamate-gated chloride channels and the mode of action of the avermectin/milbemycin anthelmintics. Parasitology 131, S85–S95. https://doi.org/10.1017/S0031182005008218

World Health Organization, United Nations Environment Programme, Internalional Labour Organization, International Programme on Chemical safety, 1986. Organophosphorus insecticides : a general introduction / published under the joint sponsorship of the United Nations Environment Programme, the International Labour Organisation, and the World Health Organization. World Health Organization; Geneva.

Wouters, F.C., Blanchette, B., Gershenzon, J., Vassão, D.G., 2016. Plant defense and herbivore counter-defense: benzoxazinoids and insect herbivores. Phytochem. Rev. 15, 1127–1151. https://doi.org/10.1007/s11101-016-9481-1

Wouters, F.C., Reichelt, M., Glauser, G., Bauer, E., Erb, M., Gershenzon, J., Vassão, D.G., 2014. Reglucosylation of the benzoxazinoid DIMBOA with inversion of stereochemical configuration is a detoxification strategy in lepidopteran herbivores. Angew. Chem. Int. Ed. Engl. 53, 11320–4. https://doi.org/10.1002/anie.201406643

Wu, M., Adesanya, A.W., Morales, M.A., Walsh, D.B., Lavine, L.C., Lavine, M.D., Fang Zhu, ·, 2019. Multiple acaricide resistance and underlying mechanisms in *Tetranychus urticae* on hops. J. Pest Sci. (2004). 92, 543–555. https://doi.org/10.1007/s10340-018-1050-5

Wybouw, N., 2015. The role of horizontally transferred genes in the xenobiotic adaptations of the spider mite Tetranychus urticae. University of Amsterdam.

Wybouw, N., Balabanidou, V., Ballhorn, D.J., Dermauw, W., Grbić, M., Vontas, J., Van Leeuwen, T., 2012. A horizontally transferred cyanase gene in the spider mite *Tetranychus urticae* is involved in cyanate

metabolism and is differentially expressed upon host plant change. Insect Biochem. Mol. Biol. 42, 881–889. https://doi.org/10.1016/j.ibmb.2012.08.002

Wybouw, N., Dermauw, W., Tirry, L., Stevens, C., Grbić, M., Feyereisen, R., Van Leeuwen, T., 2014. A gene horizontally transferred from bacteria protects arthropods from host plant cyanide poisoning. Elife 3, e02365. https://doi.org/10.7554/eLife.02365

Wybouw, N., Kosterlitz, O., Kurlovs, A.H., Bajda, S., Greenhalgh, R., Snoeck, S., Bui, H., Bryon, A., Dermauw, W., Van Leeuwen, T., Clark, R.M., 2019. Long-term population studies uncover the genome structure and genetic basis of xenobiotic and host plant adaptation in the herbivore *Tetranychus urticae*. Genetics 211, 1409–1427. https://doi.org/10.1534/genetics.118.301803

Wybouw, N., Pauchet, Y., Heckel, D.G., Leeuwen, T. Van, 2016. Horizontal gene transfer contributes to the evolution of arthropod herbivory. Genome Biol. Evol. 8, 1785–1801. https://doi.org/10.1093/gbe/evw119

Wybouw, N., Van Leeuwen, T., Dermauw, W., 2018. A massive incorporation of microbial genes into the genome of *Tetranychus urticae*, a polyphagous arthropod herbivore. Insect Mol. Biol. 27, 333–351. https://doi.org/10.1111/imb.12374

Wybouw, N., Zhurov, V., Martel, C., Bruinsma, K.A., Hendrickx, F., Grbic, V., Van Leeuwen, T., 2015. Adaptation of a polyphagous herbivore to a novel host plant extensively shapes the transcriptome of herbivore and host. Mol. Ecol. 24, 4647–4663. https://doi.org/10.1111/mec.13330

Xie, S., You, L., Zeng, S., 2007. Studies on the flavonoid substrates of human UDP-glucuronosyl transferase (UGT) 2B7. Pharmazie 62, 625–9. https://doi.org/10.1691/ph.2007.8.6779

Xie, W., Wu, Q., Wang, S., Jiao, X., Guo, L., Zhou, X., Zhang, Y., 2014. Transcriptome analysis of host-associated differentiation in *Bemisia tabaci* (Hemiptera: Aleyrodidae). Front. Physiol. 10, 487. https://doi.org/10.3389/fphys.2014.00487

Yang, X., Buschman, L.L., Zhu, K.Y., Margolies, D.C., 2009. Susceptibility and detoxifying enzyme activity in two spider mite species (Acari: Tetranychidae) after selection with three insecticides. J. Econ. Entomol. 95, 399–406. https://doi.org/10.1603/0022-0493-95.2.399

Yang, X., Yan Zhu, K., L. Buschman, L., C. Margolies, D., 2001. Comparative susceptibility and possible detoxification mechanisms for selected miticides in Banks grass mite and two-spotted spider mite (Acari: Tetranychidae). Exp. Appl. Acarol. 25, 293–299. https://doi.org/10.1023/A:1017926920389

Yeoh, C.L., Kuwano, E., Eto, M., 1982. Effects of the fungicide IBP as a synergist on the metabolism of malathion in insects. J. Pestic. Sci. 7, 31–40. https://doi.org/10.1584/jpestics.7.31

Young, M.D., Wakefield, M.J., Smyth, G.K., 2010a. goseq : Gene ontology testing for RNA-seq datasets reading data. Gene 1–21.

Young, M.D., Wakefield, M.J., Smyth, G.K., Oshlack, A., 2010b. Gene ontology analysis for RNA-seq: accounting for selection bias. Genome Biol. 11, R14. https://doi.org/10.1186/gb-2010-11-2-r14

Young, S.J., Gunning, R. V., Moores, G.D., 2006. Effect of pretreatment with piperonyl butoxide on pyrethroid efficacy against insecticide-resistant *Helicoverpa armigera* (Lepidoptera: Noctuidae) and *Bemisia tabaci* (Sternorrhyncha: Aleyrodidae). Pest Manag. Sci. 62, 114–119. https://doi.org/10.1002/ps.1127

Young, S.J., Gunning, R. V, Moores, G.D., 2005. The effect of piperonyl butoxide on pyrethroid-resistance-associated esterases in *Helicoverpa armigera* (Hübner) (Lepidoptera: Noctuidae). Pest Manag. Sci. 61, 397–401. https://doi.org/10.1002/ps.996

Yu, J., Han, J.-C., Hua, L.-M., Gao, Y.-J., 2013. In vitro characterization of glucuronidation of vanillin: identification of human UDP-glucuronosyltransferases and species differences. Phyther. Res. 27, 1392–1397. https://doi.org/10.1002/ptr.4885

Yuk, H.J., Lee, J.H., Curtis-Long, M.J., Lee, J.W., Kim, Y.S., Ryu, H.W., Park, C.G., Jeong, T.S., Park, K.H., 2011. The most abundant polyphenol of soy leaves, coumestrol, displays potent α-glucosidase inhibitory activity. Food Chem. 126, 1057–1063. https://doi.org/10.1016/j.foodchem.2010.11.125

Yusa, K., Tsuruo, T., 1989. Reversal mechanism of multidrug resistance by verapamil: direct binding of

verapamil to p-glycoprotein on specific sites and transport of verapamil outward across the plasma membrane of K562/ADM cells. Cancer Res. 49, 5002–5006.

Zalucki, M., Furlong, M., 2017. Behavior as a mechanism of insecticide resistance: evaluation of the evidence. Curr. Opin. Insect Sci. 21, 19–25. https://doi.org/10.1016/J.COIS.2017.05.006

Zdobnov, E.M., Apweiler, R., 2001. InterProScan - An integration platform for the signature-recognition methods in InterPro. Bioinformatics 17, 847–848. https://doi.org/10.1093/bioinformatics/17.9.847

Zhan, S., Huang, J., Guo, Q., Zhao, Y., Li, W., Miao, X., Goldsmith, M.R., Li, M., Huang, Y., 2009. An integrated genetic linkage map for silkworms with three parental combinations and its application to the mapping of single genes and QTL. BMC Genomics 10, 389. https://doi.org/10.1186/1471-2164-10-389

Zhang, H., Tian, W., Zhao, J., Jin, L., Yang, J., Liu, C., Yang, Y., Wu, S., Wu, K., Cui, J., Tabashnik, B.E., Wu, Y., 2012. Diverse genetic basis of field-evolved resistance to Bt cotton in cotton bollworm from China. Proc. Natl. Acad. Sci. 109, 10275–10280. https://doi.org/10.1073/PNAS.1200156109

Zhang, J., Dean, A.M., Brunet, F., Long, M., 2004. Evolving protein functional diversity in new genes of *Drosophila*. Proc. Natl. Acad. Sci. 101, 16246–16250. https://doi.org/10.1073/pnas.0407066101

Zhang, J., Yang, H., Long, M., Li, L., Dean, A.M., 2010. Evolution of enzymatic activities of testis-specific short-chain dehydrogenase/reductase in *Drosophila*. J. Mol. Evol. 71, 241–249. https://doi.org/10.1007/s00239-010-9384-5

Zhang, X., Wang, J., Liu, J., Li, Y., Liu, X., Wu, H., Ma, E., Zhang, J., 2017. Knockdown of NADPH-cytochrome P450 reductase increases the susceptibility to carbaryl in the migratory locust, Locusta migratoria. Chemosphere 188, 517–524. https://doi.org/10.1016/J.CHEMOSPHERE.2017.08.157

Zhang, Z., Hsieh, B., Poe, A., Anderson, J., Ocorr, K., Gibson, G., Bodmer, R., 2013. Complex genetic architecture of cardiac disease in a wild type inbred strain of *Drosophila melanogaster*. PLoS One 8, e62909. https://doi.org/10.1371/journal.pone.0062909

Zhao, J.-Y., Zhao, X.-T., Sun, J.-T., Zou, L.-F., Yang, S.-X., Han, X., Zhu, W.-C., Yin, Q., Hong, X.-Y., 2017. Transcriptome and proteome analyses reveal complex mechanisms of reproductive diapause in the two-spotted spider mite, *Tetranychus urticae*. Insect Mol. Biol. 26, 215–232. https://doi.org/10.1111/imb.12286

Zhou, H.-J., Tsai, S.Y., Tsai, M.-J., 2003. RNAi technology and its use in studying the function of nuclear receptors and coregulators. Nucl. Recept. Signal. 1, e008. https://doi.org/10.1621/nrs.01008

Zhou, H., Zhang, Y.-Q., Lai, T., Liu, X.-J., Guo, F.-Y., Guo, T., Ding, W., 2019. Acaricidal mechanism of scopoletin against *Tetranychus cinnabarinus*. Front. Physiol. 10, 164. https://doi.org/10.3389/fphys.2019.00164

Zhu, F., Xu, J., Palli, R., Ferguson, J., Palli, S.R., 2011. Ingested RNA interference for managing the populations of the Colorado potato beetle, *Leptinotarsa decemlineata*. Pest Manag. Sci. 67, 175–182. https://doi.org/10.1002/ps.2048

Zhurov, V., Navarro, M., Bruinsma, K.A., Arbona, V., Santamaria, M.E., Cazaux, M., Wybouw, N., Osborne, E.J., Ens, C., Rioja, C., Vermeirssen, V., Rubio-Somoza, I., Krishna, P., Diaz, I., Schmid, M., Gomez-Cadenas, A., Van de Peer, Y., Grbic, M., Clark, R.M., Van Leeuwen, T., Grbic, V., 2014. Reciprocal responses in the interaction between *Arabidopsis* and the cell-content-feeding chelicerate herbivore spider mite. Plant Physiol. 164, 384–399. https://doi.org/10.1104/pp.113.231555

Zickermann, V., Wirth, C., Nasiri, H., Siegmund, K., Schwalbe, H., Hunte, C., Brandt, U., 2015. Mechanistic insight from the crystal structure of mitochondrial complex I. Science (80-.). 347, 44–49. https://doi.org/10.1126/science.1259859

Zimmer, C.T., Panini, M., Singh, K.S., Randall, E.L., Field, L.M., Roditakis, E., Mazzoni, E., Bass, C., 2017. Use of the synergist piperonyl butoxide can slow the development of alpha-cypermethrin resistance in the whitefly *Bemisia tabaci*. Insect Mol. Biol. 26, 152–163. https://doi.org/10.1111/IMB.12276

Zou, C., Wang, P., Xu, Y., 2016. Bulked sample analysis in genetics, genomics and crop improvement. Plant

Biotechnol. J. 14, 1941–1955. https://doi.org/10.1111/pbi.12559

Zou, X., Xu, Z., Zou, H., Liu, J., Chen, S., Feng, Q., Zheng, S., 2016. Glutathione S-transferase SlGSTE1 in *Spodoptera litura* may be associated with feeding adaptation of host plants. Insect Biochem. Mol. Biol. 70, 32–43. https://doi.org/10.1016/J.IBMB.2015.10.005

Summary

In **Chapter 1** the protagonist of this PhD, the two-spotted spider mite *T. urticae*, is introduced. This mite can thrive on a wide range of host plants and develops resistance against a diverse array of pesticides. Previously reported molecular mechanisms that, in part, underlie this extreme xenobiotic adaptation potential are briefly discussed. Finally, features of *T. urticae* that led to its genome sequencing are highlighted and bio-informatic approaches that could aid in unraveling the molecular mechanisms of xenobiotic adaptation in *T. urticae* are discussed.

In **Chapter 2**, a bulked segregant analysis (BSA) was used to identify loci underlying resistance to three different METI-I pesticides (fenpyroximate, pyridaben and tebufenpyrad). Our results suggest that selection with structural different METI-I pesticides resulted in both a common (the known H92R target-site mutation) and compound specific resistance mechanisms. A genomic region that included cytochrome P450-reductase (CPR) was associated with resistance against both pyridaben and tebufenpyrad. CPR is an essential electron donor for microsomal P450s (phase I detoxification enzyme family). Furthermore, a genomic region linked with tebufenpyrad resistance harbored a non-canonical member of the nuclear hormone receptor 96 (NHR96) gene family. This NHR96 gene does not encode a DNA-binding domain (DBD), an uncommon feature in arthropods, and belongs to a newly discovered and expanded family of 47 NHR96 proteins lacking DBDs in *T. urticae*.

RNA-seq was used in **Chapter 3**, to study the genome-wide transcriptional responses upon application of four synergists (DEF, DEM, PBO and CsA) in a pesticide resistant *T. urticae* strain. Synergists can counteract metabolic resistance by inhibiting detoxification enzymes or transporters. Hence, synergists are used for the elucidation of resistance mechanisms. Exposure to PBO and DEF resulted in a broad and partly shared transcriptional response, including phase I (P450s) and II (UGTs) detoxification families. CsA treatment mainly resulted in downregulation of the phase III detoxification Major Facilitator Superfamily, while application of the synergist DEM did not result in a profound transcriptomic response.

In **Chapter 4**, we profiled the transcriptome of *T. urticae* upon long-term transfer from *Phaseolus vulgaris* to a similar, but chemically defended, host (cyanogenic *Phaseolus lunatus)* and to multiple economically important crops (*Glycine max, Gossypium hirsutum*, *Solanum lycopersicum* and *Zea mays*). It is known that *T. urticae* rapidly acclimatizes and adapts to new hosts, and hereby overcomes nutritional challenges and novel plant defenses (both constitutive and induced plant defenses). Multiple studies investigated transcriptomic responses of generalist arthropod herbivores shortly after host plant transfer to a single or very few new hosts, but it remains uncertain to what extent this is a general stress response or a host-specific adaptation. Hence, we profiled the transcriptome of *T. urticae* minimal five generations after host plant transfer to five diverse plant species. Distinct transcriptomic responses were found with only a limited overlap in both specificity and directionality, suggestive of a fine-tuned transcriptional plasticity. Nonetheless, analysis at the gene family level uncovered overlapping functional processes, recruiting genes from both well-known and newly discovered detoxification families, including short-chain dehydrogenases and

single PLAT domain proteins. Manual genome annotation showed that these two families were expanded in *T. urticae*. Our results shed new light on the molecular mechanisms underlying the remarkable adaptive potential for host plant use of generalist arthropods and set the stage for functional validation of important players in *T. urticae* detoxification of plant secondary metabolites.

Chapter 5 focusses on the phase II detoxification UDP-glycosyltransferases (UGTs), which catalyzes the addition of UDP-sugars to small hydrophobic molecules, turning them into more water-soluble metabolites. Only recently, arthropod UGTs were linked to detoxification and sequestration of plant toxins and insecticides, but functional evidence for *T. urticae* UGTs was still lacking. A set of eight UGT genes were selected for functional expression based on a phylogenetic analysis and their transcription profile upon pesticide resistance and long-term acclimation to new host plants (chapter 4). All of them were shown to be catalytically active and the majority preferred UDP-glucose as activated donor for glycosylation of model substrates. A high-throughput substrate screening with plant secondary metabolites and pesticides revealed patterns of both substrate specificity and promiscuity. Nine enzyme-substrate combinations were selected for more comprehensive analysis and steady-state kinetic parameters were determined. Among others, plant metabolites such as capsaicin and several flavonoids were shown to be glycosylated. The acaricide abamectin was also glycosylated by two UGTs and one of them was also overexpressed in an abamectin resistant strain. Our study corroborates the potential role of *T. urticae* UGTs in detoxification of both synthetic and natural xenobiotic compounds and paves the way for rapid substrate screening of arthropod UGTs.

Finally, in **Chapter 6**, the potential of trait mapping by using bulked segregant analysis in *T. urticae* and other arthropods is discussed. Additionally, potential strategies are highlighted for the validation of hypotheses brought forward in the previous chapters.

Samenvatting

Hoofdstuk 1 introduceert de protagonist van dit doctoraat, de bonenspintmijt, *T. urticae*. Deze mijt kan zich voeden op een brede waaier van waardplanten en ontwikkelt heel snel resistentie tegen gewasbestrijdingsmiddelen (pesticiden). Eerst werden de reeds gekende moleculaire mechanismen besproken die aan de basis liggen van dit uitzonderlijk adaptatievermogen. Vervolgens werden de kenmerken van de bonenspintmijt belicht die geleid hebben tot het sequentiëren van zijn genoom. Tot slot werden bio-informatica analyses voor het ontrafelen van de moleculaire mechanismen van het adaptatievermogen van *T. urticae* besproken.

In **Hoofdstuk 2**, werd een “bulked segregant analysis” (BSA) uitgevoerd, om loci gerelateerd aan resistentie tegen METI-I pesticiden (fenpyroximate, pyridaben en tebufenpyrad) te identificeren. Naast een gemeenschappelijk resistentie mechanisme voor de drie METI-Is (de gekende H92R “target-site” mutatie), werden ook twee pesticide specifieke loci terug gevonden. Een genoom locatie die het cytochroom P450 reductase (CPR) gen bevat werd gelinkt aan resistentie tegen zowel pyridaben als tebufenpyrad. CPR is een essentiële elektronendonor voor microsomale P450s (fase 1 detoxificatie mechanisme). Daarnaast werd een locus die een atypische nucleaire hormonale receptor 96 (NHR96) bevat (geen DNA-binding domein (DBD)), gelinkt aan tebufenpyrad resistentie. Ondanks dat “DBD-lacking NHR96-like” genen amper voorkomen in geleedpotigen, werd een expansie teruggevonden in het *T. urticae* genoom (47 genen).

In **Hoofdstuk 3** werd RNA-seq gebruikt om te onderzoeken wat het effect is van synergisten (DEF, DEM, PBO en CsA) op *T. urticae* genexpressie. Synergisten kunnen metabole resistentie verhinderen door inhibitie van detoxificatie enzymen en membraan transporters. Bijgevolg worden synergisten vaak gebruikt voor het ontrafelen van de bijdrage van detoxificatie enzymen en transporters in pesticide resistentie. Blootstelling aan PBO en DEF resulteerden in een uitgebreide en partieel gedeelde respons van het transcriptoom, inclusief fase 1 (P450s) en fase 2 (UGTs) detoxificatie gen families. Behandeling met CsA resulteerde in de neerregulatie van een fase 3 detoxificatie gen familie (de “Major Facilitator Superfamily (MFS)” transporter familie). Een DEM behandeling had geen sterk effect op het transcriptoom van de spintmijt.

Hoofdstuk 4 focust op de transcriptoom respons van *T. urticae* mijten nadat deze werden overgebracht naar ofwel een waardplant van dezelfde plantenfamilie maar met een chemisch verschillende plantafweer (*Phaseolus lunatus*) of naar economisch belangrijke gewassen van andere plantenfamilies (*Glycine max, Gossypium hirsutum*, *Solanum lycopersicum* and *Zea mays*). Het werd reeds eerder aangetoond dat *T. urticae* zich snel aanpast aan nieuwe waardplanten, en hierbij wordt blootgesteld aan diverse plantafweer mechanismen die zowel constitutief kunnen aanwezig zijn of geïnduceerd kunnen worden. Meerdere studies onderzochten reeds eerder het transcriptoom van geleedpotigen kort na het overzetten naar één of enkele nieuwe waardplanten. In Hoofdstuk 4 wordt het *T. urticae* transcriptoom echter bestudeerd minimaal vijf generaties na de waardplant transfer. Er werd een beperkte gemeenschappelijke respons waargenomen op gen expressie niveau. Dit suggereert een zeer specifieke en fijn afgestelde respons afhankelijk van de nieuwe waardplant. Desalniettemin zijn gelijkaardige gen families betrokken bij de verschillende

waardplant transfers. Inclusief gekende detoxificatie gen families, als gen families die niet eerder gelinkt werden aan waardplant acclimatisatie (“short-chain dehydrogenases” en “single PLAT domain proteins”). Naast een nieuwe inkijk in de onderliggende mechanismen van waardplant acclimatisatie werden kandidaat genen ontmaskerd voor verder onderzoek.

Hoofdstuk 5 focust op UDP-glycosyltransferases (UGTs), een fase 2 detoxificatie gen familie. UGTs katalyseren de additie van een UDP suiker aan kleine hydrofobe moleculen, resulterend in beter wateroplosbare metabolieten. Slechts recentelijk werden UGTs van geleedpotigen gelinkt aan de detoxificatie en sequestratie van plant toxines en pesticiden, maar functioneel bewijs voor de mogelijke rol van *T. urticae* UGTs ontbreekt nog steeds. Acht UGTs van *T. urticae* werden geselecteerd voor functionele expressie gebaseerd op fylogenetisch onderzoek en hun expressie profiel (na waardplant transfer (Hoofdstuk 4) en in pesticide resistente populaties). Alle acht UGT enzymen waren katalytisch actief en de meerderheid verkoos UDP-glucose als geactiveerde donor voor de glycosylatie van modelsubstraten. Zowel plant secundaire metabolieten als pesticiden werden getest als potentieel substraat voor de UGTs, en zowel zeer uitgebreide als specifieke substraat spectra werden teruggevonden. Vervolgens werden de “steady-state” kinetische parameters bepaald voor negen UGT enzym-substraat combinaties. Meerdere plant secundaire metabolieten werden geglycosyleerd in onze studie, waaronder capsaicin en enkele flavonoiden. Bovendien werd ook het pesticide abamectine geglycosyleerd door twee UGTs waarvan één ook sterk tot expressie kwam in een abamectine resistente *T. urticae* populatie. Onze studie toont aan dat *T. urticae* UGTs een rol kunnen spelen in de detoxificatie van zowel synthetische al natuurlijke xenobiotische verbindingen, en bevat een protocol voor de screening van mogelijke substraten van UGTs van geleedpotigen.

In **Hoofdstuk 6**, wordt tot slot het potentieel van BSAs in *T. urticae* en andere geleedpotigen besproken. Daarnaast worden mogelijke strategieën ter validatie van hypotheses in de voorgaande hoofdstukken besproken.

Curriculum vitae

Personal information

Full name: Simon Pieter Snoeck

Address: Kroonstraat 7, 9000 Gent

Birth date and place: 17 July 1992, Oudenaarde

Telephone: +32 (0)497 39 82 34

E-mail: simon.snoeck@gmail.com

Education

2015-present	PhD applied biological sciences (Ghent University)
2013-2015	Master bio-science engineer in agricultural sciences (Ghent University)
2010-2013	Bachelor bio-science engineer (Ghent University)

Publications

Kurlovs*, A., S. Snoeck*, O. Kosterlitz, T. Van Leeuwen, R.M. Clark, 2019. Trait mapping in diverse arthropods by bulked segregant analysis. Curr. Opin. Insect Sci. 36 (IF 4.171)

Snoeck*, S., A. Kurlovs*, S. Bajda, R. Feyereisen, E. Villacis-Perez, O. Kosterlitz, W. Dermauw, R.M. Clark, T. Van Leeuwen, 2019. High-resolution QTL mapping in Tetranychus urticae reveals acaricide-specific responses and common target-site resistance after selection by different METI-I acaricides. Insect Biochem. Mol. Biol. 110: 19–33. (IF 3.562)

Snoeck*, S., N. Pavlidi*, D. Pippini, J. Vontas, W. Dermauw, T. Van Leeuwen, 2019 Substrate specificity and promiscuity of horizontally transferred UDP-glycosyltransferases in the generalist herbivore *Tetranychus urticae*. Insect Biochem. Mol. Biol. 109: 116–127. (IF 3.562)

Simma*, E. A., W. Dermauw*, V. Balabanidou, S. Snoeck, A. Bryon, R.M. Clark, Y. Delenasaw, J. Vontas, L. Duchateau, T. Van Leeuwen, 2019 Genome-wide gene expression profiling reveals that cuticle alterations and P450 detoxification are associated with pyrethroid resistance in *Anopheles arabiensis* populations from Ethiopia. Pest Manag. Sci. 5374. (IF 3.249)

Wybouw*, N., O. Kosterlitz*, A. H. Kurlovs, S. Bajda, R. Greenhalgh, S. Snoeck, H. Bui, A. Bryon, W. Dermauw, T. Van Leeuwen, R.M. Clark, 2019 Long-term population studies uncover the genome structure and genetic basis of xenobiotic and host plant adaptation in the herbivore *Tetranychus urticae*. Genetics 211: 1409-1427. (IF 4.075)

Snoeck*, S., N. Wybouw*, T. Van Leeuwen, W. Dermauw, 2018 Transcriptomic plasticity in the arthropod generalist *Tetranychus urticae* upon long-term acclimation to different host plants. G3 (Bethesda). 8: 3865–3879. (IF 2.742)

Snoeck, S., R. Greenhalgh, L. Tirry, R. M. Clark, T. Van Leeuwen, W. Dermauw, 2017 The effect of insecticide synergist treatment on genome-wide gene expression in a polyphagous pest. Sci. Rep. 7: 13440. (IF 4.122)

Piot, N., S. Snoeck, M. Vanlede, G. Smagghe, I. Meeus, 2015 The effect of oral administration of dsRNA on viral replication and mortality in *Bombus terrestris*. Viruses 7: 3172–3185. (IF 3.761)

Oral* and poster presentations

2019	8th International symposium on molecular insect science, Sitges
2019*	14th International IUPAC conference of crop protection, Ghent
2018*	ESA, ESC and ESBC joint annual meeting, Vancouver
2018*	XI European congress of entomology, Napels
2017	National symposium for applied biological sciences NSABS, Leuven

Award

2018 XI European congress of entomology, Napels, student competition (oral presentation)

International mobility

14/03 – 30/04/2016	Department of Biology, University of Utah (prof. dr. Richard M. Clark)
11-16/06 & 4-14/07/2017	Institute for Biodiversity and Ecosystem Dynamics (IBED), University of Amsterdam (dr. Nena Pavlidi)
16/11 – 20/12/2017	Department of Biology, University of Utah (prof. dr. Richard M. Clark)

Other academic services

Peer reviewer	scientific reports (2019) and pest management science (2019)
Undergraduate mentoring	Vandenhende Gunar (2016-2017), Ghent University

Ongoing research

I am currently involved in a project about the genomics of host race formation in *T. urticae*, and three articles about pesticide resistance against METI-I, coumaphos and abamectin in *Panonychus citri*, *Varroa destructor* and *T. urticae*, respectively. I also contributed to the genome annotation of *Frankliniella occidentalis*.